Investigating the biological role of γ-tubulin phosphorylation in spindle alignment and assembly

Kristian Lee Shulist

Department of Biology
McGill University
Montreal, Quebec, Canada

August 2018

A thesis submitted to McGill University in partial fulfillment of the requirements of the degree of Doctor of Philosophy

Acknowledgements

I would like to express my appreciation to Dr. Jackie Vogel for providing me with this opportunity and for guiding me along the ups and downs associated with doing a PhD. She taught me about science and about myself. Most importantly, she taught me that my weaknesses do not have to hold me back.

I am also grateful to my supervisory committee Dr. Damien D'Amours and Dr. Tony Mittermaier for their productive feedback and stimulating discussions over the course of my research project. I am very thankful to the past and present Vogel lab members especially Eric Yen, Allen Leary, Yohann Faivre, Sana Thabet, Shannon Sim and Vincent Rouger for their friendship and fruitful scientific discussion. I am also thankful to Alycia Noë for her friendship and support during the last (and most difficult) years of my PhD. I am extremely grateful to Elena Nazarova, not only for establishing the basis for much of the microscopy analysis, and for teaching me how to use the microscope, but also for her continued friendship during her PhD and after she graduated. Additionally, I am extremely thankful to Susi Kaitna both for all her help in the lab, especially in the preparation and carrying out the SGA, but also in being a very dear friend throughout the course of my PhD; all the laughs during our lunches and coffee breaks made the stress of a PhD much easier to handle.

I would like to sincerely thank my family, especially my parents who have supported and encouraged me throughout my whole life. Additionally, I cannot express enough appreciation and thanks to my wonderful husband Keith Oxby. He has been through every misstep with me and shared my frustration; he has been there for every success and celebrated with me. He knows more about γ-tubulin than any engineer ought to and I deeply appreciate his love and listening over the years. I most definitely could not have done this without his support.

Finally, I would like to acknowledge the generous financial support from Jackie Vogel through her grants from the National Sciences and Engineering Research Council and the Canadian Institute of Heath Research.

Table of contents

List of tables

List of figures

List of abbreviations

(-)end	Microtubule minus end
(+)end	Microtubule plus end
α-factor	Alpha-factor
γ-tubulin	Gamma-tubulin
γ-TuRC	γ-Tubulin ring complex
γ-TuSC	γ-Tubulin small complex
+TIP	Plus-end tracking proteins
APC	Adenomatous polyposis coli tumor suppressor
APC/C	Anaphase promoting complex/cyclosome
CDK	Cyclin-dependent kinase
CPC	Chromosome passenger complex
EB1	End binding protein 1
EGFP	Enhanced green fluorescent protein
GAMER	Genetic array with mixed effects regression
GRIP	Gamma-tubulin ring complex interacting protein
IDR	Intrinsically disordered region
KT	Kinetochore
MAP	Microtubule-associated protein
MCC	Mitotic checkpoint complex
MEN	Mitotic exit network
mNG	Monomeric NeonGreen fluorescent protein
MT	Microtubule
MTOC	Microtubule organizing center
OyCD	Optimized yeast cytosine deaminase
PCA	Protein-fragment complementation assay
PCM	Pericentriolar material
PI	Phosphoinhibitory
PM	Phosphomimetic
PTM	Post-translational modification
SAC	Spindle assembly complex
SAF	Spindle assembly factor
SC	Sister chromatid
SGA	Synthetic genetic array
SGI	Synthetic genetic interaction
SPB	Spindle pole body
SPIN	Spindle pole body inheritance network
SPOC	Spindle orientation checkpoint

Author contribution

All the data collection and results obtained during my PhD are presented here as two manuscript-based chapters (Chapters 2 and 3). Chapters 1 and 4 were written entirely by myself—including the literature search and all figures—for the purpose of this thesis.

Chapter 2 is a manuscript in preparation:

I constructed all the γ-tubulin mutants and conducted all the growth assays and genetic crosses. Alexandra Decterov assisted me with this. I preformed all the microscopy and the subsequent analysis. Integrated pole intensities were extracted using a graphical user interface developed by Eric Yen. I preformed the literature review described within this chapter. I wrote the summary, introduction, materials and methods, results, discussion and figure legends. I also made all the figures in this chapter. I developed the research plan with Jackie Vogel.

Jackie Vogel established the original scientific plan and basis for this research. She guided this research and supervised my progress during this project. She also edited all sections of this chapter.

Chapter 3 is a published manuscript:

Shulist K., Yen E.A., Kaitna S., Leary A., Decterov A., Gupta D., and Vogel J. (2017). Interrogation of γ-tubulin alleles using high-resolution fitness measurements reveals a distinct cytoplasmic function in spindle alignment. *Sci Rep*. 2017; 7: 11398.

I constructed all strains, performed all growth assays, and conducted all live cell imaging and subsequent analysis. I created Figures 3.1, 3.3, 3.5, 3,6, 3.7, 3.8 and 3.9 and finalized them with Jackie Vogel.

Eric Yen developed the software and mathematical model for the GAMER analysis. He created Figures 3.2 and 3.4 and finalized them with Jackie Vogel. Susi Kaitna established and coordinated the experimental SGA screens, preformed all the quality controls for these screens and contributed to the overall discussion for the manuscript. Alexandra Decterov assisted with the construction of strains and growth assays. Debarun Gupta assisted with the statistical analysis for GAMER. Allen Leary contributed to the concept of Figure 3.6 and edited the manuscript. Eric Yen, Jackie Vogel and myself wrote and edited the manuscript.

Jackie Vogel established the original scientific plan and basis for this research. She provided the original idea behind the GAMER method and coined the idea of perfect alignment. She supervised mine and Eric Yen's progress during this project.

Abstract

Accurate chromosome segregation requires both the correct assembly of the mitotic spindle, as well as the proper placement of the spindle relative to the plane of cell division. Interruption of either of these processes can lead to severe consequences such as cell death or, in high eukaryotes, cancer. Spindle assembly and spindle placement are largely driven by the function of microtubules. Microtubules are primarily nucleated from microtubule organizing centers (MTOCs) by an evolutionarily conserved protein complex: the γ-tubulin ring complex (γ-TuRC). While canonically involved in microtubule nucleation, the γ-TuRC is also involved in numerous nucleation-independent cellular processes. How the γ-TuRC is regulated such that it participates in both nucleation-dependent and -independent cellular functions is unclear. Here, we use the budding yeast, *Saccharomyces cerevisiae*, to investigate the regulation of γ-tubulin through phosphorylation.

We systematically characterized the phosphorylation sites of γ-tubulin which is associated with the spindle pole body (the yeast MTOC) by creating phospho-mutants at each site both independently and in tandem. We found that the G1-specific phosphorylation sites, T130 and T227, contribute to chromosome attachment in a manner independent of microtubule dynamics. Additionally, we identified an intramolecular relationship between sites S360 and Y445 which regulates spindle assembly. Lastly, we identified a novel γ-tubulin allele, Y362E, which participates in spindle placement through the regulation of astral microtubule number.

Collectively, this work furthers our understanding of γ-tubulin regulation and its role in the processes of spindle assembly and spindle placement. Additionally, as the majority of the phosphorylation sites in yeast γ-tubulin are well-conserved across species, this regulation is likely an evolutionarily conserved mechanism to control γ-tubulin function.

Résumé

La ségrégation ordonnée des chromosomes lors de la mitose nécessite la formation correcte d'un fuseau mitotique ainsi que son bon positionnement dans le plan de la division cellulaire. Le dérèglement de l'une de ces conditions engendre des conséquences sévères telles que la mort cellulaire, ou encore le cancer chez les eucaryotes supérieurs. L'organisation et le positionnement du fuseau mitotique sont principalement associés à la fonction des microtubules. Les microtubules émanent de centres organisateurs de microtubules (COMT). Ils sont initialement nucléés par un complexe protéique conservé au cours de l'évolution appelé l'anneau de γ-tubuline. Connu pour sa fonction de nucléateur, ce complexe est aussi impliqué dans d'autres fonctions régulatrices des microtubules, indépendamment de la nucléation. Malgré le nombre important des travaux sur ce sujet, l'implication et la régulation de l'anneau de γ-tubuline dans les fonctions cellulaires, dépendantes et indépendantes de la nucléation, restent encore peu comprises. Le but de cette étude est d'approfondir nos connaissances sur la régulation du complexe par phosphorylation en utilisant le modèle eucaryote, la levure *Saccharomyces cerevisiae*.

Dans cette étude, les sites de phosphorylations de la γ-tubuline, située aux corps polaires du fuseau (COMT de la levure), ont été systématiquement caractérisés en construisant les phospho-mutants correspondants contenant une simple ou une double mutation. Les sites spécifiques à la phase G1 du cycle cellulaire, T130 et T227, ont été démontrés comme étant impliqués dans l'attachement des chromosomes indépendamment de la dynamique des microtubules. De plus, une relation intramoléculaire entre les sites S360 et Y445 a été mise en évidence et impliquée dans la formation du fuseau mitotique. Enfin, un nouvel allèle de γ-tubuline, Y362, a été identifié comme acteur important dans le positionnement du fuseau mitotique en régulant le nombre des microtubules astraux.

En conclusion, cette étude a permis une meilleure compréhension de la régulation de l'anneau de γ-tubuline ainsi que son rôle dans la formation et le positionnement du fuseau mitotique. De plus, la majorité des sites de phosphorylation sont conservés à travers les espèces, il est donc probable que cette régulation soit également conservée chez les eucaryotes multicellulaires notamment chez l'Homme.

Introduction

The main driving force behind all life is reproduction, the need to pass on one's genetic material to the next generation. At the basis of this is the proper segregation of genetic material upon cell division. In eukaryotic cells, genetic material is typically in the form of chromosomes and is segregated through the activity of a large biological machine known as the mitotic spindle. Many events must unfold for the proper functioning of the mitotic spindle. Specifically, the spindle must be assembled correctly, and additionally, it must be aligned perpendicularly to the plane of cell division such that each progeny cell inherits exactly one copy of the set of chromosomes. Failures in accurate segregation of genetic material leads to serious consequences such as cell death or cancer in higher eukaryotes.

The mitotic spindle includes several different components including: microtubules, which provide the flexible support required to separate chromosomes; chromosomes and kinetochore complexes, which are bound to the (+)end of microtubules; microtubule-associated proteins, which act as the force generators to pull the sister chromatids apart; and microtubule organizing centers (MTOCs) which nucleate and anchor the (-)end of microtubules. MTOCs nucleate microtubules through the evolutionary conserved protein, γ-tubulin, which, along with several other proteins forms the γ-tubulin ring complex (γ-TuRC)—a spiral-like structure that provides a template for microtubule growth. Though the canonical role of the γ-TuRC is nucleation, it also participates in a number of other cellular functions. One way that cells manage the various functions of proteins is through regulation by post-translational modifications.

Here, we used the budding yeast, *Saccharomyces cerevisiae,* to study how phosphorylation of γ-tubulin contributes to its function. The simplicity of the budding yeast cell cycle and mitotic spindle combined with its ease of use and genetic manipulation make it an excellent model organism to explore this important question. In yeast, γ-tubulin is phosphorylated at eight different residues when associated with the spindle pole body (the yeast MTOC)[1]. Only two of these sites have been investigated at any capacity[1-3]. Phosphorylation of conserved residue S360 contributes to spindle assembly by mediating the number of antiparallel microtubules forming the central core bundle of the spindle. A mutation which prevented

phosphorylation at this site (S360A) resulted in additional interpolar microtubules and increased spindle stability[2]. Consistently, when this site was mutated to an amino acid that mimicked the electrostatic nature of a phosphorylation (S360D), there was a complete lack of cross-linked interpolar microtubules resulting in an unstable spindle[2]. Similarly, a phosphomimetic mutation at residue Y445 led to spindle defects and increased chromosome loss[3,4]. Taken together, these studies highlight γ-tubulin's role in spindle assembly. However, the biological significance of the remaining sites remains unclear.

The first major focus of my research was to investigate the function of all remaining γ-tubulin phosphorylation sites (phospho-sites); this is outlined in Chapter 2 of my thesis. I did this using a systematic approach by first creating both phosphoinhibitory and phosphomimetic mutations at each phospho-site. I then subjected each mutant to an initial series of assays to help characterize the mutant and determine if microtubule-based processes were disrupted. Mutants that showed sensitivities at various stages of the initial characterization were followed up with more fine-grained analysis, such as live cell microscopy. From this systematic characterization, I identified a mutant of the G1-phase specific phospho-sites, T130D-T227D, which was dependent on the spindle assembly checkpoint for viability. The SAC monitors chromosomes for proper microtubule attachment. Previous work on γ-tubulin mutants show a correlation between SAC sensitivity and perturbed microtubule dynamics (often seen as temperature sensitivity)[1-3]. However, T130D-T227D showed no indication of having disrupted microtubule dynamics, thus, we propose that this mutant contributes to chromosome attachment independent of microtubule dynamics.

Additionally, my initial characterization of γ-tubulin mutants identified a unique relationship between sites S360 and Y445 in the regulation of spindle assembly. This was further studied in Chapter 3 of my thesis where we confirmed that the phosphomimetic mutant Y445D was involved in spindle assembly by analyzing its spindle dynamics and investigating its synthetic genetic interaction profile using a method we developed, called GAMER. Moreover, sites S360 and Y445 appear to be phosphorylated in a coordinated manner as mixing the phospho-mutant status (i.e. either phosphoinhibitory or phosphomimetic) simultaneously at each site was lethal.

Lastly, I identified a novel separation-of-function allele in Chapter 2 of my thesis (Y362E) which became the second major focus of my thesis. Chapter 3 outlines an in-depth investigation of this mutant allele. By investigating this allele, we discovered that this phospho-site contributes to proper spindle alignment prior to chromosome segregation. This is the first instance of a γ-tubulin phospho-site contributing to spindle placement. We show that the Y362E mutation caused an increase in astral microtubule number and a more symmetric distribution of microtubule occupancy across the two spindle pole bodies. We hypothesize that this is either occurring through the regulation of nucleation, or through the modification of microtubule-associated protein behaviour.

The results presented in this paper provide insight into γ-tubulin's function in budding yeast, specifically in spindle assembly and spindle placement. Additionally, as the majority of the relevant phospho-sites are well-conserved across species, this regulation may represent an evolutionarily conserved mechanism to control γ-tubulin function.

Chapter 1: Literature Review

1.1 Overview of the cell cycle

Cell division is one of nature's most ancient and conserved cellular processes, in which one cell replicates its DNA and divides into two cells. This ensures that both resulting cells inherit exactly one copy of the genome. There are four ordered phases in the cycle of cell division: G1-, S-, G2- and M-phase. In G1-phase, the cell prepares for replication of its genome which occurs in S-phase. The cell ensures S-phase is complete and prepares for mitosis in G2-phase. Lastly, M-phase is when the cell undergoes mitosis and consists of several sub-stages: prophase (chromosome condensation), prometaphase (formation of the mitotic spindle), metaphase (chromosome alignment along the metaphase plate), anaphase (separation of sister chromatids) and telophase (cytokinesis). The phases of cell division are driven by the activity of cyclin-dependent kinases (CDKs) partnered with their regulatory subunits, the cyclins. Correct progression of the cell cycle is crucial for high fidelity chromosome inheritance, and its absence can lead to aneuploidy; this often results in non-viable or highly defective cells.

At the center of the cell division process lies a large molecular machine known as the mitotic spindle. The spindle pulls sister chromatids to opposite ends of the dividing cell. Many intricate processes contribute to the overall success of the spindle, including its intrinsic dynamics, as well as proper spindle assembly, placement and breakdown.

Much of our knowledge of the mechanisms governing the cell cycle comes from research on the unicellular budding yeast, *Saccharomyces cerevisiae*. This is largely due to its amenability to genetic manipulation, its high level of evolutionary conservation with metazoans, and the vast amount of resources available for this organism.

1.2 Components of the mitotic spindle

The mitotic spindle is composed of several different key components. Microtubules (MTs) make up the majority of the spindle and are the key to its function. There are three types of MTs found in mitotic spindles: astral MTs, interpolar MTs, and kinetochore MTs. Astral MTs interact

with the cell cortex and generate the force needed to orient the spindle. Interpolar MTs interdigitate at the spindle midzone, forming an antiparallel core bundle to push the poles apart during mitosis. Kinetochore MTs bridge the microtubule organizing centers (MTOCs), at the cellular poles, to the chromosomes, at the cellular center, and allow for the separation of sister chromatids[5]. Kinetochore MTs do not come in contact with the DNA directly, but instead form stable attachments with centromere-bound kinetochore complexes. In addition, MTs are decorated with several different microtubule-associated proteins (MAPs). These proteins work together to stabilize the mitotic spindle and to generate the forces required to separate sister chromatids.

1.2.1 Microtubules

Microtubules (MTs) are polarized biopolymers made of globular tubulin subunits (α- and β-tubulin) and form an essential component of the eukaryotic cytoskeleton, along with other cellular systems such as the mitotic spindle, vesicular transport, and ciliary and flagellar movement. α-Tubulin and β-tubulin heterodimerize together in a head-to-tail fashion to form a linear protofilament. Typically, 13 protofilaments interact laterally to form a hollow cylinder measuring 25 nm in diameter; this forms the structure of a singlet MT. The lateral and longitudinal contacts among tubulin subunits within and between protofilaments gives MTs the stiffness required by the mitotic spindle to segregate chromosomes without the spindle buckling in on itself[6]. The polarity of a MT originates from the head-to-tail arrangement of the α- and β-subunits; new subunits are preferentially added at the “head”, or (+)end (plus end) of the MT rather than the (-)end (minus end)[7,8].

Additionally, MTs have an intrinsic dynamic instability which is critical to their function ([9] and recently reviewed in Brouhard, 2015[10]). Both α- and β-tubulin monomers can bind guanosine triphosphate (GTP). Hydrolysis of β-tubulin-bound GTP occurs at a fixed probability per unit time[9]. Thus, during rapid MT growth, the rate of subunit incorporation exceeds the rate of hydrolysis resulting in the formation of a GTP cap which prevents depolymerization[9]. As the concentration of free GTP-bound monomers decreases, the rate of growth slows and the GTP cap shrinks[9]. Eventually, the rate of hydrolysis catches up with the rate of polymerization resulting in exposed GDP-bound subunits; their low affinity for the MT lattice results in rapid

depolymerization of the MT (termed "catastrophe")[9]. Interestingly, recent *in vitro* data suggests that though the cause of catastrophe is undoubtedly related to the loss of the GTP cap[11,12], the age of the MT (rather than its length or growth rate) is the dominant predictor of catastrophe[13]. This implies that MTs 'remember' their past, possibly through the accumulation of defects within the lattice[14] or though the increase in (+)end tapering of older MTs[15].

The interplay between growth and catastrophe creates the intrinsic dynamic instability of MTs. It allows them to efficiently probe their environment in search of their targets and is important for their role in force generation[16].

1.2.2 Microtubule-associated proteins

All types of MTs are decorated with many microtubule-associated proteins (MAPs). The only criteria for a protein to be considered a MAP is that it interacts with MTs, thus, there are a vast number of MAPs which contribute to different MT-related processes. Generally, MAPs affect the dynamics and behaviour of MTs. MAPs have been known to regulate MT dynamics, to bundle and cross-link neighbouring MTs, or to link them to other structures, such as membranes or other cytoskeletal elements. As there are hundreds of different MAPs across all types of species and cell types, this section will only mention those relevant to this work.

a. Molecular microtubule motors

Molecular motors are a class of proteins that move along the surface of a substrate, usually a cytoskeletal filament. They do this by converting chemical energy into mechanical work through the process of ATP hydrolysis; this is the basis of their mechanochemical cycle. Generally, ATP is bound to the motor, hydrolyzed to ADP, and then released so that another ATP molecule may bind. Each of these chemical steps is coupled with a conformational change in the protein that alters its affinity to the filament. Molecular motors accomplish many feats with their mechanical movement, including vesicular and organelle transport, flagellar and ciliary movement, and spindle elongation during mitosis. There are three types of molecular motor proteins: myosins (which are track along actin motors), kinesins, and dynein (both of which are microtubule motors). This section will only discuss the molecular microtubule motors: kinesins and dynein.

Kinesins are a large super-family of motors with at least 14 distinct sub-families. They are structurally related to myosin motors and use a "hand-over-hand" motion to traverse the MT. While humans have upwards of ~50 kinesin proteins[17], budding yeast have only six: Kip2, Kar3, Kip3, Cin8, Kip1, and Smy1.

Kip2/Kinesin-7:

Kip2 is a type of kinesin-7, the same family as the highly-studied human protein, CENP-E, involved in chromosome congression (the movement of chromosomes to the metaphase plate)[18-20]. In budding yeast, Kip2 targets three other MAPs—Bik1 (CLIP-170 homolog), Kar9, and dynein—to the (+)ends of astral MTs[21,22]. This promotes spindle placement by facilitating the interaction between MTs and the cell cortex via Kar9 and dynein (discussed below). Additionally, the deposit of Bik1 on the (+)end stabilizes MTs[22]. Kip2 also interacts with Bim1 (EB1 homolog) *in vivo*[23]. Based on *in vitro* data, it is thought that Bim1, along with Bik1, act as processivity factors for Kip2 (processivity is a motor's capacity to carry out several consecutive rounds of its catalytic cycle leading to longer run lengths along the filament)[24]. Kip2 is not essential in yeast; its absence leads to rare and short astral MTs at both poles[25]. Presumably this is due to the loss of Bik1 at the (+)ends, though Kip2 also promotes MT growth *in vitro*[26]. Inactivation of Kar3, another kinesin motor, rescues this *kip2Δ* phenotype[27]. Consistently, overexpression of Kip2 leads to abnormally long astral MTs via Bik1[22].

Kar3/Kinesin-14:

Kar3 is a (-)end directed motor in the kinesin-14 family. Across different species, kinesin-14s provide the inward directed force to balance the outward directed force of kinesin-5s during pre-anaphase spindle assembly[28,29]. They do this by cross-linking and sliding MTs in the core bundle[30,31]. This is essential for bipolar spindle formation and allows for the fine-tuning of forces within the spindle. Kar3 has several unique characteristics that set it apart from other kinesin-14s. Firstly, Kar3 makes up only half of the traditionally homodimeric motor. It forms the catalytic motor head and requires either Cik1 or Vik1 as a non-catalytic motor head to complete the dimeric structure[32]. The two binding partners of Kar3 regulate its localization and function[32]. When Kar3 is partnered with Vik1, it is primarily found close to the spindle pole bodies (SPBs) where it cross-links parallel MTs[32-34]. Alternatively, when Kar3 is bound with Cik1, it localizes to

the spindle midzone where it mediates antiparallel MT cross-linking and kinetochore capture[28,35-39]. Kar3-Cik1 also functions to fuse the two haploid nuclei together (called karyogamy) during mating[40,41].

Secondly, Kar3-Cik1/Vik1 has recently been shown to exhibit robust processive movement[37]. This differs from most kinesin-14s, which are nonprocessive and are released from the MT after every catalytic cycle, thus, they rely on concerted activity within an ensemble to carry out their functions[30,31,42-46].

In vitro, Kar3 exhibits (+)end MT depolymerase activity[47]; however, it is still debated whether this occurs *in vivo*[37,40,41,48]. *In vivo*, Kar3 also regulates astral MTs, as the loss of Kar3 causes symmetrically long and frequent astral MTs on both poles[48]. This can be rescued by knock-out of *KIP2*[27].

Kip3/Kinesin-8:

Kinesin-8 family member Kip3 is a hybrid motor that can both walk along and depolymerize MTs[13,49-52]. Kip3 is found on both astral MTs and nuclear MTs—it localizes to the (+)ends of astral MTs throughout the cell cycle and to the nuclear MTs in mitosis[49]. On the astral MTs, Kip3 may play a role in the Kar9-dependent pathway for spindle placement, though the details of this are unclear[25,53,54]. The loss of Kip3 reduces the frequency of MT catastrophe[49], resulting in cells with increased MT length and mispositioned spindles[25,53,54]. Additionally, *in vitro*, Kip3 induces catastrophe in a MT length-dependent manner[13,50,55]. Thus, it is thought that Kip3 regulates the length and dynamics of cortically attached MTs. When left unregulated (i.e. in *kip3Δ*), cortically attached MTs grow inappropriately and push the spindle away from the proper aligned state[49]. On nuclear MTs, Kip3 has MT sliding activity which, along with its depolymerizing activity, promotes spindle assembly and controls spindle length and stability[56-60]. As such, Kip3 facilitates spindle disassembly at the end of anaphase by depolymerizing spindle MTs[58]. Kip3 has also been implicated in regulating kinetochore clustering and dynamics[61-63].

Cin8/Kip1/Kinesin-5:

Across nearly all eukaryotes, kinesin-5s are a family of motors which perform the essential functions of spindle establishment, maintenance and elongation (for a review, see Ferenz *et al*., 2010[64]). Kinesin-5s provide the outward pushing force at the spindle midzone, preventing spindle

collapse and causing eventual spindle elongation. They are unique from other kinesin motors in that they are homotetrameric complexes (as opposed to the typical homodimeric kinesin). Two sets of dimers assemble in a bipolar fashion (tail-to-tail) so that the motor heads are at the distal ends of the complex[65-67]. This allows kinesin-5s to cross-link and slide two antiparallel MTs[68,69]. Budding yeast have two kinesin-5s: Cin8 and Kip1. There is functional redundancy between them, however, Cin8 plays a more dominant role in spindle assembly[70,71]. Additionally, unlike Kip1, Cin8 experiences a myriad of both genetic and physical interactions with various partners suggesting it has many different cellular functions[72-79].

Cells which are lacking functional copies of both kinesin-5s (Kip1 and Cin8) are non-viable and arrest with duplicated but unseparated SPBs[70]. Loss of Cin8 in yeast also perturbs chromosome attachment and segregation[80-82]. Cin8 localizes to the kinetochore where it functions to cluster the kinetochores together[61]. This is likely related to Cin8's role in the coordinated movement of individual pericentromeres (the chromatin and interchromosomal linkages around the centromere)[82]. Cin8 is proposed to cross-link neighbouring kinetochore MTs attached to different chromosomes and lock them into coordinated movement, a process thought to aid in the orientation and stabilization of the spindle[82]. Additionally, Cin8 also contributes to chromosome congression by promoting depolymerization of longer kinetochore MTs[83].

Kinesin-5s are typically (+)end directed, however, Cin8 and Kip1 exhibit both (+)end and (-)end directed motility[84-87]. When bound to a single MT, lone Cin8 motors move in the (-)end direction; this switches when Cin8 is cross-linking antiparallel MTs as a group ensemble[84,85,88]. Similar observations are seen for Kip1[87]. It is thought that the bi-directionality of Cin8 allows for accumulation of Cin8 at the SPBs prior to pole separation (via (-)end directed motility); here Cin8 is poised to cross-link interpolar MTs and push the poles apart from each other thereby establishing bipolarity (discussed below)[88].

Dynein:

Dynein is a highly conserved multi-subunit motor protein which translocates towards the (-)end of MTs. It is unrelated to kinesins or myosins and "walks" in a much more stochastic manner, somewhat akin to a "drunken sailor"[89]. In most organisms, it regulates many different

processes including centrosome separation, spindle placement, and transport of organelles or vesicles[90-92]. In yeast, however, intracellular trafficking of organelles and other cargo is primarily carried out using the actin cytoskeleton in a dynein-independent manner[93]. Moreover, dynein is not involved in SPB separation like it is in metazoans; in fact, the only known role for dynein in budding yeast is spindle positioning during cell division[90]. Here, it works with the Kar9 pathway to ensure proper spindle placement (described below). Unlike in animals, dynein is not essential in yeast. However, absence of dynein causes aberrant anaphase due to spindle mispositioning and delays spindle disassembly and cytokinesis[94-98].

b. Non-motor +TIPs

+TIPs (plus-end tracking proteins) are a large family of MAPs that track the (+)end of MTs. There are three ways that a protein can track the (+)end of a MT: (1) plus-end directed motor activity, (2) plus-end binding affinity, and (3) hitchhiking on another MAP that is capable of either of the first two behaviours[99]. Plus-end directed motors also fall into the large family of molecular motor proteins (as discussed above). Another class of +TIPs are those that inherently have an affinity for the MT (+)end. Usually this involves what is called "treadmilling" or "surfing"[100]. Treadmilling occurs when a protein binds with high affinity to the GTP cap (e.g. EB1) and, as a population, carries out cycles of GTP-cap-binding followed by dissociation from the older GDP lattice[12,101,102]. Surfing occurs when a protein associates with the (+)end and stays associated as the end grows (e.g. XMAP215). This section will cover the relevant +TIPs which are not motor proteins.

Bim1/EB1:

End-binding protein 1 (EB1) is an evolutionarily conserved treadmilling +TIP. EB1 is thought to track the (+)end of growing MTs by preferentially binding to GTP-tubulin or GDP-P_i-tubulin[103]. *In vivo*, EB1 participates in many cellular processes because of its general role of recruiting various other hitchhiking +TIPs to the (+)end (for a review, see Lansbergen, 2006[104]). The inherent effects of EB1 are under debate due to several conflicting *in vitro* observations[12,102,105-110]. EB1's activity *in vivo* is similarly confounding: it has been shown to promote growth[111], increase rescue frequency[112,113], increase catastrophes[112,113], and suppress

catastrophes[114-116]. These differences are likely due to the different MAP binding partners that EB1 interacts with depending on the species and cell type.

In budding yeast, EB1 is known as Bim1 and is found on both the astral and nuclear MTs where it carries out distinct functions. On the astral MTs, Bim1 physically interacts with the adenomatous polyposis coli (APC) homolog, Kar9[117-119], where it assists in spindle placement (described below). Inside the nucleus, Bim1 regulates the dynamics of kinetochore MTs thus influencing kinetochore capture[120]. Additionally, Bim1 localizes to interpolar MTs where it stabilizes the core bundle by promoting polymerization; this lengthens the zone of MT overlap and maintains antiparallel cross-linking[34]. In anaphase, Bim1 is phosphorylated by Aurora B kinase (Ipl1 in yeast) which reduces its affinity for MTs and permits proper spindle breakdown[121]. Bim1 is not essential in yeast, but removing it results in short MTs. Shorter cytoplasmic MTs lead to perturbed spindle positioning[112] and shortening of the overlap between interpolar MTs leads to an unstable spindle[34]. Additionally, *bim1Δ* cells experience a higher frequency of chromosome loss[81,122] due to their role in kinetochore capture.

Kar9/APC:

Kar9 is the yeast homolog of mammalian APC. It tracks MT (+)ends by hitchhiking on Bim1. In mammals, APC is a multi-function protein with roles in cell adhesion, migration, proliferation, and differentiation, as well as MT stabilization, kinetochore capture and chromosome segregation (for a review, see Zhang and Shay, 2017[123]). Its latter three roles involve its association with MTs either directly or indirectly through binding EB1. Kar9 does not share significant sequence similarity with APC, except in its Bim1-binding site which is conserved with APC's C-terminal EB1-binding domain[124]. Thus, Kar9 is considered homologous only with respect to APC's EB1-related functions. In yeast, Kar9 is most well-known for its role on the astral MTs. Here, it binds to Bim1 and translocates to the (+)end where it mediates interactions between the MTs and the cell cortex during spindle placement (discussed below). In mammals, APC also interacts with EB1[125] and translocates to the (+)end of MTs[126-128]. Additionally, APC and EB1 have been implicated in spindle positioning[129-131]; however, unlike in yeast, APC can bind directly to MTs[126,132-134].

Recently, Kar9 has also been shown to localize to the nucleus along spindle MTs and at the kinetochore where it is ubiquitinated and targeted for degradation[135]. It is proposed that this exists to control the amount of Kar9 on the astral MTs[135]. Interestingly, Kar9 also contributes to proper chromosome segregation, similar to APC[135]. It is not yet clear whether this is a direct consequence of Kar9 activity at the kinetochore. Kar9 is not essential in yeast, but its absence leads to spindle and nuclear positioning defects[136,137] and an increase in chromosome instability[135].

Stu2/XMAP215:

Stu2 is the yeast homolog of the well-studied, evolutionarily conserved XMAP215 (ch-TOG in humans). These proteins are characterized in part by their multiple tubulin-binding TOG domains. While XMAP215 has five TOG domains, Stu2 only has two; however, this may be compensated by the fact that Stu2 functions as a homodimer while XMAP215 exists as a monomer[138-141]. Like Bim1/EB1, Stu2 and XMAP215 show varying effects on MTs. Generally, in metazoans, XMAP215/ch-TOG promotes MT growth *in vivo* and *in vitro*[138,142-144]. Most recently, in yeast, Stu2 has been shown to promote growth and reduce catastrophes *in vitro*[145]. *In vivo*, it promotes both catastrophe and rescue[146,147]. XMAP215/Stu2 increases MT polymerization by capturing tubulin dimers and facilitating their incorporation into the MT lattice[138,140,148]. The TOG domains work in tandem to allow for processive movement of Stu2 as the MT grows[148].

In the cell, Stu2 plays a central role in kinetochore capture (discussed below). Firstly, it is essential to the nucleation of kinetochore-derived MTs[149]. Secondly, it mediates kinetochore-dependent MT rescue[38,150]. Lastly, Stu2 stabilizes tension-bearing kinetochore attachments and destabilizes tension-lacking attachments[151]. Interestingly, other XMAP215 family members also seem to have kinetochore-related functions[152-155], though the details have not been elucidated as they have in budding yeast. Stu2 also exists in the cytoplasm where it localizes to astral MT (+)ends and SPBs. At the (+)ends, it increases the dynamics of astral MTs[146]. At the SPBs, it interacts with Spc72, the outer plaque γ-TuRC acceptor[156,157]. Here, it helps anchor MTs to the SPB and regulates (+)end dynamics[156]. Like other XMAP215 family members, Stu2 is essential for cell viability.

Bik1/CLIP-170:

Bik1 is the yeast homolog of CLIP-170. CLIP-170 was the first true (+)end tracking protein described[158]. It links MTs to kinetochores, endocytic vesicles and to the leading edge of a migratory cell[159]. *In vitro*, CLIP-170 promotes MT growth and bundling[160]. In yeast, Bik1 localizes to MT (+)ends, SPBs, and kinetochores. As mentioned above, Bik1 is targeted to astral MT (+)ends by Kip2 where it positively regulates growth[22]. Additionally, Bik1, along with Bim1, may act as a processivity factor for Kip2[24]. Bik1 also plays a role in spindle positioning by recruiting dynein to the (+)ends of astral MTs and by facilitating phosphorylation of Kar9 by Cdk1-Clb5 (described below)[22,161,162]. At the SPBs, Bik1 localization is dependent on Stu2[22]. Instead of SPB-localization being a prerequisite for MT loading (as is the case for Kar9), SPB-localization of Bik1 is thought to sequester it in order to prevent it from regulating (+)end dynamics[22]. Inside the nucleus, Bik1 localizes to the nuclear MTs and the kinetochore in a Kip2-independent manner[22,163,164]. Its role here is unclear but likely contributes indirectly to kinetochore capture by stimulating the dynamics of kinetochore MTs[120,165]. Bik1 is not essential in yeast and its absence results in very short astral MTs, defects in nuclear positioning, and aberrant spindle elongation[166].

1.2.3 Microtubule organizing centers

Often, the (-)end of a MT is anchored at a microtubule organizing center (MTOC) which limits this end's dynamic behaviour. The MTOC is the structure responsible for orientating the MTs spatially within the cell and is a site of MT nucleation. MTOCs participate in two main processes: (1) organizing MTs in eukaryotic flagella and cilia, and (2) organizing MTs in the mitotic and meiotic spindle. Flagellar and ciliary MTs are nucleated and organized at the cell body by MTOCs known as basal bodies. Basal bodies are made up of nine groups of fused triplet MTs arranged radially in a cartwheel configuration, and are close relatives of the metazoan centriole. Centrioles form the core of the centrosome, the MTOC responsible for the organization of the mitotic spindle in animal cells.

Centrosomes have two orthogonally-arranged centrioles at their center which, like basal bodies, consist of radial arrays of triplet MTs. The pericentriolar material (PCM) which surrounds the centrioles was believed to be an amorphous mass of proteins until recently; however, high-resolution microscopy has revealed that the PCM is actually highly structured with various layers

of proteins required for MT anchorage and nucleation[167-170]. MT nucleation is carried out by the evolutionarily conserved γ-tubulin ring complex (γ-TuRC)[171]. The γ-TuRC is comprised of smaller γ-tubulin-containing subunits known as γ-tubulin small complexes (γ-TuSCs) arranged in a ring-like structure along with other γ-TuRC-interacting proteins (known as GRIPs)[171,172].

In budding yeast, the MTOC is called the spindle pole body (SPB) and does not contain centrioles. Though the last eukaryotic common ancestor is thought to have had centrioles, some species of fungi have lost them over evolutionary time and replaced them with SPBs[173]. The SPB is embedded in the yeast nuclear envelope and consists of the inner, central and outer plaques, and the half bridge (the site of SPB duplication)[174]. Both inner and outer plaques contain the γ-TuSC which, in yeast, is comprised of two γ-tubulin molecules (Tub4) and two GRIPs (Spc97 and Spc98)[174], and is capable of assembling into γ-TuRCs to initiate MT nucleation[175,176]. The outer plaque nucleates astral (cytoplasmic) MTs and the inner plaque nucleates both interpolar MTs and kinetochore MTs.

1.2.4 Kinetochores and chromosomes

Kinetochores are large multiprotein-DNA structures which link the centromeres of sister chromatids to the mitotic spindle during cell division. Centromeric DNA can range in size from point centromeres in yeast (125 base pairs) to large, regional centromeres of humans (five megabase pairs)[6]. The number of MT attachments to a kinetochore scales accordingly: one per budding yeast point centromere or multiple attachments for regional centromeres[6]. This makes yeast an excellent binary model for studying microtubule-kinetochore interactions. Upon correct MT attachment to the kinetochores, the sister chromatids—specifically their centromeres—experience tension that opposes the pulling force of the MTs[177,178]. During mitosis, budding yeast centromeres and the DNA surrounding them form intramolecular loops held together by the cohesin complex[179]. These loops (along with their associated proteins) behave like springs which contribute to the inward tension of sister chromatids[178].

In the canonical description of the cell cycle, spindle MTs only have access to the chromosomes and kinetochores upon nuclear envelope breakdown. However, yeast undergoes closed mitosis. Its nuclear envelope does not break down during mitosis and as the SPBs are embedded in the nuclear envelope, the nuclear MTs have continual access to the nuclear

material. Therefore, yeast kinetochores are more or less continually attached to kinetochore MTs, except during DNA replication of the centromere[180,181].

1.3 MTOC duplication

One of the first steps of spindle assembly is duplication of the MTOC. This provides two poles between which to build the spindle. In metazoan cells, centrosomes duplicate in a semi-conservative fashion. After a round of cell division has been completed, centrioles exist in the tight orthogonal arrangement canonically seen within the centrosome. Shortly afterwards, in G1, the centrioles drift apart from each other and are tethered by a loose fibrous connection in a process called centriole disengagement (for a review, see Mardin, 2012[182]). This process renders the centrioles "duplication-competent" and is crucial to ensure that centrosomes are duplicated only once[183]. Next, during S-phase, each centriole stems a procentriole—the centriole-precursor—orthogonally from its base. The two procentrioles elongate throughout G2-phase but do not reach full maturity (indicated by development of appendages) until G2-phase of the *following* cell cycle. The fibrous connection between the pairs of duplicated centrioles is severed. Prior to mitosis, each mother centriole accumulates more PCM in preparation for increased MT nucleation during spindle assembly.

Yeast spindle pole bodies duplicate conservatively (although there is some exchange of newly-made proteins with each pole) and first involves the extension of a structure known as the half-bridge in early G1-phase. The half bridge is a specialized section of nuclear envelope which lies directly adjacent to the SPB. On the cytoplasmic side of the half bridge is a thin layer composed of many copies of the long, flexible protein, Sfi1, arranged parallelly; this serves as a scaffold for other half bridge proteins[184,185]. The first step of SPB duplication involves the lengthening of this Sfi1 scaffold through the recruitment and incorporation of a second group of Sfi1 molecules, arranged anti-parallelly to the first[184,185]. Next, a subset of SPB proteins are recruited to the distal end of the second Sfi1 molecule and form the satellite, a small SPB-precursor[186]. As more SPB proteins are recruited, the satellite develops into a duplication plaque, a structure that resembles the cytoplasmic side of a mature SPB. At this point, the plaque is inserted into the nuclear envelope through a mechanism that is still under investigation but

involves nuclear pore complexes (for a review, see Jaspersen and Ghosh, 2012[187]). Once embedded, the nuclear components of the SPB are assembled. Early in S-phase, the SPBs separate after a "half bridge cleavage"; however, to date, it is unknown if protease cleavage is required to split the half bridge. Instead, recent studies suggest that half-bridge splitting and SPB separation is regulated by phosphorylation[188,189], which is consistent with the failure of several CDK-cyclin mutants to separate poles[190-192].

1.4 Spindle assembly

1.4.1 Initial pole separation

After MTOCs are duplicated, the cell must separate them to assemble the mitotic spindle. In metazoans, as cells exit G2-phase and begin prophase, their interphase MT network is rapidly disassembled and duplicated centrosomes are separated by kinesin-5 (Eg5) and dynein[193]. Eg5 cross-links and slides antiparallel interpolar MTs past one another, thereby generating an outward force, pushing the duplicated centrosomes apart. Dynein, on the other hand, is anchored in the nuclear envelope and slides astral MTs along the nucleus providing an outward pulling force[193]. In budding yeast, dynein is strictly cytosolic with no nuclear localization. Instead, SPBs are initially separated with kinesin-5s.

Currently, it is proposed that immediately after SPB duplication, when the poles are sitting side-by-side, single Cin8 motors collect near the SPB through their (-)end directed motility[88]. This clustered accumulation promotes a switch to (+)end directed motility and Cin8 motors then cross-link and slide antiparallel MTs emanating from the side-by-side SPBs thus leading to initial pole separation[88]. The discrepancy in this model is that a Cin8 motor mutant, Cin8-R196K, which has severely reduced (+)end motility, was still capable of initial SPB separation and spindle assembly[68,194]. It is not known if Cin8-R196K mutants have reduced (-)end motility as well; however, this implies that at least (+)end motility is not required for SPB separation. Further research is required on the motility of the Cin8-R196K mutant to determine the Cin8 requirements for initial SPB separation.

1.4.2 Metaphase spindle assembly

After pole separation and the establishment of bipolarity, the spindle must align all chromosomes at the plane of cell division. In animal cells, the nuclear envelope breaks down in prophase, allowing MTs access to the chromatids during prometaphase. MTs are nucleated from three separate locations—the centrosome, the chromatin, and from other MTs—all of which contribute to successful alignment and segregation of sister chromatids (for a review, see Prosser and Pelletier, 2017[195]). These three different MT nucleation locations show remarkable synergy and provide the spindle with the flexibility to quickly respond to various perturbations[196,197].

In most animal cells, the centrosome is the major site of MT nucleation. MTs nucleated from here probe the cellular space for kinetochores (KTs) in a process called "search and capture" (originally proposed by Kirschner and Mitchison in 1986[198], and recently reviewed in Heald and Khodjakov, 2015[199]). The inherent dynamic instability of MTs allows them to repeatedly grow and shrink in variable trajectories to "search" for KTs; once "captured" by a KT, the (+)end of the MT is stabilized. However, due to the stochastic nature of this process, if cells exclusively used the "search and capture" mechanism in an unbiased manner, chromosome attachment would take considerably more time than the length of mitosis[200]. Thus, MT nucleation from chromatin increases the density of MTs around the KT and increases the probability of a successful chromosome attachment. This contributes to the timely success of the "search and capture" process.

Chromatin-mediated nucleation is promoted through several different mechanisms. The most prominent of the mechanisms is through the RAN-GTP gradient. RAN is a small GTPase belonging to the RAS super-family and, like all GTPases, is active when bound to GTP and inactive when bound to GDP. The opposing activities of RAN's guanine nucleotide exchange factor (bound to chromatin) and GTPase-activating protein (in the cytoplasm) establishes a gradient of activated RAN-GTP centered around the chromatin. RAN-GTP indirectly simulates the release of many different spindle assembly factors (SAFs) (for a review, see Clarke and Zhang, 2008[201]). These SAFs include many different proteins that contribute to the increased nucleation and polymerization of MTs in the immediate vicinity of the chromatin.

In metazoans, MT nucleation can occur specifically at the KT[202-204]. Some of the SAFs released by RAN-GTP are those which specifically increase nucleation or polymerization near the KT. Interestingly, KT-derived MTs exist with their (+)ends oriented at the kinetochore and their (-)ends distal towards the cytoplasm; thus new tubulin subunits are incorporated at the kinetochore and MT growth pushes the (-)end further away from the chromosome[203,204]. This ensures that KT-derived MTs have the same polarity as centrosomal MTs and can be readily incorporated into the spindle[203]. How a KT can both nucleate a MT and bind its (+)end remains unclear. However, it is proposed that kinetochores do not necessarily nucleate MTs, but rather capture the (+)ends of short MTs nucleated in their vicinity[203]. When centrosomal MTs come into contact with KT-derived MTs during "search and capture", the KT-derived MTs are transported (via dynein) along the centrosomal MT until they are incorporated into the spindle bundle and often are transported all the way to the centrosome[203,204]. This increases the probability of a successful chromosome attachment during "search and capture".

MTs can also be nucleated off the lattice of pre-existing MTs. This is mediated through the Augmin complex. The Augmin complex localizes to the spindle in late prometaphase, after centrosomal-MTs are established[205,206]. At the MT lattice, Augmin interacts with the γ-TuRC adaptor protein, NEDD1; NEDD1 then recruits the γ-TuRC. Newly-nucleated MTs branch off pre-existing MTs at shallow angles to ensure that all neighbouring MTs have the same polarity[207,208]. Eventually, the (-)ends of MT-nucleated MTs are transported towards the centrosome by dynein to generate more parallel bundles[209]. Augmin-mediated MT nucleation increases the density of MTs in the mitotic spindle, contributing to its robustness[210].

Budding yeast have less complicated means of metaphase spindle assembly and nucleate the vast majority of their MTs at the SPB using the "search and capture" mechanism. Interestingly, like metazoans, yeast kinetochores are also capable of nucleating MTs[149]. In this case, however, the (-)ends are bound to the kinetochore and the (+)ends extend distally from the chromosomes[149]; this is the reverse polarity to what is seen in animal cells[203,204]. As a result, yeast KT-derived MTs are short-lived and are not incorporated into the spindle[149]. Instead, they exist to facilitate the capture of kinetochores by SPB-derived MTs[211]. Additionally, yeast KT-derived MTs are not nucleated by the γ-TuRC; instead, they are generated by Stu2[149].

Once a KT-derived MT makes lateral contact with a SPB-derived MT, the KT-derived MT is cross-linked and pulled along the length of the SPB-derived MT (in an antiparallel orientation) until the kinetochore makes contact with and is loaded onto the lattice of the SPB-derived MT[212]. Once the kinetochore is loaded, the KT-derived MT is readily disassembled and new MT growth from the loaded kinetochore is suppressed[149]. Regardless of whether a kinetochore is captured with or without the help of a KT-derived MT, it almost certainly makes initial contact with a SPB-derived MT through a "lateral attachment" (i.e. the kinetochore is bound to the lattice of the SPB-derived MT, also known as a "side-on attachment") as opposed to an "end-on attachment" (i.e. the kinetochore is bound to the tip of the MT's (+)end)[38]. This is because the MT lattice provides a much larger surface area for contact than just the tip of the MT (+)end[212]. End-on and lateral attachments are not equivalent. End-on attachments are more stable and separate chromatids faster than lateral attachments[38,39,213,214]. Additionally, end-on attachments require the Dam1 complex for poleward pulling, while lateral attachments require Kar3[38,39]. Thus, after initial lateral attachment of a kinetochore to a SPB-derived MT, the kinetochore is transported poleward by Kar3[38,39]. Meanwhile, the SPB-derived MT will often shrink back to the laterally-attached kinetochore but will not surpass it[38]. Instead, the SPB-derived MT experiences a rescue once it reaches the kinetochore[38,150]. This controlled shrinkage is mediated by kinetochore-bound Stu2[38,150]. Stu2 is also transported towards the (+)end of the SPB-derived MT in a Kip3-dependent manner to promote rescue ahead of the kinetochore[150]. Eventually, these SPB-derived MT dynamics lead to a stable end-on attachment for the kinetochore[38,39].

Interestingly, yeast kinetochore-MT attachments experience what is called "tension selectivity" *in vitro*. This means that as force (and thus, tension) increases, the kinetochore attachment becomes more stable (up to a certain point)[215]. Stu2 plays an essential role in this tension selectivity, though the details are unclear[151].

Once one kinetochore is stably attached to a MT, its sister-kinetochore attaches in much the same way. When both sisters-kinetochores are attached to MTs from different poles, it is called an amphitelic attachment. This is synonymous with biorientation and leads to anaphase onset. Other types of attachments, like monotelic (when only one sister-kinetochore is attached to a SPB-derived MT) or syntelic (when both sister-kinetochores are attached to the same pole)

trigger a cell cycle arrest until amphitelic attachment is achieved. Prior to anaphase, there exists a highly conserved checkpoint—called the spindle assembly checkpoint—to ensure the proper amphitelic attachment of sister-kinetochores.

1.4.3 The spindle assembly checkpoint

The spindle assembly checkpoint (SAC) is a highly conserved surveillance mechanism which monitors the kinetochores for proper bioriented spindle attachment during the anaphase-to-metaphase transition and delays the onset of anaphase until this requirement is met. In metazoans, this checkpoint is essential; however, in yeast, it is only essential when the cell experiences extraneous kinetochore-MT attachment perturbations. The vast majority of the SAC was discovered and elucidated in budding yeast[216,217]. The checkpoint is centered around several key players: the mitotic checkpoint complex (MCC), the anaphase promoting complex/cyclosome (APC/C—not to be confused with APC) and Aurora B kinase.

The MCC is made up of four components: Mad2, BubR1, Bub3 and Cdc20[218,219]. The main function of the MCC is to sequester Cdc20 until all chromosomes are properly attached. Cdc20 is the coactivator of the APC/C, the E3 ubiquitin ligase that is responsible for triggering the onset of anaphase. Without Cdc20, APC/C is kept inactive and unable to promote anaphase. APC/C, bound to Cdc20, ubiquitinates and causes the degradation of two targets important for the progression into mitosis: (1) securin, and (2) B-type cyclins (Clb1-5 in yeast). Securin inhibits separase, the protease responsible for cleaving the cohesin complex that binds sister chromatids together. Degradation of B-type cyclins prevents further Cdk1-Clb activity, allowing for the dephosphorylation of Cdk1 mitotic targets in preparation for anaphase.

The details of how an unattached kinetochore triggers formation of the MCC remain unclear but involve the step-wise recruitment of SAC proteins to the unattached kinetochore. Currently, it is thought that SAC kinase Bub1 is the most upstream protein governing this recruitment (for a review, see Lara-Gonzalez *et al*., 2012[220]). Bub1 then recruits Mad1 which subsequently recruits the other MCC components[221,222].

Similarly, the details of how a subsequently attached kinetochore ceases MCC formation are not fully clear. In yeast, which have point centromeres, it is thought that MT binding to the kinetochore prevents Mad1 binding, either by completely displacing it or by causing a

conformational change in kinetochore proteins that dislodge it. Recent research suggests that MT attachment prevents MCC formation by inhibiting recruitment of Bub1[221]. In metazoans, dynein is recruited to the kinetochore and, upon MT attachment, transports SAC components (including the MCC) along the attached MT, towards the centrosome in a process called "stripping"[223] (for a review, see Kops and Shah, 2012[224]).

Upon activation of the checkpoint, the improperly-attached sister-kinetochores must be corrected. This process is mediated through the activity of Aurora B kinase, or Ipl1 in yeast[225,226] (for a review, see Lampson and Cheeseman, 2011[227]). Aurora B localizes to the centromere and is activated. Afterward, it is released and diffuses away from the centromere; this establishes a gradient of Aurora B activity around the centromere. When sister-kinetochores experience improper attachments (e.g. monotelic or syntelic attachments), the kinetochores remain in the zone of Aurora B activity and are phosphorylated, leading to a reduction in MT binding. Loss of attachment then triggers the MCC-dependent mechanism of the SAC. When sister-kinetochores experience amphitelic attachments and become bioriented, two MTs pull the centromeres in opposite directions, putting them under tension. This draws the sister-kinetochores away from each other and out of the zone of Aurora B activity[228]. Unable to be phosphorylated, kinetochores continue to be stably attached to MTs and contribute to SAC silencing.

The combination of these two processes (MCC-dependent halting of the cell cycle and Aurora B-dependent detachment of kinetochores) means that the SAC is sensitive to both MT occupancy (via the MCC) and centromere tension (via Aurora B). Despite numerous advances in understanding the SAC since its discovery, the question as to how exactly a MT attachment silences the SAC is unclear. Whether it is satisfied through MT occupancy or through the subsequently generated tension is still debated with evidence supporting both cases (for a review, see Manic *et al*., 2017[229]).

1.5 Asymmetric division of cellular materials

Symmetric cell division occurs when a cell divides its components equally into two identical daughter cells. Cells can also undergo asymmetric cell division where two resulting cells have different cellular fates due to structural and/or biochemical differences. This can occur

extrinsically, where initially identical cells rely on signaling and cues from the environment to become different, or intrinsically, where cells rely on their initial internal differences. Asymmetric cell division is especially important in multicellular organisms where it creates cell-type diversity. Intrinsic asymmetric division always requires segregation of some type of cellular component prior to cell division and then positioning of the spindle such that the proper daughter cells inherit the right components. Frequently, asymmetric cell division is thought of in reference to metazoan development (e.g. in stem cells) where these polarized components are called cell fate determinants and are usually proteins (e.g. the PAR proteins in *C. elegans*). However, in the last ten to fifteen years, two notions have become more prominent. The first is that across a number of different species—including bacteria—many different cellular materials are polarized resulting in their asymmetrical segregation (for reviews, see Lerit *et al*., 2013, Tajbakhsh and Gonzalez, 2009, and Holt and Bullock, 2009[230-232]). This includes chromatin[233-243], mRNA[244-246], and organelles (such as mitochondria[247-249], endoplasmic reticulum[250,251], centrosomes[129,252-257] and SPBs[258]). Often this changes the fate of the resulting daughter cells, indicating that, despite not being proteins, these components are still cell fate determinants.

The second is that most cell divisions—even those previously considered to be symmetric—are, in fact, inherently asymmetric. This is because the inheritance of centrosomes (or SPBs) is asymmetric; after centrosome duplication, one centrosome has older components than the other. Thus, one cell will inherit an older centrosome while the other cell will inherit a younger one. This alters the fate of symmetrically dividing cultured cells: the cell which inherits the pre-existing (older) centrosome is the first to build its primary cilium[259]. Strikingly, even bacterial cells (which undergo morphologically symmetrical cell division) experience "pole" asymmetry leading to a difference in cell fates[260]. The cell which inherits the old end (or "pole" —in this case pole refers to the end area of the cell and not to an organelle) has a diminished growth rate, decreased offspring production and an increased incidence of death[260]. This indicates that asymmetric division of cellular material is an ancient phenomenon.

Budding yeast are an ideal model for asymmetric cell division. Not only do they experience a clear physical asymmetry, but they have also been shown to asymmetrically segregate all cellular material listed above[236,247,248,250,251]. In most cases, this contributes to

increased aging in the mother cell and/or increased fitness of the daughter cell[247,250,251,261,262]. One exception is yeast asymmetric pole inheritance, for which 95% of the time the pre-existing (old) pole is inherited by the daughter cell[258]. The evolutionary advantage for this is not yet clear but may prove to be important during meiosis or in sub-optimal growth conditions[263-265].

To asymmetrically segregate cellular material, the cell must first establish its polarity. In budding yeast, the first step in polarity establishment is choosing the presumptive bud site[266,267]. Cortical landmark proteins leftover from the previous cell cycle are located at the former site of cell division (i.e. the bud scar) where they guide the choice of the next bud site by recruiting a set of bud-site selection proteins[268-279]. This leads to the recruitment and activation of the conserved Rho-like GTPase Cdc42. Cdc42 orchestrates the polarization of the actin cytoskeleton, septin organization, cell wall biogenesis and exocytosis—all of which contribute to bud emergence and growth[280-282].

Upon polarization of the actin cytoskeleton, the cell is now primed to carry out asymmetric segregation of cellular material and proper spindle placement. This ensures each progeny cell inherits the correct components. Spindle placement depends on interactions between the MT cytoskeleton and polarized actin filaments such that the spindle can be moved towards the bud neck.

1.6 Spindle placement in budding yeast

In existing literature, spindle positioning, alignment and orientation are often used interchangeably. In this work, spindle positioning will refer to the movement of the spindle towards the plane of cell division, spindle alignment will refer to the angle between the polarity axis and the spindle, and spindle orientation will refer to the identity of the pole inherited by the mother and daughter cell (Figure 1.1). Spindle placement will refer to the overall process involving these three components. Spindle placement is considered correct once a spindle is positioned close to the bud neck, aligned perpendicular to the plane of cell division, and has the proper pole oriented proximal to the daughter cell.

In budding yeast, there are two main pathways governing spindle positioning: the Kar9 pathway and the dynein pathway which act earlier or later in the cell cycle, respectively. These

pathways are partially redundant in that they can compensate for each other, but both carry out unique functions as indicated by their individual genetic interaction profiles. Earlier-acting Kar9 is responsible for positioning the spindle close to the bud neck and is solely responsible for correct pole inheritance, while upon anaphase entry, later-acting dynein accurately separates the poles to their respective compartments. These two pathways are discussed further in the forthcoming sections.

Figure 1.1 | The process of spindle placement. (A) Spindle positioning refers to the movement of the nucleus and spindle towards the bud neck. (B) Spindle orientation refers to the identity of the pole proximal to the bud neck. When the old pole is proximal to the bud neck, the spindle is considered properly oriented and this leads to correct pole inheritance. When the new pole is proximal to the bud neck, the spindle is considered misoriented and this leads to pole misinheritance. (C) Spindle alignment refers to the angle between the polarity axis (mother-bud axis) and the spindle (visualized as a purple arc).

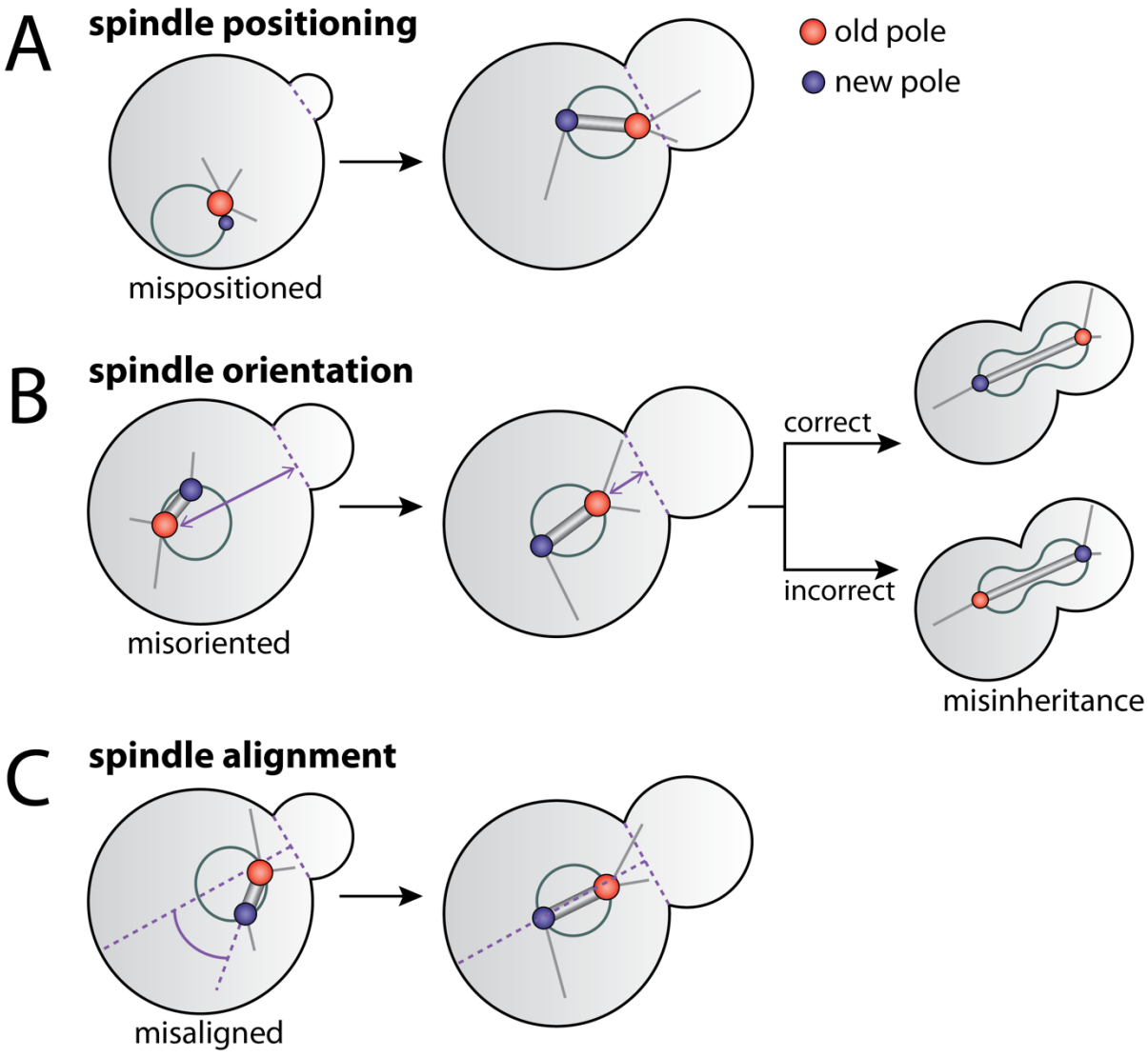

1.6.1 The Kar9 pathway

The earlier-acting pathway is dependent on actin filaments and is centered around Kar9. Kar9 physically interacts with the EB1 (+)end tracker homolog, Bim1[117-119], and is dependent on this interaction for its SPB localization and subsequent loading onto astral MTs[283]. Once loaded, the Kar9-Bim1 complexes track the (+)end of the astral MTs through Bim1's +TIP activity. Kinesin motor protein Kip2 also transports Kar9 to the astral MT (+)ends[21], but unlike Bim1, it is not required for Kar9 localization to the SPB or MT (+)ends[162,283]. At the astral MT (+)ends, Kar9 (in complex with Bim1) interacts with and becomes cargo for the myosin V motor protein, Myo2[283-286].

Myo2 walks along actin filaments towards the polarisome, located at the bud tip[284]. This results in the bud-directed movement of Kar9-Bim1, the attached astral MT, and the SPB from which the astral MT emanates[283-286]. While Bim1 localizes to both SPBs and their associated cytoplasmic and nuclear MTs[137,283,287], Kar9 localizes specifically to the pre-existing pole[21,283,288]. This asymmetric targeting is carried out by several different post-translational modifications (PTMs): Cdk1 phosphorylation, Siz1/Siz2 sumoylation and Dbf2/Dbf20 phosphorylation all contribute.

a. Cdk1 phosphorylation

Cdk1 (cyclin-dependent kinase 1) phosphorylates Kar9 on at least two sites—S197 and S496—which contributes to Kar9 asymmetry[21,162,283,289,290]. However, both the cyclin responsible for this phosphorylation and how this phosphorylation translates to Kar9 asymmetry are still debated. There are two favored models.

One model proposes that both sites are phosphorylated by Cdk1-Clb4 at the distal pole; this inhibits the interaction between Kar9 and Bim1 and thus decreases distal-pole localization[283]. In this model, Clb5 is proposed to indirectly affect Kar9 asymmetry through the action of the SAC and the mitotic exit network (MEN) in a pathway parallel to that involving Clb4 (discussed below)[291]. It is thought that Clb5 activity is required to satisfy the SAC and relieve a SAC-dependent inhibition of metaphase MEN activity[291]. However, the details of this process—including how Clb5 contributes to SAC satisfaction and how the SAC inhibits metaphase MEN activity—are still unknown[291].

The second model suggests that the two Kar9 phospho-sites are phosphorylated by different Cdk1-cyclin complexes[290]. In contrast to previous reports, phosphorylation at either site (S197 or S496) did not affect Kar9 interaction with Bim1[290] and therefore, could not be used to explain Kar9's phospho-dependent asymmetry as suggested in the first model. Instead, it is proposed that Cdk1-Clb5, facilitated by Bik1, phosphorylates Kar9 at S496 which enables Kar9 to recognize an intrinsic SPB asymmetry[21,162,290]. Furthermore, instead of directly impacting Kar9 asymmetry, Cdk1-Clb4 is thought to antagonize the interaction of astral MTs with the bud cortex[289,290]. Another related observation indicates that the phospho-status of S197 affects Kar9's interaction with Stu2, suggesting a role for Stu2 in the establishment of Kar9 asymmetry[290].

Neither model excludes the possibility that there are additional, related Cdk1 sites on Kar9 (or other related proteins); in fact, several observations suggest that this is the case[162,283,290,292]. Moreover, there are four other Cdk1 consensus sites in the Kar9 sequence[289]. Though the identities of all the Cdk1-Clb4 targeted residues may be unknown, it is agreed that Cdk1-Clb4 does phosphorylate Kar9[162,283,289,290].

Taken together, it is clear that Kar9 regulation by Cdk1 phosphorylation is very complex and requires further study in order to fully understand and reconcile the differing observations. Many aspects of each model need not be mutually exclusive and resolving the contrasting data has been attempted[290]. Further clarification of the specific roles of the Cdk1-Clbs and other MAPs (e.g. Bik1, Stu2), and the identification of other factors involved in Kar9 behaviour, will greatly aid in our understanding of Kar9-dependent spindle placement.

b. Siz1/Siz2 sumoylation

Kar9 is sumoylated on at least four residues *in vivo* by yeast SUMO E3 ligases, Siz1/Siz2[293,294]. Inhibition of sumoylation at these sites caused an increase in symmetric Kar9 localization in metaphase cells and perturbed spindle alignment[293,294]. Whether this sumoylation is independent of Cdk1 phosphorylation is controversial[293,294], and how sumoylation promotes Kar9 localization to the old SPB is still unknown. Although, more recently, prevention of sumoylation at these residues severely reduced Kar9's ability to bind to Bim1 *in vitro*[295]. This is surprising since Bim1 is required for Kar9's SPB localization[283] and *in vivo* Kar9 sumoylation mutants were still capable of SPB localization, albeit symmetrically[293,294]. Further studies are

required to understand the relationship between sumoylation, Cdk1 phosphorylation, and resulting Kar9 asymmetry.

c. Dbf2/Dbf20 phosphorylation

The yeast mitotic exit network (MEN) is reminiscent of the Hippo pathway, important for cell proliferation, differentiation and apoptosis in animals. While the ultimate function of the MEN is the dephosphorylation and inactivation of mitotic cell cycle components (e.g. Cdk1) through the action of Cdc14 phosphatase, as of yet, no instances of Cdc14 regulation by the Hippo pathway have been reported in metazoans (for a review, see Hergovich, 2016[296]). In yeast, the MEN involves a signaling cascade which begins with the GTPase Tem1 and requires SPB component Nud1 as a scaffolding platform[297-301]. Tem1 activates kinase Cdc15, which in turn phosphorylates NDR/LATS-related kinases Dbf2 and Dbf20. Dbf2/Dbf20 then promote the release of Cdc14 from its sequestering partner. While the MEN pathway is predominantly activated in late mitosis, recent work indicates its activity in the Kar9 spindle placement pathway as early as metaphase[291]. MEN kinases Dbf2/Dbf20 phosphorylate Kar9 at three consensus sites; phosphoinhibition at these sites perturbed the asymmetric localization of Kar9 to the SPBs and disturbed spindle alignment[291]. As mentioned previously, this MEN-dependent regulation of Kar9 asymmetry is promoted by Clb5-dependent inactivation of the SAC[136]. Interestingly, while Cdk1 phosphorylation and Siz1/Siz2 sumoylation do not affect SPB inheritance, MEN mutants do, suggesting that this pathway plays a role in proper spindle orientation[291].

d. Spindle orientation: how pole age is differentiated

The aforementioned PTMs affect Kar9 asymmetric localization to the pre-existing pole, however, they still require upstream pole differentiation to 'recognize' pole identity. What distinguishes the poles, and how regulatory proteins interpret this difference, has only very recently been clarified. There are two general hypotheses: that pole differentiation is driven by structural differences, or by PTM differences. Recent high-resolution analysis of the pole outer plaques concluded that there are no significant structural differences, supporting the idea that the poles are differentiated through modifications[288].

Recent work has identified a set of enzymes which make up the spindle pole body inheritance network (SPIN): kinases Swe1 and Kin3, and the acetyltransferase complex NuA4[263].

This network is responsible for differentiating the poles as pre-existing or newly-formed. Swe1, the budding yeast homolog of Wee1, localizes to the SPB in G1-phase, prior to pole duplication. Here, Swe1 phosphorylates Nud1 at two residues, marking it as the pre-existing pole[263]. Swe1 is then relocalized to the bud neck where it is phosphorylated and rapidly degraded[263,302,303]. This ensures that only the pre-existing SPB inherited from the previous cell cycle is marked, and the newly-formed SPB is not. Interestingly, Swe1 phosphorylation is only important for marking SPBs prior to their first duplication to establish them as pre-existing and is not required to re-establish the markings during the following cell cycle. This indicates that Swe1 modification of the pre-existing pole is maintained from one generation to the next. This maintenance is carried out by kinase Kin3 and the acetyltransferase complex NuA4 which 'read' the markings (e.g. Swe1 phosphorylation) and preserve them or relay them through other modifications.

How SPIN modifications lead to proper Kar9 asymmetry and pole inheritance is not yet fully understood but is proposed to occur through the activity of the Bfa1-Bub2 complex[263]. Bfa1-Bub2 bridges the spindle orientation checkpoint (SPOC) and the MEN. Bfa1-Bub2 physically interacts with Nud1 and localizes asymmetrically to the pre-existing SPB where it prevents activation of the MEN by inhibiting Tem1[258,263,297,299,304,305]. Bfa1-Bub2 is, itself, inhibited by polo-like kinase, Cdc5, through the SPOC. Two polarized proteins, Kin4 and Lte1, which localize to the mother compartment or the bud cortex, respectively, antagonistically regulate Cdc5's inhibition of Bfa1-Bub2. When the spindle is improperly aligned and pole-localized Bfa1-Bub2 is in the mother compartment, Kin4 is localized to both poles and prevents Cdc5 inhibition of Bfa1-Bub2 thereby preventing mitotic exit. Alternatively, when pole-localized Bfa1-Bub2 is in the bud compartment, Lte1 inhibits Kin4 activity[306] which permits Cdc5 inhibition of Bfa1-Bub2, thereby allowing Tem1 to initiate mitotic exit.

The asymmetric localization of both Bfa1-Bub2 and Tem1 to the pre-existing pole is important for proper asymmetric Kar9 establishment[307]. Furthermore, several other MEN components are active during spindle orientation and alignment, when Kar9 asymmetry is being established[291,307]. The details of how this works are not yet clear, but Bfa1-Bub2 pole localization is dependent in part on SPIN modification of Nud1[263].

Though further research is required to articulate the details of pole differentiation and how that translates into proper pole inheritance, huge strides have been made in recent years, providing a solid foundation from which to proceed.

1.6.2 The dynein pathway

Dynein participates later in the spindle placement process and, unlike the Kar9 pathway, it does not require filamentous actin[308]. In yeast, dynein is first recruited to the astral MT (+)ends, then it is offloaded and anchored into the bud cortex. Here, it becomes activated and begins to walk along the astral MT to the (-)end, however, since it is anchored, the astral MT slides along the cortex of the bud, pulling the attached SPB towards the bud. In higher eukaryotes, dynein also accumulates on MT (+)ends[309-313] and at the cortex[314,315], and is involved in spindle placement (see reviews by Markus *et al*., 2012 or Kotak and Gönczy, 2013[316,317]) which exhibits its conservation of function.

a. Recruitment to astral MT (+)ends in yeast

The hypothesis of how a (-)end directed motor could end up enriched on MT (+)ends has been slowly refined over the past two decades. The discovery of four MAPs which are necessary for this robust (+)end recruitment—Bik1, Kip2, Pac1, and Ndl1—greatly aided in the development of the current hypothesis. Work done by several groups has helped piece together the puzzle[22,161,318-320]; however, it was not until 2011 that the details of how Bik1, Kip2, Pac1 and Ndl1 influence dynein localization were clarified further.

Recall that Bik1 is transported by Kip2 to the astral MT (+)ends where it is deposited and prevents depolymerization[22]. Dynein is also transported by Kip2 (through its association with Bik1) to MT (+)ends[22], however, this does not seem to be the dominant mechanism of dynein recruitment[320]. Instead, the current model suggests that Pac1 and dynein must form a complex in the cytoplasm prior to astral MT localization[320]. Then, the dynein-Pac1 complex is recruited to (+)ends by Bik1 and partially by Ndl1[161,319,320]. Interestingly, though Bik1 is found both at MT (+)ends and along the length of MTs (when translocating with Kip2)[22,163], dynein-Pac1 complexes specifically bind to Bik1 located at the (+)end[320]. How dynein-Pac1 complexes can differentiate between the pools of (+)end-bound Bik1 and length-bound Bik1 is unclear. As Kip2-independent mechanisms of Bik1 (+)end localization exist[22,320], it is possible that the (+)end pool of Bik1 is

dissociated from Kip2, or is in complex with another protein. In other organisms, homologous Bik1 (+)end recruitment is dependent on EB1[12,102,321,322]; whether this occurs in budding yeast is still controversial[22,110,320,323]. Clearly, the mechanism of how dynein is recruited to MT (+)ends still needs further investigation and refinement, specifically how dynein-Pac1 recognizes tip-bound Bik1.

b. Regulation of dynein activation

Once dynein is recruited to MT (+)ends, it is offloaded and anchored in the bud cortex, where it is then activated. Regulation of dynein activity is especially important because, though its (+)end localization increases upon mitosis onset, dynein is often found on astral MT (+)ends regardless of the cell cycle phase[161]. Additionally, although dynein offloading predominantly occurs at the bud cortex[324], dynein foci are frequently observed all along the mother cortex[318,325]. As a result, dynein activity must be regulated in a cell cycle-dependent and spatially-dependent manner. Indeed, inhibition of dynein activity (indicated by lack of MT sliding along the cortex) is observed throughout metaphase until onset of anaphase[95,326-328].

The details of how this regulation works are not completely clear; however, several regulators of dynein have been identified. Dynactin, a multimeric complex, not only regulates dynein's processivity, but is required for nearly all dynein functions both in yeast and other organisms[91,329-331]. In higher eukaryotes, dynactin regulates dynein during organelle and vesicular transport[90,91]. It does so by stabilizing the tethering of dynein to its cargo (for a review, see Schroer, 2004[91]). In yeast, dynactin regulates dynein by offloading it to the cell cortex—a step necessary for dynein function[318,324,332]. Offloading of dynein is analogous to cargo tethering in higher eukaryotes which exhibits dynactin's conserved function. Once offloaded at the cortex, dynein is anchored by Num1 (i.e. its 'cargo')[324,333]. Both dynactin and Num1 regulate dynein by satisfying the prerequisites necessary for dynein function (offloading and anchoring).

She1 regulates dynein by preventing recruitment of dynactin until anaphase onset[320,334]. Additionally, She1 selectively inhibits dynein activity in the mother cortex, allowing pulling forces to be polarized towards the bud[335]. PP1 phosphatase Glc7 and its regulatory subunit, Bud14, regulate dynein activity as well. Genetic studies indicate that Glc7-Bub14 is a positive regulator

of dynein at the cortex, but the details are not known[336]. Lastly, *in vitro* evidence suggests that in addition to dynein recruitment, Pac1 also regulates dynein motor activity after anchoring[337].

As mentioned earlier, dynein must be regulated in a cell cycle-dependent manner and a spatially-dependent manner. However, there is much left to discover as to how this regulation works. Of note, Glc7-Bud14 is regulated in both a cell cycle-dependent and a spatially-dependent manner and may provide the link. Alternatively, spatial dynein regulation may be accomplished similarly to Kar9—by asymmetric targeting of dynein to MTs emanating specifically from the pre-existing pole. In fact, asymmetric distribution of dynein has been observed *in vivo*[328], but similar to Kar9, the mechanisms which determine this asymmetry are still being determined.

c. Asymmetric localization of dynein

Prior to activation, dynein asymmetrically localizes to the proximal SPB and its associated MTs throughout metaphase[328]. This asymmetry disappears at anaphase onset during spindle elongation, when dynein becomes symmetric and pulls the poles apart[328]. It is unknown whether the proximity of the pole or its age designates dynein accumulation. Like Kar9 and dynein, astral MTs also experience an asymmetric bias in terms of MT number and state: the astral MTs emanating from the proximal/pre-existing pole are generally longer, more abundant, and less dynamic than those at the distal/newly-formed pole[283,338]. In fact, unlike Kar9, whose asymmetry is dictated by pole age, astral MT asymmetry is dictated by pole proximity to the bud, regardless of age[288]. Because of this inherent astral MT asymmetry, several MAPs appear to localize to astral MTs in a partially asymmetric manner, including Bik1, Kip2 and Bim1[328]. Dynein asymmetric localization, however, is independent of MT asymmetry[328]. It is also independent of Kar9 asymmetry, as constitutively symmetric Kar9 mutants have no effect on dynein localization[328]. However, in the absence of Kar9 completely, dynein asymmetry is essential[328].

Dynein asymmetry requires Cdk1-Clb1/Clb2, SPB component Cnm67, and morphogenesis factors Elm1, Hsl1 and Gin4[328]. Cdk1-Clb2 localizes to the outer plaque of SPBs[339] in a Cnm67-dependent manner[328]. Elm1, Hsl1 and Gin4 regulate the morphogenesis checkpoint, which involves the hyper-phosphorylation and subsequent degradation of Swe1 upon proper bud formation. It is proposed that Elm1, Hsl1 and Gin4 induce dynein asymmetry after astral MTs from one pole interact with the bud neck cortex. Consistently, dynein asymmetry is partially

dependent on MTs contacting the bud neck[328]. This asymmetry is then amplified by Cdk1 and Cnm67-dependent silencing on the opposite pole[328].

1.7 Nucleation-independent roles of MTOCs and γ-tubulin

The canonical function of MTOCs is to nucleate MTs (through the activity of γ-tubulin) and organize them into defined functional arrays. However, MTOCs—and specifically γ-tubulin complexes—have increasingly been found to participate in nucleation-independent functions, including regulation of MT (+)end dynamics, cell cycle progression, and checkpoint response (Reviewed in Cuschieri *et al*., 2007 and Oakley, 2015[340,341]).

Evidence across different species suggests that γ-tubulin complexes contribute to the regulation of (+)end MTs dynamics. As γ-tubulin complexes exist at the (-)end of MTs, it is often thought that they exert their (+)end effects through behaviour modification of MAPs. In budding yeast, Stu2 (XMAP215 homolog) forms a cooperative complex with the γ-TuRC and Spc72 by directly binding to Spc72 at the SPBs; this interaction regulates (+)end MT dynamics though the details are still unclear[156,157]. Similarly, defects in the fission yeast Spc72 homolog (Mto1) and the Spc97/GCP2 homolog (Alp4) caused abnormal MT dynamics by changing (+)end levels of the CLIP170/Bik1 homolog (Tip1)[342]. In *Drosophila*, downregulation of γ-TuRC component Dgrip75/GCP4 significantly increased the dynamics of astral MTs and altered the localization of EB1[343]. Mutations within γ-tubulin itself have also been associated with a change in (+)end dynamics. A γ-tubulin structural mutation in budding yeast (*tub4-dsyl*Δ) changed the behaviour of Kar9 on astral MT (+)ends, causing a suppression of MT dynamics; additionally, this mutation altered the distribution of Bim1 on the SPBs and astral MTs[344]. Similarly, a phosphomimetic mutation of the tyrosine (Y445) within that structural motif increased the MT elongation time and the rate of MT depolymerization[3]. Lastly, in fission yeast, mutation of a conserved γ-tubulin residue (P301) increased MT stability so that MTs displayed a very exaggerated fishhook spindle[345]. In most cases, γ-tubulin complexes exert their effects indirectly through the modulation of MAPs, possibly by controlling their recruitment and deployment onto MTs[342,344,346,347]. However, MTOCs also act as scaffolds for regulators (e.g. kinases) to modify their

substrates (e.g. Nud1's role in the MEN); thus, it is possible that γ-tubulin complexes provide a "meeting ground" for MAPs and their regulators.

Several key processes are required for the successful completion of the cell cycle. DNA replication, centrosome duplication, spindle assembly, spindle placement, chromosome alignment, chromosome segregation and cytokinesis must successively occur in a coordinated, timely fashion. MTOCs, γ-TuRC and/or γ-tubulin have been implicated in all these different processes.

The G1/S-phase transition closely follows a key moment in the cell cycle—the moment when the cell irreversibly commits to cell division. This is known as START in yeast and the restriction point in mammalian cells. At this point, the transcription of hundreds of G1/S-phase genes is upregulated, leading to the start of DNA synthesis. This transcription is mediated by transcription factors SBF and MBF in yeast, and E2F in mammals. Additionally, the APC/C (still active from the previous anaphase) is normally inactivated at the G1/S boundary, permitting cyclin B activity. γ-Tubulin has been implicated in both these G1/S processes. In mammalian cells, γ-tubulin enters the nucleus where it interacts with and negatively regulates the activity of E2F transcription factors[348,349]. This nuclear localization is dependent on the phosphorylation of γ-tubulin residue S385 by SADB kinase[350]. In the filamentous fungi, *Aspergillus nidulans*, a nucleation-competent γ-tubulin mutant prevented the dissociation of the APC/C activator, Cdh1 from the SPBs[351]. This resulted in a failure to inactivate the APC/C at the G1/S boundary, leading to a cell cycle arrest[352].

Concurrent to DNA replication, another essential S-phase process is centrosome/SPB duplication. In mammalian cells, phosphorylation of γ-tubulin residue S131 by SADB kinase governs centrosome duplication possibly by increasing local MT polymerization to build the daughter centriole during duplication[353]. Subsequently, BRCA1-dependent ubiquitination of γ-tubulin is thought to mark centrosomes post-duplication to prevent re-duplication and amplification[354-356]. While BRCA1 is heavily involved in DNA damage, BRCA1 ubiquitination of γ-tubulin is not linked to the DNA damage response[355,356]. In fact, while γ-tubulin ubiquitination is important in many cell lines, BRCA1 was only required as an E3 ubiquitin ligase in mammary cell lines[355].

After centrosome/SPB duplication comes spindle assembly and placement. In budding yeast, phosphorylation at residue S360 was found to be crucial for proper spindle assembly[1,2]. A phosphomimetic mutation at S360 resulted in an under-built spindle lacking a core MT bundle, while phosphoinhibitory mutants had over-built spindles with additional overlapping MTs[2]. Similarly, altering the dosage of γ-TuSC components perturbs the ratio of kinetochore to interpolar MTs in budding yeast[357]. Furthermore, the role of the γ-TuRC and γ-tubulin in spindle assembly is emphasized by its involvement in the spindle assembly checkpoint. There are many instances where disturbances in γ-TuRC components led to a failure of the SAC when spindle assembly was severely disrupted and premature mitotic exit[358-362]. The γ-TuRC is also directly linked to the SAC. Several SAC-related proteins directly interact with γ-tubulin or other γ-TuRC components[363,364]. Lastly, in filamentous fungi, a γ-tubulin mutant causes mislocalization of SAC components which completely abolishes the checkpoint[365].

SPBs have a well-documented role in spindle positioning—mainly the spindle positioning checkpoint (SPOC) where several important components localize to the SPB: Bfa1-Bub2 (Tem1 inhibitor), Cdc5, and Kin4[258,366,367]. This localization is important for SPOC function. Bfa1-Bub2's pole localization is required for Tem1 inactivation[368] and occurs through direct interaction with Nud1[297]. Furthermore, in response to spindle misalignment, Kin4 and Bfa1-Bub2 are localized to both poles where Kin4 maintains Bfa1-Bub2's activity (and thus, Tem1 inactivation)[367]. Kin4 SPB localization is dependent on γ-TuRC outer plaque receptor, Spc72[369]. Apart from contributing to the SPOC, γ-TuRC components contribute to the actual process of spindle placement. Depletion of the γ-TuRC component Dgrip75/GCP4 in *Drosophila* and mammals result in perturbed spindle positioning while not affecting the nucleation capacity of cells[343]. Similarly, characterization of the structural DSYL motif in budding yeast found these residues to be important in regulating the behaviour of proteins Kar9 and Bim1 (as mentioned above), two proteins which are involved in spindle placement[344]. As a result, *tub4-dsylΔ* cells have a significantly higher incidence of mispositioned spindles[344]. Recently, my own work, described in Chapter 3, identifies a γ-tubulin phospho-mutant (Y362E) which perturbs proper spindle alignment.

Another checkpoint shown to be related to MTOCs and γ-tubulin in more recent years is the DNA damage checkpoint. A number of proteins involved in the DNA damage checkpoint

localize to the centrosome in mammalian cells, including the initial DNA damage checkpoint kinases, ATM and ATR, as well as the downstream effector kinases, Chk1 and Chk2, among others[370]. γ-Tubulin has also been shown to directly interact with several DNA damage proteins such as ATR, BRCA1, the DNA damage recombinase, Rad51, and the DNA damage checkpoint protein, C53[370-373].

Rounding off the end of the cell cycle is the mitotic exit network (MEN) and cytokinesis, both of which involve MTOCs and γ-tubulin complexes. The majority of the MEN occurs at the SPBs and requires the scaffolding protein Nud1 for its signal transduction[374-377]. A similar process is seen in fission yeast, though instead of scaffolding MEN components, the SPBs scaffold components of the septin initiation network (SIN), which facilitates proper timing of cytokinesis[378-380]. Interestingly, in *Arabidopsis*, cells depleted for γ-tubulin could progress through mitosis but completion of cytokinesis was strongly perturbed[381].

In summary, MTOCs, and specifically γ-TuRCs, affect MT (+)end dynamics, contribute to cell cycle processes and progression, and participate in various checkpoint responses. A current model exists to explain the diverse number of processes that MTOCs are involved in: they function as scaffolds which coordinate cell cycle signaling and regulation with the dynamic properties and organization of the spindle. Along with carrying out chromosome segregation, the MT cytoskeletal network also bridges distinct areas of the cell. In yeast, the spindle connects the nucleus to the actin cytoskeletal network to allow for nuclear movement and in higher eukaryotes, MTs act as highways for vesicular transport. Central to this are MTOCs, the hub of the MT cytoskeleton. This places MTOCs (and γ-TuRCs) in a prime position to act as the integration point for incoming and outgoing cellular signals.

Despite ample evidence that γ-tubulin is involved in nucleation-independent roles, the mechanisms through which this happens are still, for the most part, unclear. One of the more understood ways γ-tubulin participates in different cellular processes is through post-translational modifications, of which there are examples in both yeast and other organisms.

1.8 γ-Tubulin modifications

Post-translational modifications (PTMs) are covalent modifications of the amino acids within a protein which affect its chemical, biological and physical properties. They influence protein folding and structure, activity, localization, turnover, and interactions, and thus, are key to governing protein behaviour. There are more than 300 types of PTMs identified[382], though the most commonly observed are phosphorylation, acetylation, glycosylation, amidation, hydroxylation, methylation and ubiquitination (from most common to least)[383].

By far, most instances of PTMs described for γ-tubulin have been phosphorylation. However, the details for the majority of these observations are unclear. For example, in *Drosophila* embryos, Dwee1 kinase (Wee1/Swe1 homolog) directly interacts with the γ-TuRC and is required for γ-tubulin phosphorylation *in vivo*[384]. This is proposed to function in centrosome positioning during embryonic syncytial cortical divisions; however, it is still not clear if Dwee1 is responsible for direct or indirect phosphorylation of γ-tubulin[384]. In the amoebae *Naegleria gruberi*, γ-tubulin becomes hyperphosphorylated during the formation of basal bodies and is expected to increase the nucleating capacity of the basal body precursor[385]. Yet how hyperphosphorylation contributes to nucleation is still under investigation. In mice embryonic carcinoma cells, γ-tubulin becomes phosphorylated during neurogenesis, the purpose of which is not known[386]. In humans, numerous high-throughput analyses have identified many γ-tubulin sites which are post-translationally modified (phosphorylated, ubiquitinated or acetylated)[387-398]; however, as is often the case with high-throughput screens, the biological significance of the majority of these sites remains unknown. Four exceptions to this are the SADB-dependent phosphorylation of S131 and S385, and the BRCA1-dependent ubiquitination of K48 and K344.

In higher eukaryotes, SADB kinase is a well-known critical regulator for neural development, but it is also involved in DNA damage and centrosome duplication. γ-Tubulin is phosphorylated at residue S131 by SADB which regulates centrosome duplication[353]. It is proposed that this phosphorylation increases local MT polymerization to build the daughter centriole during duplication[353]. At residue S385, SADB phosphorylation increases the nuclear localization of γ-tubulin, thereby permitting it to interact with and regulate E2F transcription

factors[348-350]. BRCA1 is a well-known tumor suppressor involved in the DNA damage response pathway, genome maintenance, DNA replication, cell cycle control and transcription[399]. It also functions as an E3 ubiquitin ligase and targets γ-tubulin as a substrate[355]. This ubiquitination decreases MT nucleation and aster formation and is proposed to mark centrosomes after duplication to prevent re-duplication and amplification[354-356].

In budding yeast, the only γ-tubulin PTM discovered thus far is phosphorylation. Two mass spectrometry-based studies identifying γ-TuSC phosphorylation sites came up with quite different results[1,400]. One study (Keck *et al*., 2011), which used isolated whole SPBs from cells arrested at various time-points, identified eight sites: T130 and T227 from a G1 arrest, and S42, S43/T44, S360, Y362, S444 and Y445 from a metaphase arrest[1]. The other study (Lin *et al*., 2011) used cell lysates isolated from asynchronous cells which were overexpressing the γ-TuSC components and identified five sites: S42, S74, S100, S346, and S415[400]. We expect that the former study's results are more biologically relevant as the proteins were present in their wild-type amounts and the phospho-sites were identified specifically from SPBs, the place of γ-tubulin's known functions. Additionally, the former study confirmed three previously identified phospho-sites (S360, Y362[401] and Y445[3]) which were not found in the latter study. Nonetheless, phospho-sites identified from the latter study could potentially represent those which are more prevalent in the cytoplasm, perhaps involved in γ-TuSC formation or novel cytoplasmic roles.

Of the sites identified by Keck *et al*., 2011, only two have been studied to any capacity: invariant sites S360 and Y445. Residue S360 is phosphorylated in a Cdk1-Clb3-dependent manner *in vivo* and *in vitro*. This phosphorylation is critical for proper spindle assembly, specifically the pairing of antiparallel MTs within the core bundle[1,2,402]. When phosphorylation was prevented at this site (S360A), cells had increased numbers of antiparallel MTs resulting in an over-stabilized spindle[2]. Accordingly, when phosphorylation was constitutively mimicked at this site (S360D), cells completely lost their core bundle of antiparallel MTs resulting in decreased spindle stability[2]. Though included in the structural DSYL motif involved in spindle positioning, phosphorylation of residue Y445 appears to have other roles in the cell. The phosphomimetic Y445D mutant behaves indistinguishably from wild-type in terms of spindle positioning[344]. Instead, Y445D cells have

altered (+)end dynamics, a higher frequency of chromosome loss, and a strict dependence on the SAC[3,4]. This suggests that Y445 phosphorylation also plays a role in spindle assembly.

Of the sites identified by Lin *et al*., 2011, only S74 and S100 phospho-mutants had growth phenotypes and were followed up on. Phosphomimetic mutations at either site were lethal at 30°C due to a Mad2-dependent SAC arrest. Furthermore, spindle assembly was perturbed. These results are hard to interpret as they are potentially confounded by the fact that all mutants were expressed non-endogenously (i.e. off of plasmids, which exist in two to five copies per cell)[403]. This is especially relevant to the γ-TuSC components as cells are sensitive to their dosage[357].

A third, more recent study investigated Hrr25-dependent phosphorylation events in γ-tubulin[404]. Hrr25 is the yeast homolog of human casein kinase 1δ (CK1δ). CK1δ is involved in a wide variety of signaling pathways and has several subcellular localizations, including an enrichment at centrosomes[405-409]. Hrr25 also localizes to SPBs in yeast and phosphorylates components of the γ-TuSC *in vivo* and *in vitro*[404]. *In vitro* kinase assays followed by mass spectrometry identified 22 different γ-tubulin sites clustered into several groups; two of these sites were previously found by Lin *et al*., 2011 (S74 and S100). Phosphoinhibitory mutations at two of these clusters (S71-S74, and S277-S279-S290-S291-S292) proved to be lethal for cells[404]. The importance of these sites *in vivo* is still unclear; however, Hrr25 stimulates MT assembly from γ-TuRCs *in vitro* suggesting a role in nucleation[404].

In summary, though several phospho-sites have been identified in γ-tubulin, research is still scratching the surface as to their biological purpose. To further investigate these sites, I conducted a systematic characterization of all SPB-bound phospho-sites (from Keck *et al*., 2011). I created phosphoinhibitory (alanine or phenylalanine) and phosphomimetic (aspartic or glutamic acid) mutations at the remaining unstudied sites (S42, S43/T44, T130, T227, Y362, S444). I tested their growth under various conditions, including those which favor MT stabilization (37°C) and those which favor destabilization (benomyl and 18°C). Additionally, I tested each mutant's dependence on the SAC. I combined different phospho-mutations together to assess for genetic interactions. Interestingly, I found that phosphomimetic mutations at the G1 sites have a strict dependence on the SAC, though their MT function seemed undisturbed. This suggests that they may be triggering the SAC in some way other than perturbed spindle assembly, perhaps by

contributing to chromosome attachment. I also identified a novel intramolecular relationship between two phosphorylated areas of γ-tubulin related to spindle assembly. This suggests the presence of a concerted signaling mechanism occurring across the protein. These results are presented and discussed in Chapter 2.

My work characterizing the SPB-bound phospho-sites led to the discovery of a novel, temperature-sensitive allele which was insensitive to loss of the SAC, suggesting that it was not disrupting spindle assembly. This prompted us to investigate this mutation further and subsequently discover that it contributed to spindle positioning. The results of this study are detailed in Chapter 3.

Chapter 2: Systematic characterization of yeast γ-tubulin phospho-sites indicate novel mechanisms of regulation

2.1 Summary

γ-Tubulin is an evolutionarily conserved protein best known as a nucleator of microtubules. It is regulated by phosphorylation in both humans and yeast and many of these phospho-sites are conserved. However, the biological significance of most of these modifications is not yet known. Here, we review current knowledge of γ-tubulin phospho-regulation using budding yeast to exemplify a systematic analysis of all γ-tubulin phospho-sites associated with the spindle pole body (yeast centrosome). We find that conserved G1-phase site mutants are lethal in the absence of the spindle assembly checkpoint despite having unperturbed spindle dynamics. This indicates that these sites may be involved in chromosome attachment independent of spindle assembly. Additionally, we identify an intramolecular coupling between two conserved phosphorylated regions of γ-tubulin and propose that this concerted phosphorylation event is a way to control the binding of γ-tubulin to a specific subset of protein interaction partners.

2.2 Introduction

Across all eukaryotic lifeforms, the essential function of microtubule (MT) nucleation is mainly carried out by γ-tubulin, a conserved member of the tubulin superfamily. In budding yeast, γ-tubulin (Tub4) forms a complex with Spc97 and Spc98 (collectively known as the γ-tubulin small complex, or γ-TuSC) and localizes to the functional centrosome equivalent: the spindle pole body (SPB). SPBs are permanently embedded in the nuclear envelope as budding yeast undergo a closed mitosis. γ-TuSCs form a larger complex, called the γ-tubulin ring complex (γ-TuRC) and nucleate both astral (cytoplasmic) and spindle (nuclear) MTs from either the outer or inner surface of the SPB. SPB-bound γ-tubulin is thought to be in an "active" conformation (i.e. nucleation competent) following the addition of activating post-translational modifications (PTMs)[175].

To date, the only PTMs identified on budding yeast γ-tubulin are phosphorylation events[1,400,401,404]. Of these, only eight residues are phosphorylated specifically on SPB-bound γ-tubulin: S42, S43/T44, T130, T227, S360, Y362, S444 and Y445[1]. Here, we give an overview of our current understanding of γ-tubulin phosphorylation at the SPB, provide new data through the systematic characterization of yeast γ-tubulin phosphorylation sites, and comment on how this relates to phosphorylation of γ-tubulin in other species.

Of the eight SPB-specific phospho-sites, two (T130 and T227) were found phosphorylated explicitly in G1 arrested cells, while the remaining were specific to an M-phase arrest[1]. Most of these sites are well-conserved both within the fungi kingdom and outside of it[1] (Figure 2.1C; for a thorough evolutionary analysis of γ-tubulin across fungi, see Keck *et al*., 2011[1]). The exceptions to this conservation include sites S42 (which does not appear in other species), T227 (although other species have a serine/threonine nearby) and S444 (whose conservation is restricted to closer yeast relatives) (Figure 2.1C and Keck *et al*., 2011[1]).

Figure 2.1 | Sequence alignment of γ-tubulin phospho-sites. (A) Phylogenetic tree for γ-tubulin across different species. This tree was created based on NCBI taxonomy using phyloT (http://phylot.biobyte.de/) and visualized using the ETE toolkit (3.0.0b34)[410]. Evolutionary distance correlates with horizontal line length; scale bar represents base pair substitutions per site. (B) Ribbon structure of budding yeast γ-tubulin (homology model based on the human γ-tubulin structure). Spheres indicate *in vivo* phospho-sites associated with the spindle pole body. The G1 sites are shown in red, and the M-phase sites are shown in blue (serines) or cyan (tyrosines). (C) Alignment of γ-tubulin in the regions surrounding the post-translationally modified sites. Yeast sites are indicated in blue, human sites in red. The *Saccharomyces cerevisiae* (S.c.) residue number is shown along the top of the alignment.

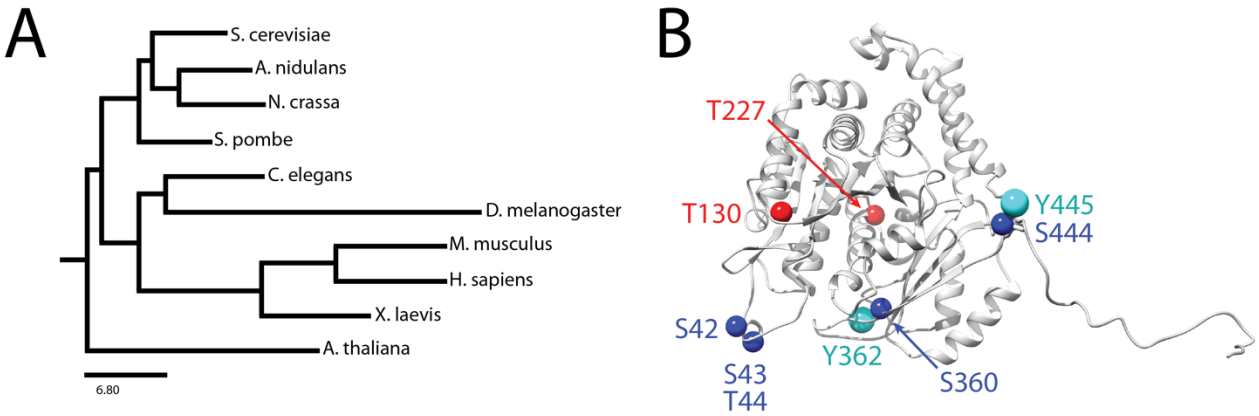
A
S. cerevisiae
A. nidulans
N. crassa
S. pombe
C. elegans
D. melanogaster
M. musculus
H. sapiens
X. laevis
A. thaliana
6.80
B
T227
T130
Y445
S444
S42
S43
T44
Y362
S360

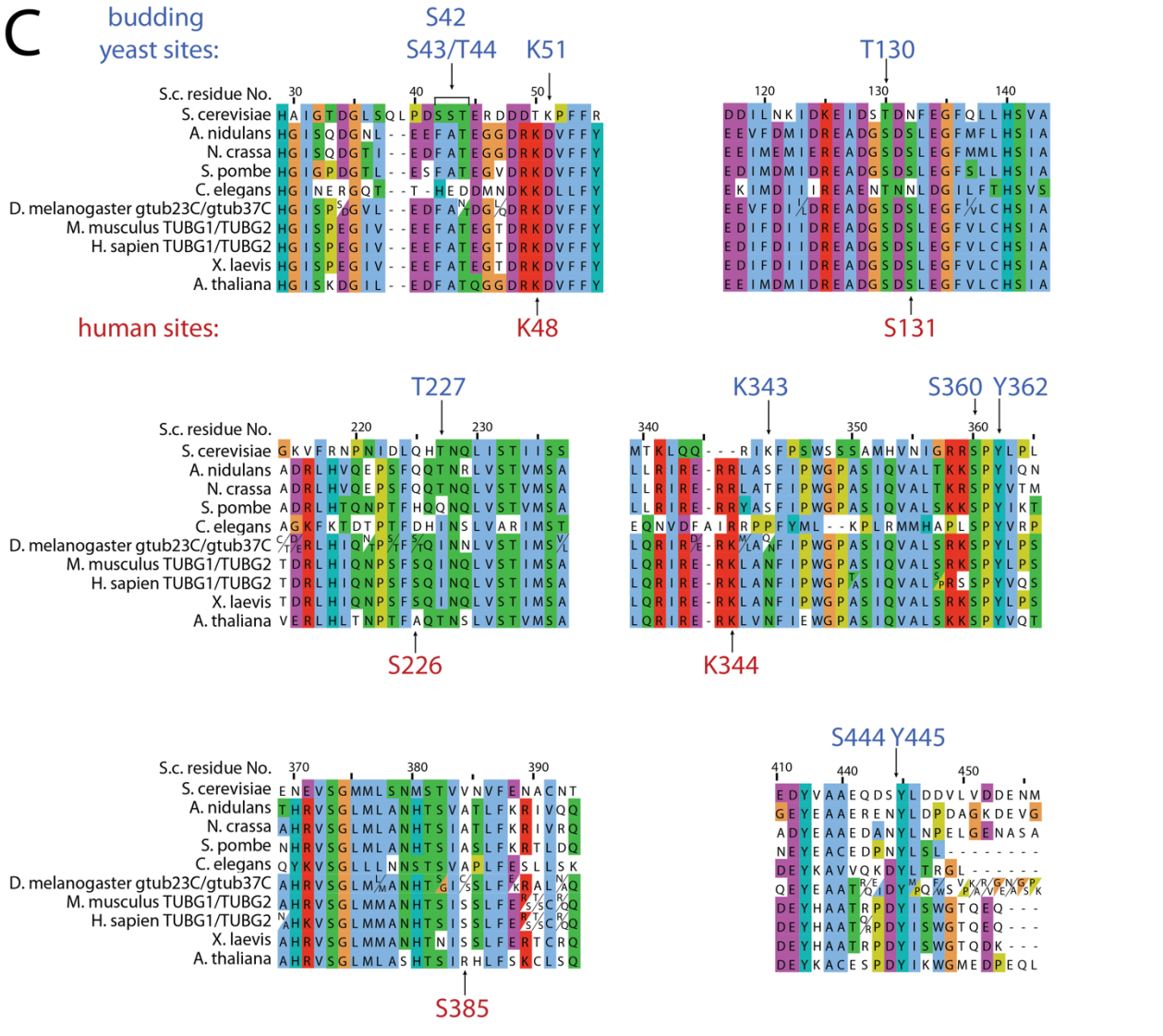
C
budding yeast sites:
S42
S43/T44
K51
T130
S.c. residue No.
S. cerevisiae
A. nidulans
N. crassa
S. pombe
C. elegans
D. melanogaster gtub23C/gtub37C
M. musculus TUBG1/TUBG2
H. sapien TUBG1/TUBG2
X. laevis
A. thaliana
human sites:
K48
S131
T227
K343
S360
Y362
S226
K344
S444
Y445
S385

The evolutionary conservation of these sites suggests that phosphorylation may be a common mechanism for regulating γ-tubulin. In humans, high-throughput analysis has identified many γ-tubulin sites which are post-translationally modified[387-398]. However, the biological significance of the majority of these sites remains unknown. Notable exceptions are the SADB-dependent phosphorylation of S131 and S385, and the BRCA1-dependent ubiquitination of K48 and K344. Phosphorylation of S131 by SADB kinase governs centrosome duplication in mammalian cells by increasing local MT polymerization to build the daughter centriole during duplication[353]. In contrast, SADB phosphorylation of residue S385 increases the nuclear pool of γ-tubulin and affects cell cycle progression[348,350]. BRCA1-dependent mono-ubiquitination of γ-tubulin decreases MT nucleation and aster formation and is thought to be a way to mark centrosomes post-duplication to prevent re-duplication and amplification[354,356].

Similar to human γ-tubulin, little is known in regard to the biological relevance of most yeast phospho-sites. The exceptions are the invariant sites S360 and Y445, which are both involved in spindle assembly[1-3]. Residue S360 is phosphorylated by Cdk1-Clb3 and is important for proper spindle formation, specifically the pairing of interpolar MTs[1,2,402]. The phosphoinhibitory mutant (S360A) has increased numbers of antiparallel MTs leading to an over-stabilized spindle. Consistently, the phosphomimetic mutant (S360D) experiences a loss of antiparallel MTs resulting in decreased spindle stability[2]. Phosphomimetic mutations at residue Y445 lead to chromosome loss and a strict dependence on the spindle assembly checkpoint (SAC; both of these phenotypes are indicative of perturbed spindle assembly [3,4].

While the individual roles of S360 and Y445 are becoming clearer, the questions of how these sites relate to each other, and of the role of the remaining six γ-tubulin phospho-sites are still outstanding. In this study, we conduct a global characterization of all the SPB-associated phospho-sites in budding yeast, as well as some conserved sites which are important to human γ-tubulin function. We provide evidence that phosphorylation in G1-phase is related to the proper attachment of chromosomes and show a clear functional interplay of the M-phase sites S360 and Y445. Additionally, we identify a unique γ-tubulin allele which becomes the basis of my investigation in Chapter 3.

2.3 Materials and methods

2.3.1 Strain construction, plasmids and growth conditions

All yeast strains used in this study are derivatives of BY4741 unless otherwise stated; see Table 2.1 for a complete list. All strains containing a gene knockout (e.g. *mad2Δ*, *san1Δ*, *tub4Δ*) were created using haploids that were isolated from the Yeast Knock-out deletion collection (genes are deleted using a *KANMX4* cassette)[411]. Strains isolated from the Yeast Knock-out deletion collection were confirmed by PCR using the following primer pair: a forward primer which binds upstream of the deleted gene, and a reverse primer which binds within the *KANMX4* cassette. Only strains with PCR fragments of the correct predicted size were used. All strains containing an EGFP tag (e.g. *TUB4-EGFP*, *SPC97-EGFP*) were created using haploids that came from the Yeast-EGFP Clone Collection (Invitrogen)[412]. All mNeonGreen (mNG) tags[413] were made using a yeast optimized version with linker 'GGTGACGGTGCTGGTTTAATTAAC'. Strains isolated from the Yeast-EGFP Clone Collection were confirmed by sequencing to scrutinize the integrity of the tagged gene.

Plasmids used in this study are listed in Table 2.2. All transformations (point mutations and fluorophore tags) used PCR-based methods and involved insertion of genetic material into the genome at the native locus and under the endogenous promoter[415-417]. Point mutants were created by first generating them on a *TUB4-NATMX6* containing plasmid (pJV0372) using the USER™ cloning method[414]. Sequence-confirmed point-mutated *TUB4-NATMX6* plasmids were then used as templates to PCR the entire mutated *tub4* coding region along with the *NATMX6* cassette. PCR fragments were transformed into *TUB4/tub4ΔKANMX4* heterozygote diploids and resulting colonies were screened for loss of the *KANMX4* cassette and gain of the *NATMX6* cassette. The *tub4* loci of positive colonies were sequenced in their entirety (from the upstream recombination junction to the downstream recombination junction) to ensure the integrity of the mutagenesis. The *NATMX6* cassette remained at the genomic locus to allow for tracking of the mutated allele in downstream analysis.

Yeast strains were grown in rich medium (YEPD: yeast extract, peptone, dextrose) at 25°C unless otherwise stated[418]; synthetic complete (SC) medium was used for all fluorescence live-

cell imaging[419]. Bacterial cultures were grown at 37°C in LB medium supplemented with 100 μg/mL of carbenicillin.

The growth properties of yeast strains were assessed by growing cultures overnight in YEPD at 25°C. The following morning, cultures were diluted to an OD_{600} of 0.2 and then grown to log phase. At this point, cultures were diluted to an OD_{600} of 0.4 and then serially diluted five times in sterile dH_2O, each time by a factor of five (unless otherwise stated). Five microliters of the starting 0.4 OD_{600} culture and the five serial dilutions were spotted onto solid YEPD media and left to dry. Spotted plates were incubated at either 18°C, 25°C, 30°C, or 37°C as indicated. Benomyl dissolved in dimethyl sulfoxide (DMSO) was added to YEPD at a final concentration of 12 μg/mL as indicated (DMSO alone was added to the control plates at a final concentration of 0.12%). At least three biological replicates were tested for each assessed mutation.

Table 2.1 | List of all yeast strains used in this study.

Yeast Strain	Genotype	Notes	Reference
YV2018-2020	*tub4-T130A-NATMX6; MATa; his3Δ1; leu2Δ0; ura3Δ0; met15Δ0*	γ-tub-T130A; isolate 1, 2, 3	This study.
YV2517-2519	*tub4-T130D-NATMX6; MATa; his3Δ1; leu2Δ0; ura3Δ0; met15Δ0*	γ-tub-T130D; isolate 1, 2, 3	This study.
YKS750-752	*tub4-T130E-NATMX6; MATa; his3Δ1; leu2Δ0; ura3Δ0; met15Δ0*	γ-tub-T130E; isolate 1, 2, 3	This study.
YKS755-757	*tub4-T227A-NATMX6; MATa; his3Δ1; leu2Δ0; ura3Δ0; met15Δ0*	γ-tub-T227A; isolate 1, 2, 3	This study.
YV2523-2525	*tub4-T227D-NATMX6; MATa; his3Δ1; leu2Δ0; ura3Δ0; met15Δ0*	γ-tub-T227D; isolate 1, 2, 3	This study.
YV2429-2431	*tub4-T130A-T227A-NATMX6; MATa; his3Δ1; leu2Δ0; ura3Δ0; met15Δ0*	γ-tub-T130A-T227A; isolate 1, 2, 3	This study.
YV2529-2531	*tub4-T130D-T227D-NATMX6; MATa; his3Δ1; leu2Δ0; ura3Δ0; met15Δ0*	γ-tub-T130D-T227D; isolate 1, 2, 3	This study.
YKS735-736	*TUB4/TUB4-GFP-HIS3MX6; MATa/MATα; his3Δ1/ his3Δ1; leu2Δ0/ leu2Δ0; ura3Δ0/ ura3Δ0; MET15/met15Δ0; LYS2/lys2Δ0*	Diploid wild-type γ-TUB-GFP; isolate 1, 2	Huh *et al*., 2003[412]
YKS888-889	*TUB4/tub4-T130D-T227D-GFP-HIS3MX6; MATa/MATα; his3Δ1/ his3Δ1; leu2Δ0/ leu2Δ0; ura3Δ0/ ura3Δ0; MET15/met15Δ0; LYS2/lys2Δ0*	Diploid γ-tub-T130D-T227D-GFP; isolate 1, 2	This study.
YV2450-2452	*tub4-T130D-T227D-NATMX6; SPC97-mNeonGreen-NATMX6; SPC42-cerulean-HYGB; MATa; his3Δ1; leu2Δ0; ura3Δ0; met15Δ0*	γ-tub-T130D-T227D; Spc97-mNeonGreen; isolate 1, 2, 3	This study.
YV2685-2687	*tub4-T130A-T227A-NATMX6; SPC97-mNeonGreen-NATMX6; SPC42-cerulean-HYGB; MATa; his3Δ1; leu2Δ0; ura3Δ0; met15Δ0*	γ-tub-T130A-T227A; Spc97-mNeonGreen; isolate 1, 2, 3	This study.
YKS626-628	*TUB4/tub4-S360A-Y445F-NATMX6; MATa/MATα; his3Δ1/ his3Δ1; leu2Δ0/ leu2Δ0; ura3Δ0/ ura3Δ0; MET15/met15Δ0; LYS2/lys2Δ0*	Diploid γ-tub-S360A-Y445F; isolate 1, 2, 3	This study.
YV1887, YV1904-1905	*TUB4/tub4-S360A-Y445D-NATMX6; MATa/MATα; his3Δ1/ his3Δ1; leu2Δ0/ leu2Δ0; ura3Δ0/ ura3Δ0; MET15/met15Δ0; LYS2/lys2Δ0*	Diploid γ-tub-S360A-Y445D; isolate 1, 2, 3	This study.
YV1906, YKS884-885	*TUB4/tub4-S360D-Y445F-NATMX6; MATa/MATα; his3Δ1/ his3Δ1; leu2Δ0/ leu2Δ0; ura3Δ0/ ura3Δ0; MET15/met15Δ0; LYS2/lys2Δ0*	Diploid γ-tub-S360D-Y445F; isolate 1, 2, 3	This study.
YKS932, 934, 945	*TUB4/tub4-S360D-Y445D-NATMX6; MATa/MATα; his3Δ1/ his3Δ1; leu2Δ0/ leu2Δ0; ura3Δ0/ ura3Δ0; MET15/met15Δ0; LYS2/lys2Δ0*	Diploid γ-tub-S360D-Y445D; isolate 1, 2, 3	This study.
YKS974-976	*tub4-Y445N-NATMX6; MATa; his3Δ1; leu2Δ0; ura3Δ0; met15Δ0*	γ-tub-Y445N; isolate 1, 2, 3	This study.
YKS1091-1093	*tub4-S360N-NATMX6; MATa; his3Δ1; leu2Δ0; ura3Δ0; met15Δ0*	γ-tub-S360N; isolate 1, 2, 3	This study.
YKS936-938	*TUB4/tub4-S360A-Y445N-NATMX6; MATa/MATα; his3Δ1/ his3Δ1; leu2Δ0/ leu2Δ0; ura3Δ0/ ura3Δ0; MET15/met15Δ0; LYS2/lys2Δ0*	Diploid γ-tub-S360A-Y445N; isolate 1, 2, 3	This study.
YKS767-769	*TUB4/tub4-S360N-Y445F-NATMX6; MATa/MATα; his3Δ1/ his3Δ1; leu2Δ0/ leu2Δ0; ura3Δ0/ ura3Δ0; MET15/met15Δ0; LYS2/lys2Δ0*	Diploid γ-tub-S360N-Y445F; isolate 1, 2, 3	This study.
YV1298-1299	*tub4-Y445D-NATMX6; MATa; his3Δ1; leu2Δ0; ura3Δ0; met15Δ0*	γ-tub-Y445D; isolate 1, 2	Vogel *et al*., 2001[3]
YV550-551	*tub4-Y445F-NATMX6; MATa; his3Δ1; leu2Δ0; ura3Δ0; met15Δ0*	γ-tub-Y445F; isolate 1, 2	Vogel *et al*., 2001[3]
YV1209, YKS001-002	*tub4-S360D-NATMX6; MATa; his3Δ1; leu2Δ0; ura3Δ0; met15Δ0*	γ-tub-S360D; isolate 1, 2, 3	Keck *et al*., 2011[1]; Nazarova *et al*., 2013[2]
YV1184-1185	*tub4-S360A-NATMX6; MATa; his3Δ1; leu2Δ0; ura3Δ0; met15Δ0*	γ-tub-S360A; isolate 1, 2	Keck *et al*., 2011[1]; Nazarova *et al*., 2013[2]
YKS1228-1229	*TUB4-mNeonGreen-NATMX6/TUB4; MATa/MATα; his3Δ1/ his3Δ1; leu2Δ0/ leu2Δ0; ura3Δ0/ ura3Δ0; MET15/met15Δ0; LYS2/lys2Δ0*	Diploid γ-TUB-mNeonGreen/γ-TUB; isolate 1, 2	This study.

YKS1273, 1275	*TUB4-mNeonGreen-NATMX6/tub4Δ; MATa/MATα; his3Δ1/ his3Δ1; leu2Δ0/ leu2Δ0; ura3Δ0/ ura3Δ0; MET15/met15Δ0; LYS2/lys2Δ0*	Diploid γ-TUB-mNeonGreen/γ-tubΔ; isolate 1, 2	This study.
YKS1330-1331	*TUB4-mNeonGreen-NATMX6/tub4-S360A-Y445D-NATMX6; MATa/MATα; his3Δ1/ his3Δ1; leu2Δ0/ leu2Δ0; ura3Δ0/ ura3Δ0; MET15/met15Δ0; LYS2/lys2Δ0*	Diploid γ-TUB-mNeonGreen/γ-tub-S360A-Y445D; isolate 1, 2	This study.
YKS1332-1333	*TUB4-mNeonGreen-NATMX6/tub4-S360D-Y445F-NATMX6; MATa/MATα; his3Δ1/ his3Δ1; leu2Δ0/ leu2Δ0; ura3Δ0/ ura3Δ0; MET15/met15Δ0; LYS2/lys2Δ0*	Diploid γ-TUB-mNeonGreen/γ-tub-S360D-Y445F; isolate 1, 2	This study.
YV922	*TUB4/TUB4; SPC97/SPC97-GFP-HIS3MX6; SPC42/SPC42-cerulean-HYGB; MATa/MATα; his3Δ1/ his3Δ1; leu2Δ0/ leu2Δ0; ura3Δ0/ ura3Δ0; MET15/met15Δ0; LYS2/lys2Δ0*	Diploid γ-TUB; Spc97-GFP; Spc42-cerulean	This study.
YKS844-845	*TUB4/tub4-S360D-NATMX6; SPC97/SPC97-GFP-HIS3MX6; SPC42/SPC42-cerulean-HYGB; MATa/MATα; his3Δ1/ his3Δ1; leu2Δ0/ leu2Δ0; ura3Δ0/ ura3Δ0; MET15/met15Δ0; LYS2/lys2Δ0*	Diploid γ-tub-S360D; Spc97-GFP; Spc42-cerulean; isolate 1, 2	This study.
YKS833-834	*TUB4/tub4-S360D-Y445F-NATMX6; SPC97/SPC97-GFP-HIS3MX6; SPC42/SPC42-cerulean-HYGB; MATa/MATα; his3Δ1/ his3Δ1; leu2Δ0/ leu2Δ0; ura3Δ0/ ura3Δ0; MET15/met15Δ0; LYS2/lys2Δ0*	Diploid γ-tub-S360D-Y445F; Spc97-GFP; Spc42-cerulean; isolate 1, 2	This study.
YKS818-819	*TUB4/tub4-Y445D-NATMX6; SPC97/SPC97-GFP-HIS3MX6; SPC42/SPC42-cerulean-HYGB; MATa/MATα; his3Δ1/ his3Δ1; leu2Δ0/ leu2Δ0; ura3Δ0/ ura3Δ0; MET15/met15Δ0; LYS2/lys2Δ0*	Diploid γ-tub-Y445D; Spc97-GFP; Spc42-cerulean; isolate 1, 2	This study.
YKS830-831	*TUB4/tub4-S360A-Y445D-NATMX6; SPC97/SPC97-GFP-HIS3MX6; SPC42/SPC42-cerulean-HYGB; MATa/MATα; his3Δ1/ his3Δ1; leu2Δ0/ leu2Δ0; ura3Δ0/ ura3Δ0; MET15/met15Δ0; LYS2/lys2Δ0*	Diploid γ-tub-S360A-Y445D; Spc97-GFP; Spc42-cerulean; isolate 1, 2	This study.
YKS527-529	*tub4-K51R-NATMX6; MATa; his3Δ1; leu2Δ0; ura3Δ0; met15Δ0*	γ-tub-K51R; isolate 1, 2, 3	This study.
YKS434-435	*tub4-K343R-NATMX6; MATa; his3Δ1; leu2Δ0; ura3Δ0; met15Δ0*	γ-tub-K343R; isolate 1, 2	This study.
YKS522-524	*tub4-K51R-K343R-NATMX6; MATa; his3Δ1; leu2Δ0; ura3Δ0; met15Δ0*	γ-tub-K51R-K343R; isolate 1, 2, 3	This study.
YV1380-1381, YKS035	*tub4-S241A-NATMX6; MATa; his3Δ1; leu2Δ0; ura3Δ0; met15Δ0*	γ-tub-S241A; isolate 1, 2, 3	This study.
YV1065-1067	*tub4-S241D-NATMX6; MATa; his3Δ1; leu2Δ0; ura3Δ0; met15Δ0*	γ-tub-S241D; isolate 1, 2, 3	This study.
YKS360-362	*tub4-S241E-NATMX6; MATa; his3Δ1; leu2Δ0; ura3Δ0; met15Δ0*	γ-tub-S241E; isolate 1, 2, 3	This study.
YKS264-266	*tub4-S269A-NATMX6; MATa; his3Δ1; leu2Δ0; ura3Δ0; met15Δ0*	γ-tub-S269A; isolate 1, 2, 3	This study.
YKS671-673	*tub4-S269D-NATMX6; MATa; his3Δ1; leu2Δ0; ura3Δ0; met15Δ0*	γ-tub-S269D; isolate 1, 2, 3	This study.
YKS399-401	*tub4-S269E-NATMX6; MATa; his3Δ1; leu2Δ0; ura3Δ0; met15Δ0*	γ-tub-S269E; isolate 1, 2, 3	This study.
YKS354-356	*tub4-S241A-S269A-NATMX6; MATa; his3Δ1; leu2Δ0; ura3Δ0; met15Δ0*	γ-tub-S241A-S269A; isolate 1, 2, 3	This study.
YKS239-240	*TUB4/tub4-S241D-S269D-NATMX6; MATa/MATα; his3Δ1/ his3Δ1; leu2Δ0/ leu2Δ0; ura3Δ0/ ura3Δ0; MET15/met15Δ0; LYS2/lys2Δ0*	Diploid γ-tub-S241D-S269D; isolate 1, 2	This study.
YV1593-1594, YV1596	*tub4-S241E-S269E-NATMX6; MATa; his3Δ1; leu2Δ0; ura3Δ0; met15Δ0*	γ-tub-S241E-S269E; isolate 1, 2, 3	This study.
YKS532-534	*tub4-S241A-S269A-K51R-NATMX6; MATa; his3Δ1; leu2Δ0; ura3Δ0; met15Δ0*	γ-tub-S241A-S269A-K51R; isolate 1, 2, 3	This study.
YKS443-445	*tub4-S241A-S269A-K343R-NATMX6; MATa; his3Δ1; leu2Δ0; ura3Δ0; met15Δ0*	γ-tub-S241A-S269A-K343R; isolate 1, 2, 3	This study.
YV1749-1751	*tub4-S241E-S269E-K51R-NATMX6; MATa; his3Δ1; leu2Δ0; ura3Δ0; met15Δ0*	γ-tub-S241E-S269E-K51R; isolate 1, 2, 3	This study.
YKS472-474	*tub4-S241E-S269E-K343R-NATMX6; MATa; his3Δ1; leu2Δ0; ura3Δ0; met15Δ0*	γ-tub-S241E-S269E-K343R; isolate 1, 2, 3	This study.
YKS031	*tub2-104; ade2(ochre); ura3-52*	Benomyl resistant (BenR) strain	Huffaker *et al.*, 1988[420]
YKS033	*tub1-1; ade2(ochre); his3Δ200; leu2-3,112; ura3-52*	Benomyl sensitive (BenS) strain	Stearns and Botstein, 1988[421]

Table 2.2 | List of all plasmids used in this study.

Plasmid	Description	Reference
pJV0372	pBKS-*tub4*-NAT	Shulist *et al.*, 2017[424]
pTB16	Plasmid with yeast optimized mNeonGreen-NAT	Gift from Rodrigo Reyes-Lamothe
BKS064	pBKS-*tub4-S42A-S43A-T44A*-NAT	This study.
BKS073	pBKS-*tub4-S42D-S43D-T44D*-NAT	This study.
BKS067	pBKS-*tub4-S42E-S43E-T44E*-NAT	This study.
BKS063	pBKS-*tub4-S42A-S43A*-NAT	This study.
BKS086	pBKS-*tub4-T130A*-NAT	This study.
BKS087	pBKS-*tub4-T130D*-NAT	This study.
BKS092	pBKS-*tub4-T130E*-NAT	This study.
BKS090	pBKS-*tub4-T227A*-NAT	This study.
BKS091	pBKS-*tub4-T227D*-NAT	This study.
BKS136	pBKS-*tub4-T130A-T227A*-NAT	This study.
BKS100	pBKS-*tub4-T130D-T227D*-NAT	This study.
BKS004	pBKS-*tub4-S360A-Y445F*-NAT	This study.
BKS111	pBKS-*tub4-S360A-Y445D*-NAT	This study.
BKS110	pBKS-*tub4-S360D-Y445F*-NAT	This study.
BKS107	pBKS-*tub4-S360D-Y445D*-NAT	This study.
BKS118	pBKS-*tub4-Y445N*-NAT	This study.
BKS132	pBKS-*tub4-S360N*-NAT	This study.
BKS122	pBKS-*tub4-S360A-Y445N*-NAT	This study.
BKS099	pBKS-*tub4-S360N-Y445F*-NAT	This study.
pJV199	pBKS-*tub4-S444A-Y445F*-NAT	This study.
pJV195	pBKS-*tub4-S42A-S43A-S360A-Y362F*-NAT	This study.
pJV196	pBKS-*tub4-S360A-Y362F-S444A-Y445F*-NAT	This study.
pJV198	pBKS-*tub4-S360A-Y362F*-NAT	This study.
BKS120	pBKS-*tub4-S360D-Y362D*-NAT	This study.
pJV194	pBKS-*tub4-S42A-S43A-T130A-T227A-S360A-Y362F-S444A-Y445F*-NAT	This study.
BKS051	pBKS-*tub4-K51R*-NAT	This study.
BKS059	pBKS-*tub4-K343R*-NAT	This study.
BKS060	pBKS-*tub4-K51R-K343R*-NAT	This study.
BKS013	pBKS-*tub4-S241D*-NAT	This study.
BKS035	pBKS-*tub4-S241E*-NAT	This study.
BKS031	pBKS-*tub4-S269A*-NAT	This study.
BKS045	pBKS-*tub4-S269D*-NAT	This study.
BKS047	pBKS-*tub4-S269E*-NAT	This study.
BKS037	pBKS-*tub4-S241A-S269A*-NAT	This study.
BKS033	pBKS-*tub4-S241D-S269D*-NAT	This study.
BKS049	pBKS-*tub4-S241E-S269E*-NAT	This study.
BKS068	pBKS-*tub4-S241A-S269A-K51R*-NAT	This study.
BKS061	pBKS-*tub4-S241E-S269E-K51R*-NAT	This study.
BKS065	pBKS-*tub4-S241A-S269A-K343R*-NAT	This study.
BKS062	pBKS-*tub4-S241E-S269E-K343R*-NAT	This study.

2.3.2 Genetic analysis

To assess different single or combined mutations for growth phenotypes and/or synthetic genetic interactions, heterozygous diploids were sporulated by growing in liquid sporulation media for three to seven days at 25°C[418]. The resulting meiotic products (tetrads) were digested with 50 μg/mL of Zymolyase enzyme and then dissected on a YEPD plate using a Nikon E400 micromanipulator. Dissected tetrads were growth at 25°C and then replica plated onto appropriate selective media to determine the segregation of mutant alleles. Common genetic markers used in this study include NATMX6, KANMX4, HygB, or HIS3MX6 which confer growth on YEPD supplemented with either 100 μg/mL of clonNAT (nourseothricin), 200 μg/mL G418 (geneticin), or 200 μg/mL hygromycin B, or SC-HIS, respectively. As both *tub4* alleles and mNG fluorophore tags were marked with NATMX6, only tetrads showing a non-parental ditype segregation pattern were screened for haploids containing both these alleles.

Protein stability of temperature-sensitive mutant alleles for genes encoding nuclear-targeted proteins can be indirectly measured in yeast by combining the mutant with loss of the major nuclear degradation pathway (*san1Δ*)[422,423]. Phenotypic rescue by *san1Δ* indicates the temperature sensitivity is caused by protein instability as opposed to loss-of-function. Lack of rescue by *san1Δ* indicates that the allele encodes a stable protein.

2.3.3 Fluorescence microscopy methods

Yeast cells expressing fluorophore tags (mNG, EGFP, or Cerulean) were grown to log phase in SC media supplemented with 2 mM of ascorbate and imaged as single time points on a custom-built spinning-disk confocal microscope as previously described[2,424]. Images were collected in a streaming regime as Z-stacks with 300 nm Z-slices across 30 focal planes. An integration time of 50 ms per focal plane was used for all EGFP tags, Cerulean tags, and for haploid mNG-tagged strains; diploid mNG-tagged strains used an integration time of 25 ms per focal plane.

2.3.4 Calculation of spindle pole body intensity and statistical analysis

Spindle pole bodies were found computationally using MatLab (Mathworks) by fitting to a 3-dimensional Gaussian; the integrated intensity was calculated from the Gaussian fit. Distributions of integrated intensities were tested for normality using a one-sample Kolmogorov-

Smirnov test; they were assessed for differences using the Kruskal-Wallis test followed by a Dunn-Šidák correction or the Wilcoxon rank sum test/Mann-Whitney U-test.

2.4 Results

Yeast γ-tubulin phospho-sites exist in four different temporal and/or spatial clusters (Figure 2.1B and C and Keck *et al*., 2011[1]). These include the G1 sites (T130 and T227), and three M-phase clusters: S42-S43/T44, S360-Y362 and S444-Y445. We hypothesized that these clusters had a functional significance. To investigate this, we systematically mutated all sites to either phosphoinhibitory (PI) or phosphomimetic (PM). PI mutations prevent the phosphorylated residue from being modified: a serine or threonine is mutated to an alanine, while a tyrosine is mutated to a phenylalanine. PM mutations mimic the electrostatic environment of a phosphorylation by using a charged amino acid, like aspartic or glutamic acid. We made these mutations individually and in combination with each other. Phospho-mutants were subsequently assessed for growth phenotypes. We assessed growth of single colonies and of populations at different conditions: different temperatures (18°C, 25°C, 30°C and 37°C), with or without the presence of benomyl (a MT destabilizing drug), and in the absence of the spindle assembly checkpoint (*mad2Δ*). PM mutations at all but one cluster (S42-S43/T44) yielded growth phenotypes either alone or when combined with other mutations (Table 2.3). Interestingly, none of the PI mutants had growth phenotypes, and preventing phosphorylation at all eight sites simultaneous resulted in only a mild temperature sensitivity (Figure 2.2). This suggests that phosphorylation of these sites is not essential for cell survival.

Table 2.3 | Summary of all mutants created in this study.

Mutant	Growth Phenotypes				Published in
	At 25°C	Temperature sensitivity	Benomyl sensitivity	mad2Δ sensitivity	
S42A-S43A	WT	WT	WT	n/a	This study
S42A-S43A-T44A	WT	WT	WT	n/a	This study
S42D-S43D-T44D	WT	WT	WT	n/a	This study
S42E-S43E-T44E	WT	n/a	n/a	n/a	This study
T130A	WT	WT	WT	WT	This study
T130D	WT	WT	Slightly sensitive at 18°C	WT	This study
T130E	WT	WT	Slightly sensitive at 18°C	WT	This study
T227A	WT	WT	WT	WT	This study
T227D	WT	WT	Slightly sensitive at 18°C	WT	This study
T130A-T227A	WT	WT	WT	WT	This study
T130D-T227D	WT	WT	Slightly sensitive at 18°C	Lethal	This study
S360A	WT	WT	WT	WT	Keck *et al*., 2011[1]
S360D	Slow growing	Temperature-sensitive	WT	Lethal	Keck *et al*., 2011[1]
S360N	WT	n/a	n/a	n/a	This study
Y362F	WT	WT	WT	WT	Shulist *et al*., 2017[424]
Y362D	WT	Temperature-sensitive	WT	Lethal	Shulist *et al*., 2017[424]
Y362E	WT	Temperature-sensitive	WT	Sensitive	Shulist *et al*., 2017[424]
Y362N	WT	n/a	n/a	n/a	This study
Y362Q	WT	n/a	n/a	n/a	This study
S360A-Y362F	WT	WT	WT	n/a	This study
S360D-Y362D	Lethal	n/a	n/a	n/a	This study
S444A	WT	WT	n/a	WT	Vogel *et al*., 2001[3]
S444D	WT	WT	WT	n/a	Vogel *et al*., 2001[3]
Y445F	WT	WT	n/a	n/a	Vogel *et al*., 2001[3]
Y445D	Slightly slow growing	Temperature-sensitive	Resistant	Lethal	Vogel *et al*., 2001[3]
Y445E	Slightly slow growing	Temperature-sensitive	n/a	Lethal	This study
Y445N	WT	Slightly temperature-sensitive	WT	n/a	This study
Y445Q	WT	WT	WT	n/a	This study
S444A-Y445F	WT	WT	WT	n/a	This study

S444D-Y445D	Slow growing	Temperature-sensitive	n/a	n/a	This study
S42A-S43A-S360A-Y362F	WT	WT	WT	n/a	This study
S360A-Y362F-S444A-Y445F	WT	WT	WT	n/a	This study
S42A-S43A-T130A-T227A-S360A-Y362F-S444A-Y445F (8-phosphoinhibitory)	WT	Slightly temperature-sensitive	WT	n/a	This study
K51R	WT	WT	WT	n/a	This study
K343R	WT	WT	WT	n/a	This study
K51R-K343R	WT	WT	WT	n/a	This study
S241A	WT	WT	WT	n/a	This study
S269A	WT	WT	WT	n/a	This study
S241D	WT	WT	WT	n/a	This study
S269D	WT	WT	WT	n/a	This study
S241E	WT	WT	WT	n/a	This study
S269E	WT	WT	WT	n/a	This study
S241A-S269A	WT	WT	WT	n/a	This study
S241D-S269D	Lethal	n/a	n/a	n/a	This study
S241E-S269E	Slow growing	Temperature-sensitive	Sensitive	n/a	This study
S241A-S269A-K51R	WT	WT	WT	n/a	This study
S241E-S269E-K51R	Slow growing	Temperature-sensitive	Sensitive	n/a	This study
S241A-S269A-K343R	WT	WT	WT	n/a	This study
S241E-S269E-K343R	Slow growing	Temperature-sensitive	Sensitive	n/a	This study
Intramolecular Mutants					
S360A-Y445F	WT	WT	WT	n/a	This study
S360D-Y445F	Lethal	n/a	n/a	n/a	This study
S360A-Y445D	Lethal	n/a	n/a	n/a	This study
S360D-Y445D	Lethal	n/a	n/a	n/a	This study
S360N-Y445F	WT	n/a	n/a	n/a	This study
S360A-Y445N	Slow growing	Temperature-sensitive	Benomyl sensitive	n/a	This study

Figure 2.2 | Mutating all eight sites to PI caused mild temperature sensitivity. Growth assays of serially diluted yeast (by a factor of ten) spotted onto solid media at different temperatures. Dashed line indicates strains were grown on the same plate but not neighbours.

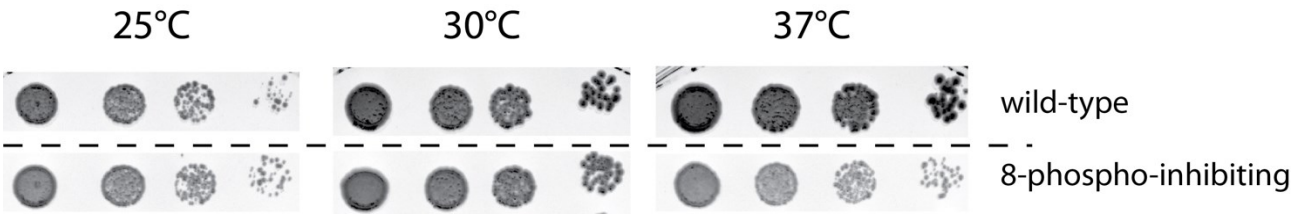

2.4.1 Combined G1 site mutants are dependent on the spindle assembly checkpoint

Two yeast γ-tubulin sites (T130 and T227) are phosphorylated during G1-phase[1]. At this point in the cell cycle, single SPBs experience many structural changes necessary to complete pole duplication[425,426]. Interestingly, duplication of human centrosomes is partially regulated at S131 of γ-tubulin by SADB kinase[353]. Human S131 lies very close to yeast T130 both in primary and tertiary structure (Figure 2.1C and Figure 2.3A, B). Both residues are located on the same loop near the interface between neighbouring γ-tubulin molecules (Figure 2.3B and C). While T227 is not exactly conserved in humans, there is a serine at the +2 position in human γ-tubulin: S226 (Figure 2.1C). S226 is located in the same helix as yeast residue T227 (Figure 2.3B, bottom).

Both G1 phospho-sites (T130 and T227) were mutated to either PM or PI singly and in tandem. PI mutants grew as wild-type in all eight growth conditions tested (18°C, 25°C, 30°C, 37°C, with and without benomyl) (Table 2.3). PM mutants grew as wild-type in seven out of the eight conditions tested: they showed benomyl sensitivity at 18°C (Table 2.3 and Figure 2.4). However, when compared to the benomyl sensitive control strain (Figure 2.4, BenS), the sensitivity of the PM mutants was very mild. Taken together, this suggests that though MT function may be reduced in these strains at 18°C, in general, we suspect that there is no significant disturbance in MT function. Next, we asked whether G1 phospho-mutants required the SAC for survival. The SAC monitors the fidelity of chromosome attachment at the metaphase-anaphase transition. Cells with defects in spindle function (like γ-tubulin mutants S360D or Y445D[1,3]) require the SAC for viability and typically die in the absence of SAC proteins. Mutants were crossed to a knockout of the SAC protein Mad2, and the haploid double-mutant progeny (tetrads; >20 per strain) of the heterozygous diploids were assessed for SGIs. No SGIs were detected for the single mutants; however, the T130D-T227D mutation was lethal when combined with *mad2Δ* (Figure 2.3D). This suggests that chromosome attachment and/or centromere tension is reduced in this mutant.

Figure 2.3 | PM mutations at the G1 sites are sensitive to loss of the spindle assembly checkpoint. (A) Overlaid ribbon structures of yeast (grey; homology model) and human γ-tubulin (blue; PDB ID: 1Z5W). T130 or S131 are indicated with a purple or blue sphere, respectively; T227 or S226 are indicated with a red or green sphere, respectively. (B) Insets of T130/S131 (top) and T227/S226 (bottom). The ribbon structure of the ten residues surrounding the G1 sites are shown in their respective colors. (C) Location of T130/S131 (purple spheres) and T227/S226 (red spheres) in the γ-TuRC (the globular structure of γ-TuRC was taken from PDB ID: 5FLZ; the C-terminal tail structure was taken from Harris *et al*., 2018[427]). (D) Representative tetrad dissections (> 40 tetrads were dissected for each strain) of G1 phospho-mutants alone and combined with loss of the SAC (*mad2Δ*). γ-Tubulin alleles are circled in blue; *mad2Δ* knockouts are circled in black. TDTD and TATA stand for T130D-T227D and T130A-T227A, respectively.

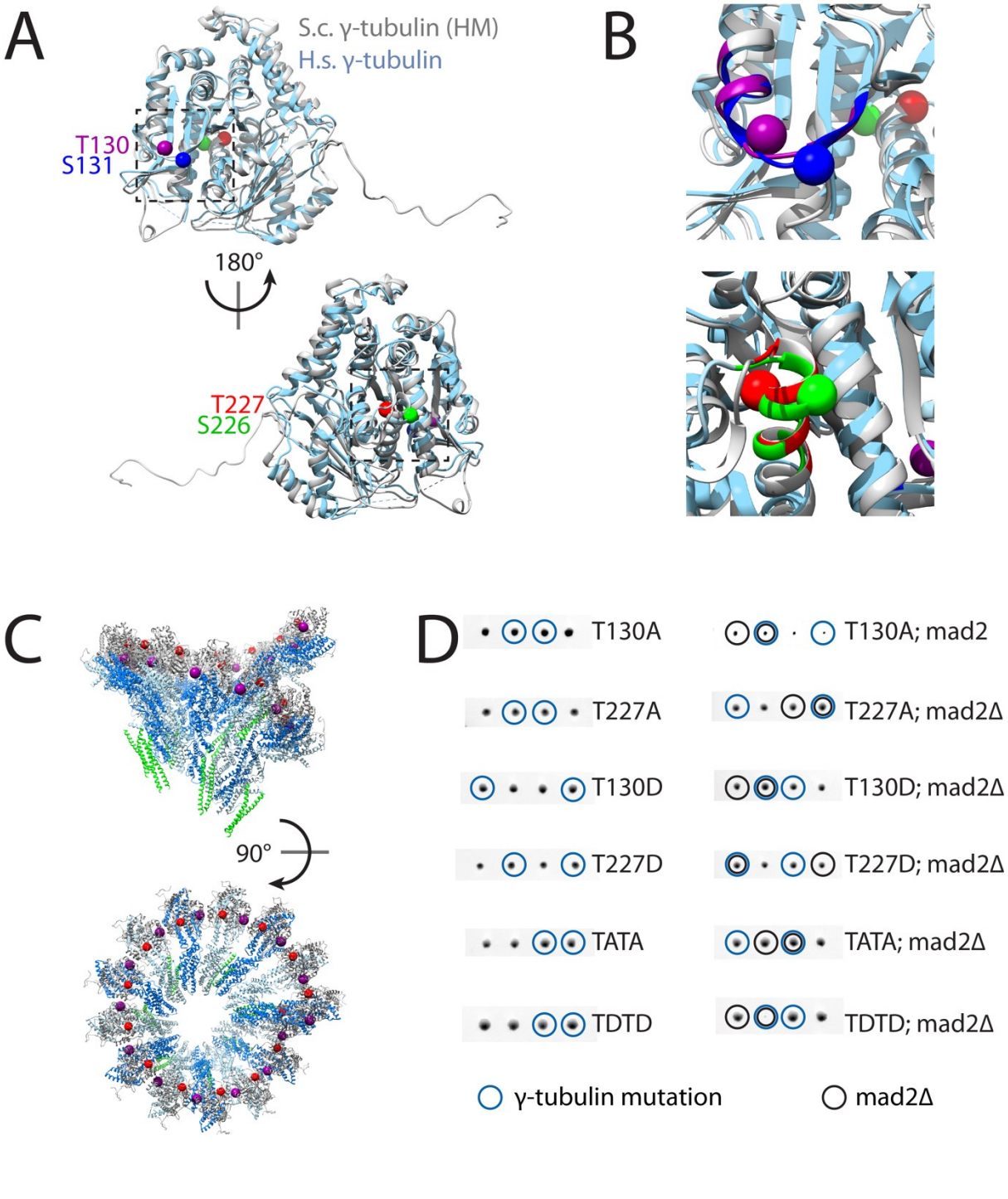
A
S.c. γ-tubulin (HM)
H.s. γ-tubulin
T130
S131
180°
T227
S226
B
C
90°
D
T130A
T130A; mad2
T227A
T227A; mad2Δ
T130D
T130D; mad2Δ
T227D
T227D; mad2Δ
TATA
TATA; mad2Δ
TDTD
TDTD; mad2Δ
γ-tubulin mutation
mad2Δ

Figure 2.4 | PM mutations at the G1 sites are sensitive to benomyl. Growth assays of serially diluted yeast spotted onto solid media showing a slight sensitivity to benomyl at cold temperatures. Dashed line indicates strains were grown on the same plate but not neighbours; solid line indicates strains were grown on separate plates. TDTD stands for T130D-T227D; BenR and BenS indicate the benomyl resistant and benomyl sensitive control strains, respectively.

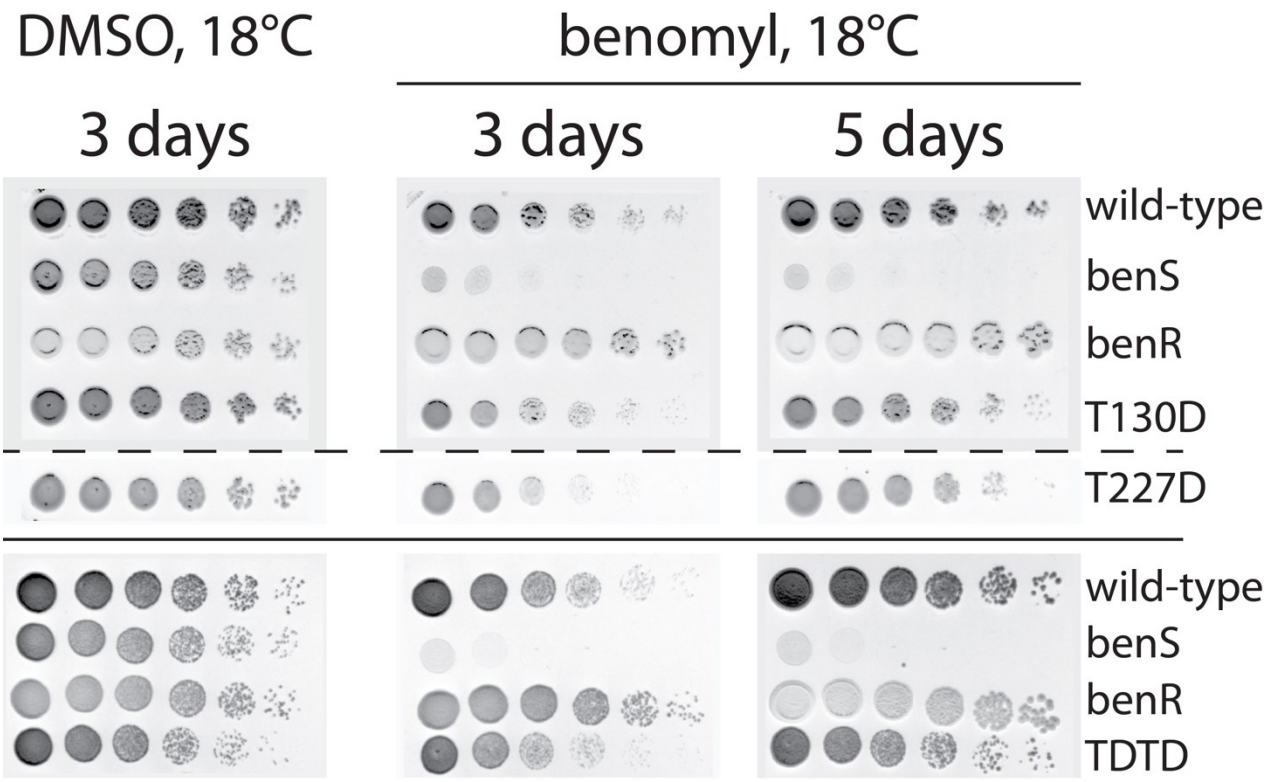

As residue S131 regulates centrosome duplication in humans, we used fluorescence microscopy to determine whether the yeast G1 phospho-mutants affected SPB duplication. Though wild-type γ-tubulin localization was investigated in the past using an EGFP tag[412], T130D-T227D became lethal when tagged with EGFP (Figure 2.5A). In fact, wild-type γ-tubulin-EGFP was sensitive to the loss of *mad2* (Figure 2.5A). The same was true for an mNeonGreen (mNG) tag suggesting that γ-tubulin C-terminal fluorescent fusion proteins are not fully functional. In budding yeast, γ-TuSC components (γ-tubulin, Spc97 or Spc98) cannot localize to the poles unless complexed together[404,428]. Thus, we used Spc97-mNG as a proxy for γ-TuSC and γ-tubulin pole localization. Although centrosome amplification is seen in human cells with γ-tubulin-S131D[353], all yeast T130D-T227D cells (n = 277) had normal SPB numbers at all cell stages (Figure 2.6A). However, based on the integrated intensity of mNG at the SPBs, there was a slight but significant decrease in γ-TuSC localization in the T130D-T227D mutant (integrated intensity means of $7.54 \times 10^5 \pm 2.20 \times 10^5$ and $7.10 \times 10^5 \pm 2.37 \times 10^5$ for wild-type and the mutant, respectively; $p = 0.0007$) (Figure 2.6C). This implies that there is less Spc97-mNG (and thus, less γ-TuSCs) at the SPB. Therefore, unlike human S131, our results indicate that the yeast G1 phospho-site T130 (and T227) does not seem to play a role in SPB duplication and instead seems to be conducive to chromosome attachment, though it may contribute slightly to γ-TuSC pole localization.

Figure 2.5 | Supplementary tetrad dissections. (A) Representative tetrad dissections indicating that tagging γ-tubulin with EGFP or mNG is not completely inert. (B) Representative tetrad dissections of strains with mutations within the S360-Y362 M-phase clusters. γ-Tubulin and Spc97 alleles are circled in blue; *mad2Δ* knockouts are circled in black. At least 40 tetrads were dissected for each strain.

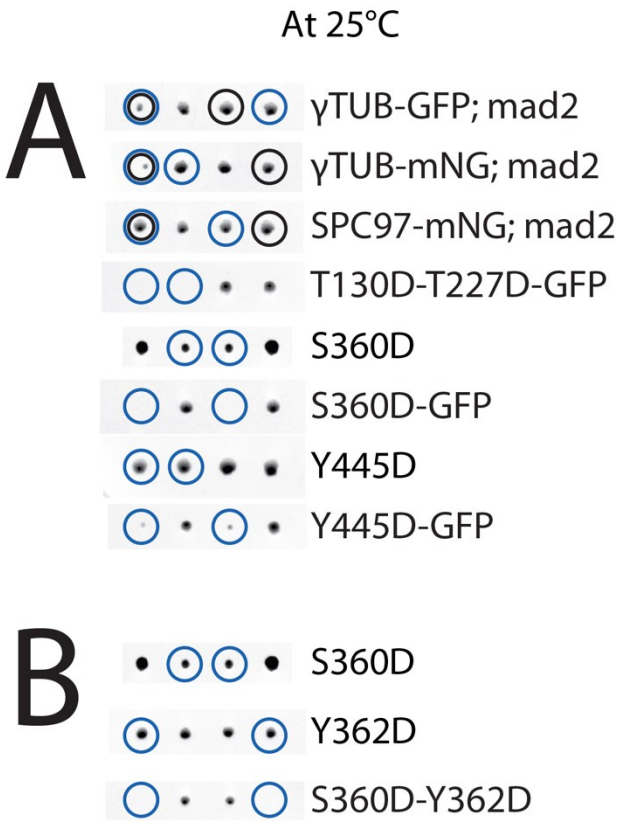

Figure 2.6 | T130D-T227D is present at poles. (A-B) Representative fields of view for wild-type, T130A-T227A and T130D-T227D (A) with boxed insets of cells shown below (B). Cell outlines are shown in white and the scale bar represents five microns. (C) Histograms showing integrated intensity of Spc97-mNG at the pole; wild-type is shown in grey in each plot. Means and standard deviations are shown as factors of 10^5.

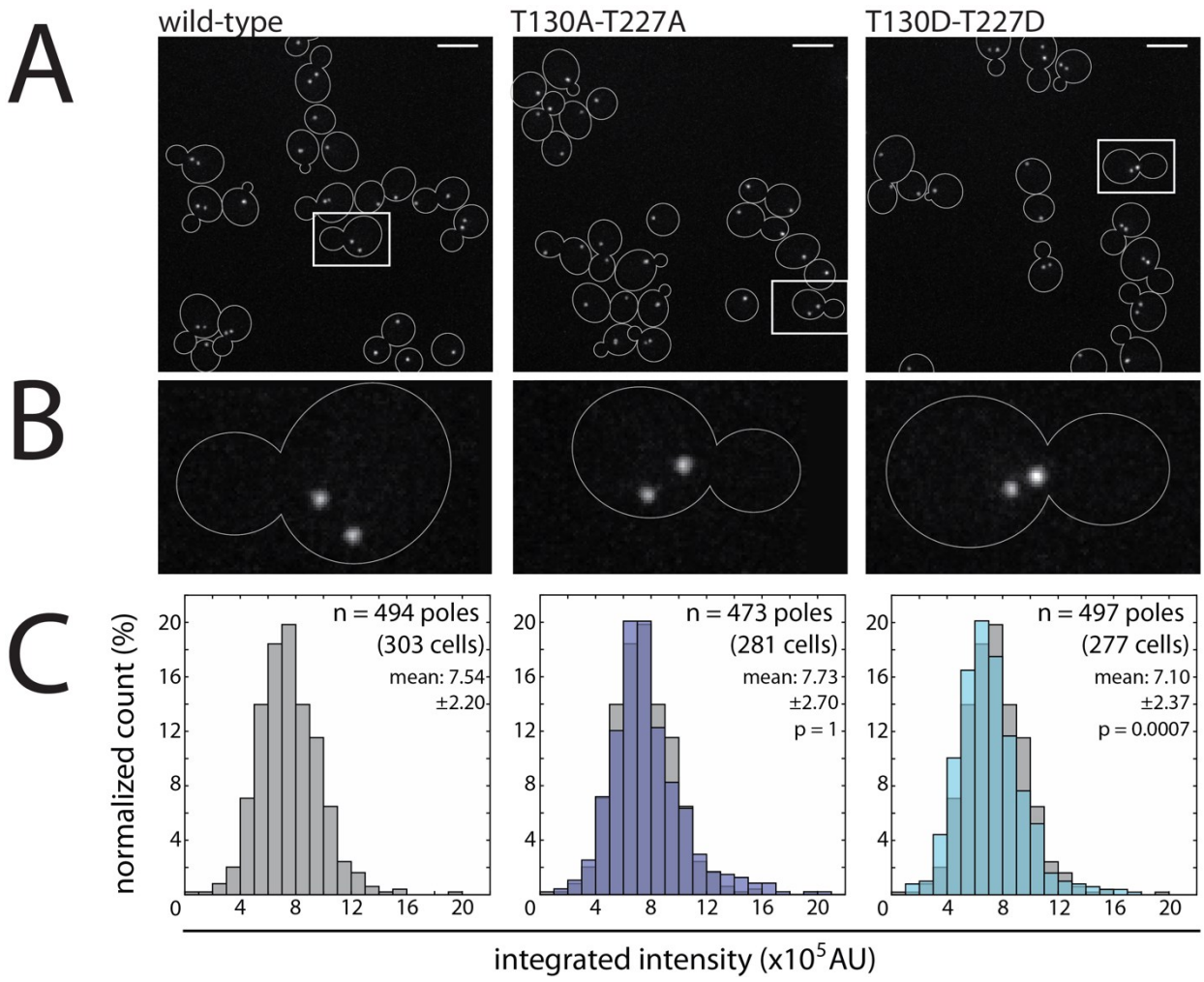

2.4.2 Modified human sites conserved in yeast

In parallel to investigating known phosphorylation sites, we also mutated conserved mammalian-modified residues. In human cell lines, BRCA1 ubiquitinates γ-tubulin at two conserved lysine residues (Figure 2.1C); prevention of which caused centrosomal amplification and increased MT nucleation[355,356]. While there is no structural homolog for BRCA1 in budding yeast, Rad9 is predicted to be a functional homolog[429,430]. Upon mutation of these conserved lysines in yeast γ-tubulin, no discernable growth phenotype was seen, indicating that ubiquitination of these sites is either not conserved or not important for viability.

Both BRCA1 and Rad9 contain tandem BRCT domains which recognize phosphorylated BRCT ligand motifs. Interestingly, both human and yeast γ-tubulin contain putative BRCT ligand motifs. This site (S385) is phosphorylated in humans by SADB and affects cell cycle progression[350]. Whether phosphorylation of S385 contributes to BRCA1 binding and/or ubiquitination of γ-tubulin has not been determined. In yeast, there are two putative BRCT ligand motifs (S241 and S269) and PM mutations at both sites were detrimental to the cell, though the allele appeared to be structurally stable (Figure 2.7). As neither S241 nor S269 have been shown to be phosphorylated *in vivo* or *in vitro*, whether these sites play an important role *in vivo* is an open question; though our results provide the first evidence that γ-tubulin BRCT ligand motifs may be important for cellular function.

Figure 2.7 | Mutating both BRCT ligand motifs to PM causes slow growth or death. (A) Location of the putative BRCT recognition motifs (S-X-X-F). (B) Representative tetrad dissections (> 40 tetrads were dissected for each strain) of phospho-mutations singly or in combination; black circles indicate mutant γ-tubulin alleles. (C) Growth assays of serially diluted yeast spotted onto solid media showing temperature and benomyl sensitivity; BenS indicates the benomyl sensitive control strain. (D) Growth assays of serially diluted yeast missing the major nuclear degradation pathway (*san1Δ*) spotted onto solid media at different temperatures. Dashed lines indicate strains were grown on the same plate but not neighbours; solid line indicates strains were grown on separate plates.

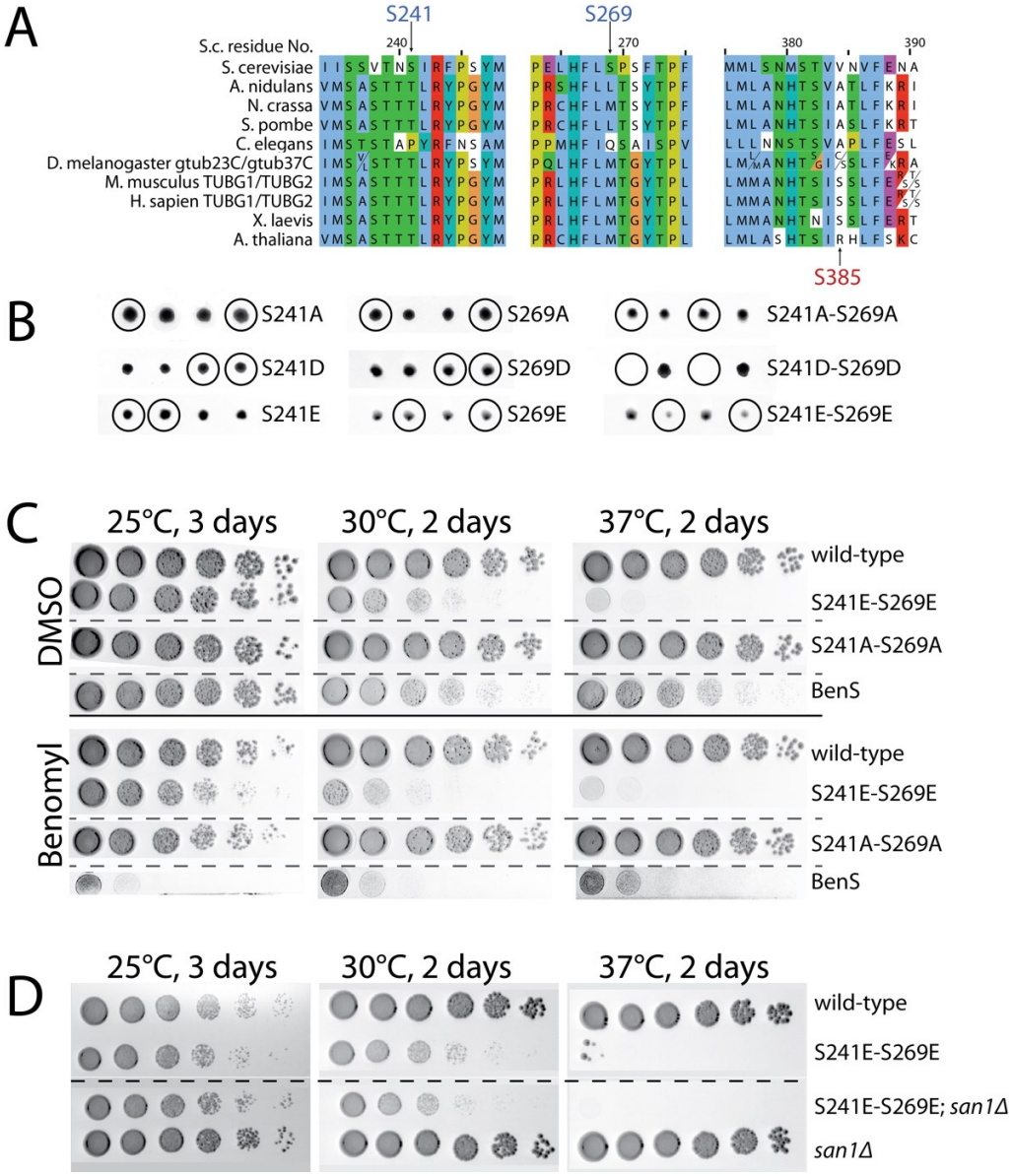

2.4.3 M-phase site clusters

The M-phase phospho-sites cluster into three groups where each group contains two sites in close proximity (either direct neighbours or separated by one residue). While only two sites were identified in the N-terminal cluster (S42-S43/T44), researchers were unable to pinpoint whether S43 or T44 was the second phosphorylated residue[1]. Additionally, phospho-mutants at residue S42 had been previously investigated with no discernable phenotype[400]. Because of this, we mutated all three residues simultaneously to either PI or PM. The phenotype of these mutants did not differ from wild-type at any condition tested indicating that phosphorylation at these sites either perform a function under specific unknown conditions (for example, in response to stress) or they participate in a cellular function of which there are other compensating pathways (Table 2.3).

Very spatially close to the S42-S43/T44 cluster lies the S360-Y362 cluster (Figure 2.1B). While S360 has been examined independently and is involved in spindle assembly[1,2], Y362 has not been studied. Initial characterizations of Y362 led to a more thorough investigation and the subsequent discovery of a role in spindle placement. The results pertaining to the Y362 phospho-mutants are presented in detail in Chapter 3.

Though S360 phosphorylation regulates spindle assembly and Y362 is related to spindle placement, two independent mass spectrometry studies found both S360 and Y362 to be phosphorylated within the same peptide[1,401]. This raises the question as to whether these sites are phosphorylated in a coordinated manner *in vivo*. Thus, we mutated both sites simultaneously to PI (S360A-Y362F) and PM (S360D-Y362D). The double PI mutant had no growth phenotype, but the double PM mutant was lethal suggesting that these sites are not phosphorylated together in a concerted manner, or that, if they are, dephosphorylation of at least one of these sites is essential for cell cycle progression (Figure 2.5B). Similarly, both residues in the S444-Y445 cluster have been investigated individually[3] but not in tandem. Individual PI mutants at these sites do not have growth phenotypes, and while Y445D experiences slow growth and is temperature-sensitive, S444D behaves like wild-type[3]. When both sites were mutated simultaneously, neither the double PI (S444A-Y445F) nor the double PM (S444D-Y445D) gave an enhanced phenotype. S444A-Y445F behaved like wild-type and the combined S444D-Y445D mutant was

indistinguishable from Y445D alone (Table 2.3). This indicates that the phospho-status of site S444 has little to no consequence on Y445.

2.4.4 There is an intramolecular relationship between S360 and Y445

Residues S360 and Y445 have been investigated independently and both are involved in spindle assembly, though how the sites relate to each other is unknown. Thus, we combined different phospho-mutations at each site in tandem. Interestingly, all combinations of phospho-mutations were lethal except a double PI mutant (S360A-Y445F) (Figure 2.8A). Both S360D and Y445D have slow growth phenotypes on their own ([1,3]; and Figure 2.8A), thus, we could not determine if the lethality of S360D-Y445D was due to an intramolecular genetic interaction or due to the additive effect of each individual mutation. Surprisingly, though individual PI mutants do not have any growth phenotypes ([1-3]; and Figure 2.8A), the mixed-phosphorylation mutants—S360A-Y445D (SAYD) and S360D-Y445F (SDYF)—were both lethal. To determine whether this was caused by intramolecular interactions (within one γ-tubulin molecule) or intermolecular interactions (between neighbouring γ-tubulin molecules), heterozygous diploids where each γ-tubulin gene carried one of the phospho-mutant alleles (S360A/Y445D or S360D/Y445F) were created. These heterozygous double mutant diploids had no growth phenotypes (Figure 2.8B) indicating that the genetic interactions are intramolecular.

To assess whether the phenotypes of PM-containing mutants were due to the change in steric effects of the residue (i.e. serine/tyrosine to aspartic acid) or due to the change in charge of the residue (charge is more relevant to phosphorylation), we mutated the phospho-sites to asparagine in place of aspartic acid. Asparagine and aspartic acid are nearly isosteric, but the former lacks the (-1) charge from the carboxyl group. This rescued the slow growth in S360D and Y445D suggesting these phenotypes are due to the addition of a negative charge and not due to steric effects (Figure 2.8C). When asparagine was combined with a PI mutation at the secondary site (S360N-Y445F or S360A-Y445N), it rescued the lethality either completely (in S360N-Y445F) or partially (in S360A-Y445N) (Figure 2.8C). This indicates that the lethality of SDYF is due to the presence of the negative charge while the lethality of SAYD is partially due to the negative charge, partially due to steric effects. Therefore, nearly all the phenotypes associated with PM mutations

at either S360, Y445 or both are caused by a change in charge and thus, are more biologically relevant to phosphorylation.

The only known essential function for γ-tubulin is nucleation. In order for γ-tubulin to nucleate MTs in yeast, it must: (1) form the γ-TuSC (with Spc97 and Spc98), (2) localize to the SPBs, and (3) be capable of nucleating MTs. If any of these three steps are impaired, the result would likely be lethality. Thus, we wanted to determine whether these three processes were affected in our lethal tandem mutants.

Figure 2.8 | Simultaneously mixing phosphorylation status between sites S360 and Y445 was detrimental for the cell. (A) Representative tetrad dissections of single and combined phospho-mutants (> 40 tetrads were dissected for each strain). (B) Growth assays of different diploids heterozygous for γ-tubulin alleles. γTUB indicates the wild-type allele. Solid line indicates strains were grown on separate plates. (C) Representative tetrad dissections for PM asparagine controls (> 40 tetrads were dissected for each strain). γ-Tubulin alleles are circled in black.

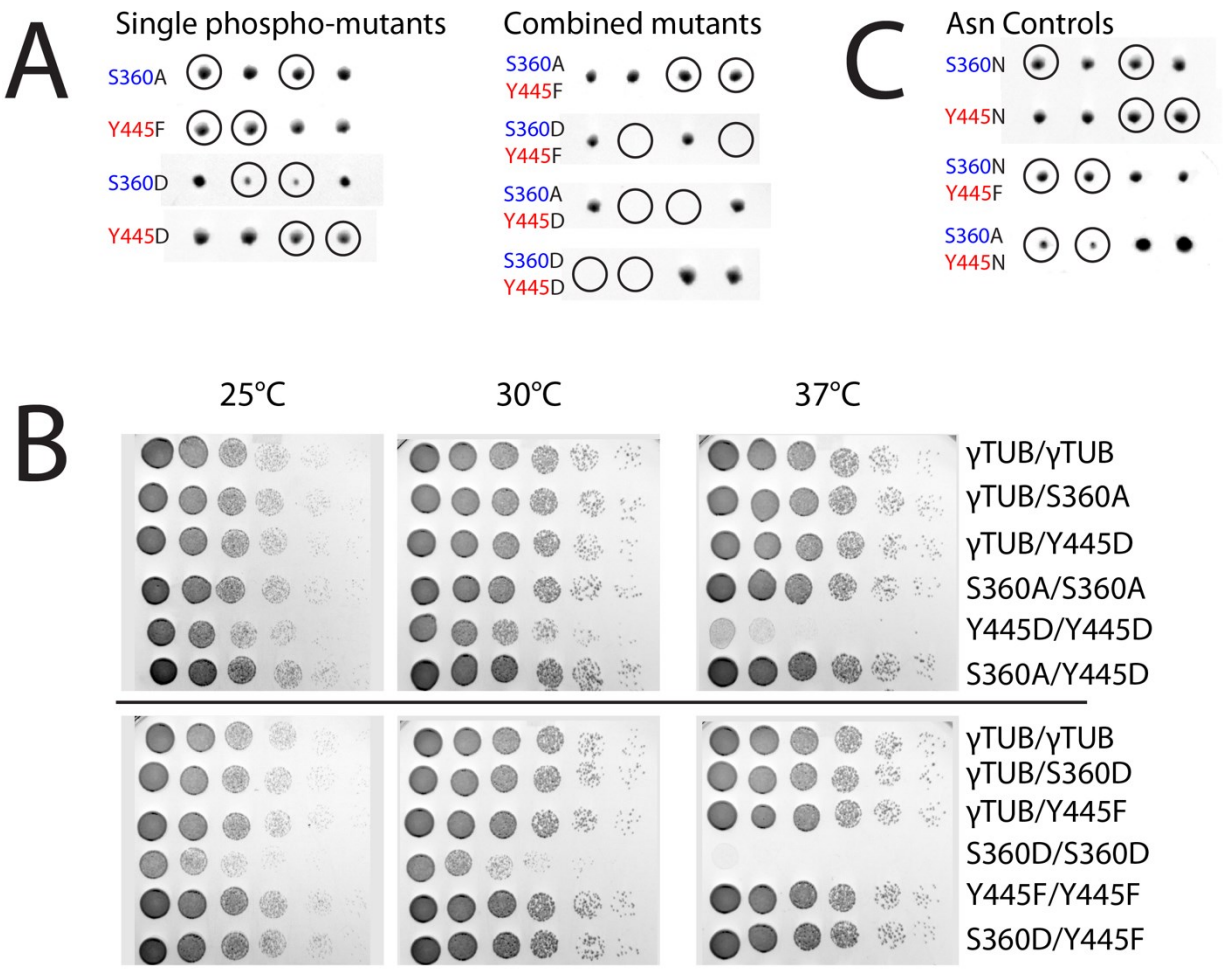

As pole localization of γ-tubulin is dependent on the formation of the γ-TuSC and subsequent interaction of Spc97/98 with Spc110 (in the nucleus) or Spc72 (in the cytosol)[404,428,431,432], the presence or absence of γ-tubulin at the SPB could be used as a read-out for the first two prerequisite steps of nucleation (first, the formation of the γ-TuSC, and second, the localization of the γ-TuSC to the SPB). We therefore sought to determine whether pole localization of γ-tubulin was affected in our lethal tandem mutants.

Initially, we tagged the mutant γ-tubulin alleles with EGFP; however, this was lethal for the S360D single mutant, (similar to when we attempted to tag the G1-phase T130D-T227D mutant) and is likely due to the added effect of the C-terminal tag (Figure 2.5A). Y445D-EGFP was not lethal but had slower growth than Y445D alone (Figure 2.5A). To account for the additional phenotypes added by the EGFP tag, we investigated mutant γ-tubulin localization indirectly by measuring changes in the localization of the wild-type allele in heterozygous diploids. We first compared the SPB integrated intensity between the wild-type control strain (γTUB-mNG/γTUB; n = 281 SPBs across 153 cells) and a γ-tubulin knockout negative control (γTUB-mNG/γtubΔ; n = 288 SPBs across 161 cells). When the γTUB-mNG allele was paired with a γ-tubulin knockout, the mean integrated intensity doubled with respect to the wild-type control (means of $4.12 \times 10^5 \pm 1.29 \times 10^5$ and $8.94 \times 10^5 \pm 2.32 \times 10^5$; $p < 1 \times 10^{-15}$; Figure 2.9A-C). This was expected as only half of the available γ-tubulin was tagged with mNG in the wild-type control, whereas all the available γ-tubulin was fluorescently tagged in the knockout negative control. This indicates that assessing the localization of the wild-type γ-tubulin allele could provide an indirect measure for the untagged mutant allele.

Figure 2.9 | Decreased localization for mixed phospho-status mutants. (A-B) Representative fields of view for diploids containing a single wild-type copy of mNG-tagged γ-tubulin (γTUB-mNG) (A); dashed boxes indicate inset cells (B). (C) Box plots showing the integrated intensity of spindle poles for γTUB-mNG/γtub mutant diploids. (D) Representative fields of view for Spc97-EGFP containing diploids. (E) Box plots showing integrated intensity of spindle poles for Spc97-EGFP heterozygous diploids. For representative fields of view, cell outlines are shown in white and the scale bars represent five microns. For box plots, red bars indicate the median of each population, box edges indicate the 25th and 75th percentile, dashed whiskers extend to the most extreme data points (not considered outliers) and outliers are shown with black asterisks. The number of poles and cells for each sample are shown below the box plots. WT, SAYD and SDYF stand for wild-type, S360A-Y445D and S360D-Y445F, respectively.

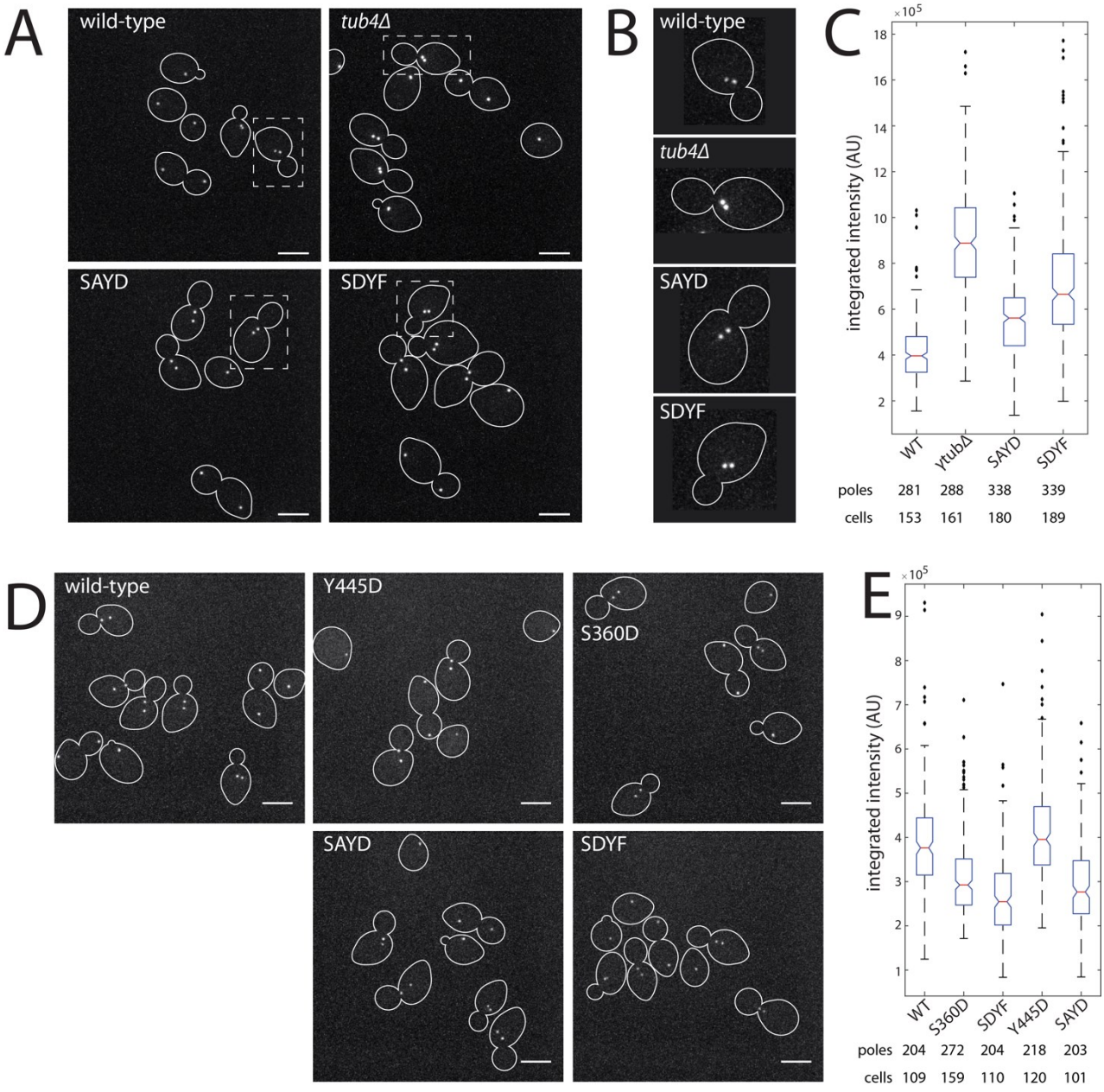
A
wild-type
tub4Δ
SAYD
SDYF
B
wild-type
tub4Δ
SAYD
SDYF
C
×10^5
integrated intensity (AU)
WT
YtubΔ
SAYD
SDYF
poles 281 288 338 339
cells 153 161 180 189
D
wild-type
Y445D
S360D
SAYD
SDYF
E
×10^5
integrated intensity (AU)
WT
S360D
SDYF
Y445D
SAYD
poles 204 272 204 218 203
cells 109 159 110 120 101

Fluorescence intensity was then measured in our lethal mutants (γTUB-mNG/γtub-SAYD and γTUB-mNG/γtub-SDYF; n = 338 SPBs across 180 cells, and 339 SPBs across 189 cells, respectively) (Figure 2.9A-C). Both mutant strains had significantly lower mean pole intensities than the knockout negative control (respective means of $5.56 \times 10^5 \pm 1.67 \times 10^5$ and $7.12 \times 10^5 \pm 2.68 \times 10^5$; $p < 1 \times 10^{-15}$ and $p = 1.33 \times 10^{-15}$, Table 2.4A and B) indicating that the mutant alleles partially localize to the poles. However, both strains also had higher intensities than the wild-type control (Figure 2.9C; $p < 1 \times 10^{-15}$ for both, Table 2.4A and B) suggesting that pole localization of the mutant γ-tubulin protein is significantly reduced and compensated for by an increased number of tagged wild-type protein on the poles. Alternatively, these lethal mutants could be acting as dominant negative alleles and reducing all levels of γ-tubulin on the poles. To verify these results, we also investigated γ-TuSC localization using a Spc97-EGFP tag (SPC97-EGFP/SPC97 diploids). Similar to the γTub-mNG results, SAYD and SDYF had significantly reduced mean pole intensities (Figure 2.9D-E; Table 2.4C and D for all means and p-values). This suggests that while pole localization of the γ-TuSC is reduced, SAYD- and SDYF-mutated γ-tubulin can form a γ-TuSC and localize to the pole.

Table 2.4 | Summary of values for fluorescence microscopy imaging of S360-Y445 lethal mutants. Number of cells, number of poles (n), mean integrated intensity of the pole and standard deviation (std dev) for γTUB-mNG-containing diploids (A) and Spc97-EGFP-containing diploids (C). Pairwise p-values for γTUB-mNG-containing diploids (B) and Spc97-EGFP-containing diploids (D).

A

strain	number of cells	number of poles	mean	± std dev
wild-type	153	281	4.12×10^5	1.29×10^5
γ-tubΔ	161	288	8.94×10^5	2.32×10^5
S360A-Y445D	180	338	5.56×10^5	1.67×10^5
S360D-Y445F	189	339	7.12×10^5	2.68×10^5

B

strain	comparison strain	p-value
wild-type	γ-tubΔ	$< 1 \times 10^{-15}$
wild-type	S360A-Y445D	$< 1 \times 10^{-15}$
wild-type	S360D-Y445F	$< 1 \times 10^{-15}$
γ-tubΔ	S360A-Y445D	$< 1 \times 10^{-15}$
γ-tubΔ	S360D-Y445F	1.33×10^{-15}
S360A-Y445D	S360D-Y445F	9.89×10^{-12}

C

strain	number of cells	number of poles	mean	± std dev
wild-type	109	204	3.90×10^5	1.15×10^5
S360D	159	272	3.11×10^5	0.90×10^5
S360D-Y445F	110	204	2.68×10^5	0.92×10^5
Y445D	120	218	4.14×10^5	1.14×10^5
S360A-Y445D	101	203	2.93×10^5	0.93×10^5

D

strain	comparison strain	p-value
wild-type	S360D	2.33×10^{-14}
wild-type	S360D-Y445F	$< 1 \times 10^{-15}$
wild-type	Y445D	0.3489
wild-type	S360A-Y445D	$< 1 \times 10^{-15}$
S360D	S360D-Y445F	8.45×10^{-5}
S360D	Y445D	$< 1 \times 10^{-15}$
S360D	S360A-Y445D	0.6014
S360D-Y445F	Y445D	$< 1 \times 10^{-15}$
S360D-Y445F	S360A-Y445D	0.0988
Y445D	S360A-Y445D	$< 1 \times 10^{-15}$

2.5 Discussion

2.5.1 Phospho-inhibiting mutants lack growth phenotypes

Pole specific γ-tubulin phosphorylation does not occur at standalone sites—all phospho-sites are clustered both spatially and/or temporally. G1 phospho-sites T130 and T227 are located on opposite faces of the protein and are ~3.1 nm apart from each other (Figure 2.1B). They are thus not clustered spatially, but rather temporally and, when combined, are sensitive to the loss of the SAC (Figure 2.3). M-phase phospho-sites are spatially clustered into three groups: S42-S43/T44, S360-Y362 and S444-Y445 (Figure 2.1). While the S42-S43/T44 phospho-mutants grew as wild-type, PM mutations at individual sites within the other clusters had phenotypes both independently and when combined ([1-3] and this study). Notably, no PI mutations had growth phenotypes—in fact, the simultaneous mutation of all eight phospho-sites to PI resulted in only a mild temperature sensitivity (Figure 2.2). This suggests that phosphorylation of γ-tubulin is not essential for viability; however, the remarkable conservation of those sites across species together with the fact that they are phosphorylated *in vivo* strongly indicate that phosphorylation provides an evolutionary advantage.

Assessment of growth is an easy way to quickly gage a phospho-sites' contribution to viability, but it is a coarse-grained method and does not reflect the requirement of the sites to a non-essential cellular function, like survival under specific circumstances. For example, in yeast, loss of the SAC (e.g. *mad2Δ*) has no growth consequence in healthy cells; however, under specific circumstances (i.e. disturbance of chromosome attachment), the SAC becomes essential. Moreover, yeast cells are robust and often have redundant mechanisms contributing to the same cellular function; for example, the two partially redundant pathways of spindle placement—Kar9 and dynein—can fully compensate each other in terms of growth but loss of them both is lethal. In fact, γ-tubulin mutant S360A clearly affects the cross-linking of MTs within the core bundle of the mitotic spindle despite its lack of growth phenotype[2]. Further investigation beyond growth assays will need to be done on the mutants with no discernable growth phenotype. The best way to cast a wide net is to use high-throughput screens, such as our recently published SGA-based GAMER method (discussed further in Chapter 3)[424].

2.5.2 G1-site mutants are involved in chromosome attachment

Phospho-residues T130 and T227 were identified from cells arrested in G1-phase using α-factor[1]. Here, we showed that the double PM mutation at these conserved residues was lethal when combined with loss of the SAC protein, Mad2 (Figure 2.3D). Otherwise mutations at these sites had no other phenotype despite a mild sensitivity to benomyl at 18°C, indicating MT function is largely undisturbed (Table 2.3 and Figure 2.4).

In yeast, SPB duplication occurs in G1-phase, beginning before the point of α-factor arrest (when T130 and T227 were identified)[174]. Interestingly, residue S131 in human γ-tubulin, located close to yeast T130 in both primary and tertiary structure (Figure 2.1C and Figure 2.3A-B), participates in centrosome duplication. SADB kinase phosphorylates human γ-tubulin at serine 131 which regulates centrosome duplication in S-phase by increasing MT polymerization locally to build the daughter centriole[353]. Intriguingly, the yeast SADB homolog, Hsl1, phosphorylated γ-tubulin in an *in vitro* high-throughput screen of yeast kinases[433]. Considering that T130 is phosphorylated at a time feasible for a role in SPB duplication, and that human residue S131 is involved in centrosome duplication, we hypothesized that these G1 sites, at least T130, may be involved in SPB duplication, possibly through the phosphorylation by Hsl1.

To determine if this was true, we assessed the number of SPBs in T130 and T227 mutants. In human cells, S131D mutants had amplified centrosome numbers, while S131A mutants had decreased numbers of centrioles[353]. Conversely, in yeast, mutating T130 (in combination with T227) did not lead to aberrant SPB numbers; all cells had normal counts of SPBs at all phases of the cell cycle (Figure 2.6A). This is not unexpected considering that, while the regulation and general function of centrosomes and SPBs are conserved, their structure and mechanism of duplication are very different[174,434-436].

Yeast SPBs are layered structures which are embedded in the nuclear envelope. Duplication is a conservative process and involves the formation of the satellite (SPB precursor) which matures and is eventually inserted into the nuclear envelope. Centrosomes, on the other hand, are made up of two general components: the centrioles which form the core, and the surrounding pericentriolar material (PCM) which is responsible for the nucleation of MTs. Duplication occurs semi-conservatively with each centriole stemming its own procentriole

(centrosome precursor) that slowly matures over two cell cycles. Despite these differences, recent high-resolution microscopy has revealed that the PCM is highly structured with various layers of proteins required for MT nucleation and anchorage, similar to the spindle pole body[167-170]. Additionally, several similarities between SPBs and the PCM have been noted including the high content of coiled-coil proteins and the similarities between Spc110 and pericentrin[186,437-442].

Interestingly, S131D had different effects on MT growth depending on whether the MTs were nucleated from within the centriole or from the PCM. This mutation increased MT polymerization at the centriole, but decreased MT polymerization from the PCM[353]. How regulation at this residue leads to opposite effects on different components of the centrosome is not known, but it is possible that studying this site in yeast may aid in understanding its role in the PCM as it is more similar to SPBs.

In yeast, the T130D-T227D mutants had a striking dependence on the SAC suggesting that these cells have difficulties with chromosome attachment. It is possible that this is due to a reduction in the number of spindle MTs, especially in light of the observed decrease in T130D-T227D γ-TuSC pole localization (Figure 2.6). In fact, the γ-tubulin mutant S360D experiences a decrease in interpolar MT number which leads to perturbed spindle assembly. As a result, S360D is lethal when combined with the loss of Mad2; however, this mutant is also severely temperature sensitive[1,2]. Similarly, all γ-tubulin phospho-mutants (to date) which are dependent on the SAC experience temperature sensitivity on account of their disrupted MT function[1-3]. Conversely, T130D-T227D does not have any temperature sensitivity and, in fact, has no other strong phenotype (Table 2.3) suggesting that MT function is largely unaffected. Thus, it is quite intriguing as to why it is sensitive to the loss of *mad2Δ* as it seems unrelated to MT function. We suspect that these sites contribute to chromosome attachment independent of spindle function, possibly through the regulation of MT associated proteins (MAPs) or other proteins involved in kinetochore capture and attachment. Measuring the spindle dynamics[2] in T130D-T227D would help determine if spindle function was truly unperturbed. Additionally, conducting a high-throughput analysis of genetic interactions (e.g. using a GAMER analysis as is described in Chapter 3) would greatly aid in narrowing the specific function of G1 phosphorylation in budding yeast[424].

2.5.3 Intramolecular relationships within M-phase clusters

The majority of the γ-tubulin phospho-sites were isolated in M-phase arrested cells and form three different clusters[1]. While mutations within the S42-S43/T44 cluster did not show any discernable growth phenotypes, the remaining two clusters had phenotypes when PM mutations were made within or between clusters, as was combining different types of phospho-mutants across the S360-Y362 and S444-Y445 clusters (Figure 2.8A).

Creating two PM mutations at S360 and Y362 was lethal for the cell (Figure 2.5B). These two sites have been implicated in separate cellular processes: S360 in spindle assembly and Y362 in spindle alignment (discussed in Chapter 3). However, γ-tubulin's roles in these processes are likely related, especially since these processes occur concurrently and both rely on the balance of forces associated with the spindle. Spindle assembly relies on the forces existing within the inner spindle (i.e. interpolar and kinetochore MTs in the nucleus), while spindle alignment depends on the forces acting on the outer spindle (i.e. astral MTs in the cytoplasm). However, nuclear and cytoplasmic MTs are not completely independent. Firstly, they share several of the same MAPs and the disruption of MAP distribution in one compartment of the cell can have detrimental effects on the spindle function in other compartments, as is seen with Kar9 and Bim1[135]. Secondly, nuclear and cytoplasmic MTs are physically connected (via the plaques of the SPB). Thus, the forces associated with these MTs are not autonomous. Fluctuations in spindle length report the relative spindle stability[2]; large fluctuations (e.g. as is seen in S360D) are thus indicative of severely unstable spindles. Spindle instability is likely to disrupt the cells' attempts to properly align its spindle. Thus, the lethality of S360D-Y362D could be explained by the simultaneous disruption of two essential and related MT-dependent functions, spindle assembly and spindle placement. Alternatively, another explanation for S360D-Y362D lethality may be that as S360D cells are sick to begin with, addition of another constitutively charged residue at this location may disrupt the structure of γ-tubulin and/or formation of the γ-TuSC. Purification of S360D-Y362D-containing γ-TuSCs followed by cryo-electron microscopy may be necessary to assess proper complex formation and structure, respectively. Regardless, we believe that S360 and Y362 are not phosphorylated in tandem and as S360 regulates spindle assembly and Y362

regulates spindle placement, we suspect phosphorylation of these sites may be restricted to different cellular compartments (the nucleus or cytoplasm, respectively).

In contrast to the S360-Y362 cluster, creating a double PM mutant at residues S444-Y445 did not enhance the phenotype of Y445D alone (Figure 2.5). This is perhaps not unexpected as S444 is often replaced with a charged amino acid (aspartic acid) in animals (Figure 2.1C). This could suggest that this residue is constitutively phosphorylated *in vivo*.

2.5.4 The intramolecular relationship across M-phase clusters

Intramolecular relationships of mutations within the same cluster were not surprising; however, relationships between different clusters were more unexpected. Several different combinations of phospho-mutations at S360 and Y445 resulted in cell lethality (Figure 2.8A). Both combinations of mixed phospho-status—S360A-Y445D (SAYD) or S360D-Y445F (SDYF)—caused unexpected lethality. This suggests that phosphorylation prevention at one site while the other is constitutively phosphorylated is detrimental to the cell. To control for the change in steric effects caused by an aspartic acid mutation, we also mutated the phospho-sites to asparagine. This rescued the slow growth of S360D and Y445D, and the lethality of SDYF suggesting that these phenotypes were not due to allosteric effects but rather to a change in charge (Figure 2.8C). However, SAYD was not fully rescued by SAYN suggesting that the lethal phenotype is in part due to the change in steric effects associated with a tyrosine to aspartic acid mutation. This is not surprising as tyrosine, unlike serine, contains an aromatic side group and is completely different in structure from aspartic acid. These asparagine controls confirmed that most of the observed phenotypic growth defects were caused by the additional charge of aspartic acid, and thus more biologically relevant for the study of phosphorylation at these sites (as phosphorylation changes the charge of the residue).

As localization of the γ-TuSC is a prerequisite for MT nucleation, these mutants were tested for disrupted γ-TuSC pole localization. Both SAYD and SDYF decreased γ-TuSC pole localization though did not prevent it entirely (Figure 2.9) suggesting that SAYD and SDYF proteins are not completely degraded and are at least partially stable. Pole localization is a proxy for γ-TuSC formation, as well as the complex's ability to locate to the pole, both of which are essential for downstream MT nucleation. So, it stands to ask whether this observed decrease in pole

localization is enough to warrant lethality by not providing adequate templates for nucleation? The difficulty in answering this question is that both the minimum number of inner plaque γ-TuRCs required for viability, as well as the total number of γ-TuRCs present at the inner plaque, are not known. However, yeast have a very characteristic inner spindle architecture with 16 kinetochore MTs, and ~4 interpolar MTs[443,444]. Thus, theoretically, they only require ~20 active γ-TuRCs on the inner plaque. However, the actual number of inner plaque γ-TuRCs has not yet been accurately quantified. It is difficult to measure as not all γ-TuRCs may be complete (i.e. composed of seven Spc97, seven Spc98 and 14 γ-tubulin molecules), some may be only partially assembled. The inner plaque γ-TuSC receptor, Spc110, can form complete or partial rings *in vitro*[175], however, the stability of partial rings has not been assessed.

Though we cannot accurately determine at this time whether SAYD and SDYF recruit enough γ-TuSC for viability, we can compare them to other diploid mutants that are known to be viable as haploids. The SAYD mutant had ~25% less γ-TuSC pole localization than wild-type; this was statistically the same as S360D's pole localization, a mutant known to be viable as a haploid ([1] and Figure 2.9E). As S360D cells do not have significantly less MTs than wild-type[2], they therefore, must have enough γ-TuSCs at the poles to nucleate a normal number of MTs. Thus, by extension, SAYD likely has enough γ-TuSC at the poles for viability and we do not think perturbed γ-TuSC formation or pole localization is the reason for its lethality.

On the contrary, SDYF had the lowest pole localization of all mutants tested (except the γ-tubulin knockout negative control) with 42% less γ-TuSC localization that wild-type in γTUB-mNG diploids and 31% less in SPC97-EGFP diploids (Figure 2.9C and E; Table 2.4). This discrepancy could be due to the different effects the fluorescent tags have on complex formation; perhaps the mNG tag perturbs the capacity of γTub-mNG and SDYF to form a complex together. Regardless, SDYF had a significantly lower γ-TuSC localization than any viable haploid mutant. As a result, we cannot determine whether this mutant has enough pole-bound γ-TuSC to perform essential MT-dependent functions.

In summary, both SAYD and SDYF had decreased γ-TuSC pole localization. SDYF had a more severe loss of γ-TuSC at the poles, thus we cannot conclude whether the lethality of SDYF is caused by inadequate amounts of γ-TuSCs on the poles. Purification of SDYF-containing γ-TuSCs

is required to investigate whether this mutation disrupts the formation of the complex (and subsequent localization) or whether γ-TuSCs form normally but are unable to localize to the pole. The latter might occur if, for example, an unknown protein binding partner is constitutively binding and sequestering γ-tubulin or the γ-TuSC. Conversely, we think it unlikely that the decreased γ-TuSC localization caused the observed lethality seen in SAYD. Instead, we suspect that the mixed phospho-status between S360 and Y445 constitutively prevents either an essential γ-tubulin-dependent function or another essential cellular function. This may be nucleation, γ-tubulin's only known essential function (as of yet); alternatively, it may prevent a protein binding partner from carrying out its own essential function.

Residue S360 is involved in spindle assembly and Y445 is also likely related to spindle assembly[2,3]—in Chapter 3, we confirm the involvement of Y445 in spindle assembly. Thus, we propose that these sites provide a structural means of communication across γ-tubulin which leads to the observed intramolecular genetic interactions. For example, phosphorylation at one site may cause a conformational change at the other, unmasking a site for protein-protein interaction. Residue Y445 exists at the base of the intrinsically disordered C-terminal tail of γ-tubulin. Recently, nuclear magnetic resonance spectroscopy and Monte Carlo simulations have shown that the wild-type C-terminal tail exists mostly in a form collapsed against the globular body of the protein[427]. However, the Y445D mutation caused millisecond timescale dynamics across the entire tail leading to a higher propensity for an extended tail conformation ([427] and Figure 2.10A). Presumably, phosphorylation at this site would allow access to areas of the protein previously masked by the collapsed tail. Thus, this residue is proposed to regulate the tail as a "tunable antenna" for the recruitment of specific γ-tubulin interacting proteins[427].

We suspect that the observed coupling between phospho-sites S360 and Y445 feeds into this structural change, either by increasing or decreasing the propensity for the extended tail conformation. The S360 residue lies at the end of a β-strand which is preceded by a looped intrinsically disordered region (Figure 2.10B). This loop is very close in proximity to Y445 and could potentially be the structural means of communication between residues S360 and Y445. High resolution structural analysis (e.g. high resolution cryo-electron microscopy or single particle analysis) of these S360-Y445 γ-tubulin mutants will help determine if this hypothesis has

any validity. Additionally, identification of loss or gain of physical interacting partners in these mutants using a high-throughput screening method, such as the optimized yeast cytosine deaminase protein-fragment complementation assay (OyCD PCA)[402] will aid greatly in understanding this coupling. Alternatively, this intramolecular protein communication may be a means to regulate nucleation. Investigating the nucleation capacity of these mutants *in vitro*[175] or *in vivo* (Trisha Davis, personal communication) will be necessary to determine whether this is the case.

Multisite phosphorylation and, more specifically, phospho-site clustering are widely-observed phenomena. Multisite phosphorylation, defined as the phosphorylation of more than one site within a protein, is ubiquitous across eukaryotes and is involved in numerous cellular processes[445-450]. Spatial phospho-site clustering is less common but is seen frequently in CDK motifs governing cell cycle control[451,452] and within the DNA damage response[453,454]. These clusters may include a mix of different regulatory elements (e.g. phospho-sites of different kinases, localization signals, degradation signals, protein-protein interaction domains, etc.)[452] and are thought to provide precise control over protein activity patterns, regulatory thresholds/switch-like responses or cooperative binding[446,452,455]. We suspect that γ-tubulin is regulated in this manner, both between the G1-phase sites and between sites S360 and Y445 (Figure 2.10C). Our results suggest that the G1 phosphorylated sites T130 and T227 are genetically linked and involved in a process related to proper chromosome attachment, though as MT growth seems largely unaffected, we suspect this is independent of spindle function (Figure 2.10C-1). Similarly, the intramolecular relationship between mitotic sites S360 and Y445 suggests a structural mechanism of spindle assembly regulation occurring across the protein (Figure 2.10C-2). This type of regulation is something that has not been described for γ-tubulin and opens an exciting new avenue for investigation of γ-tubulin regulation and its potential role as a hub for protein regulation.

Figure 2.10 | Conceptualizing the interplay of γ-tubulin regulation. (A) The γ-tubulin C-terminal tail exists mostly collapsed against the globular portion of the protein (top); Y445D (green) causes a higher propensity for the tail to take on an extended conformation (bottom)[427]. (B) Ribbon structure of the last 130 residues of γ-tubulin (residues 343-473). Residues S360 and Y445 are indicated by blue or cyan spheres, respectively. Intrinsically disordered regions (IDRs) are shown in yellow, β-strand in green, α-helices in blue, and the intrinsically disordered C-terminal tail is shown in purple. (C) Schematic summary of the coupling of residues across γ-tubulin. (C-1) Phospho-sites T130 and T227 are temporally linked and when mutated to PM together required the presence of the SAC for survival. The reason behind this is not known but is likely independent of spindle function. (C-2) S360 and Y445 are both involved in spindle assembly and have strong intramolecular genetic interactions suggesting a method of across-protein regulation. (C-3) Spindle assembly and spindle positioning occur concurrently and as inner and outer plaque MTs are both physically connected and share many of the same MAPs, disruption of one is likely to disrupt the other.

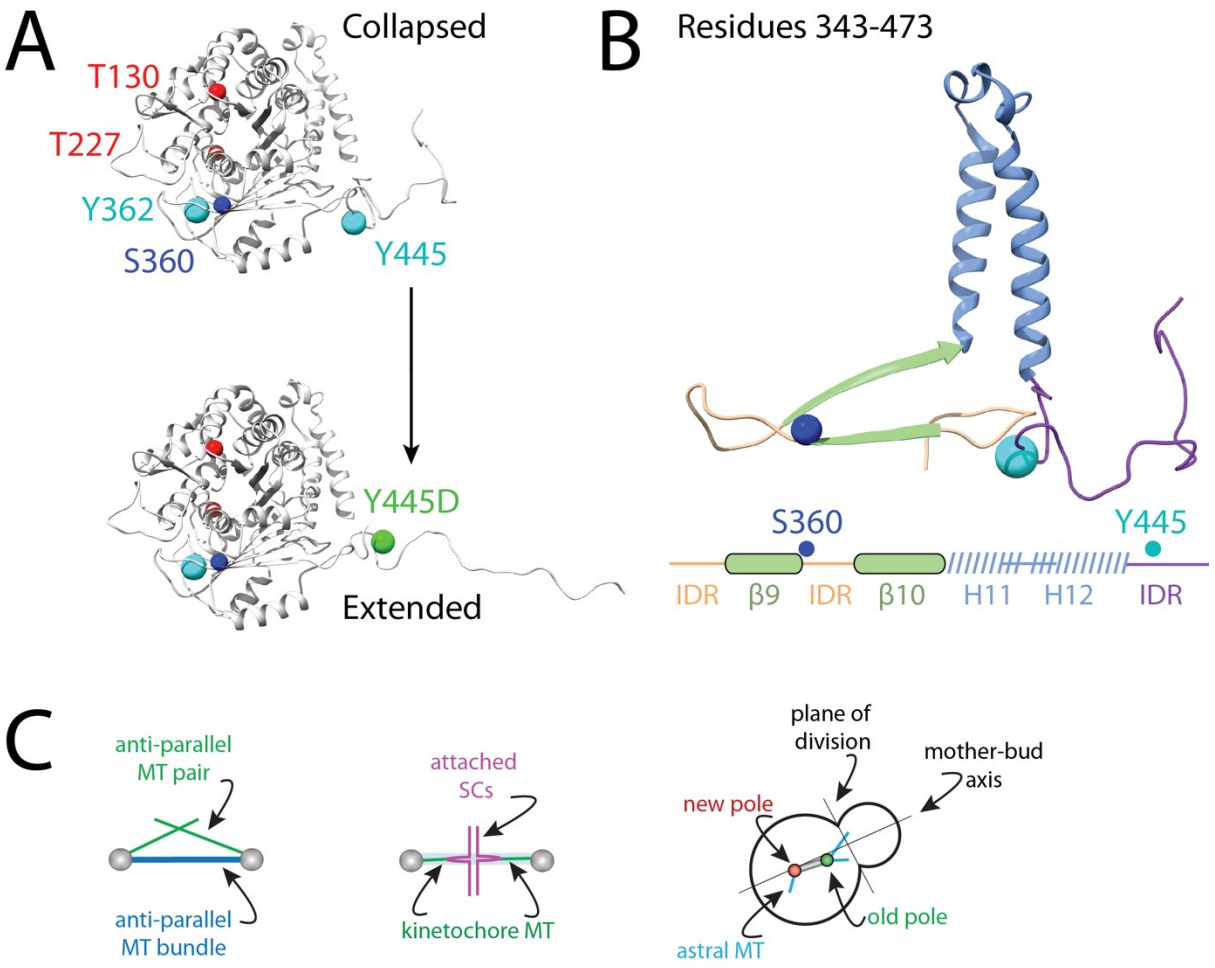
A
Collapsed
T130
T227
Y362
S360
Y445
Y445D
Extended
B
Residues 343-473
S360
Y445
IDR
β9
IDR
β10
H11
H12
IDR
C
anti-parallel
MT pair
anti-parallel
MT bundle
attached
SCs
kinetochore MT
plane of
division
mother-bud
axis
new pole
old pole
astral MT
T130D
1
T227D
?
S360D
2
Y445D
unstable
chromosome loss
3
?
mis-aligned
Y362E

Chapter 3: Interrogation of γ-tubulin alleles using high-resolution fitness measurements reveals distinct cytoplasmic function in spindle alignment

3.1 Summary

γ-Tubulin has a well-established role in nucleating the assembly of microtubules, yet how phosphorylation regulates its activity remains unclear. Here, we use a time-resolved, fitness-based SGA approach to compare two γ-tubulin alleles (Y362E and Y445D). We find that the genetic interaction profile of Y362E is enriched in spindle positioning and cell polarity genes relative to that of Y445D, which is enriched in genes involved in spindle assembly and stability. In Y362E cells, we find a defect in spindle alignment and an increase in the number of astral microtubules at both spindle poles. Our results suggest that the Y362E allele is a separation-of-function mutation that reveals a role for γ-tubulin phospho-regulation in spindle alignment. We propose that phosphorylation of the evolutionarily conserved Y362 residue of budding yeast γ-tubulin both contributes to regulating the number of astral microtubules associated with spindle poles, and promotes efficient pre-anaphase spindle alignment.

3.2 Introduction

γ-Tubulin is an evolutionarily conserved member of the tubulin superfamily[456,457] whose essential function is the nucleation of microtubules (MTs) in eukaryotic cells[457-462]. In budding yeast, γ-tubulin is encoded by the essential gene *TUB4*[463]. γ-Tubulin, Spc97 and Spc98 form the γ-tubulin ring complex (γ-TuRC) located on the nuclear and cytoplasmic surfaces of spindle pole bodies (SPBs). SPBs serve as the centrosome in yeast cells and remain embedded in the nuclear envelope throughout mitosis[464-466]. The γ-TuRC nucleates both spindle (nuclear) and astral (cytoplasmic) MTs[426,431,467]. At the SPB, γ-tubulin is proposed to be in the form of "active" γ-TuRCs (i.e. nucleation competent)[175]. The pool of γ-tubulin bound to purified SPBs is phosphorylated at eight residues: two (T130 and T227) are specific to cells arrested in G1-phase, and six (S42, S43/T44, S360, Y362, S444 and Y445) are specific to cells arrested in metaphase[1]. Residues S360, Y362 and Y445 (Figure 3.1A) are extremely well-conserved[1,3]. Phosphorylation of residues S360, Y362 and Y445 occurs between S-phase and metaphase, before the anaphase transition[1]. This is a time in the cell cycle that is functionally relevant to spindle assembly and sister chromatid attachment[468].

The conservation of S360, Y362 and Y445 between yeast and human[1] suggests that phospho-regulation of these residues is a general mechanism for controlling the activity of γ-tubulin. To date, there is no evidence that phosphorylation of the pool of γ-tubulin bound to the SPBs contributes to the activation of γ-TuRCs[175]. Phosphorylation of S360 and Y445 likely contribute to events in spindle assembly (Figure 3.1B). Mutation of S360 alters the number of antiparallel MTs that provide stability to the spindle. An alanine substitution at this residue increases the number of antiparallel MTs and stabilizes the spindle, while substitutions—such as aspartic or glutamic acid—that introduce a local negative charge and mimic constitutive phosphorylation block the formation of antiparallel MTs and decreases spindle stability[2]. Mutation of Y445 disrupts spindle function[3] and causes chromosome loss[4]; as a result, Y445D cells cannot survive in the absence of the spindle assembly checkpoint (SAC)[3,217,469]. An internal deletion of S444, Y445 and their adjacent residues (DSYL) within the intrinsically disordered C-terminus of γ-tubulin perturbs both spindle assembly and pre-anaphase spindle positioning[338,344].

As with S360 and Y445, Y362 is also evolutionarily conserved, however the biological function of this modification is unknown.

Separation-of-function mutations are extremely useful genetic tools in cell biology, and aid in understanding the biological significance of γ-tubulin phospho-regulation. Separation-of-function mutations can be identified through the analysis of synthetic genetic interactions (SGIs) discovered by conducting synthetic genetic array (SGA) screens[470]. The SGA screen is a robotic-assisted method used to assess genetic interactions of mutations arrayed on plates; typically, the array consists of non-essential gene knock-outs[73,411,471,472]. The relative growth of each strain (wild-type controls, query, array and double mutants) is extracted using end-point analysis of colony size, with the growth of the double mutant compared to that of each single mutant. If the double mutant has an unexpected phenotype, an SGI is inferred. For null or loss-of-function mutations, the SGI profiles of functionally redundant genes converge, with genes in one pathway showing strong SGI congruence with those in parallel, redundant pathways[73]. However, a subset of unique SGIs is expected in the case of separation-of-function mutations when comparing SGI profiles for a series of alleles. Analysis of alleles presents an additional challenge, as they may exhibit phenotypic differences dependent on the process that is perturbed by the mutation. For example, an allele with a mutation that perturbs one of two spindle placement pathways may exhibit a weak phenotype in comparison to an allele with a mutation that perturbs chromosome attachment. An SGA-based approach for detection of separation-of-function mutations must therefore be sensitive to differences in relative fitness of both single and double mutants, and also be precise in measurements such that the SGI profiles for multiple alleles of the same gene can be compared.

In this study, we describe GAMER (Genetic Array with Mixed Effects Regression)—a time-resolved and fitness-based SGA method—and use this approach to perform a comparative functional analysis between two γ-tubulin alleles (Y362E and Y445D). We did this by using both alleles as query mutations and extracting their SGIs when combined with ~4,700 SGA deletion mutations. Growth rates were computed and used to calculate the fitness of all strains (wild-type controls, query, array and double mutants), and to compare relative fitness of the two γ-tubulin query alleles. The SGI profile for the previously described Y445D mutation[3] was enriched for

genes that are involved in spindle assembly and stability, act in chromosome segregation, or function in the SAC monitoring the fidelity of sister chromatid attachment. The SGI profile for the Y362E mutation showed convergence with the Y445D mutant for a subset of genes involved in mitosis, but also had a distinct set of SGIs with genes acting in spindle placement, as well as cell polarity. Live cell analysis of spindle stability and movements relative to the bud neck and polarity axis revealed that the Y362E mutation does not alter spindle stability but is defective in pre-anaphase spindle alignment. We report that in the Y362E mutant, the number of astral MTs is increased, and the bias of astral MTs to the pre-existing SPB relative to the newly-formed SPB is lost. This leads to inefficient spindle alignment. Our results provide new evidence that the phosphorylation of an evolutionarily conserved tyrosine residue (Y362) contributes to γ-tubulin function: Y362 controls the number of astral MTs associated with both SPBs during S- to M-phase and influences the efficiency of pre-anaphase spindle alignment relative to the future plane of cell division.

3.3 Materials and methods

3.3.1 Strains, plasmids, genetic manipulation and growing conditions

All yeast strains are derivatives of BY4741[473] and are listed in Table 3.1. All plasmids used in this study are listed in Table 3.2. Point mutations (Y362E, Y445D*,* etc.) were generated on plasmids using USER™ cloning[414] followed by sequencing to confirm error-free introduction of the desired mutation. PCR-based methods were used to integrate point mutations and fluorophore tags into the native gene locus on the chromosome under the endogenous promoter[474]. Venus-Tub1 was made by integrating pHIS3p:Venus-Tub1+3'UTR::HIS3 (gift from Wei-Lih Lee, Addgene plasmid # 50656)[475,476] into the knocked out *his3Δ1* locus of BY4741, with the Venus-Tub1 fusion expressed under the native *HIS3* promoter. Yeast strains were grown in rich medium (YEPD: yeast extract, peptone, dextrose)[418] at 25°C unless otherwise stated. For fluorescence live-cell microscopy, cells were grown in synthetic complete (SC) medium[419]. Bacterial cells used from cloning were grown at 37°C in LB medium supplemented with 100 μg/mL of carbenicillin.

3.3.2 Live cell microscopy

Yeast cells expressing Spc42-Cerulean were grown to log phase in SC medium supplemented with 2 mM of ascorbate, and imaged at 25°C on a custom-built spinning-disk confocal microscope as previously described[2]. Briefly, the following components were installed on a Leica DM6000 inverted microscope: a 100x/1.46 numerical aperture plan apochromatic objective, an XY stage with a Z top piezo (Applied Scientific Instrumentation), a Borealis head (a Quorum conversion of a Yokogawa QLC-100). Solid state lasers (446 and 515 nm) with an emission filter wheel were used for multicolor imaging. A Hamamatsu ImagEM EM-CCD camera was used for detection. MetaMorph (Molecular Devices) was used for image acquisition. Images were collected in a streaming regime as Z-stacks (200 or 300 nm Z-steps across 31 or 30 focal planes, respectively) with an integration time of 50 ms per focal plane. For spindle dynamics and alignment studies, cells were imaged over ten minutes with a ten second time step between stack acquisitions. For imaging astral MTs in live cells, strains containing Venus-Tub1 were imaged over five minutes with a five second time step between stack acquisitions (the Spc42-Cerulean pole reporter was collected with ten second time steps in these strains).

3.3.3 Analysis of spindle stability, alignment, positioning and orientation

Pole-tracking was implemented using MatLab (Mathworks) as previously described[2]. Briefly, SPBs were fit to 3-dimensional gaussians and tracked by nearest neighbour analysis. Spindle stability was measured by computing the standard deviation of the instantaneous spindle lengths (referred to as spindle fluctuations) of each cell over the ten-minute time course. For spindle positioning and alignment, the bud neck was defined by manually drawing a line through the neck in the brightfield image. Spindle positioning at the bud neck was measured by calculating the mean distance between the SPB proximal to the bud and the bud neck. This distance was normalized to the length of the mother to adjust for minor differences in the size of the mother compartment. One-dimensionally projected spindle length was calculated by projecting the SPB coordinates onto the polarity axis, perpendicular to the bud neck plane (Figure 3.6A). Spindle orientation was assessed by first assigning the SPBs as either pre-existing (old) or newly-formed (new) based on the mean integrated intensity of Spc42-Cerulean over the ten-minute time course, with the brighter SPB identified as the old SPB[2]. A spindle was considered misoriented if

the SPB proximal to the bud neck had a lower mean integrated intensity (i.e. was the new SPB) than the distal pole. Spindle alignment heatmaps were generated first as bivariate histograms of 30 x 30 bins and then smoothed with bicubic interpolation to give 180 x 180 bins. The color indicates the normalized frequency of data points in each bin across all analyzed cells; the maximum normalized frequency (dark red) indicates all bins with a normalized frequency ≥ 0.015.

3.3.4 Analysis of astral MTs

Wild-type and Y362E cells with Venus-Tub1-labeled astral MTs were analyzed using Fiji[477]. Astral MTs projecting from each SPB (labeled with Spc42-Cerulean) were detected in maximum projections and counted manually in all time points (61 time points per cell over five minutes, with a time step of five seconds). Astral MTs were only counted once they were resolvable from the central spindle and could be observed for at least two time points. This dataset was used to compute the mean number of astral MTs per spindle, the mean number of astral MT per SPB, and the number of time points where both SPBs had at least one astral MT during the five-minute acquisition. Intensity of astral MTs was not considered (i.e. we did not discriminate between bundled astral MTs which would appear brighter than a single astral MT), therefore, these data may underestimate the number of astral MTs per spindle/SPB.

3.3.5 Statistics used for image analysis

Distributions were tested for normality using a one-sample Kolmogorov-Smirnov test. To test for differences in spindle fluctuations, the variance of changes in spindle length (i.e. between two neighbouring time points) was assessed between strains using a Bartlett's test. Distributions for normalized mean distance from the neck were assessed using the Kruskal-Wallis test followed by a Dunn-Šidák correction. Distributions for the mean number of astral MTs per spindle and for the percentage of total time both poles had astral MTs were assessed for differences using the Wilcoxon rank sum test/Mann-Whitney U-test.

Table 3.1 | Yeast strains used in this study.

Yeast Strain	Genotype	Notes	Reference
YV838, YV856, YV2175, YV2176	*SPC42-cerulean-HYGB; MATa; his3Δ1; leu2Δ0; ura3Δ0; met15Δ0*	wild-type; isolate 1, 2, 3, 4	Nazarova, *et al*., 2013[2] and this study.
YV2275, YV2276, YV2464	*tub4-Y362E-NAT; SPC42-cerulean-HYGB; MATa; his3Δ1; leu2Δ0; ura3Δ0; met15Δ0*	γ-tub-Y362E; isolate 1, 2, 3	This study.
YV2098, YV2361, YV2362	*tub4-Y445D-NAT; SPC42-cerulean-HYGB; MATa; his3Δ1; leu2Δ0; ura3Δ0; met15Δ0*	γ-tub-Y445D; isolate 1, 2, 3	This study.
YV2230, YV2231, YV2232	*kar9Δ::KAN*; *SPC42-cerulean-HYGB; MATa; his3Δ1; leu2Δ0; ura3Δ0; met15Δ0*	kar9Δ; isolate 1, 2, 3	This study.
YV2235, YV2236, YV2237	*dyn1Δ::KAN*; *SPC42-cerulean-HYGB; MATa; his3Δ1; leu2Δ0; ura3Δ0; met15Δ0*	dyn1Δ; isolate 1, 2, 3	This study.
YV2331, YV2332, YV2333	*tub4-Y362E-NAT; kar9Δ::KAN*; *SPC42-cerulean-HYGB; MATa; his3Δ1; leu2Δ0; ura3Δ0; met15Δ0*	γ-tub-Y362E; kar9Δ; isolate 1, 2, 3	This study.
YV2492, YV2493	*tub4-Y362E-NAT; dyn1Δ::KAN*; *SPC42-cerulean-HYGB; MATa; his3Δ1; leu2Δ0; ura3Δ0; met15Δ0*	γ-tub-Y362E; dyn1Δ; isolate 1, 2	This study.
YV2500, YV2501, YV2502	*HIS3::venus-TUB1; SPC42-cerulean-HYGB; MATa; his3Δ1; leu2Δ0; ura3Δ0; met15Δ0*	wild-type; isolate 1, 2, 3	This study.
YV2509, YV2510, YV2511	*tub4-Y362E-NAT, HIS3::venus-TUB1; SPC42-cerulean-HYGB; MATa; his3Δ1; leu2Δ0; ura3Δ0; met15Δ0*	γ-tub-Y362E; isolate 1, 2, 3	This study.

Table 3.2 | Plasmids used in this study.

Plasmid	Description	Reference
pJV0372	pBKS-*tub4*-NAT	This study.
pJV0373	pBKS-*tub4-Y362E*-NAT	This study.
pJV0374	pBKS-*tub4-Y445D*-NAT	This study.
Addgene #50656	pHIS3p:Venus-Tub1+3'UTR::HIS3	Markus *et al*., 2015[475]

3.3.6 Synthetic genetic array

Strains undergoing the SGA process were iteratively grown to select for double mutants using previously described media[471] with the aid of a Beckman Coulter Biomek robot. In order to measure the growth rates, an additional robotics platform (based on Beckman Coulter's robotic Orca Arm) photographs each final selection plate every two hours for 72 hours using a Nikon DSLR camera.

3.3.7 SGA image processing

After data acquisition, the density of each single colony was extracted from every image. Density is calculated from the integrated intensity of the pixels within the colony. As pixel intensity increases with colony height, density is a read out of both colony size and colony volume. To maximize colony detection, a computationally generated grid was overlaid on each plate. Each grid tile contained at most a single colony and was analyzed for the presence of a colony from the last time point back to the first time point. A watershed algorithm was then applied to separate the colony from the background, and density was measured as the integrated intensity over the background of these pixels.

To generate a grid which does not intersect a colony, we first identified colonies using a coarse-grained method based on the circular Hough transform. Since the colonies are pinned in a regular pattern, circular objects that were either too close or too far from one another were removed. The grid lines were fit to these objects such that they did not intersect with the objects and followed the regular pattern of the pin tool. This resulted in grid tiles containing at most one colony. When an insufficient number of objects was found for grid fitting (less than 100), the grid lines from the later time point were used.

In order to measure the fitness of a colony, the densities were fit to a Gompertz growth equation of the form:

$$Density(time) = A * \exp(B * \exp(-GR * time)) \quad (1)$$

where *A* is the maximum density of the colony, *B* is proportional to the initial size at time zero, *exp* is the exponential function with base e, *GR* is the growth rate, and *time* is the elapsed time since the first data point. Here, the growth rate parameter is akin to the doubling time of a

single cell and represents the health of the colony. We then normalized the colony densities such that

(2) $$Density(time) = 1 * \exp(B * \exp(-GR * time))$$

Then, we applied a double logarithm to transform the Gompertz equation into a simple linear equation:

(3) $$\log(\log(Density(time)) = \log(B) - GR * time$$

which is of the form: $y = b + m * x$. Since the parameter of interest is the growth rate, we re-centered time such that $\log(\mathrm{B}) = 0$, giving the equation:

(4) $$\log(\log(Density(time')) = -GR * time'$$

where $time'$ is the shifted time.

3.3.8 GAMER mathematical model

We defined the competitive fitness of strain i as: $F_i = GR_i/GR_{WT}$ where GR_i is the growth rate of strain i and GR_{WT} is the growth rate of the wild-type reference. A true genetic interaction was inferred when the fitness of the double mutant was significantly different from its expected fitness (defined as the product of the individual mutants' fitness)[478-481]:

(5) $$F_{ij} = F_i * F_j$$

where F_{ij} is the fitness of the double mutant with mutations i and j.

This definition of the expected fitness of the double mutant is appropriately modelled by a single linear mixed-effects model. This allowed us to model the growth rates of each colony for the four genotypes (WT, *i*, *j*, *ij*) using two categorical variables. The only assumption of the model is that all the yeast mutants we screened are derived from a common background strain. This allowed us to assume that any observable growth defects in the mutants (both the single and double mutants) can be attributed to the mutation(s).

For the single mutant *i*, the growth rate was modelled as: $GR_i = GR_{WT} + d_i$, where d_i is the measurable defect in the growth rate associated to the mutation relative to the common background strain. In the case of the double mutant, the growth rate was modelled as $GR_{ij} = GR_{WT} + d_i + d_j + d_{ij}$, where d_{ij} is the measurable growth defect present only in the double

mutant. The expected value of d_{ij} was determined by substituting the fitness terms in the expected fitness equation with the growth rate terms:

(6) $$\frac{GR_{ij}}{GR_{WT}} = \frac{GR_i}{GR_{WT}} * \frac{GR_j}{GR_{WT}}$$

(7) $$GR_{ij} = \frac{GR_i * GR_j}{GR_{WT}}$$

(8) $$GR_{WT} + d_i + d_j + d_{ij} = \frac{(GR_{WT}+d_i)*(GR_{WT}+d_j)}{GR_{WT}}$$

(9) $$GR_{WT}{}^2 + GR_{WT} * d_i + GR_{WT} * d_j + GR_{WT} * d_{ij}$$
$$= GR_{WT}{}^2 + GR_{WT} * d_i + GR_{WT} * d_j + d_i * d_j$$

(10) $$GR_{WT} * d_{ij} = d_i * d_j$$

(11) $$d_{ij} = \frac{d_i * d_j}{GR_{WT}}$$

We therefore found the expected value for the defect to be:

(12) $$d_{ij} = \frac{d_i * d_j}{GR_{WT}}$$

From this model, a genetic interaction was inferred between the two mutations when the experimentally measured value for d_{ij} was significantly different from the expected value. The GAMER scores were calculated as:

(13) $$GAMER\ score = d_{ij_{expected}} - d_{ij_{observed}}$$

To calculate p-values, we bootstrapped the model 20,000 times and calculated the probability of observing a more extreme value than the expected d_{ij}. Finally, we corrected the p-values for multiple hypothesis testing by the false discovery rate.

3.4 Results

3.4.1 The Y362E mutation does not reduce spindle stability

Cells with defects in spindle function require the activity of the SAC for survival, and typically die in the absence of these checkpoint proteins[469]. The viability of γ-tubulin alleles and their dependence on SAC activity was tested by analysis of progeny (tetrads; 20 per strain) obtained from diploids heterozygous for γ-tubulin alleles S360D, Y445D or Y362E, and the *mad2Δ* null mutation which blocks SAC activation. γ-Tubulin mutations S360D, Y445D and Y362E are viable under normal growth conditions (25-30˚C), with a weak growth defect observed for S360D and Y445D ([1,3] and Figure 3.1C). As previously shown, the S360D and Y445D mutations are lethal in combination with the *mad2Δ* mutation[1,3]. The Y362E mutant did not show a similar sensitivity to the loss of the SAC (Figure 3.1C).

We next examined fluctuations in spindle length, which reports relative spindle stability[2]. Length fluctuations were computed from the standard deviation of spindle length (σ) and assessed with respect to the mean spindle length (Figure 3.1D). The S360D mutation disrupts the formation of interpolar antiparallel cross-linked MTs[2]. As a result, spindles in S360D cells are unstable and undergo very large length fluctuations relative to wild-type cells ($p = 1.888 \times 10^{-85}$). Similarly, in Y445D, spindles also experience large length fluctuations relative to wild-type cells ($p = 8.977 \times 10^{-41}$). The length fluctuations of Y362E spindles are similar to those of wild-type spindles ($p = 1.881 \times 10^{-6}$), and both wild-type and Y362E spindles are stable relative to the spindles of S360D and Y445D.

Figure 3.1 | Effects of γ-tubulin phosphomimetic (D/E) mutations on spindle function and spindle stability. (A) ribbon structure of yeast γ-tubulin (homology model based on the human γ-tubulin structure) with loops and structured domains of the final 132 residues shown in green and blue, and the predicted intrinsically disordered C-terminus shown in pink. Spheres indicate the positions of the residues phosphorylated at the SPBs *in vivo*; S360 (blue), Y362 (green) and Y445 (red). A schematic representing the primary sequence of the 132 residues is shown below with the intrinsically disordered regions (IDRs) shown in green, the α-helices and β-strands shown in dashed blue and solid blue (respectively), and the C-terminus shown in pink. (B) Schematic depicting the role of S360 in architecture of the antiparallel microtubule (MT) bundle and spindle stability (top panel); schematic depicting the role of Y445 in the attachment of sister chromatids (SCs) and the resulting chromosome loss (bottom panel). (C) Representative tetrad dissections of S360D, Y445D and Y362E, alone and in combination with *mad2Δ* (> 40 tetrads were dissected for each strain). Unlike S360D and Y445D, the Y362E; *mad2Δ* double mutant is viable, with a slight growth defect, at 25°C. (D) Spindle length fluctuations in wild-type, Y362E, S360D and Y445D cells plotted as a function of mean spindle length. Wild-type fluctuations are shown in grey in each plot. Fluctuations for each spindle (σ) are computed as the standard deviation of length.

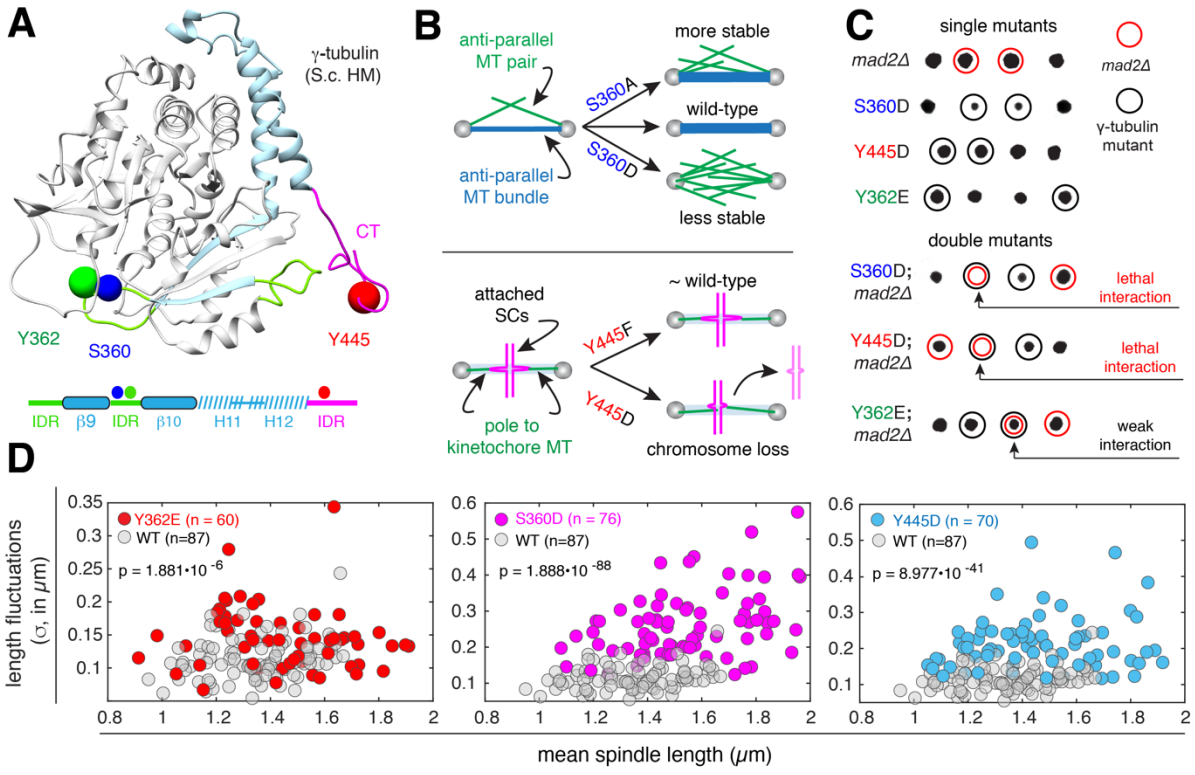

3.4.2 GAMER analysis reveals common and distinct SGIs for Y362E and Y445D alleles

GAMER analysis uses a modified SGA method that provides a growth rate parameter. After the final pinning for selection of *MATa* double mutants, plates were photographed at two-hour intervals for 72 hours. From the resulting images, the density of each colony was extracted from the colony's integrated intensity and used to calculate the growth rates and relative fitness of each strain (Figure 3.2A). Linkage group analysis for the *TUB4* locus extending 150 kilobases in both directions (approximately 50 centiMorgans[482-484]) was conducted using both GAMER and a standard endpoint colony size characterization method (Figure 3.3). Due to technical issues arising from experimental procedures (e.g. colony position on the array plate), growth characterization of the endpoint colony sizes had much larger variances. These issues can be corrected during post-processing[481]. In contrast, the resulting GAMER growth rates for the *TUB4* linkage groups had a higher measured precision and showed more uniformity across the genes without additional post-processing.

In agreement with the *mad2Δ* genetic analysis shown in Figure 3.1C, Y445D was found to have a strong synthetically lethal interaction with *mad2Δ* (relative fitness of 0%, $p < 10^{-4}$, Figure 3.2B). GAMER is also suitable for detection of weak SGIs; the Y362E mutation had a weak but significant interaction with *mad2Δ* (relative fitness of 61%, $p = 8.88 \times 10^{-3}$, Figure 3.2C). This interaction was not apparent when colony size of Y362E and *mad2Δ* were compared with the double mutant (Figure 3.1C) highlighting the sensitivity of the GAMER method. Fitness-based experiments using GAMER overcome potential technical variations that could influence the interpretation of results; for example, *mad2Δ* colonies appear to increase in size faster than wild-type due to their increased endpoint densities (Figure 3.2B, C; black growth curves in left panels). However, our analysis reveals that the growth rates of *mad2Δ* and wild-type colonies are not statistically different—both have a fitness of 100% (Figure 3.2B, C; right panels).

Figure 3.2 | Identification of SGIs based on relative fitness using GAMER. (A) Overview of the GAMER method, which includes imaging every two hours (τ) over a 72-hour period. Images were processed computationally, and fitness was extracted and used to calculate the GAMER scores of the double mutants. (B-C) SGA growth curves (left panels) for six isolates of wild-type, Y445D (B) or Y362E (C), *mad2Δ* and the combined double mutant. Values of the observed and expected growth defects (d_{ij}) for the respective double mutants (right panels).

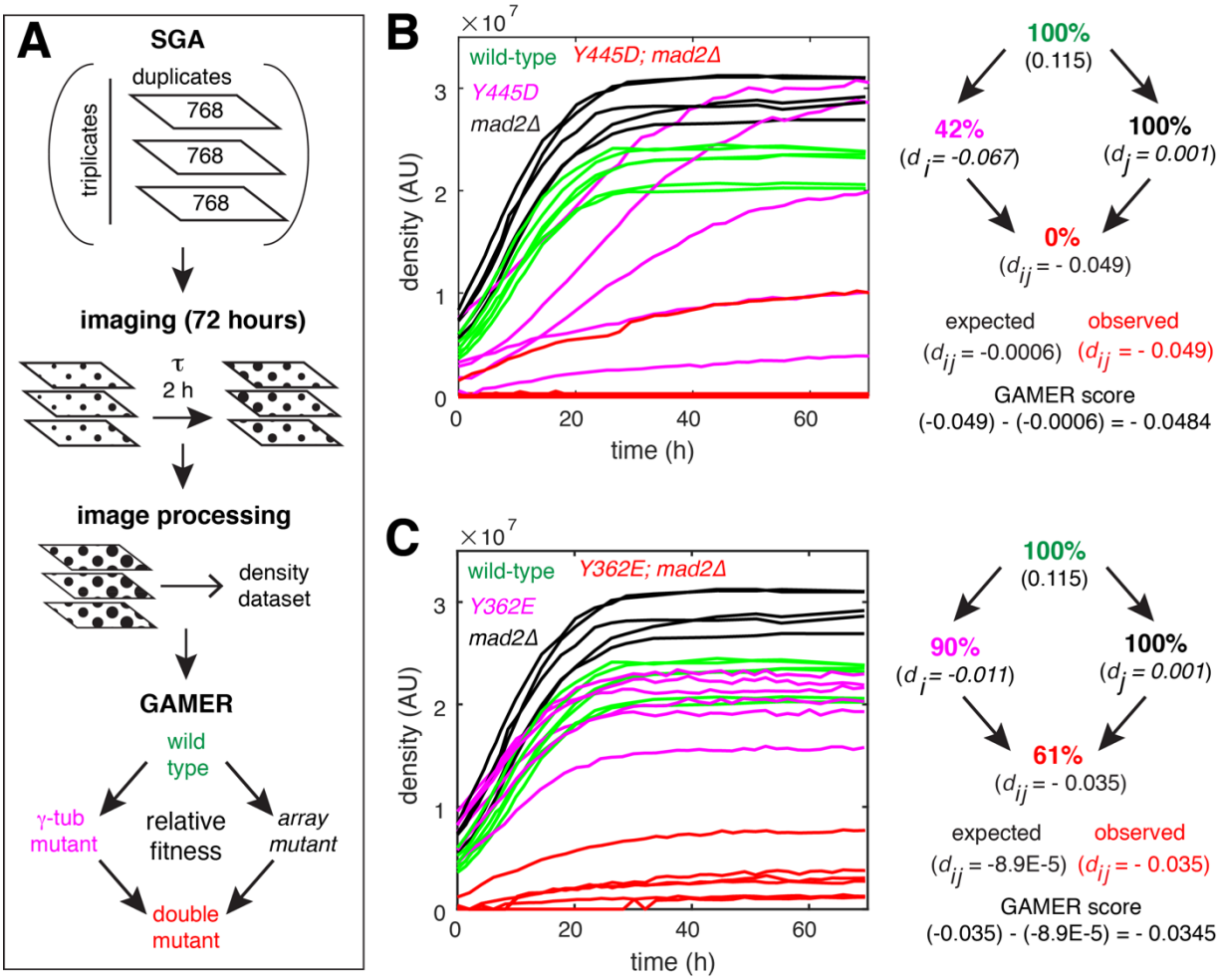

Figure 3.3 | Growth rates reflect strain fitness independently of initial conditions. (A-B) Linkage group analysis for Y445D and Y362E alleles based on endpoint colony size (A) or GAMER-measured growth rates (B). A linkage group extending ~150 kb (50 centiMorgans) on either side of the *TUB4* locus was detected for the Y445D and Y362E alleles using both methods. Colony sizes at 24 hours have a large variance that increases with distance from the query gene. This variance arises from initial conditions and experimental procedures and must be corrected in post-processing. In contrast, GAMER-measured growth rates for double mutants have increased precision and accuracy as a consequence of relatively uniform growth rates across replicates and duplicates.

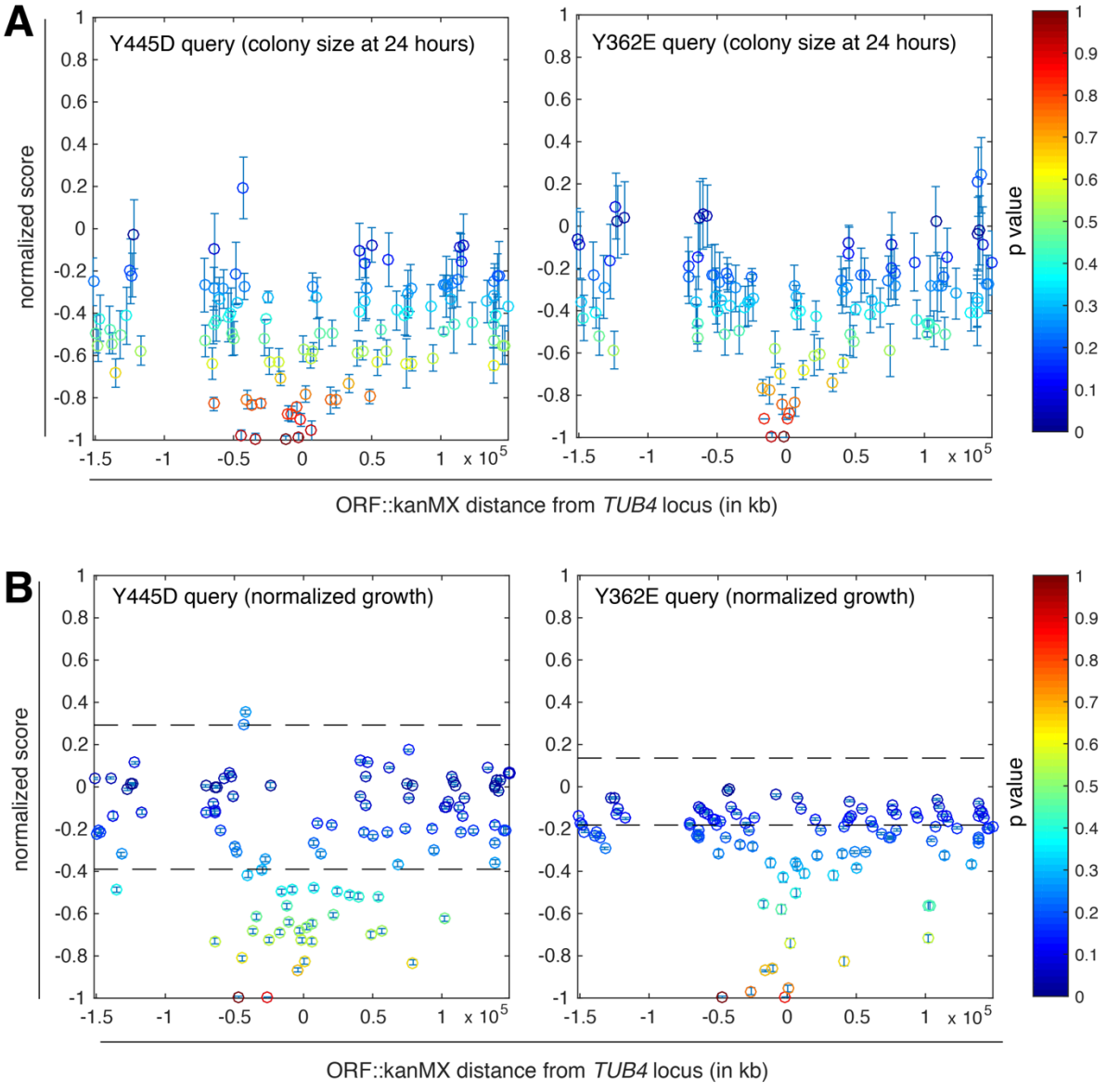

GAMER identified 1035 SGIs across the Y362E and Y445D screens (Figure 3.4A). To directly compare the relative fitness between SGIs of the two alleles, we projected the two sets of GAMER scores for each array mutant (Y362E and Y445D). This organized SGIs into four quadrants: (1) rescues in both screens, where the fitness of the double mutant (γ-tubulin allele and array mutant together) was increased relative to all single mutants (γ-tubulin allele alone, or array mutant alone) in *both* the Y445D and the Y362E screens (Figure 3.4B, top right quadrant). (2) Y445D rescue/Y362E sick, where the fitness of the Y445D double mutant was increased relative to all single mutants while the fitness of the Y362E double mutant was decreased relative to all single mutants (leading to a synthetic sick or lethal SGI) (Figure 3.4B, top left quadrant). (3) Y445D sick/Y362E rescue, where the fitness of the Y445D double mutant was decreased relative to all single mutants while the fitness of the Y362E double mutant was increased relative to all single mutants (Figure 3.4B, bottom right quadrant). (4) Y445D sick/Y362E sick, where the fitness of both double mutants was decreased relative to all single mutants (Figure 3.4B, bottom left quadrant). The latter group (Y445D sick/Y362E sick) is divided at the point where the fitness was equivalently reduced for both Y362E and Y445D double mutants (Figure 3.4B, dashed diagonal line). Below this boundary, the Y445D double mutant's fitness is worse than the Y362E double mutant's fitness; above this boundary, the opposite is the case. Genes in the linkage group (Figure 3.4C, pink) tend to cluster close to the boundary as they similarly reduce the fitness of both γ-tubulin alleles.

Comparison of the GAMER-derived SGIs of Y362E and Y445D revealed that the proportion of SGIs common to both alleles was smaller than the set of SGIs unique to each allele. We identified 123 SGIs in common, but a larger number of SGIs were unique, with 524 SGIs for Y445D and 380 SGIs for Y362E. Y362E did not have an SGI with the *mad3Δ* mutation and the normalized scores for the Y362E interactions with *mad1Δ* and *mad2Δ* mutations were less severe than the corresponding scores for Y445D (Figure 3.4D) supporting our observation that Y362E is not dependent on the SAC (Figure 3.1C). The Y362E allele had no SGIs with genes that strictly contribute to the function of spindle/nuclear microtubules (Figure 3.4D). In contrast, SGIs specific to the Y445D allele were consistent with defects in both antiparallel (*ase1Δ* and *slk19Δ*) and parallel (*vik1Δ*) nuclear MT cross-linking. Antiparallel cross-linking is required to form the

interpolar MTs that stabilizes the spindle[32,33,485,486]. This is consistent with Y445D participating in the process of spindle assembly. SGIs common to both alleles were often genes that function in both spindle MT- and astral MT-dependent processes or coordinate the completion of spindle placement with mitotic exit. Cik1, which has been shown to function on both the spindle and astral MTs[47], was a common SGI for both alleles (*cik1Δ*). The Y362E SGI profile revealed a dependence on the cell cycle kinase Kin4 (Figure 3.4E), which inhibits the mitotic exit network (MEN) when the spindle positioning checkpoint is activated[367,487]. Additionally, the Y362E SGI profile was enriched for SGIs with genes acting in Kar9- and dynein-dependent spindle placement as well as cell polarity (Figure 3.4F). This group of SGIs included mutations in *bub2Δ* and *lte1Δ*, as well as mutations of components of the dynactin complex (*arp1Δ*, *jnm1Δ*, *ldb18Δ*, *nip100Δ*) and the kinase Pac1. Dynactin and Pac1 both regulate the activity of cytoplasmic dynein during spindle placement. SGIs specific to Y362E also included components of the polarisome (*rho2Δ*, *bem3Δ*, *rom2Δ*, *rgl1Δ*) and actin cables (*abp140Δ*), which are critical for both Kar9- and dynein-dependent spindle placement. These results suggested that the Y362E mutation likely perturbs a function of γ-tubulin that is directly linked to spindle placement and actin organization rather than the previously characterized role in spindle assembly (i.e. in S360D and Y445D).

Despite their spatial separation in both primary sequence and tertiary structure, the S360D and Y445D γ-tubulin mutants both exhibit spindle instability (Figure 3.1A, D). Residues S360 and Y362 are positioned within an unstructured loop on the opposite surface of the molecule to the intrinsically disordered C-terminal-containing Y445. Based on work done in Chapter 2 of my thesis, we knew that S360 and Y445 were functionally coupled, thus, we asked if Y362 and Y445 were similarly coupled by assessing the viability of intramolecular double mutants. Individual phosphoinhibitory mutations (alanine or phenylalanine) in S360, Y362 and Y445 are viable ([1-3] and Figure 3.5A) while intramolecular double mutants S360A-Y445D or S360D-Y445F are lethal (Chapter 2 and Figure 3.5B). Previously, we reported that S360 phosphorylation by Cdk1 requires the early mitotic cyclin Clb3 *in vivo*[402]. This may be the cause of the lethal interaction identified in our GAMER analysis between the Y445D and *clb3Δ* mutants (Figure 3.4E). The Y445D; *clb3Δ* double mutant may phenocopy the S360A-Y445D mutant as both S360A and *clb3Δ* prevent phosphorylation at site S360. When mutations in Y362 and Y445 were

combined, only the Y362F-Y445D double mutant showed a growth phenotype (Figure 3.5C). As Y445D has a growth defect on its own, it is possible that the growth phenotype of Y362F-Y445D is completely due to Y445D. The lack of intramolecular interactions between Y362 and Y445 suggest that these sites are not coupled like S360 and Y445. Taken together with the GAMER results, our analysis of intramolecular genetic interactions suggests that the phosphorylation of S360 and Y445 must be coordinated with respect to each other during spindle assembly. Moreover, the phosphorylation of Y362 is uncoupled from Y445 and regulates γ-tubulin activity in a process that involves genes acting in spindle placement and cell polarity (Figure 3.5D).

Figure 3.4 | GAMER identifies distinct and common SGIs for Y445D and Y362E alleles. (A) Growth rates for all array mutants when combined with Y445D were plotted against their growth rates when combined with Y362E. The blue points represent all significant hits between the two GAMERs; grey represents the genes with no genetic interactions. Genes that caused lethal phenotypes when combined with Y445D or Y362E cluster along the x- or y-axis, respectively. (B) The resulting GAMER scores for Y445D and Y362E were projected on the same axis organizing SGIs into four quadrants depending on the respective scores: (1) hits that increased fitness (rescued) for both alleles (upper, right). (2) Hits that increased fitness for Y445D but reduced fitness for Y362E (upper, left). (3) Hits that reduced fitness for Y445D but increased fitness for Y362E (lower, right). (4) Hits that reduced the relative fitness in both alleles (lower, left). Quadrant (4) is divided in half along a diagonal line (---) which indicates hits that reduced fitness similarly for both alleles. Below this line, fitness was reduced more for Y445D than Y362E, while above this line, the opposite is true. (C) GAMER scores for all SGA mutants including those that were unique hits for Y445D (green), those that were unique hits for Y362E (red), those that were common hits for both alleles (blue), the linkage group (pink) and those that did not have SGIs with either allele (grey). (D-F) SGIs related to the SAC and spindle stability (D), to the cell cycle (E), and to spindle placement and cell polarity (F).

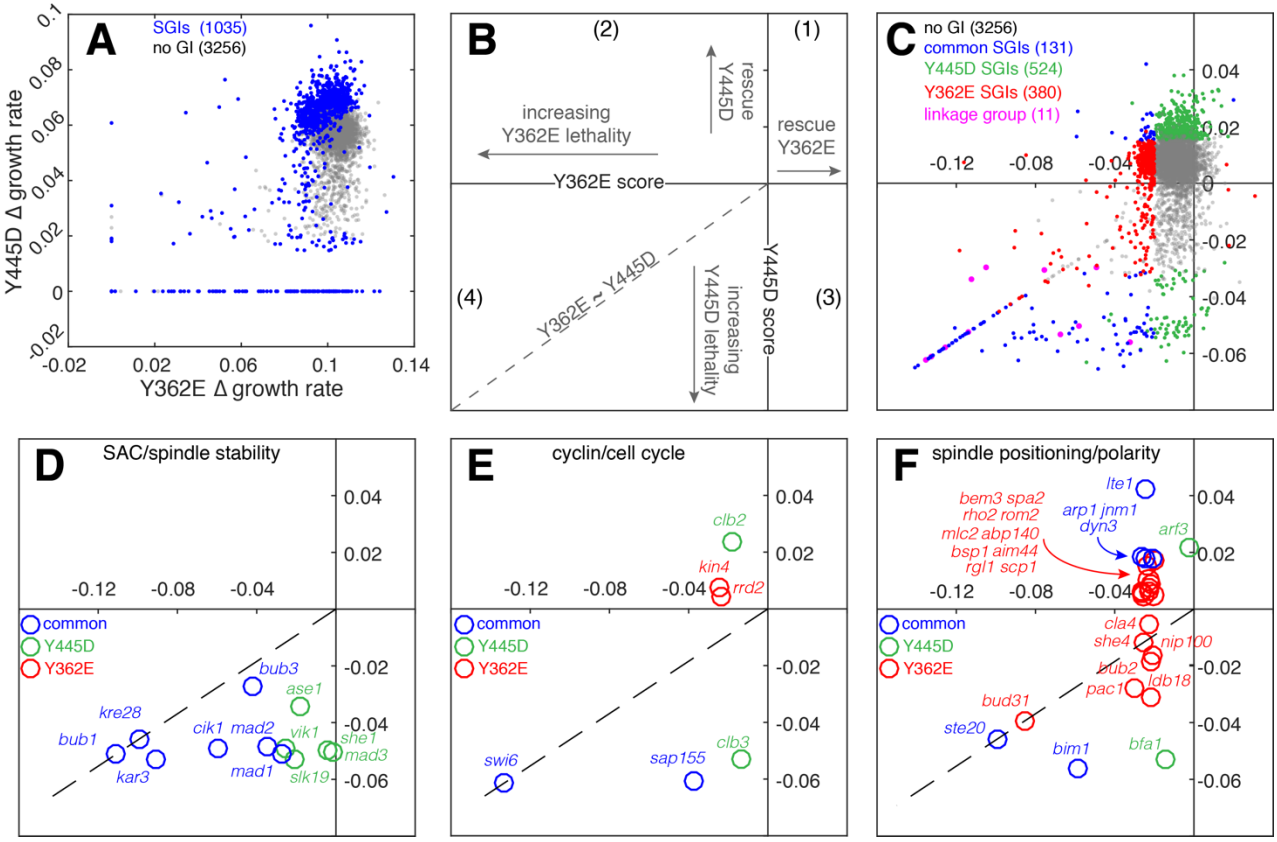
A
SGIs (1035)
no GI (3256)
Y445D Δ growth rate
Y362E Δ growth rate
B
(2)
(1)
(4)
(3)
increasing Y362E lethality
rescue Y445D
rescue Y362E
Y362E score
Y445D score
Y362E ~ Y445D
increasing Y445D lethality
C
no GI (3256)
common SGIs (131)
Y445D SGIs (524)
Y362E SGIs (380)
linkage group (11)
D
SAC/spindle stability
common
Y445D
Y362E
bub3
ase1
kre28
bub1
cik1
mad2
vik1
she1
mad3
kar3
mad1
slk19
E
cyclin/cell cycle
clb2
kin4
rrd2
swi6
sap155
clb3
F
spindle positioning/polarity
lte1
bem3 spa2 rho2 rom2 mlc2 abp140 bsp1 aim44 rgl1 scp1
arp1 jnm1 dyn3
arf3
cla4
she4
nip100
bud2
pac1
ldb18
bud31
ste20
bim1
bfa1

Figure 3.5 | Y362E is a separation-of-function allele. (A-C) Meiotic outcomes of single phosphoinhibitory (PI) mutants (A) and intramolecular phospho-mutants between S360 and Y445 (B) and Y362 and Y445 (C). While individual phosphoinhibitory mutations S360A, Y362F and Y445F have no detectable growth phenotype, lethality is observed when combined with phosphomimetic mutations S360D or Y445D. Intramolecular co-lethality suggests functional coupling between S360 and Y445. A weak growth defect is observed between the Y362F and Y445D mutant. (D) Residues S360 and Y445 contribute to spindle stability, while Y362 contributes to spindle placement.

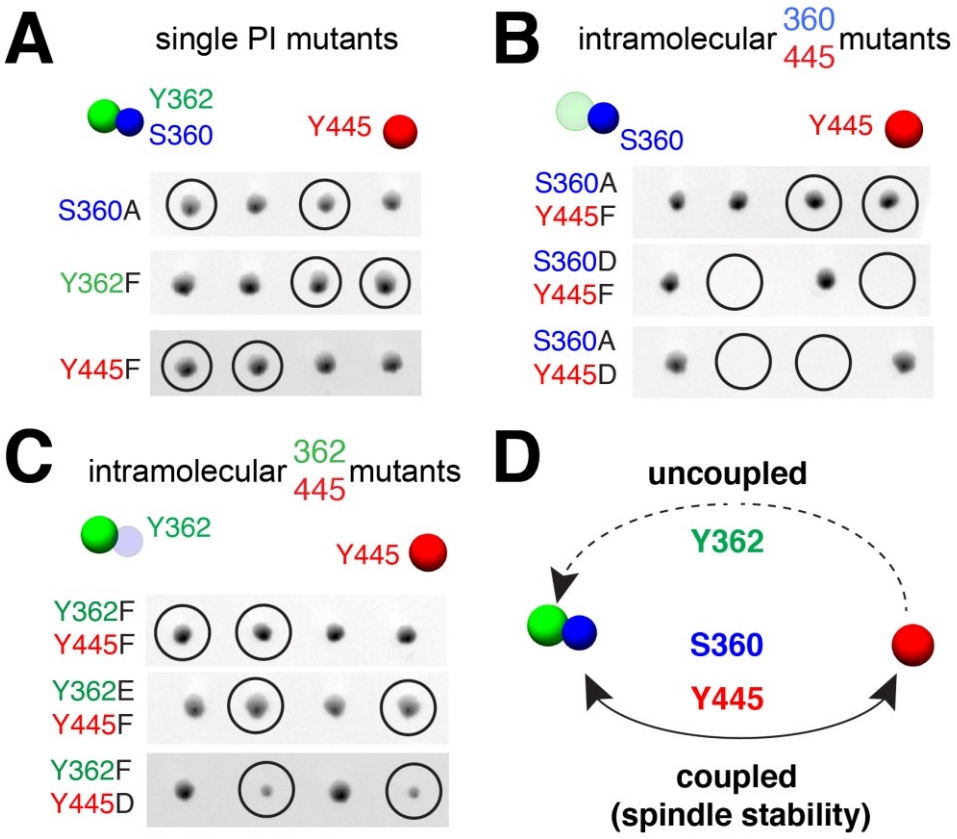

3.4.3 A geometric definition for perfect alignment of the metaphase spindle in budding yeast

A budding yeast cell is asymmetric once the bud has formed, with a polarity axis that is normal to the plane of the bud neck (the future site of cytokinesis). As the spindle is assembled, it becomes positioned close to the bud neck and is aligned parallel to the polarity axis and normal to the bud neck plane, with a strong bias for the older SPB (formed in the previous cell cycle) to be oriented proximal to the neck[258]. This condition, which we define as perfect alignment, is the reference for our measurement of spindle placement in wild-type and mutant cells (Figure 3.6A). Perfect alignment ensures that the anaphase spindle will elongate through the bud neck and a full complement of chromosomes are inherited by the mother and daughter cells at the end of cell division. If the spindle is not positioned at the neck and/or not aligned normal to the bud neck plane, anaphase may occur in the mother cell, resulting in aneuploidy and cell death. To compare an observed spindle to this reference, we project it (in 3D) to a perfectly aligned spindle (1D). If the spindle is perfectly aligned, the true (3D) and projected (1D) lengths are approximately the same, while spindles rotated 90˚ off the polarity axis would have a projected length of zero. As spindle alignment proceeds, the true and projected length of the spindle are expected to converge.

3.4.4 The Y362E mutation does not perturb spindle positioning at the bud neck

We measured spindle positioning at the bud neck in wild-type and Y362E cells, as well as in mutants lacking either cytoplasmic dynein (*dyn1Δ*) or the APC-like +TIP protein, Kar9 (*kar9Δ*), both of which are central to the two functionally redundant spindle placement pathways in budding yeast. To measure spindle position relative to the bud neck, we analyzed the trajectories of the SPBs—which are diffraction-limited, point-like objects whose position can be precisely determined[2,488]—over a ten-minute window in single cells. We then extracted the mean distance of the proximal SPB to the neck plane and the mean spindle length using 3-dimensional data collected at ten-second intervals. The distance of the proximal SPB to the neck plane was computed for metaphase spindles with an average length < 2 µm and initial lengths between 0.8-2 µm for wild-type (n=88 cells), single mutant (Y362E n=61 cells, *kar9Δ* n=60 cells, *dyn1Δ* n=68 cells) and double mutant strains (Y362E; *kar9Δ* n=48 cells, Y362E; *dyn1Δ* n=49 cells). In the majority of wild-type, Y362E, *dyn1Δ* and Y362E; *dyn1Δ* cells, the normalized mean distance of the

proximal pole to the neck is less than 25% of the diameter of the mother cell regardless of the mean spindle length (Figure 3.6B and Figure 3.7). In contrast, in the majority of *kar9Δ* and Y362E; *kar9Δ* cells, the mean distance of the proximal pole to the neck is >25% of the mother cell diameter and is significantly increased relative to wild-type, as well as to the other mutants ($p < 0.0001$; Figure 3.6B and Figure 3.7). Movement of the spindle to the neck occurs even in the absence of cytoplasmic dynein and is not significantly perturbed by the Y362E mutation.

3.4.5 Spindle alignment is defective in the Y362E mutant

Next, we simultaneously investigated the alignment and orientation of the spindles in wild-type and mutant strains. For each strain, alignment is shown as the normalized frequency of projected (1D) lengths in a distribution of 3D length bins for all time points. Two white lines indicate where 1D and 3D lengths converge, either "perfect alignment" (aligned with proper orientation: the old SPB proximal to the neck) or "incorrect orientation" (aligned with incorrect orientation: the new SPB proximal to the neck). In wild-type cells, perfect alignment is correlated with increasing 3D spindle length, with most spindles ≥ 1.5 µm in length maintaining perfect alignment (Figure 3.6C, upper left panel). In the Y362E mutant, spindles exhibit a defect in achieving or maintaining perfect alignment. Furthermore, the frequency of incorrect orientation for spindles ≥ 1.5 µm in length is increased relative to wild-type (Figure 3.6C, upper right panel). Spindle alignment is observed in *dyn1Δ* cells (Figure 3.6C, lower left panel); however, the majority of spindles in *kar9Δ* cells do not achieve or maintain perfect alignment regardless of spindle length (Figure 3.6C lower right panel). Instead, spindles in *kar9Δ* cells tend to explore orientations centered around a parallel alignment to the bud neck and 90˚ to the polarity axis (i.e. projected 1D length of zero). We directly compared spindle alignment in wild-type cells with mutants by computing the difference between the conditions, with wild-type compared to Y362E, *dyn1Δ* or *kar9Δ* (Figure 3.6D). Spindles in Y362E cells explore many orientations relative to the bud neck plane. The frequency of incorrect orientation is increased in both Y362E cells, and to a lesser amount in *dyn1Δ* cells, relative to wild-type cells.

To better understand the nature of the spindle alignment defect in Y362E cells, we plotted instantaneous projected spindle length as a function of true spindle length for representative wild-type and Y362E cells taken from mean 3D length bins of 1 µm, 1.3 µm and 1.5 µm (Figure

3.6E, F). In wild-type cells, spindles with an average length less than 1.2 μm are not aligned; however, longer spindles either undergo alignment or remain aligned during the ten minutes of observation (Figure 3.6E). In contrast, Y362E spindles are frequently misaligned independent of spindle length, and approach but do not maintain perfect alignment as spindle length increases (Figure 3.6F).

3.4.6 The Y362E mutation enhances alignment defects of Kar9 and dynein mutants

To understand how the Y362E mutation might affect the function of Kar9 or dynein, we next investigated spindle alignment in Y362E cells when combined with *dyn1Δ* or *kar9Δ* mutations. When Y362E is combined with *dyn1Δ*, such that spindle placement is dependent on Kar9, the frequency of incorrect orientation increases for spindles ≤1.5 μm (Figure 3.6G, upper panels). Interestingly, while the majority of spindles in *kar9Δ* cells were biased to orientations parallel to the bud neck axis (i.e. projected 1D length of zero; Figure 3.6C), in Y362E; *kar9Δ* double mutants, spindle orientation appears to be random relative to the bud neck plane (Figure 3.6G, lower panels).

Figure 3.6 | Pre-anaphase spindle alignment is perturbed in Y362E cells. (A) Schematic depicting the method used to compute both the distance between proximal pole and bud neck (for assessment of spindle positioning), and the spindle alignment in relation to "perfect alignment". Perfect alignment is defined as a spindle with a 1D projected spindle length approximately equal to its 3D spindle length. (B) Distance of the proximal pole from the bud neck; error bars show standard deviation. Asterisks indicates statistical difference with $p < 0.0001$; n.s. denotes no significant difference. (C) Heatmaps showing the projected 1D spindle length as a function of true 3D spindle length in wild-type (WT), Y362E, *dyn1Δ* and *kar9Δ* cells. Color bar shows the frequency of time points normalized to the total number of time points of all cells. Incorrect orientation occurs when the new pole is proximal to the bud. (D) Plots exhibiting the differences between the spindle alignment heatmaps shown in (C). WT is compared to Y362E (top), *dyn1Δ* (middle) and *kar9Δ* (bottom). Green indicates areas where the frequency of the WT was increased relative to the mutant, red indicates areas where the frequency of the mutant was increased relative to WT. (E-F) Instantaneous projected 1D spindle length plotted as a function of true 3D spindle length for representative WT (E) and Y362E (F) cells. Time is indicated by the color gradation from dark (start) to light (end). (G) The Y362E mutation increases the range of unaligned spindle orientations, and the occurrence of incorrect orientation when combined with *kar9Δ* and *dyn1Δ* mutants. Heatmaps showing the projected 1D spindle length in double mutants Y362E; *dyn1Δ* (upper left) and Y362E; *kar9Δ* cells (lower left). Plots showing the differences between the single mutants and double mutants spindle alignment heatmaps. Green indicates areas where the frequencies of the single mutant were increased relative to the double mutants, red indicates areas where the frequencies of the double mutants were increased.

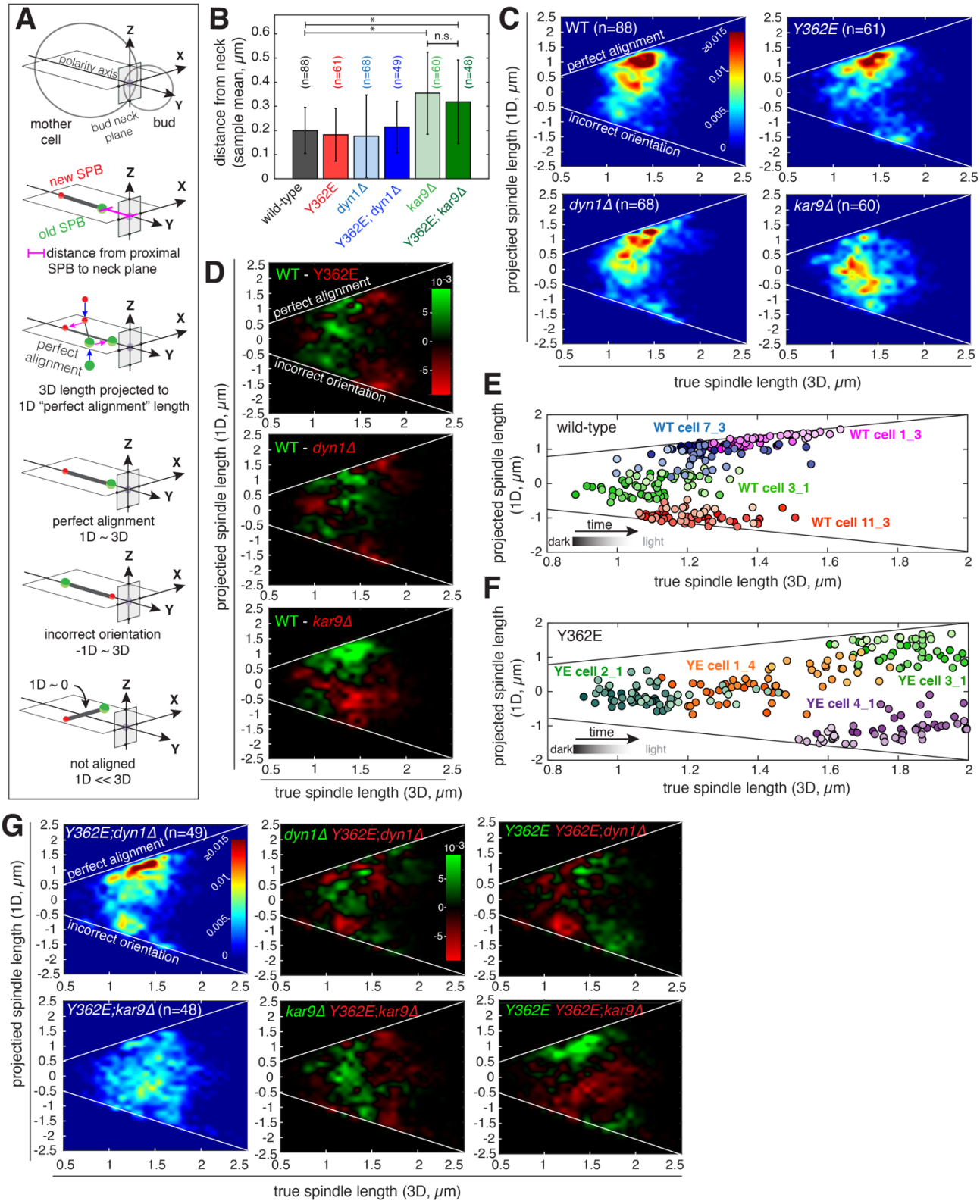
A
polarity axis
mother cell
bud neck plane
bud
new SPB
old SPB
distance from proximal SPB to neck plane
perfect alignment
3D length projected to 1D "perfect alignment" length
perfect alignment 1D ~ 3D
incorrect orientation -1D ~ 3D
1D ~ 0
not aligned 1D << 3D
B
distance from neck (sample mean, μm)
(n=88)
(n=61)
(n=68)
(n=49)
(n=60)
(n=48)
n.s.
wild-type
Y362E
dyn1Δ
Y362E; dyn1Δ
kar9Δ
Y362E; kar9Δ
C
WT (n=88)
Y362E (n=61)
dyn1Δ (n=68)
kar9Δ (n=60)
perfect alignment
incorrect orientation
projected spindle length (1D, μm)
true spindle length (3D, μm)
D
WT - Y362E
WT - dyn1Δ
WT - kar9Δ
projected spindle length (1D, μm)
true spindle length (3D, μm)
E
wild-type
WT cell 7_3
WT cell 1_3
WT cell 3_1
WT cell 11_3
time
dark
light
projected spindle length (1D, μm)
true spindle length (3D, μm)
F
Y362E
YE cell 2_1
YE cell 1_4
YE cell 3_1
YE cell 4_1
time
dark
light
projected spindle length (1D, μm)
true spindle length (3D, μm)
G
Y362E;dyn1Δ (n=49)
dyn1Δ Y362E;dyn1Δ
Y362E Y362E;dyn1Δ
Y362E;kar9Δ (n=48)
kar9Δ Y362E;kar9Δ
Y362E Y362E;kar9Δ
perfect alignment
incorrect orientation
projected spindle length (1D, μm)
true spindle length (3D, μm)

Figure 3.7 | Y362E does not perturb spindle positioning at the bud neck. Distance from the proximal pole to the bud neck was found and normalized to the initial length of the mother cell. This was plotted as a function of mean spindle length for wild-type cells, single mutants (Y362E, *kar9Δ*, *dyn1Δ*) and double mutants (Y362E; *kar9Δ* and Y362E; *dyn1Δ*).

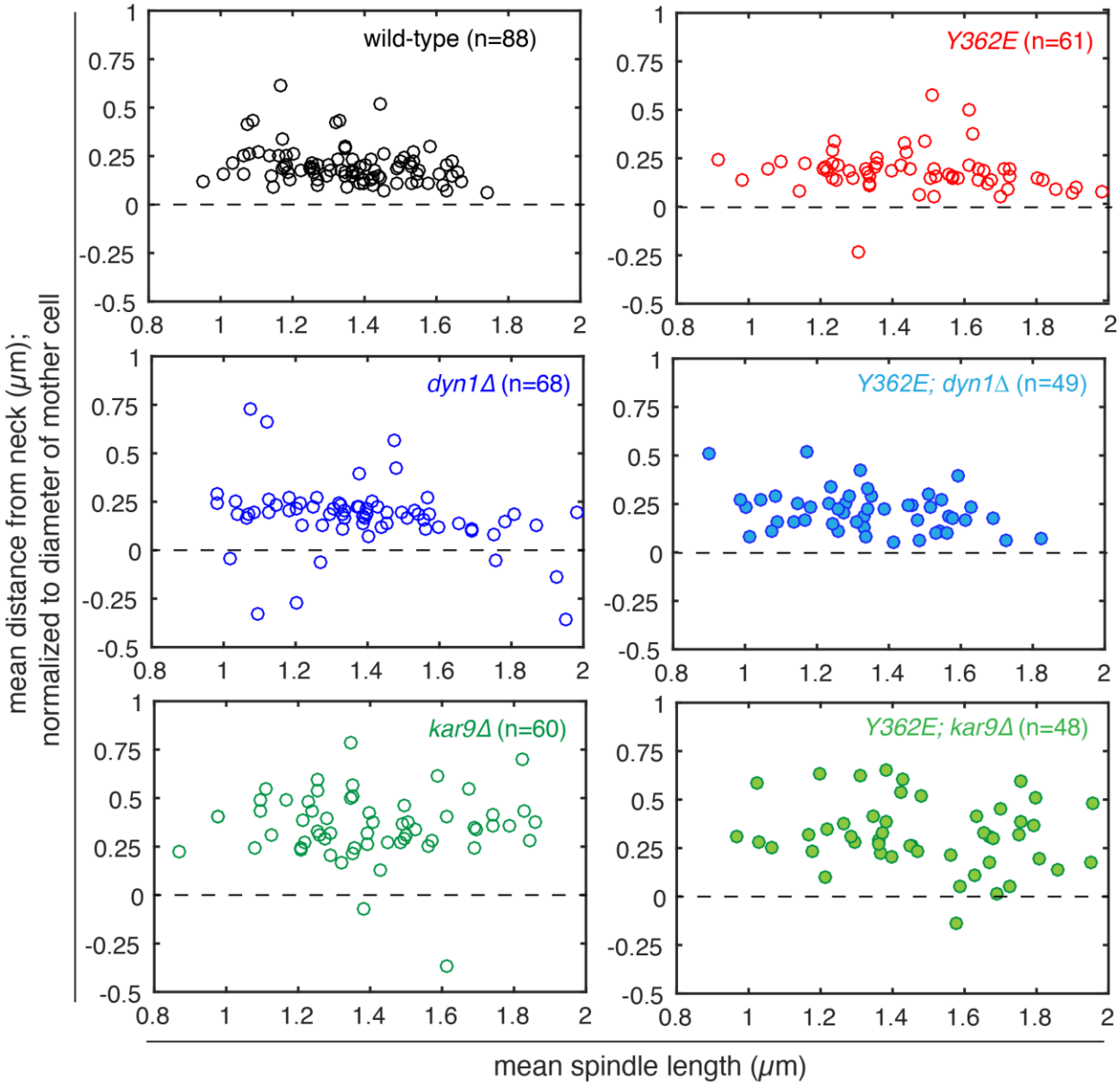

3.4.7 The Y362E mutation increases the number of astral MTs at the old and new SPBs

Forces produced by astral MTs are important for spindle placement[489-492]. Thus, we investigated the effect of the Y362E mutation on the behaviour and number of astral MTs in metaphase cells. Representative wild-type and Y362E cells expressing a Venus-Tub1 (α-tubulin) MT reporter and a Spc42-Cerulean SPB reporter are shown in Figure 3.8A. In wild-type cells, pre-anaphase spindles typically have one to two astral MTs (mean of 1.28 $\pm$ 0.568), in agreement with published data[493]. Pre-anaphase spindles in the Y362E mutant had almost two-fold more astral MTs than wild-type (mean of 2.59 $\pm$ 0.616, $p = 1.5 \times 10^{-9}$).

We next investigated the astral MT number at each SPB. Astral MTs associated with the pre-existing (old) SPB are thought to persist longer due to an increased stability cause by the asymmetric loading of MT +TIP proteins, such as Bim1 and Kar9, during spindle alignment[21,283,494]. The increased stability of astral MTs loaded with +TIP proteins likely contributes to the increased number of astral MTs associated with the old SPB (0.89 $\pm$ 0.312) relative to the new SPB (0.45 $\pm$ 0.362, $p= 1.1 \times 10^{-6}$) in wild-type cells (Figure 3.8B). However, in Y362E cells, the number of astral MTs is increased on both old and new SPBs relative to wild-type (Figure 3.8C). The number of astral MTs associated with the old SPB increased 1.6-fold (1.42 $\pm$ 0.417, $p = 1.1 \times 10^{-6}$) and the number of astral MTs associated with the new SPB increased two-fold (0.94 $\pm$ 0.331, $p = 1.0 \times 10^{-6}$). Interestingly, despite having increased numbers of astral MTs, only one astral MT entered the bud at a time in Y362E cells, as is seen in wild-type (Figure 3.9). The increase in the number of astral MTs at both old and new SPBs in Y362E cells results in a significant shift towards symmetry of astral MT occupancy and away from the asymmetric bias of astral MT occupancy to the old SPB found in wild-type cells (Figure 3.8D, $p = 1.3 \times 10^{-7}$). Symmetry of astral MT occupancy is defined as having at least one astral MT on both SPBs over the five-minute acquisition window (e.g. 80% symmetry of astral MT occupancy indicates the cell has at least one astral MT on both poles for 80% of the acquisition time). In the Y362E mutant, 40% of cells (14 of 35 cells) had ≥ 80% symmetry of astral MT occupancy, a condition that was not observed in wild-type cells (n=35). Over 80% of Y362E cells (29 cells) had astral MTs on both SPBs during at least 50% of the five-minute acquisition window, while in wild-type cells, the frequency of symmetry of astral MT occupancy ≥50% was relatively rare (8 cells, 23%). Our analysis suggests that the majority of

spindle movements during Y362E pre-anaphase spindle placement are predominantly influenced by astral MTs associated with both old and new SPBs, rather than by astral MTs associated with the old SPB as in wild-type cells.

Figure 3.8 | The number of astral MTs associated with old and new SPBs is increased in Y362E cells. (A) Representative metaphase spindles (two SPBs 0.8-2 μm apart) in wild-type (WT) and Y362E cells. MTs are tagged with Venus-Tub1 (shown in green) and SPBs are tagged with Spc42-Cerulean (shown in red). Corresponding explanatory schematics for astral MT organization are shown to the right. (B-C) Astral MT count for old and new SPBs in wild-type (B) and Y362E (C) cells. (D) Percentage of total time both SPBs have astral MTs in WT and Y362E cells. (E) Proposed mechanism for loss of alignment in Y362E cells. (1) During normal spindle alignment, Kar9-Bim1 complexes are loaded onto astral MTs and track the MT plus end. Kar9 binds to the type-5 myosin Myo2 which guides the astral MT plus end towards the bud by walking on actin cables along the bud cortex. (2) Astral MTs projecting into the mother cell are typically short lived but are capable of "pushing" the spindle away from the mother cell cortex. (3 and 4) Astral MTs terminating in the bud exert a "pulling" force, via Kar9 or dynein. An increase in the number of astral MTs in Y362E cells results in uncoordinated pushing and pulling forces at both SPBs, resulting in failure to achieve or maintain spindle alignment.

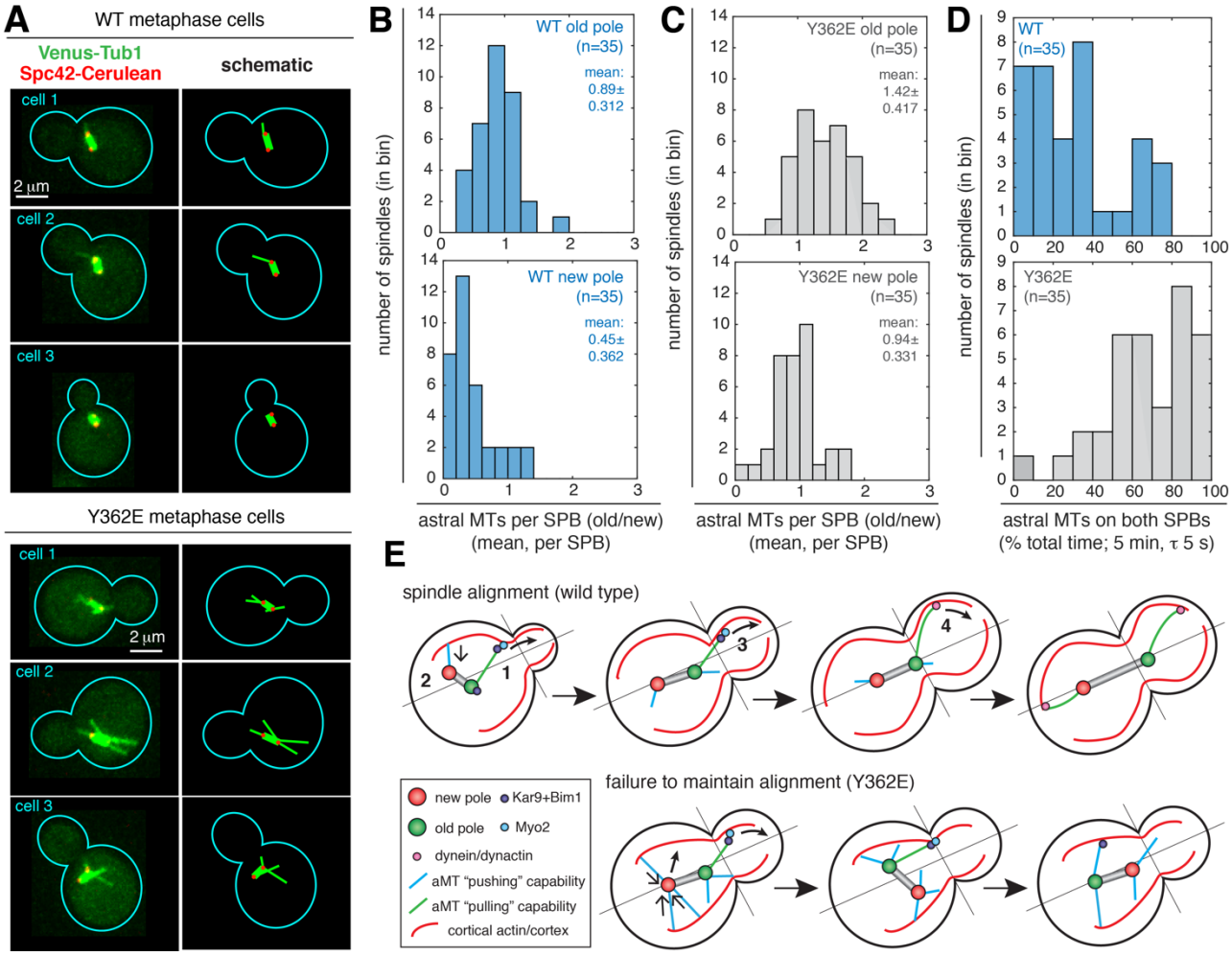
A
WT metaphase cells
Venus-Tub1
Spc42-Cerulean
schematic
cell 1
cell 2
cell 3
2 μm
Y362E metaphase cells
B
WT old pole
(n=35)
mean:
0.89±
0.312
WT new pole
(n=35)
mean:
0.45±
0.362
number of spindles (in bin)
astral MTs per SPB (old/new)
(mean, per SPB)
C
Y362E old pole
(n=35)
mean:
1.42±
0.417
Y362E new pole
(n=35)
mean:
0.94±
0.331
number of spindles (in bin)
astral MTs per SPB (old/new)
(mean, per SPB)
D
WT
(n=35)
Y362E
(n=35)
number of spindles (in bin)
astral MTs on both SPBs
(% total time; 5 min, τ 5 s)
E
spindle alignment (wild type)
1
2
3
4
new pole
Kar9+Bim1
old pole
Myo2
dynein/dynactin
aMT "pushing" capability
aMT "pulling" capability
cortical actin/cortex
failure to maintain alignment (Y362E)

Figure 3.9 | A single astral MT enters the bud in both wild-type and Y362E cells. The number of bud-directed astral MTs never exceeds one per five-second time point in both wild-type (n = 12 cells) and Y362E (n = 14 cells). (A-B) The frequency of time points in which cells had zero, one or greater than one bud-directed (A) or mother-directed (B) astral MT(s).

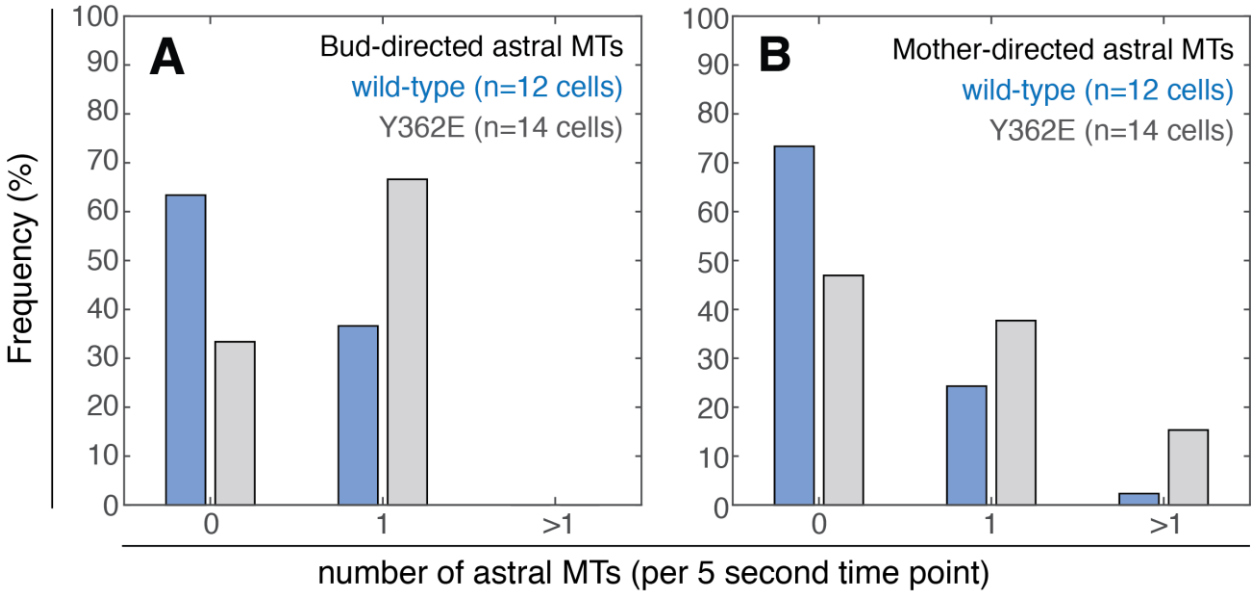

3.5 Discussion

In this study, we developed GAMER, a novel SGA-based approach that identifies subtle differences amongst alleles of one gene (Y445D, Y362E). In previous SGA screens, the assumption that SGIs are rare events[495] forms the basis of the analysis leading to "rare" being defined contextually amongst the queried double mutants. In contrast, GAMER measures growth rates of individual colonies in combination with mixed effects regression to overcome the limitations that are solved by assuming SGIs are rare, leading to an increased sensitivity in the method. It is ideally suited for discerning the subtle differences between an allelic series and also for identifying SGIs of mutants with subtle growth phenotypes (such as the Y362E mutant). The sensitivity and precision of the GAMER approach enabled the detection of a set of specific SGIs for the Y362E allele that revealed a sensitivity to mutations in genes acting in spindle placement and cell polarity, but not in genes acting in spindle assembly or the spindle assembly checkpoint. These results motivated a quantitative analysis of spindle positioning and alignment; this uncovered novel evidence that phosphorylation of Y362 may control the number of astral MTs during spindle placement. Lastly, our GAMER method can uniquely be applied to both large-scale and small-scale assays, allowing the functional screening of new candidates using sub-arrays of the SGA. Taken together, and considering its success in detecting subtle differences between γ-tubulin alleles, we believe GAMER to be a useful improvement on the standard SGA method as it facilitates the comparative analysis of an allelic series and aids in the identification of separation-of-function mutants.

GAMER results indicated that the Y445D and Y362E alleles perturb different aspects of γ-tubulin's function, with the former acting in spindle assembly as previously described[3], and the latter involved in spindle alignment relative to the bud neck plane. Our high-throughput GAMER results recapitulate previous SGIs identified by tetrad dissection[3,344], and the identified Y445D SGIs are consistent with a previously reported decrease in chromosome transmission fidelity for this mutant[4]. We confirmed Y362E's involvement in spindle alignment by quantitatively measuring the ability of a metaphase spindle to reach the state of perfect alignment in wild-type, the Y362E mutant, and in the spindle placement mutants *kar9Δ* and *dyn1Δ*. Unexpectedly, we found that Y362E cells have an increased number of astral MTs on both old and new SPBs, which

reduces the asymmetry of astral MT pole occupancy that is normally biased to the old SPB. The increase in astral MT symmetry is correlated with an increase in the frequency of spindle misalignment independent of spindle length.

GAMER analysis combined with analysis of intramolecular mutations provided new insights into the role of S360 and Y445 phosphorylation in spindle assembly. Mutations that substitute negatively charged amino acids (D/E) at S360 and Y445 decrease spindle stability ([2,3] and this study). For S360, this instability is not due to a lack of spindle MTs, but instead arises from a defect in the organization of these MTs—in particular the formation of a stabilizing core bundle of antiparallel interpolar MTs, which is promoted in the S360A mutant and defective in the S360D mutant[2,3]. The *ase1Δ* and *slk19Δ* SGIs with the Y445D allele are consistent with a similar defect in the function of the interpolar MTs of the spindle. The phosphorylation state of S360 and Y445 may be involved in tuning the architecture of the spindle MTs, with the phospho-state either promoting MT cross-linking (i.e. unphosphorylated S360 and/or Y445) or preventing excessive or inappropriate MT cross-linking (i.e. phosphorylated S360 and/or Y445).

In budding yeast, there are two pathways that can execute pre-anaphase spindle placement—the Kar9/Bim1 pathway (APC/EB1 in metazoans) and the dynein pathway—both of which act by applying a pulling force on astral MTs and, as a result, on the spindle as a whole[94,95,137,284]. We investigated both of these pathways' role in the achievement of perfect alignment (where the spindle must translocate towards the bud neck and align with the old SPB proximal to the bud neck plane). The process of spindle positioning and alignment begins between S- and M-phase, and in the absence of Kar9, short spindles (<2 μm in length) fail to achieve perfect alignment. We found that spindles in *kar9Δ* cells are unable to accomplish proper spindle positioning and are frequently oriented parallel to the bud neck plane, consistent with previous studies demonstrating that *kar9Δ* mutants exhibit defects in nuclear migration as well as in spindle alignment[136,137]. Deletion of dynein did not affect spindle positioning to the bud neck plane but resulted in an increase in time points where the new SPB is proximal to the bud neck (incorrect spindle orientation). Our results confirm that Kar9 is the dominant pathway for early spindle placement.

Our analysis of spindle alignment in the Y362E mutant combined with *dyn1Δ* or *kar9Δ* mutations reveals that both pathways depend on astral MT asymmetry to achieve perfect alignment (Figure 3.6E). In the absence of Kar9, the Y362E mutation enhances misalignment such that spindles appear to explore many more orientations. This observation suggests that dynein may be sensitive to either the increase in astral MT number, and/or to the symmetry of pole occupancy resulting from the Y362E mutation. This would be unexpected, as the asymmetric distribution of dynein to the astral MTs of the old SPB in late-metaphase has previously been shown to be independent of astral MT number and symmetry[328]. The increase in astral MTs on both SPBs therefore may lead to an increase in pushing forces applied to both poles. These pushing forces would arise from the polymerization of astral MTs rather than Kar9 or dynein. When the plus ends of astral MTs come into contact with the cortex of the mother cell, the MT exerts a pushing force on the SPB, causing it to displace[95]; astral MT pushing forces are also observed in G1 cells, prior to SPB separation[494]. Pushing forces applied by astral MTs do not normally interfere with spindle placement at the bud neck[326] if they are properly balanced by astral MTs that exert pulling forces on the old SPB.

Kar9 and dynein can both pull astral MT plus ends into the bud through their association with cortical actin. Due to the asymmetric localization of Kar9 and dynein, pulling forces are almost exclusively biased to the old SPB in wild-type cells. Pulling forces are usually restricted to one bud-directed astral MT at a time (Figure 3.9); this is likely why Kar9 is typically only seen at one focus at a time when fluorescently tagged[137,283,489]. Every astral MT has the potential to apply either a pulling force (bud-directed) or a pushing force (mother-directed). If there is an increase in the number of astral MTs at both SPBs (i.e. a shift towards symmetry of astral MT occupancy), as is seen in the Y362E mutant, an increase in the frequency of pushing forces by astral MTs at both SPBs will compete with pulling forces that are biased to the astral MTs of one SPB (Figure 3.8E). Interestingly, wild-type and Y362E cells have at most a single bud-directed astral MT at any given time (Figure 3.9). This suggests that the surplus of astral MTs projecting into the mother cell in the Y362E mutant are applying pushing forces. As a result, Y362E cells must contend with the potential for both pushing and pulling forces applied to the old pole. Taken together, these

consequences are expected to produce the spindle movements that are decoupled from the polarity axis of the cell that we observe in Y362E cells.

γ-Tubulin phospho-regulation appears to contribute to both spindle assembly and placement ([2,3] and this study), processes that occur in the nucleus and cytoplasm, respectively. Given the unaltered spindle stability as well as the two-fold increase in astral MTs, we speculate that Y362 phosphorylation mainly occurs in the cytoplasmic compartment of the cell. As well, we suggest that S360 and Y445 phosphorylation mainly occurs in the nucleus and affects nuclear MTs and their organization. In either compartment, phosphorylation may also be restricted to a sub-population of γ-TuRCs. Kollman *et al.* (2015) proposed that S360 and Y362, which are located on the inner side of the γ-TuRC, can only be accessed by a kinase when the γ-TuRC is not occupied by a MT[175]. Phosphorylation of Y362 is therefore likely to occur prior to nucleation of a MT by the γ-TuRC.

Apart of the astral MTs, the appearance of metaphase spindles in Y362E cells is similar to metaphase spindles in wild-type cells (Figure 3.8A), thus it is unclear at this point whether the number of nuclear MTs is increased by the Y362E mutation. In budding yeast, kinetochores bind to single MTs, and thus surplus nuclear MTs would increase the number of interpolar MTs; this has been shown to not significantly alter spindle function[2]. In wild-type cells, the formation of interpolar MTs does not compete with the capture of kinetochores by free MT plus ends[357], and cross-linking proteins such as Ase1 or Cin8 may limit the number of stable interpolar MTs that can be formed[2]. Nuclear MTs not bound to a kinetochore or cross-linked to another MT are relatively unstable, and for this reason the formation of surplus spindle MTs during spindle assembly may not result in major changes in spindle architecture.

The Y362E mutation introduces a negatively charged amino acid (E) in place for a phosphorylated tyrosine[1]. Our investigation of this mutant suggests that phosphorylation of Y362 is likely to increase the number of astral MTs. This may occur either by stabilizing and thereby increasing the lifetime of astral MTs, or by favoring the formation of astral MTs. Surprisingly, the increase in symmetry of astral MT occupancy that we observed in Y362E cells did not appear to block translocation of the spindle to the bud neck in the absence of dynein; this suggests that Kar9 is functional even when astral MTs are present on both SPBs and is consistent with published

data[136,263,283]. Furthermore, while both poles are associated with more astral MTs in the majority of spindles in Y362E cells, the number of astral MTs associated with the old SPB (1.42 $\pm$ 0.412) is greater than that of the new SPB (0.94 $\pm$ 0.331, $p = 8.2 \times 10^{-6}$). In fact, the difference in astral MT number between the old and new poles does not change significantly between wild-type and Y362E (0.44 ± 0.081 and 0.48 ± 0.090, respectively; p = 0.92). This suggests that although astral MT occupancy becomes symmetric, factors contributing to differences in astral MT number remain active in Y362E cells.

Regardless of the mechanism by which the number of astral MTs is increased, our analysis of Y362E suggests that γ-tubulin contributes to determining the number of astral MTs associated with the spindle during metaphase, and consequently contributes to spindle alignment. Our findings raise several fascinating questions for future studies. We speculate that phosphorylation of Y362 may increase the number of astral MTs associated with the old SPB thereby increasing the efficiency of pre-anaphase spindle alignment by Kar9. Alternatively, phosphorylation of Y362 may promote astral MT symmetry and the efficiency of dynein in maintaining the position of the SPBs in the mother and bud compartments. The two-fold increase in the number of astral MTs associated with the new SPB—which frequently lacks astral MTs in wild-type cells—opens the possibility that phosphorylation of Y362 may contribute to γ-TuRC activation, which has previously been shown to increase nucleation by a factor of two[175]. Given the evolutionary conservation of Y362 across eukaryotes, phosphorylation could be part of a general mechanism for control of microtubule number.

Chapter 4: Discussion

4.1 The caveats of phosphomimetic mutations

Phosphomimetic (PM) mutations have be in use for at least 30 years[496] and despite having several important limitations, a newer method to replace their use does not exist. The largest caveat of using PM mutations is that the mutation will never substitute exactly for a phosphorylation. Though an aspartic acid resembles a phosphorylated serine, the carboxylate group of an aspartic acid (COO^{-1}) is different in both charge and shape (i.e. steric effects) to the phosphate group ($O\text{-}PO_3^{-2}$) of a phospho-serine. An aspartic acid resembles a phospho-threonine even less so and bears no resemblance at all to a phospho-tyrosine. In fact, PM mutations are not recognized by phospho-specific antibodies highlighting the difference in chemical structure[497]. PM mutations simply create an electrostatic environment similar to a phosphorylated site. However, whether this environment elicits the same biological response as a phosphorylation is difficult to predict and depends on the protein in question. This is especially hard to assess when the function of the phosphorylation is unknown. As phospho-mutants are generally used as a tool to understand phosphorylation, this is often the case. However, there are many instances of enzymes (e.g. kinases, transcription factors, etc.) which are either activated or repressed upon phosphorylation[498-503]; in these cases, it was more straight forward to assess whether a PM mutation elicits a true phosphorylated response. Although less frequently reported, several instances exist where PM mutations fail to elicit the same behaviour as the phosphorylation event[504-509].

When no prior knowledge is known about the purpose of a phosphorylation, the use of PM mutations can leave the researcher guessing as to whether the mutation is eliciting the proper behaviour. One method which is almost always employed is to make both the phosphoinhibitory and the PM mutation. If the mutations cause clear opposite effects, it is generally considered strong evidence that the phospho-mutants are capturing near biological responses. However, biological control mechanisms are not always simple off-and-on switches and may not always cause opposite responses.

Another way to determine whether the PM mutation is causing a phosphorylation-like response is to substitute the PM mutation for an isosteric uncharged amino acid (asparagine or glutamine). This controls for the change in steric effects caused by the PM substitution; however, exceptions have occurred where asparagine/glutamine substitutions also elicited the phosphorylated behaviour[510].

For *in vitro* work, researchers have several options to create purified protein preparations with phosphorylated residues[511]. For the study of constitutive phosphorylation *in vivo*, however, researchers have less choice. One option, which is only available if the kinase is known, is to increase the activity of the kinase. However, this can have confounding effects if the kinase has other activities as well. Some researchers have had luck by fusing or trapping the kinase to the protein of interest[512]; however, not all proteins are tolerable of these types of fusions. One of the most promising techniques to be recently discovered is the incorporation of an unnatural amino acid into the genome of *E. coli*[513]. Researchers engineered a unique tRNA and a corresponding tRNA synthetase to incorporate a phospho-serine into a protein of interest during translation using the amber stop codon[513].

The resulting phosphorylated residues are still susceptible to phosphatase activity meaning that the phosphatase has to be removed in order to achieve constitutive phosphorylation. Perhaps if this method could be modified to instead encode for phosphatase-resistant phospho-serine analogs, like phosphonated serine or phospho-cysteine[514]. The complications with carrying this system over to yeast is that while *E. coli* rarely use the amber stop codon (751 instances), budding yeast encode it more frequently (3312 instances)[515,516]. Thus, it would certainly be a big undertaking to transfer this system to yeast, let alone other eukaryotes.

Apart from the chemical differences between PM mutations and true phospho-residues, another caveat of PM mutations is the constitutive nature of them. All protein exists in a phosphorylated form, regardless of temporal or spatial regulation. This can confound the interpretation of the results. For example, if a protein has both cytoplasmic and nuclear localization but is exclusively phosphorylated in the cytoplasm, PM mutations of this protein would introduce its phosphorylated form into the nucleus, a place it would never occur naturally.

Taken together, though the use of PM mutations has several limitations, at this point, it still appears to be one of the best methods for studying the effect of phosphorylation *in vivo*, especially when little is known otherwise. No method is perfect and data interpretation should always be done in light of the methodology.

4.2 Understanding the biological significance of γ-tubulin phosphorylation

The most important questions to answer when investigating phosphorylation of a protein include the when, the where, the why and the who. When is the phosphorylation taking place, where is it happening, why is it happening, and who (i.e. which kinase) is responsible for it? For the phosphorylation of yeast γ-tubulin, these are ongoing questions, though the work I have outlined in this thesis has brought us closer to the answers. Based on the data presented in this thesis and on the current literature, I speculate as to the answers of these questions in the following sections.

4.2.1 When are these phosphorylation events taking place?

The general time frames for these phosphorylation events were found by Keck *et al*. (2011)[1] who identified the SPB phospho-sites from different pools of synchronized cells. Keck *et al*. synchronized the cells two different ways: by using α-factor to arrest the cells in G1-phase, and by using a repressible copy of Cdc20 to arrest the cells at metaphase. α-Factor triggers the mating response pathway which halts the cell cycle at an early stage of SPB duplication. Cdc20 is an activator of the APC/C and, when repressed, prevents the degradation of the M-phase cyclins and thereby prevents anaphase onset.

Thus, γ-tubulin sites identified from the α-factor-arrested cells are most likely to be modified in G1-phase prior to SPB duplication; however, as γ-tubulin has little turnover during anaphase and G1[517], these sites may be phosphorylated during anaphase and remained so until the following G1. At the G1/S transition, γ-tubulin experiences high protein turnover concurrent with SPB duplication and recruitment of γ-TuSCs to the newly-formed pole; after binding to SPBs, γ-tubulin stays stably bound over the course of mitosis[517]. Therefore, phospho-sites identified from the metaphase-arrested cells are likely to be phosphorylated between S-phase and metaphase. In yeast cells, this is a fairly long window of time when many S-phase-specific and M-

phase-specific cell cycle advancements occur simultaneously (including bud formation, DNA replication, kinetochore attachment, spindle assembly and spindle placement).

By analyzing the phenotypes of the phospho-mutations at these M-phase sites, we have gained insight into the precise timing of the phosphorylation. Site S360—which is involved in spindle assembly—is phosphorylated in a Cdk1-Clb3-dependent manner[2,402]. Clb3 levels start to rise in S-phase and peak at the start of mitosis[518]. This is consistent with S360's role in spindle assembly. M-phase site Y445 also participates in spindle assembly[3] and my own work suggests that it is phosphorylated in a concerted manner with S360. Based on these observations, I suspect that Y445 is modified at a similar time to S360—specifically in S-phase during early to mid-spindle assembly.

In Chapter 3 of my work, I showed that the γ-tubulin M-phase site, Y362, is involved in spindle placement. A PM mutation at this site increased the number of astral MTs thereby increasing the symmetry of astral MT occupancy across the two SPBs (Figure 3.8). This led to aberrations in spindle alignment, but not spindle positioning (Figure 3.6 and Figure 3.7). We hypothesized that Y362 phosphorylation may increase local astral MT number on the outer plaque of the pre-existing pole to increase the efficiency to spindle placement by Kar9, or alternatively, that it may promote astral MT symmetry to increase dynein's efficiency in maintaining the spindle within the mother and bud compartment. If Y362 promotes efficiency of Kar9 activity, I would expect it to be phosphorylated earlier in spindle placement when Kar9 is more dominant; however, if Y362 promotes dynein function, I would expect it to be phosphorylated later in spindle placement (closer to metaphase) when dynein becomes more active. Though, it is important to note that while traditionally, dynein is seen as being active later in spindle placement, several observations suggest that this is an oversimplification and dynein might be active much earlier[98,162,326]. Further work is required in understanding the mechanism of Y362E astral MT regulation in order to pinpoint the time of phosphorylation, but it most likely occurs some time during spindle placement.

Other M-phase mutants S42-S43/T44 and S444 had no discernable growth phenotypes and thus, we do not have enough information as of yet to specify the point when these sites are phosphorylated (other than somewhere between S-phase and metaphase).

In summary, I suspect that the G1-identified γ-tubulin phospho-sites (T130 and T227) are phosphorylated in G1, prior to SPB duplication. M-phase sites S360 and Y445 are likely phosphorylated in mid-S-phase during spindle assembly. Similarly, I expect Y362 to be phosphorylated in S-phase during spindle placement.

4.2.2 The role of γ-tubulin G1-site phosphorylation in budding yeast

In Chapter 2, I showed that when mutating both G1 phospho-sites (T130 and T227), cells behaved nearly identically to wild-type in MT stabilizing or destabilizing conditions indicating that MT function is largely unperturbed (Figure 2.4). Despite this, the mutant had a striking dependence on the SAC (Figure 2.3). This is the first instance of a γ-tubulin phospho-mutant whose dependence on the SAC is not due to perturbed MT function. Instead, I propose that these sites play a role in the eventual attachment of chromosomes to kinetochore MTs.

As yeast undergo a closed mitosis, kinetochore MTs have continual access to the chromosomes throughout the cell cycle except during centromere replication in early S-phase[180,181,519]. Additionally, in late G1-phase, SPB duplication completes and MTs from the newly-formed pole begin to search for kinetochore attachments. Thus, at the G1/S-phase transition and into early S-phase, MTs from the old pole are searching to reattach to kinetochores (after centromeric DNA replication), and MTs from the new pole are searching to make new kinetochore attachments. This places the phosphorylation of T130 and T227 at the right time to participate in the process of chromosome attachment. We suspect that modification at these sites contributes to this process. As the phosphoinhibitory mutant (T130A-T227A) is not sensitive to the loss of the SAC (*mad2Δ*), we hypothesize that phosphorylation does not promote chromosome attachment. Instead, phosphorylation may inhibit chromosome attachment; this would explain why constitutive phosphorylating conditions (i.e. PM mutations) are lethal in the absence of Mad2 (Figure 2.3).

At this point, we can only speculate as to how this regulation contributes to chromosome attachment. Perhaps these G1 mutations are inherently affecting the MT's attachment ability by changing the lattice of the MT. However, it would be unlikely that changing the lattice would not also change the dynamics of the MTs, and as previously noted, the dynamics of T130D-T227D

seem largely undisturbed (Figure 2.4). Instead, we suspect that phosphorylation of T130 and T227 is eliciting its effects through the regulation of binding partners.

There is a finite number of proteins which both localize to the SPB and are involved in kinetochore attachment (although this may change as new discoveries are made). For example, several MAPs, like Kar3, Stu2 and Cin8 localize at, or very close to, SPBs around the G1/S transition, and they participate in kinetochore attachment[32,88,156,157,520]. Alternatively, this γ-tubulin-dependent regulation need not strictly involve MAPs. For example, kinase Mps1 localizes to both SPBs and kinetochores[521]. Importantly, all these proteins carry out kinetochore-independent processes while localized near the SPB. Kar3, when partnered with Vik1, is found close to the SPB and cross-links parallel MTs[32-34]. Stu2 localizes to the SPB where it helps to anchor MTs and regulate (+)end dynamics[156]. Cin8 collects near the SPBs in order to mediate SPB separation[88]. Lastly, Mps1 mediates SPB duplication while localized to the poles, and the spindle assembly checkpoint at the kinetochores[521].

Perhaps phosphorylation of γ-tubulin stimulates the timely execution of the SPB-related function of a protein, and then, upon γ-tubulin dephosphorylation, the protein is promoted to participate in its kinetochore-related function. This regulation of the unknown protein's activity may occur through the γ-tubulin-dependent recruitment of modification enzymes (e.g. kinases, phosphatases, etc.). All three MAPs and Mps1 are regulated by at least phosphorylation[401,434,522-526]. In fact, phosphorylation of Cin8 alters both its motile properties and its localization[527-529]. Additionally, several modifying enzymes localize to SPBs, including Cdk1, Swe1, and several mitotic exit kinases[263,530,531].

In summary, we hypothesize that γ-tubulin contributes to chromosome attachment by regulating the behaviour of kinetochore-related proteins (possible through indirectly contributing to their modification). Investigation of the T130D-T227D mutant's SGI profile using our GAMER analysis method would be beneficial to understanding how this mutation contributes to chromosome attachment and may even identify any candidate kinetochore-related proteins involved in the process.

4.2.3 What kinase(s) phosphorylates the G1 sites?

At this point, we cannot determine whether sites T130 and T227 are phosphorylated by the same kinase or by separate kinases. The intramolecular genetic relationship between the two sites does not necessarily mean a single kinase phosphorylates them both. However, the following section discusses the most likely kinases to phosphorylate either or both of the sites.

Seeing as SADB phosphorylates S131 in humans[353], it follows that the SADB homolog in yeast, Hsl1, is a prime kinase candidate for the phosphorylation of T130 in yeast. Moreover, Hsl1 phosphorylated γ-tubulin in a high-throughput *in vitro* screen[433]. However, Hsl1 is ubiquitinated and degraded by APC/C from late-metaphase until after the onset of S-phase[532,533]. Thus, Hsl1 is absent from the cell during G1 and is not likely responsible for the phosphorylation of T130 or T227.

Dual specificity kinase Mps1 localizes to the SPBs in G1 where it phosphorylates several SPB components contributing to many steps of SPB duplication[432,530,534-537]. Two of Mps1's targets include components of the γ-TuRC—Spc110 and Spc98[432,534]—meaning that Mps1 exists at precisely the right time and place to phosphorylate γ-tubulin sites T130 and/or T227. Additionally, Mps1 localizes to the kinetochore later in the cell cycle where it participates in the spindle assembly checkpoint and chromosome attachment[530,538-540]. This could potentially provide the link for T130D-T227D's involvement in chromosome attachment.

Cdk1 is active during G1 when partnered with cyclins Cln1-3. Cln1 and Cln2 localize to both the cytoplasm and nucleus, while Cln3 localizes primarily to the nucleus[541-544]. Though distinct SPB foci have not been seen for Cln localization, similar to Mps1, Cdk1-Clns phosphorylates pole-specific proteins[1,434,534] and are required for SPB duplication[425,545]. Thus, Cdk1 in complex with the G1 cyclins may be responsible for the phosphorylation of T130 and/or T227.

The yeast homolog of casein kinase 1δ, Hrr25, localizes to SPBs in a γ-TuSC-dependent manner and phosphorylates Spc98 *in vivo* and *in vitro*[404]. Additionally, loss of Hrr25 kinase activity results in abnormally long astral MTs specific to G1-phase indicating the importance of Hrr25 activity at this time[404]; thus, it may be involved in γ-tubulin phosphorylation. However, when

identifying Hrr25-dependent *in vitro* phospho-sites on γ-tubulin, neither T130 nor T227 were found[404], suggesting that Hrr25 is not the kinase responsible.

In summary, I believe that either Mps1 or Cdk1 are the most likely candidates for γ-tubulin G1-site phosphorylation. Both localize and modify proteins at the spindle pole body during G1 and are thus, in the right place at the right time to carry out these modifications.

4.2.4 The contribution of S360 and Y445 to spindle assembly

Previously work done in our lab has shown that S360 phosphorylation contributes to the construction of the spindle midzone (or core bundle) during spindle assembly[2]. When phosphorylation was blocked at this site (S360A), spindles formed additional interpolar-like MTs leading to an overbuilt core bundle and less dynamic spindle fluctuations. Conversely, when a PM mutation was made at this site (S360D), there was a significant lack of antiparallel interpolar MTs causing a complete loss of the core bundle. In this case, spindles experienced large fluctuations indicative of severe instability ([2] and Figure 3.1D).

Similarly, we suspected that phospho-site Y445 also contributed to spindle assembly as PM mutants at this site (Y445D) often exhibited a fishhook spindle—when an anaphase spindle hyperelongates past the length of the cell and buckles as it hits the cell cortex[3]. Fishhook spindles occur when the cell has defects in spindle disassembly. Spindle disassembly involves the depolymerization of interpolar MTs out of the plane of cell division to allow for cytokinesis. This requires the APC/C-dependent degradation of stabilizing MAPs, the Ipl1-dependent phosphorylation and removal of Bim1, and the depolymerization activity of Kip3[58]. Perturbations in spindle disassembly are often preconditioned by improper spindle assembly.

We confirmed our suspicions that Y445 was related to spindle assembly in the work presented in Chapter 3 of my thesis. Similar to S360D, Y445D spindles experiences large fluctuations indicative of spindle instability (Figure 3.1D); additionally, Y445D had an SGI profile consistent with perturbed spindle assembly (Figure 3.4D). Lastly, by making simultaneous phospho-mutations at both S360 and Y445, we determined that these sites are likely phosphorylated in a coordinated manner (Figure 2.8 and Figure 3.5). Based on the data presented in this thesis and on published data[2,3], we suspect that these phosphorylation events occur predominantly within the nucleus where they can exert their effects on spindle assembly.

These sights may contribute to nucleation as γ-tubulin likely requires modification in order to reach its full nucleation capacity[175]. Indeed, too many or too few spindle MTs may lead to erroneous spindle assembly. However, electron tomographic reconstructions of S360A and S360D spindles show no significant change in total nuclear MT number suggesting that nucleation is unchanged[2]. Regardless, the nucleation capacity of S360-Y445 phospho-mutants must be verified to ensure this essential process is not being disrupted. Relatedly, the S360-Y445 mutants may be changing the lattice of the MT, leading to changes in MAP behaviour (e.g. changes in a motor's ability to track a MT, or in a depolymerase's ability to disassemble MTs). Though, this is expected to have global effects on most MAPs, and would probably be detrimental to the cell leading to lethality for PM mutants (e.g. S360D or Y445D); however, S360D and Y445D mutants are viable. Nonetheless, cryo-electron microscopy of MTs polymerized off of purified yeast γ-TuRCs from S360-Y445 phospho-mutants may be necessary to assess lattice conformation.

Alternatively, we hypothesize that phosphorylation of S360 is related to the Y445-dependent structural changes of the γ-tubulin C-terminal tail[427]. Phosphorylation of Y445 increases the propensity for γ-tubulin's C-terminal tail to take on an extended confirmation which is thought to regulate the recruitment of specific γ-tubulin-interaction proteins [427]. We propose that S360 phosphorylation feeds into this structural change. How might this work, and how would this contribute to spindle assembly? First of all, S360 and Y445 phosphorylation probably contribute to different steps in the same process. If they contributed redundantly to the same step, then the mixed phospho-mutants SDYF and SAYD would be no worse than S360D or Y445D alone, respectively. Secondly, it is important to note that these two steps are not essential for cell viability as S360A-Y445F has no growth phenotype, instead it is only when one of these steps is constitutively triggered that the other one becomes essential. This explains why S360D and Y445D have milder phenotypes when compared to SDYF and SAYD, because in the single mutants, the second residue is still available for phosphorylation. Lastly, while phosphorylation at one residue is required to suppress the otherwise lethal phenotype caused by a PM at the other, this is something that must be regulated in a timely manner, since PMs at both sites is also lethal, indicating that at some point, dephosphorylation of at least one of the residues is required

for cell cycle progression. In summary, constitutive triggering of one step is not detrimental to the cell as long as the other step can cycle between “on” and “off” states.

An example of how these two steps might be coordinated is as follows: during spindle assembly, phosphorylation of one residue (e.g. S360) recruits a MAP, while phosphorylation of the other (e.g. Y445) recruits an enzyme which modifies the MAP (henceforth known as “the modifier”) and changes its behaviour (i.e. prevents MT cross-linking) (Figure 4.1). After modification, both MAP and modifier are released from the pole. The slow growth seen in the single S360D mutant may be due to increased behaviour changes in the MAP (i.e. increased prevention of MT cross-linking) or due to increased sequestering of the MAP at the SPBs (Figure 4.1B). In Y445D, the slow growth may be due to increased sequestering of the modifier, which could have essential functions elsewhere in the cell. However, in the case of the single mutants (S360D or Y445D), MAP modification and subsequent release would still be occurring somewhat as the other non-mutated residue (Y445 or S360, respectively) would still be available for modification. In the mixed phospho-status mutants, SDYF and SAYD, phosphorylation is prevented completely at the other residue (Y445F or S360A, respectively). This means that, in the case for SDYF, the MAP is constitutively localizing to the pole, but cannot be released because no modifier is being recruited; similarly, in the case of SAYD, the modifier is constitutively localizing to the pole, but cannot be released because the MAP is not being recruited. If the MAP and modifier have essential functions elsewhere in the cell or at different times in the cell cycle, this may result in lethality, especially if either are not abundant in cellular concentration.

This proposed model brings to mind the question as to the identity of the MAP involved. MAPs involved in cross-linking MTs, like Cin8, are the most likely candidates. In fact, Cin8 distribution across the spindle seems to differ between wild-type, S360A and S360D mutants (E. Nazarova, unpublished observations). In S360D spindles, Cin8 experiences a biased accumulation at/near the old pole, perhaps due to either an increased sequestering in this region, or due to a change in Cin8 behaviour which inhibits its ability to cross-link properly. In addition to having a complete lack of a core bundle, S360D mutants also frequently have increased MT length[2]. Therefore, other MAP candidates include Kip3 or Kar3, both of which localize to the nuclear MTs and contribute to spindle stability, and both of which can depolymerize MTs.

Figure 4.1 | Proposed model for the contribution of S360 and Y445 to spindle assembly. (A) Phosphorylation of S360 increases recruitment of a MAP; phosphorylation of Y445 increases recruitment of the MAP modifier. Upon modification of the MAP, both proteins are released and able to carry out their downstream functions which, for the MAP, would be to prevent MT cross-linking. (B) Proposed explanation of observed phenotypes for S360-Y445 mutants. S360A prevents MAP recruitment leading to higher levels of cross-linking; S360D increases MAP recruitment leading to prevention of cross-linking and possible sequestering of the MAP; SDYF leads to constitutive sequestering of the MAP, resulting in lethality; SAYD leads to constitutive sequestering of the modifier, resulting in lethality.

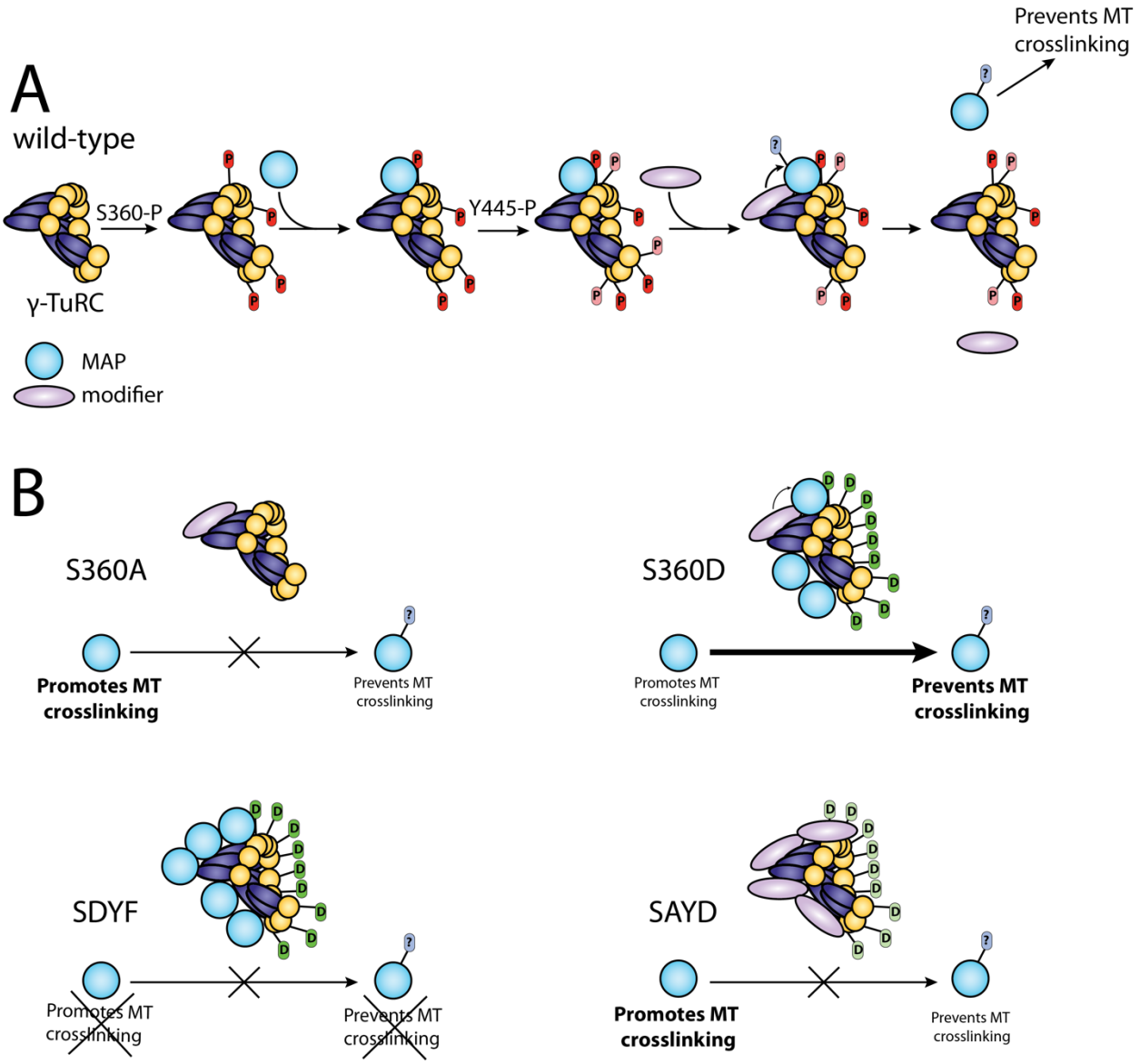

What would be the benefit of decreasing a MT's ability to cross-link to other MTs, especially since having an abundance of cross-linking MTs (as is seen in S360A) has no obvious consequences? Considering the evolutionary conservation of these sites, it is likely that regulation at these sites procures an advantage over evolutionary time, something we might not see when growing yeast short-term in optimal laboratory conditions. Mitotic spindles are crucial in ensuring the proper inheritance of genetic material and thus, must exhibit a robustness to changing environmental conditions. For example, in vertebrates, spindles are so robust that they can undergo mitosis even in the absence of centrosomes[197]. I suspect that regulation at these residues contributes to the robustness of the yeast spindle. The negative consequences associated with the yeast γ-tubulin PM mutations (e.g. S360D and Y445D have slow growth) suggests that not all γ-tubulin in all γ-TuRCs are phosphorylated at one time; perhaps only a subpopulation of γ-TuRCs or γ-TuSCs are phosphorylated. This would allow for a sliding scale of precise control over the stability of the spindle and contribute to a more adaptable spindle. The cell would be able to modulate its spindle to preform optimally in growth conditions both where a stiffer spindle, or where a flexible spindle is more beneficial.

In summary, we speculate that regulation at γ-tubulin sites S360 and Y445 function in separate steps in the same related process that ultimately contributes to spindle stability via interpolar MT cross-linking. We suspect this involves the regulation of MAP behaviour and only occurs on a subset of γ-TuRCs at the poles. Investigation of the physical interaction profiles of different phospho-mutants at S360 and Y445 using a high-throughput protein-protein interaction assay, like the optimized yeast cytosine deaminase protein-fragment complementation assay (OyCD PCA)[402] would aid greatly in assessing whether γ-tubulin participates in any sequestering behaviour.

4.2.5 The contribution of Y362 to spindle placement

In Chapter 3, we characterized the novel γ-tubulin allele, Y362E, and discovered a role for it in spindle placement. During the process of spindle placement, the forces produced by astral MTs are key for proper positioning and alignment[489-492]. Under normal conditions, astral MTs emanating from the pre-existing pole persist longer due to both the increased stability caused by the asymmetric loading of +TIP proteins (like Bim1 and Kar9), as well as the closer proximity to

the bud neck[21,283,288,494]. This presumably leads to an increased number of astral MTs associated with the pre-existing SPB relative to the newly-formed SPB, and thus, an asymmetric distribution of astral MTs between the poles. Y362E spindles have an increase number of astral MTs on both poles and a shift from asymmetric to symmetric pole MT occupancy. This likely explains Y362E's perturbed spindle alignment. Due to Y362E's role in spindle alignment, we propose that this regulation event is mostly restricted to the cytoplasm, on the outer plaque of the SPB where it would solely affect the astral MTs and not the nuclear MTs.

Increased number of astral MTs could lead to spindle misalignment in several different ways. At the most basic level, more astral MTs means more external force for the spindle to contend with when properly aligning. Spindle placement requires a balance of pulling and pushing forces administered by the astral MTs. Pulling forces are the result of Kar9/Bim1 or dynein (+)end localization and interaction with cortical actin. Due to the largely asymmetric SPB localization of Kar9 and dynein, most pulling forces are biased to MTs associated with the old pole and are usually restricted to one bud-directed astral MT at a time ([137,283,489] and Figure 3.9). Pushing forces occur in a Kar9- and dynein-independent manner through the polymerization and subsequent contact of astral MTs with the cortex[494]. Y362E spindles continue to have only one bud-directed astral MT at a time, indicating that the number of pulling MTs remains unchanged (Figure 3.9). Thus, all additional astral MTs in Y362E are likely to be applying a pushing force to the spindle. This would produce spindle movements that are decoupled from the polarity axis and lead to defects in spindle alignment as is observed in Y362E.

The question that follows is what causes the increase in astral MT number? This may be a direct result of increased nucleation. γ-Tubulin likely requires modification in order to reach its full nucleation capacity[175]; additionally, the location of this residue on γ-tubulin suggests that it can only be accessed by a kinase when the γ-TuRC is unoccupied by a MT (i.e. prior to nucleation)[175]. As of such, the nucleation capacity of Y362E must be assayed either *in vivo* or *in vitro* (Trisha Davis, personal communication; [175]).

Aside from activation of the γ-TuRC and increased nucleation, the Y362E mutation could also increase astral MT number more indirectly through the modulation of MAPs. Changes in MAP behaviour can have strong effects on spindle alignment. For example, when Kar9 is localized

to both poles using a mutant which blocks the two Cdk1-Clb4 phosphorylation sites (*kar9-AA*), both sets of astral MTs are targeted to the bud and the vast majority of spindles are misaligned[283]. Additionally, several MAPs, including Kar9-Bim1-Myo2 complexes, stabilize the dynamics of MTs leading to an increased astral MT number[494]. Though, if the increase astral MT number was the sole result of increased or misdirected Kar9 activity, we would not expect the combined *Y362E; kar9Δ* mutant to have a worse phenotype than the *kar9Δ* mutant alone, as was observed (Figure 3.6C and G). Thus, though Kar9 behaviour may be perturbed in a different manner in Y362E, it is not likely responsible for the increase in astral MT number. Instead, we suspect another MAP may be responsible, perhaps dynein, Kip2 or Kip3.

Like Kar9, dynein also experiences asymmetrical localization to the SPBs throughout metaphase[328]. At anaphase onset and during spindle elongation, dynein localization becomes symmetric so that it may pull the SPBs in opposite directions[71,328]. It is possible that γ-tubulin contributes to dynein regulation through residue Y362. For example, if Y362E mislocalizes or misregulates dynein which contributes to increased astral MT number and spindle misalignment, we would expect the combination of Y362E with *dyn1Δ* to be no worse at aligning than *dyn1Δ* alone. This is close to what we observe—there is little difference between *dyn1Δ* and *Y362E; dyn1Δ* in terms of spindle alignment (Figure 3.6C and G). Additionally, we would expect that the combination of misregulation of dynein with the *kar9Δ* mutation would be more severe because both spindle placement pathways would be perturbed. Indeed, we do see a more severe alignment phenotype with *Y362E; kar9Δ* than with *kar9Δ* alone (Figure 3.6C and G). Lastly, Y362E spindles persist to longer lengths prior to anaphase more often than wild-type spindles (Figure 3.1D or Figure 3.7; compare mean spindle length data points)—it is possible this is due to premature symmetrical pulling on the spindle. This length persistence would be expected to disappear upon deletion of dynein. We do see a reduction in the frequency of spindles greater than or equal to 1.5-1.6 µm in *Y362E; dyn1Δ* when compared to *Y362E* alone (Figure 3.6G; top right panel, green areas) especially for those spindles which are aligned but misoriented. Taken together, these data suggest that dynein regulation could be perturbed in Y362E cells. Investigating dynein localization in Y362E cells would help to ascertain this hypothesis.

Kinesin-7 motor protein, Kip2, is a good candidate for causing increased astral MT numbers in the Y362E mutant. It is already involved in spindle placement by transporting Kar9 and dynein to astral MT (+)ends[21,22]. Additionally, Mck1-dependent phospho-regulation of Kip2 modulates the length and number of astral MTs as well as the amount of Kar9 and dynein on the astral MT (+)ends[23]. While loss of Kip2 leads to rare and short astral MTs at both poles[25], PI mutations at the Mck1-dependent phospho-sites of Kip2 lead to an increased number of abnormally long astral MTs, similar to what we see in the γ-tubulin Y362E mutant[23]. Like Y362E, this increase in astral MT number and length leads to a perturbation in spindle alignment[23]. Thus, it is possible that site Y362 contributes to the phospho-regulation of Kip2. It would be interesting to combine Y362E with the PI mutations of Kip2 to investigate whether this enhances each individual phenotype; lack of enhancement would indicate that these phospho-sites participate in the same pathway.

Lastly, Kip3 is a candidate for contributing to the increase astral MT number in Y362E. Kip3 has been implicated in the Kar9-dependent pathway for spindle placement, though the details are unclear[25,53,54]. Kip3 is thought to regulate the length and dynamics of cortically attached astral MTs; in the absence of Kip3, astral MTs grow inappropriately and push the spindle away from the aligned state[49]. This is what we believe is contributing to spindle misalignment in the Y362E mutant.

In summary, we propose that Y362E contributes to spindle placement either by directly or indirectly regulating astral MT number. It may directly contribute to astral MT number through regulation of γ-TuRC activation and nucleation. Alternatively, it may indirectly contribute to astral MT number through the regulation of MAP behaviour, like Kar9, dynein, Kip2 or Kip3.

Why would a cell want to control the number of astral MTs during spindle placement? We propose that this regulation might be restricted to the outer plaque of the pre-existing pole, to locally increase astral MT number in order to increase the efficiently of Kar9-dependent spindle alignment. Alternatively, this regulation may occur on the outer plaque of both poles to promote astral MT symmetry during dynein-dependent spindle alignment and elongation.

4.2.6 The kinase(s) responsible for γ-tubulin tyrosine phosphorylation

In yeast, all predicted or confirmed kinases (except two histidine kinases) are members of the serine/threonine (S/T) kinase family from a strictly sequential perspective—conventional tyrosine kinases are lacking[546]. However, tyrosine phosphorylation does occur in yeast. Instead, yeast seem to have co-opted the traditional S/T kinases to carry out tyrosine phosphorylation; indeed, out of 119 screened kinases, 27 of them readily phosphorylated tyrosine[433]. These kinases are often referred to as dual-specificity kinases as they can phosphorylate both S/T and tyrosine substrates (though sometimes prefer one to the other)[546]. This significantly narrows down the number of possible kinase candidates for Y362 and Y445. At this point, we do not know whether the same kinase phosphorylates both Y362 and Y445 but, seeing as these sites are involved in different functions and regulate separate sets of microtubules (astral MTs or nuclear MTs, respectively), we suspect that different kinases may modify these sites. Additionally, based on our data, we hypothesize that Y362 is mostly phosphorylated on the outer plaque of the SPB (meaning the kinase would access the SPBs from the cytoplasm) while Y445 is mostly phosphorylated on the inner plaque (meaning the kinase would gain access from the nucleus). Of the kinases confirmed to phosphorylate tyrosines *in vivo*, the prime candidates are those that are known to be in the right place at the right time. For Y362 or Y445, this includes Mck1, Swe1 or Mps1.

Mck1 is a dual-specificity kinase and the yeast homolog of the highly conserved glycogen synthase kinase 3 (GSK-3). In yeast, it is involved in chromosome segregation, meiotic entry, and most recently, spindle placement[23,547,548]. Mck1 phosphorylates the MAP, Kip2, which regulates the length and number of astral MTs as well as the amount of Kar9 or dynein on the astral MT (+)ends[23]. PI mutations at the Mck1-dependent phospho-sites of Kip2 lead to an increased number of abnormally long astral MTs, similar to what we see in the γ-tubulin PM mutant, Y362E[23]. Like Y362E, this increase in astral MT number and length leads to a perturbation in spindle alignment[23]. Additionally, Mck1 localizes to the SPBs from S-phase until anaphase[23], the time frame when Y362 is phosphorylated. Taken together—Mck1's timely SPB localization and its involvement in not only spindle alignment but in causing a phenotype very similar to Y362E's phenotype—Mck1 is a good candidate kinase for phosphorylating γ-tubulin at the Y362 site.

Swe1 is a cell cycle regulated dual-specificity kinase which accumulates from G1- to S-phase to prevent premature entry into M-phase by inhibiting the activity of Cdk1-Clb complexes. In G1, Swe1 accumulates in the nucleus, and then relocalizes to the bud neck in S-phase where it is hyper-phosphorylated and degraded allowing for entry into mitosis. Thus, Swe1 is in the right place (the nucleus) at the right time (S-phase) to be capable of phosphorylating Y445 on the inner plaque.

Independent of its role in Cdk1 inhibition, Swe1 also influences SPB inheritance. Swe1 has recently been shown to localize to the SPBs and phosphorylate SPB component Nud1[263]. Phosphorylation of Nud1 marks it as the pre-existing pole to ensure proper Kar9 asymmetry and subsequent spindle orientation[263]. Swe1 phosphorylates Nud1 in G1-phase; upon S-phase onset, when Nud1 is recruited to the newly-formed SPB, Swe1 is relocalized to the bud neck where it is rapidly degraded[263,302,303]. This ensures that only the pre-existing SPB is marked; by the time the new SPB recruits Nud1, Swe1 is no longer on the poles. Moreover, as Nud1 is an outer plaque protein, Swe1 must localize specifically to the outer plaque in G1. Therefore, Swe1 is also a prime candidate for the phosphorylation of Y362 as it localizes to the outer plaque where it phosphorylates Nud1 and contributes to proper spindle placement and pole inheritance.

In human cells, Mps1 localizes to the centrosomes during interphase[549] where it mediates centrosome duplication[550]. From the start of M-phase until anaphase onset, Mps1 enters the nucleus and localizes to the kinetochores where it is indispensable for the SAC and chromosome alignment[549,551-555]. In yeast, Mps1 localization seems to follow a similar pattern: it localizes to the SPBs early in the cell cycle to mediate the process of SPB duplication, then is found on the kinetochores during M-phase where it participates in the SAC. Whether Mps1 leaves the SPBs completely upon kinetochore localization is not known as detection of fluorescently tagged Mps1 using standard microscopy techniques is difficult[556]. Regardless, Mps1 localizes to the SPBs and is likely to be there even after the G1/S transition. Additionally, Mps1 protein levels stay high throughout the course of the cell cycle until after the onset of anaphase[557]. Thus, as Mps1 is a dual specificity kinase, it is good candidate for the phosphorylation of γ-tubulin tyrosines.

4.3 Conclusions

γ-Tubulin and the γ-TuRC have long been known to be the cell's primary nucleator of MTs. However, even this well-studied function is not fully understood. In yeast, γ-TuRCs do not exhibit strong nucleation capacity on their own and likely require modifications for activation[175] but what these modifications are is not yet known. In addition to nucleation, γ-TuRCs are hypothesized to play a role at the MTOC as a general signalling hub for the cell. In support of this, γ-tubulin and the γ-TuRC participate in many nucleation-independent roles. Additionally, γ-TuRCs are in a prime position to coordinate cellular signaling and regulation with the dynamic properties and organization of the spindle. Being primarily located at MTOCs, γ-TuRCs are at the center of the vast cytoskeletal network allowing them to act as an ideal integration points for incoming and outgoing signals.

Through my work, we have furthered our understanding of γ-tubulin and its roles during the cell cycle. The discovery that G1-specific sites (T130 and T227) influence chromosome attachment independent of spindle assembly opens up the possibility of γ-tubulin contributing more directly to kinetochore capture, possibly by regulation of kinetochore-related proteins. Moreover, the clarification of Y445's role in spindle assembly and its likely coupling to S360 shed light on the concerted regulation of γ-tubulin and its role in building a functional mitotic spindle. Lastly, the investigation of the novel Y362E allele and the discovery that it regulates astral MT number is the first instance of a γ-tubulin phospho-site participating in spindle placement. Whether this residue affects MT nucleation, or the behaviour of MAPs, both are exciting avenues for further study. Moreover, the high conservation of these sites among other eukaryotes suggests that γ-tubulin phosphorylation may be an evolutionarily conserved means to regulate γ-tubulin function. Overall, the work that I have done has contributing both to our understanding of γ-tubulin phosphorylation, but also to γ-tubulin's overall functions both as a nucleator and as a hub of cellular signal integration.

List of references

1 Keck, J. M. *et al.* A cell cycle phosphoproteome of the yeast centrosome. *Science* **332**, 1557-1561 (2011).

2 Nazarova, E. *et al.* Distinct roles for antiparallel microtubule pairing and overlap during early spindle assembly. *Mol Biol Cell* **24**, 3238-3250, doi:10.1091/mbc.E13-05-0232 (2013).

3 Vogel, J. *et al.* Phosphorylation of gamma-tubulin regulates microtubule organization in budding yeast. *Dev. Cell* **1**, 621-631 (2001).

4 Stirling, P. C. *et al.* The complete spectrum of yeast chromosome instability genes identifies candidate CIN cancer genes and functional roles for ASTRA complex components. *PLoS Genet* **7**, e1002057 (2011).

5 Morgan, D. O. *The Cell Cycle: Principles of Control*. (OUP/New Science Press, 2007).

6 Alberts, B. *et al.* Molecular Biology of the Cell, (Garland Science, New York, 2008). *Google Scholar*, 652 (2002).

7 Lodish, H. *et al. Molecular cell biology*. Vol. 3 (WH Freeman New York, 1995).

8 Bergen, L. G. & Borisy, G. G. Head-to-tail polymerization of microtubules in vitro. Electron microscope analysis of seeded assembly. *The Journal of Cell Biology* **84**, 141-150 (1980).

9 Mitchison, T. & Kirschner, M. Dynamic instability of microtubule growth. **312**, 237-242 (1984).

10 Brouhard, G. J. Dynamic instability 30 years later: complexities in microtubule growth and catastrophe. *Molecular biology of the cell* **26**, 1207-1210 (2015).

11 Maurer, S. P. *et al.* EB1 accelerates two conformational transitions important for microtubule maturation and dynamics. *Current Biology* **24**, 372-384 (2014).

12 Bieling, P. *et al.* Reconstitution of a microtubule plus-end tracking system in vitro. *Nature* **450**, 1100-1105 (2007).

13 Gardner, M. K., Zanic, M., Gell, C., Bormuth, V. & Howard, J. Depolymerizing kinesins Kip3 and MCAK shape cellular microtubule architecture by differential control of catastrophe. *Cell* **147**, 1092-1103 (2011).

14 Bowne-Anderson, H., Zanic, M., Kauer, M. & Howard, J. Microtubule dynamic instability: a new model with coupled GTP hydrolysis and multistep catastrophe. *Bioessays* **35**, 452-461 (2013).

15 Coombes, C. E., Yamamoto, A., Kenzie, M. R., Odde, D. J. & Gardner, M. K. Evolving tip structures can explain age-dependent microtubule catastrophe. *Current Biology* **23**, 1342-1348 (2013).

16 Desai, A. & Mitchison, T. J. Microtubule polymerization dynamics. *Annual review of cell and developmental biology* **13**, 83-117 (1997).

17 Endow, S. A., Kull, F. J. & Liu, H. Kinesins at a glance. *J Cell Sci* **123**, 3420-3424 (2010).

18 Thrower, D. A., Jordan, M., Schaar, B., Yen, T. & Wilson, L. Mitotic HeLa cells contain a CENP-E-associated minus end-directed microtubule motor. *The EMBO Journal* **14**, 918 (1995).

19 Shrestha, R. L. & Draviam, V. M. Lateral to end-on conversion of chromosome-microtubule attachment requires kinesins CENP-E and MCAK. *Current biology* **23**, 1514-1526 (2013).
20 Bancroft, J., Auckland, P., Samora, C. P. & McAinsh, A. D. Chromosome congression is promoted by CENP-Q-and CENP-E-dependent pathways. *J Cell Sci* **128**, 171-184 (2015).
21 Maekawa, H., Usui, T., Knop, M. & Schiebel, E. Yeast Cdk1 translocates to the plus end of cytoplasmic microtubules to regulate bud cortex interactions. *EMBO J.* **22**, 438-449 (2003).
22 Carvalho, P., Gupta, M. L., Hoyt, M. & Pellman, D. Cell cycle control of kinesin-mediated transport of Bik1 (CLIP-170) regulates microtubule stability and dynein activation. *Dev. Cell* **6**, 815-829 (2004).
23 Drechsler, H., Tan, A. N. & Liakopoulos, D. Yeast GSK-3 kinase regulates astral microtubule function through phosphorylation of the microtubule-stabilizing kinesin Kip2. *J. Cell. Sci.* **128**, 3910-3921 (2015).
24 Roberts, A. J., Goodman, B. S. & L, R.-P., Samara. Reconstitution of dynein transport to the microtubule plus end by kinesin. *Elife* **3**, e02641 (2014).
25 Miller, R. K. *et al.* The kinesin-related proteins, Kip2p and Kip3p, function differently in nuclear migration in yeast. *Mol Biol Cell* **9**, 2051-2068 (1998).
26 Hibbel, A. *et al.* Kinesin Kip2 enhances microtubule growth in vitro through length-dependent feedback on polymerization and catastrophe. *eLife* **4**, e10542 (2015).
27 Huyett, A., Kahana, J., Silver, P., Zeng, X. & Saunders, W. The Kar3p and Kip2p motors function antagonistically at the spindle poles to influence cytoplasmic microtubule numbers. *J. Cell. Sci.* **111 (Pt 3)**, 295-301 (1998).
28 Hepperla, A. J. *et al.* Minus-end-directed Kinesin-14 motors align antiparallel microtubules to control metaphase spindle length. *Dev. Cell* **31**, 61-72 (2014).
29 Saunders, W. & Hoyt, M. Kinesin-related proteins required for structural integrity of the mitotic spindle. **70**, 451-458 (1992).
30 Braun, M., Drummond, D. R., Cross, R. A. & McAinsh, A. D. The kinesin-14 Klp2 organizes microtubules into parallel bundles by an ATP-dependent sorting mechanism. *Nature cell biology* **11**, 724-730 (2009).
31 Fink, G. *et al.* The mitotic kinesin-14 Ncd drives directional microtubule–microtubule sliding. *Nature cell biology* **11**, 717-723 (2009).
32 Manning, B. D., Barrett, J. G., Wallace, J. A., Granok, H. & Snyder, M. Differential regulation of the Kar3p kinesin-related protein by two associated proteins, Cik1p and Vik1p. *The Journal of cell biology* **144**, 1219-1233 (1999).
33 Allingham, J. S., Sproul, L. R., Rayment, I. & Gilbert, S. P. Vik1 modulates microtubule-Kar3 interactions through a motor domain that lacks an active site. *Cell* **128**, 1161-1172 (2007).
34 Gardner, M. K. *et al.* The microtubule-based motor Kar3 and plus end–binding protein Bim1 provide structural support for the anaphase spindle. **180**, 91-100 (2008).
35 Shanks, R. M., Kamieniecki, R. J. & Dawson, D. S. The Kar3-interacting protein Cik1p plays a critical role in passage through meiosis I in Saccharomyces cerevisiae. *Genetics* **159**, 939-951 (2001).

36 Middleton, K. & Carbon, J. KAR3-encoded kinesin is a minus-end-directed motor that functions with centromere binding proteins (CBF3) on an in vitro yeast kinetochore. *Proceedings of the National Academy of Sciences* **91**, 7212-7216 (1994).
37 Mieck, C. *et al.* Non-catalytic motor domains enable processive movement and functional diversification of the kinesin-14 Kar3. *Elife* **4** (2015).
38 Tanaka, K. *et al.* Molecular mechanisms of kinetochore capture by spindle microtubules. **434**, 987-994 (2005).
39 Tanaka, K., Kitamura, E., Kitamura, Y. & Tanaka, T. U. Molecular mechanisms of microtubule-dependent kinetochore transport toward spindle poles. *The Journal of cell biology* **178**, 269-281 (2007).
40 Maddox, P. S., Stemple, J. K., Satterwhite, L., Salmon, E. & Bloom, K. The minus end-directed motor Kar3 is required for coupling dynamic microtubule plus ends to the cortical shmoo tip in budding yeast. *Current biology* **13**, 1423-1428 (2003).
41 Gibeaux, R., Politi, A. Z., Nédélec, F., Antony, C. & Knop, M. Spindle pole body-anchored Kar3 drives the nucleus along microtubules from another nucleus in preparation for nuclear fusion during yeast karyogamy. *Genes & Development* **27**, 335-349 (2013).
42 Foster, K. A., Correia, J. J. & Gilbert, S. P. Equilibrium binding studies of non-claret disjunctional protein (Ncd) reveal cooperative interactions between the motor domains. *Journal of Biological Chemistry* **273**, 35307-35318 (1998).
43 Pechatnikova, E. & Taylor, E. W. Kinetic mechanism of monomeric non-claret disjunctional protein (Ncd) ATPase. *Journal of Biological Chemistry* **272**, 30735-30740 (1997).
44 Endres, N. F., Yoshioka, C., Milligan, R. A. & Vale, R. D. A lever-arm rotation drives motility of the minus-end-directed kinesin Ncd. *Nature* **439**, 875-878 (2006).
45 Pechatnikova, E. & Taylor, E. Kinetics processivity and the direction of motion of Ncd. *Biophysical journal* **77**, 1003-1016 (1999).
46 Fondecave, R. M., Clarke, L. A., Schmidt, C. F. & Stewart, R. J. Working strokes by single molecules of the kinesin-related microtubule motor ncd. *Nature cell biology* **2**, 724-729 (2000).
47 Sproul, L. R., Anderson, D. J., Mackey, A. T., Saunders, W. S. & Gilbert, S. P. Cik1 targets the minus-end kinesin depolymerase kar3 to microtubule plus ends. *Current biology* **15**, 1420-1427 (2005).
48 Saunders, W., Hornack, D., Lengyel, V. & Deng, C. The Saccharomyces cerevisiae kinesin-related motor Kar3p acts at preanaphase spindle poles to limit the number and length of cytoplasmic microtubules. *The Journal of cell biology* **137**, 417-431 (1997).
49 Gupta, M. L., Carvalho, P., Roof, D. M. & Pellman, D. Plus end-specific depolymerase activity of Kip3, a kinesin-8 protein, explains its role in positioning the yeast mitotic spindle. **8**, 913-923 (2006).
50 Varga, V. *et al.* Yeast kinesin-8 depolymerizes microtubules in a length-dependent manner. *Nature cell …* (2006).
51 Mayr, M. I. *et al.* The human kinesin Kif18A is a motile microtubule depolymerase essential for chromosome congression. *Current Biology* **17**, 488-498 (2007).

52 Tischer, C., Brunner, D. & Dogterom, M. Force-and kinesin-8-dependent effects in the spatial regulation of fission yeast microtubule dynamics. *Molecular systems biology* **5**, 250 (2009).
53 Cottingham, F. R. & Hoyt, M. A. Mitotic spindle positioning in Saccharomyces cerevisiae is accomplished by antagonistically acting microtubule motor proteins. *The Journal of cell biology* **138**, 1041-1053 (1997).
54 DeZwaan, T. M., Ellingson, E., Pellman, D. & Roof, D. M. Kinesin-related KIP3 of Saccharomyces cerevisiae is required for a distinct step in nuclear migration. *The Journal of cell biology* **138**, 1023-1040 (1997).
55 Varga, V., Leduc, C., Bormuth, V., Diez, S. & Howard, J. Kinesin-8 motors act cooperatively to mediate length-dependent microtubule depolymerization. *Cell* (2009).
56 Straight, A., Sedat, J. & Murray, A. Time-lapse microscopy reveals unique roles for kinesins during anaphase in budding yeast. *J. Cell Biol.* **143**, 687-694 (1998).
57 Cottingham, F. R., Gheber, L., Miller, D. L. & Hoyt, A. M. Novel Roles for Saccharomyces cerevisiae Mitotic Spindle Motors. *The Journal of cell …* (1999).
58 Woodruff, J. B., Drubin, D. G. & Barnes, G. Mitotic spindle disassembly occurs via distinct subprocesses driven by the anaphase-promoting complex, Aurora B kinase, and kinesin-8. *The Journal of cell biology* **191**, 795-808 (2010).
59 Woodruff, J. B., Drubin, D. G. & Barnes, G. Spindle assembly requires complete disassembly of spindle remnants from the previous cell cycle. *Molecular biology of the cell* **23**, 258-267 (2012).
60 Su, X. *et al.* Microtubule-sliding activity of a kinesin-8 promotes spindle assembly and spindle-length control. *Nat. Cell Biol.* **15**, 948-957 (2013).
61 Tytell, J. D. & Sorger, P. K. Analysis of kinesin motor function at budding yeast kinetochores. *J. Cell Biol.* **172**, 861-874 (2006).
62 Wargacki, M. M., Tay, J. C., Muller, E. G., Asbury, C. L. & Davis, T. N. Kip3, the yeast kinesin-8, is required for clustering of kinetochores at metaphase. *Cell Cycle* **9**, 2581-2588 (2010).
63 Su, X. *et al.* Mechanisms underlying the dual-mode regulation of microtubule dynamics by Kip3/kinesin-8. *Molecular cell* **43**, 751-763 (2011).
64 Ferenz, N. P., Gable, A. & Wadsworth, P. in *Seminars in cell & developmental biology.* 255-259 (Elsevier).
65 Gordon, D. M. & Roof, D. M. The kinesin-related protein Kip1p of Saccharomyces cerevisiae is bipolar. *Journal of Biological Chemistry* **274**, 28779-28786 (1999).
66 Kashina, A. *et al.* A bipolar kinesin. *Nature* **379**, 270 (1996).
67 Scholey, J. E., Nithianantham, S., Scholey, J. M. & Al-Bassam, J. Structural basis for the assembly of the mitotic motor Kinesin-5 into bipolar tetramers. *Elife* **3**, e02217 (2014).
68 Gheber, L., Kuo, S. & Hoyt, M. Motile properties of the kinesin-related Cin8p spindle motor extracted from Saccharomyces cerevisiae cells. *J. Biol. Chem.* **274**, 9564-9572 (1999).
69 Kapitein, L. C. *et al.* The bipolar mitotic kinesin Eg5 moves on both microtubules that it crosslinks. *Nature* **435**, 114-118 (2005).
70 Hoyt, M., He, L., Loo, K. & Saunders, W. Two Saccharomyces cerevisiae kinesin-related gene products required for mitotic spindle assembly. *The Journal of cell biology* (1992).

71 Saunders, W. S., Koshland, D., Eshel, D., Gibbons, I. R. & Hoyt, M. A. Saccharomyces cerevisiae kinesin-and dynein-related proteins required for anaphase chromosome segregation. *The Journal of cell biology* **128**, 617-624 (1995).
72 Collins, S. R. *et al.* Functional dissection of protein complexes involved in yeast chromosome biology using a genetic interaction map. *Nature* **446**, 806-810 (2007).
73 Costanzo, M. *et al.* The genetic landscape of a cell. *Science* **327**, 425-431 (2010).
74 Geiser, J. *et al.* Saccharomyces cerevisiae genes required in the absence of the CIN8-encoded spindle motor act in functionally diverse mitotic pathways. *Mol. Biol. Cell* **8**, 1035-1050 (1997).
75 Hoppins, S. *et al.* A mitochondrial-focused genetic interaction map reveals a scaffold-like complex required for inner membrane organization in mitochondria. *J Cell Biol*, jcb. 201107053 (2011).
76 Pan, X. *et al.* A robust toolkit for functional profiling of the yeast genome. *Mol. Cell* **16**, 487-496 (2004).
77 Newman, J. R., Wolf, E. & Kim, P. S. A computationally directed screen identifying interacting coiled coils from Saccharomyces cerevisiae. *Proceedings of the National Academy of Sciences* **97**, 13203-13208 (2000).
78 Wang, Y. *et al.* Coiled-coil networking shapes cell molecular machinery. *Molecular biology of the cell* **23**, 3911-3922 (2012).
79 Wong, J. *et al.* A protein interaction map of the mitotic spindle. *Mol. Biol. Cell* **18**, 3800-3809 (2007).
80 Ouspenski, I. I., Elledge, S. J. & Brinkley, B. New yeast genes important for chromosome integrity and segregation identified by dosage effects on genome stability. *Nucleic acids research* **27**, 3001-3008 (1999).
81 Yuen, K. W. *et al.* Systematic genome instability screens in yeast and their potential relevance to cancer. *Proceedings of the National Academy of Sciences* **104**, 3925-3930 (2007).
82 Stephens, A. D. *et al.* Individual pericentromeres display coordinated motion and stretching in the yeast spindle. *J Cell Biol*, jcb. 201307104 (2013).
83 Gardner, M. K. *et al.* Chromosome congression by Kinesin-5 motor-mediated disassembly of longer kinetochore microtubules. *Cell* **135**, 894-906 (2008).
84 Roostalu, J. *et al.* Directional switching of the kinesin Cin8 through motor coupling. *Science* **332**, 94-99 (2011).
85 Gerson-Gurwitz, A. *et al.* Directionality of individual kinesin-5 Cin8 motors is modulated by loop 8, ionic strength and microtubule geometry. *EMBO J.* **30**, 4942-4954 (2011).
86 Thiede, C., Fridman, V., Gerson-Gurwitz, A., Gheber, L. & Schmidt, C. F. Regulation of bi-directional movement of single kinesin-5 Cin8 molecules. *Bioarchitecture* **2**, 70-74 (2012).
87 Fridman, V. *et al.* Kinesin-5 Kip1 is a bi-directional motor that stabilizes microtubules and tracks their plus-ends in vivo. **126**, 4147-4159 (2013).
88 Shapira, O., Goldstein, A., Al-Bassam, J. & Gheber, L. A potential physiological role for bi-directional motility and motor clustering of mitotic kinesin-5 Cin8 in yeast mitosis. *J Cell Sci* **130**, 725-734 (2017).

89 Qiu, W. *et al.* Dynein achieves processive motion using both stochastic and coordinated stepping. *Nature structural & molecular biology* **19**, 193-200 (2012).
90 Moore, J. K., Stuchell-Brereton, M. D. & Cooper, J. A. Function of dynein in budding yeast: mitotic spindle positioning in a polarized cell. *Cytoskeleton* **66**, 546-555 (2009).
91 Schroer, T. A. Dynactin. *Annu. Rev. Cell Dev. Biol.* **20**, 759-779 (2004).
92 Tanenbaum, M. E. & Medema, R. H. Mechanisms of centrosome separation and bipolar spindle assembly. *Developmental cell* **19**, 797-806 (2010).
93 Fagarasanu, A. & Rachubinski, R. A. Orchestrating organelle inheritance in Saccharomyces cerevisiae. *Current opinion in microbiology* **10**, 528-538 (2007).
94 Li, Y.-Y., Yeh, E., Hays, T. & Bloom, K. Disruption of mitotic spindle orientation in a yeast dynein mutant. *Proceedings of the National Academy of Sciences* **90**, 10096-10100 (1993).
95 Adames, N. R. & Cooper, J. A. Microtubule interactions with the cell cortex causing nuclear movements in Saccharomyces cerevisiae. *J Cell Biol* **149**, 863-874 (2000).
96 Farkasovsky, M. & Küntzel, H. Yeast Num1p associates with the mother cell cortex during S/G2 phase and affects microtubular functions. *The Journal of Cell Biology* **131**, 1003-1014 (1995).
97 Eshel, D. *et al.* Cytoplasmic dynein is required for normal nuclear segregation in yeast. *Proceedings of the National Academy of Sciences* **90**, 11172-11176 (1993).
98 Yeh, E., Skibbens, R., Cheng, J., Salmon, E. & Bloom, K. Spindle dynamics and cell cycle regulation of dynein in the budding yeast, Saccharomyces cerevisiae. *J. Cell Biol.* **130**, 687-700 (1995).
99 Carvalho, P., Tirnauer, J. S. & Pellman, D. Surfing on microtubule ends. *Trends in cell biology* **13**, 229-237 (2003).
100 Asbury, C. L. XMAP215: a tip tracker that really moves. *Cell* **132**, 19-20 (2008).
101 Bieling, P. *et al.* CLIP-170 tracks growing microtubule ends by dynamically recognizing composite EB1/tubulin-binding sites. *J Cell Biol* **183**, 1223-1233 (2008).
102 Dixit, R. *et al.* Microtubule plus-end tracking by CLIP-170 requires EB1. *Proceedings of the National Academy of Sciences* **106**, 492-497 (2009).
103 Zanic, M., Stear, J. H., Hyman, A. A. & Howard, J. EB1 recognizes the nucleotide state of tubulin in the microtubule lattice. *PloS one* **4**, e7585 (2009).
104 Lansbergen, G. & Akhmanova, A. Microtubule plus end: a hub of cellular activities. *Traffic* **7**, 499-507 (2006).
105 Ligon, L. A., Shelly, S. S., Tokito, M. & Holzbaur, E. L. The microtubule plus-end proteins EB1 and dynactin have differential effects on microtubule polymerization. *Molecular biology of the cell* **14**, 1405-1417 (2003).
106 Vitre, B. *et al.* EB1 regulates microtubule dynamics and tubulin sheet closure in vitro. *Nature cell biology* **10**, 415 (2008).
107 Sandblad, L. *et al.* The Schizosaccharomyces pombe EB1 homolog Mal3p binds and stabilizes the microtubule lattice seam. *Cell* **127**, 1415-1424 (2006).
108 Zanic, M., Widlund, P. O., Hyman, A. A. & Howard, J. Synergy between XMAP215 and EB1 increases microtubule growth rates to physiological levels. *Nature cell biology* **15**, 688 (2013).

109 Manna, T., Honnappa, S., Steinmetz, M. O. & Wilson, L. Suppression of microtubule dynamic instability by the+ TIP protein EB1 and its modulation by the CAP-Gly domain of p150glued. *Biochemistry* **47**, 779-786 (2008).
110 Blake-Hodek, K. A., Cassimeris, L. & Huffaker, T. C. Regulation of microtubule dynamics by Bim1 and Bik1, the budding yeast members of the EB1 and CLIP-170 families of plus-end tracking proteins. *Molecular biology of the cell* **21**, 2013-2023 (2010).
111 Kita, K., Wittmann, T., Näthke, I. S. & Waterman-Storer, C. M. Adenomatous polyposis coli on microtubule plus ends in cell extensions can promote microtubule net growth with or without EB1. *Molecular biology of the cell* **17**, 2331-2345 (2006).
112 Tirnauer, J., E, O. T., Berrueta, L., Bierer, B. & Pellman, D. Yeast Bim1p promotes the G1-specific dynamics of microtubules. (1999).
113 Rogers, S. L., Rogers, G. C., Sharp, D. J. & Vale, R. D. Drosophila EB1 is important for proper assembly, dynamics, and positioning of the mitotic spindle. *The Journal of cell biology* **158**, 873-884 (2002).
114 Tirnauer, J. S., Grego, S., Salmon, E. D. & Mitchison, T. J. EB1–microtubule interactions in Xenopus egg extracts: role of EB1 in microtubule stabilization and mechanisms of targeting to microtubules. *Molecular biology of the cell* **13**, 3614-3626 (2002).
115 Busch, K. E. & Brunner, D. The microtubule plus end-tracking proteins mal3p and tip1p cooperate for cell-end targeting of interphase microtubules. *Current Biology* **14**, 548-559 (2004).
116 Komarova, Y. *et al.* Mammalian end binding proteins control persistent microtubule growth. *The Journal of cell biology* **184**, 691-706 (2009).
117 Korinek, W. S., Copeland, M. J., Chaudhuri, A. & Chant, J. Molecular linkage underlying microtubule orientation toward cortical sites in yeast. *Science* **287**, 2257-2259 (2000).
118 Lee, L. *et al.* Positioning of the mitotic spindle by a cortical-microtubule capture mechanism. *Science* **287**, 2260-2262 (2000).
119 Miller, R. K., Cheng, S. C. & Rose, M. D. Bim1p/Yeb1p mediates the Kar9p-dependent cortical attachment of cytoplasmic microtubules. *Molecular biology of the cell* **11**, 2949-2959 (2000).
120 Tanaka, T. U., Stark, M. J. & Tanaka, K. Kinetochore capture and bi-orientation on the mitotic spindle. *Nature reviews Molecular cell biology* **6**, 929-942 (2005).
121 Zimniak, T., Stengl, K., Mechtler, K. & Westermann, S. Phosphoregulation of the budding yeast EB1 homologue Bim1p by Aurora/Ipl1p. *J. Cell Biol.* **186**, 379-391 (2009).
122 Measday, V. *et al.* Systematic yeast synthetic lethal and synthetic dosage lethal screens identify genes required for chromosome segregation. *Proceedings of the National Academy of Sciences of the United States of America* **102**, 13956-13961 (2005).
123 Zhang, L. & Shay, J. W. Multiple roles of APC and its therapeutic implications in colorectal cancer. *Journal of the national cancer institute* **109**, djw332 (2017).
124 Bienz, M. Spindles cotton on to junctions, APC and EB1. *Nature cell biology* **3**, E67 (2001).
125 Su, L.-K. *et al.* APC binds to the novel protein EB1. *Cancer research* **55**, 2972-2977 (1995).

126 Mimori-Kiyosue, Y., Shiina, N. & Tsukita, S. Adenomatous polyposis coli (APC) protein moves along microtubules and concentrates at their growing ends in epithelial cells. *The Journal of cell biology* **148**, 505-518 (2000).
127 Mimori-Kiyosue, Y., Shiina, N. & Tsukita, S. The dynamic behavior of the APC-binding protein EB1 on the distal ends of microtubules. *Current biology* **10**, 865-868 (2000).
128 Mogensen, M. M., Tucker, J. B., Mackie, J. B., Prescott, A. R. & Näthke, I. S. The adenomatous polyposis coli protein unambiguously localizes to microtubule plus ends and is involved in establishing parallel arrays of microtubule bundles in highly polarized epithelial cells. *The Journal of cell biology* **157**, 1041-1048 (2002).
129 Yamashita, Y. M., Jones, D. L. & Fuller, M. T. Orientation of asymmetric stem cell division by the APC tumor suppressor and centrosome. *Science* **301**, 1547-1550 (2003).
130 McCartney, B. M. *et al.* Drosophila APC2 and Armadillo participate in tethering mitotic spindles to cortical actin. *Nature cell biology* **3**, 933 (2001).
131 Lu, B., Roegiers, F., Jan, L. Y. & Jan, Y. N. Adherens junctions inhibit asymmetric division in the Drosophila epithelium. *Nature* **409**, 522 (2001).
132 Munemitsu, S. *et al.* The APC gene product associates with microtubules in vivo and promotes their assembly in vitro. *Cancer research* **54**, 3676-3681 (1994).
133 Smith, K. J. *et al.* Wild-type but not mutant APC associates with the microtubule cytoskeleton. *Cancer Research* **54**, 3672-3675 (1994).
134 Zumbrunn, J., Kinoshita, K., Hyman, A. A. & Näthke, I. S. Binding of the adenomatous polyposis coli protein to microtubules increases microtubule stability and is regulated by GSK3β phosphorylation. *Current Biology* **11**, 44-49 (2001).
135 Schweiggert, J., Panigada, D., Tan, A. N. & Liakopoulos, D. Kar9 controls the nucleocytoplasmic distribution of yeast EB1. *Cell Cycle* **15**, 2860-2866 (2016).
136 Hotz, M. *et al.* Spindle pole bodies exploit the mitotic exit network in metaphase to drive their age-dependent segregation. *Cell* **148**, 958-972 (2012).
137 Miller, R. K. & Rose, M. D. Kar9p is a novel cortical protein required for cytoplasmic microtubule orientation in yeast. *J Cell Biol* **140**, 377-390 (1998).
138 Brouhard, G. J. *et al.* XMAP215 is a processive microtubule polymerase. *Cell* **132**, 79-88 (2008).
139 De Wulf, P., McAinsh, A. D. & Sorger, P. K. Hierarchical assembly of the budding yeast kinetochore from multiple subcomplexes. *Genes & development* **17**, 2902-2921 (2003).
140 Al-Bassam, J., Van Breugel, M., Harrison, S. C. & Hyman, A. Stu2p binds tubulin and undergoes an open-to-closed conformational change. *J Cell Biol* **172**, 1009-1022 (2006).
141 van Breugel, M., Drechsel, D. & Hyman, A. Stu2p, the budding yeast member of the conserved Dis1/XMAP215 family of microtubule-associated proteins is a plus end–binding microtubule destabilizer. *J Cell Biol* **161**, 359-369 (2003).
142 Tournebize, R. *et al.* Control of microtubule dynamics by the antagonistic activities of XMAP215 and XKCM1 in Xenopus egg extracts. *Nature cell biology* **2**, 13 (2000).
143 Gard, D. L. & Kirschner, M. W. A microtubule-associated protein from Xenopus eggs that specifically promotes assembly at the plus-end. *The Journal of cell biology* **105**, 2203-2215 (1987).
144 Goshima, G., Wollman, R., Stuurman, N., Scholey, J. M. & Vale, R. D. Length control of the metaphase spindle. *Current Biology* **15**, 1979-1988 (2005).

145 Podolski, M., Mahamdeh, M. & Howard, J. Stu2, the budding yeast XMAP215/Dis1 homolog, promotes assembly of yeast microtubules by increasing growth rate and decreasing catastrophe frequency. *Journal of Biological Chemistry* **289**, 28087-28093 (2014).
146 Kosco, K. A. *et al.* Control of Microtubule Dynamics by Stu2p Is Essential for Spindle Orientation and Metaphase Chromosome Alignment in Yeast. **12**, 2870-2880 (2001).
147 Pearson, C. G., Maddox, P. S., Zarzar, T. R., Salmon, E. D. & Bloom, K. Yeast Kinetochores Do Not Stabilize Stu2p-dependent Spindle Microtubule Dynamics. (2003).
148 Ayaz, P., Ye, X., Huddleston, P., Brautigam, C. A. & Rice, L. M. A TOG: αβ-tubulin complex structure reveals conformation-based mechanisms for a microtubule polymerase. *Science* **337**, 857-860 (2012).
149 Kitamura, E. *et al.* Kinetochores generate microtubules with distal plus ends: their roles and limited lifetime in mitosis. *Developmental cell* **18**, 248-259 (2010).
150 Gandhi, S. R. *et al.* Kinetochore-dependent microtubule rescue ensures their efficient and sustained interactions in early mitosis. *Developmental cell* **21**, 920-933 (2011).
151 Miller, M. P., Asbury, C. L. & Biggins, S. A TOG protein confers tension sensitivity to kinetochore-microtubule attachments. *Cell* **165**, 1428-1439 (2016).
152 Gergely, F., Draviam, V. M. & Raff, J. W. The ch-TOG/XMAP215 protein is essential for spindle pole organization in human somatic cells. *Genes & development* **17**, 336-341 (2003).
153 Meraldi, P., Draviam, V. M. & Sorger, P. K. Timing and checkpoints in the regulation of mitotic progression. *Developmental cell* **7**, 45-60 (2004).
154 Hsu, K.-S. & Toda, T. Ndc80 internal loop interacts with Dis1/TOG to ensure proper kinetochore-spindle attachment in fission yeast. *Current biology* **21**, 214-220 (2011).
155 Tang, N. H., Takada, H., Hsu, K.-S. & Toda, T. The internal loop of fission yeast Ndc80 binds Alp7/TACC-Alp14/TOG and ensures proper chromosome attachment. *Molecular biology of the cell* **24**, 1122-1133 (2013).
156 Usui, T., Maekawa, H., Pereira, G. & Schiebel, E. The XMAP215 homologue Stu2 at yeast spindle pole bodies regulates microtubule dynamics and anchorage. *The EMBO Journal* **22**, 4779-4793 (2003).
157 Chen, X. P., Yin, H. & Huffaker, T. C. The yeast spindle pole body component Spc72p interacts with Stu2p and is required for proper microtubule assembly. *The Journal of cell biology* **141**, 1169-1179 (1998).
158 Perez, F., Diamantopoulos, G. S., Stalder, R. & Kreis, T. E. CLIP-170 highlights growing microtubule ends in vivo. *Cell* **96**, 517-527 (1999).
159 Maekawa, H. & Schiebel, E. CLIP-170 family members: a motor-driven ride to microtubule plus ends. *Developmental cell* **6**, 746-748 (2004).
160 Slep, K. C. & Vale, R. D. Structural basis of microtubule plus end tracking by XMAP215, CLIP-170, and EB1. *Molecular cell* **27**, 976-991 (2007).
161 Sheeman, B. *et al.* Determinants of S. cerevisiae dynein localization and activation: implications for the mechanism of spindle positioning. *Curr Biol* **13**, 364-372 (2003).
162 Moore, J. K., D'Silva, S. & Miller, R. K. The CLIP-170 homologue Bik1p promotes the phosphorylation and asymmetric localization of Kar9p. *Mol Biol Cell* **17**, 178-191, doi:10.1091/mbc.E05-06-0565 (2006).

163 Lin, H. *et al.* Polyploids require Bik1 for kinetochore-microtubule attachment. *J Cell Biol* **155**, 1173-1184, doi:10.1083/jcb.200108119 (2001).
164 He, X., Rines, D. R., Espelin, C. W. & Sorger, P. K. Molecular analysis of kinetochore-microtubule attachment in budding yeast. *Cell* **106**, 195-206 (2001).
165 Wolyniak, M. J. *et al.* The regulation of microtubule dynamics in Saccharomyces cerevisiae by three interacting plus-end tracking proteins. *Molecular biology of the cell* **17**, 2789-2798 (2006).
166 Berlin, V., Styles, C. A. & Fink, G. R. BIK1, a protein required for microtubule function during mating and mitosis in Saccharomyces cerevisiae, colocalizes with tubulin. *The Journal of Cell Biology* **111**, 2573-2586 (1990).
167 Mennella, V. *et al.* Subdiffraction-resolution fluorescence microscopy reveals a domain of the centrosome critical for pericentriolar material organization. *Nature cell biology* **14**, 1159 (2012).
168 Sonnen, K. F., Schermelleh, L., Leonhardt, H. & Nigg, E. A. 3D-structured illumination microscopy provides novel insight into architecture of human centrosomes. *Biology open* **1**, 965-976 (2012).
169 Fu, J. & Glover, D. M. Structured illumination of the interface between centriole and peri-centriolar material. *Open biology* **2**, 120104 (2012).
170 Lawo, S., Hasegan, M., Gupta, G. D. & Pelletier, L. Subdiffraction imaging of centrosomes reveals higher-order organizational features of pericentriolar material. *Nature cell biology* **14**, 1148 (2012).
171 Zheng, Y., Wong, M. L., Alberts, B. & Mitchison, T. Nucleation of microtubule assembly by a γ-tubulin-containing ring complex. *Nature* **378**, 578 (1995).
172 Oegema, K. *et al.* Characterization of two related Drosophila γ-tubulin complexes that differ in their ability to nucleate microtubules. *The Journal of cell biology* **144**, 721-733 (1999).
173 Carvalho-Santos, Z., Azimzadeh, J., Pereira-Leal, J. B. & Bettencourt-Dias, M. Tracing the origins of centrioles, cilia, and flagella. *J Cell Biol* **194**, 165-175 (2011).
174 Jaspersen, S. L. & Winey, M. The budding yeast spindle pole body: structure, duplication, and function. *Annu. Rev. Cell Dev. Biol.* **20**, 1-28 (2004).
175 Kollman, J. M. *et al.* Ring closure activates yeast γTuRC for species-specific microtubule nucleation. *Nat. Struct. Mol. Biol.* **22**, 132-137 (2015).
176 Kollman, J. M., Polka, J. K., Zelter, A., Davis, T. N. & Agard, D. A. Microtubule nucleating γ-TuSC assembles structures with 13-fold microtubule-like symmetry. *Nature* **466**, 879 (2010).
177 Tanaka, T., Fuchs, J., Loidl, J. & Nasmyth, K. Cohesin ensures bipolar attachment of microtubules to sister centromeres and resists their precocious separation. *Nature cell biology* **2**, 492 (2000).
178 Stephens, A. D., Haase, J., Vicci, L., Taylor, R. M. & Bloom, K. Cohesin, condensin, and the intramolecular centromere loop together generate the mitotic chromatin spring. *The Journal of cell biology* **193**, 1167-1180 (2011).
179 Yeh, E. *et al.* Pericentric chromatin is organized into an intramolecular loop in mitosis. *Current Biology* **18**, 81-90 (2008).

180 Kitamura, E., Tanaka, K., Kitamura, Y. & Tanaka, T. U. Kinetochore–microtubule interaction during S phase in Saccharomyces cerevisiae. *Genes & development* **21**, 3319-3330 (2007).
181 Winey, M. & O'Toole, E. T. The spindle cycle in budding yeast. *Nature Cell Biology* **3**, E23-E27 (2001).
182 Mardin, B. R. & Schiebel, E. Breaking the ties that bind: new advances in centrosome biology. *J Cell Biol* **197**, 11-18 (2012).
183 Tsou, M.-F. B. & Stearns, T. Controlling centrosome number: licenses and blocks. *Current opinion in cell biology* **18**, 74-78 (2006).
184 Kilmartin, J. V. Sfi1p has conserved centrin-binding sites and an essential function in budding yeast spindle pole body duplication. *The Journal of cell biology* **162**, 1211-1221 (2003).
185 Li, S. *et al.* Structural role of Sfi1p–centrin filaments in budding yeast spindle pole body duplication. *The Journal of Cell Biology* **173**, 867-877 (2006).
186 Adams, I. R. & Kilmartin, J. V. Localization of core spindle pole body (SPB) components during SPB duplication in Saccharomyces cerevisiae. *The Journal of cell biology* **145**, 809-823 (1999).
187 Jaspersen, S. L. & Ghosh, S. Nuclear envelope insertion of spindle pole bodies and nuclear pore complexes. *Nucleus* **3**, 226-236 (2012).
188 Elserafy, M. *et al.* Molecular mechanisms that restrict yeast centrosome duplication to one event per cell cycle. *Current Biology* **24**, 1456-1466 (2014).
189 Avena, J. S. *et al.* Licensing of yeast centrosome duplication requires phosphoregulation of sfi1. *PLoS genetics* **10**, e1004666 (2014).
190 Yeong, F. M., Lim, H. H., Wang, Y. & Surana, U. Early expressed Clb proteins allow accumulation of mitotic cyclin by inactivating proteolytic machinery during S phase. *Molecular and cellular biology* **21**, 5071-5081 (2001).
191 Fitch, I. *et al.* Characterization of four B-type cyclin genes of the budding yeast Saccharomyces cerevisiae. **3**, 805-818 (1992).
192 Lim, H. H., Goh, P.-Y. & Surana, U. Spindle pole body separation in Saccharomyces cerevisiae requires dephosphorylation of the tyrosine 19 residue of Cdc28. *Molecular and cellular biology* **16**, 6385-6397 (1996).
193 Raaijmakers, J. A. *et al.* Nuclear envelope-associated dynein drives prophase centrosome separation and enables Eg5-independent bipolar spindle formation. *The EMBO Journal* **31**, 4179-4190 (2012).
194 Crasta, K., Huang, P., Morgan, G., Winey, M. & Surana, U. Cdk1 regulates centrosome separation by restraining proteolysis of microtubule-associated proteins. *The EMBO journal* **25**, 2551-2563 (2006).
195 Prosser, S. L. & Pelletier, L. Mitotic spindle assembly in animal cells: a fine balancing act. *Nature Reviews Molecular Cell Biology* **18**, 187-201 (2017).
196 Hayward, D., Metz, J., Pellacani, C. & Wakefield, J. G. Synergy between Multiple Microtubule-Generating Pathways Confers Robustness to Centrosome-Driven Mitotic Spindle Formation. *Dev. Cell* (2014).
197 Khodjakov, A., Cole, R. W., Oakley, B. R. & Rieder, C. L. Centrosome-independent mitotic spindle formation in vertebrates. *Current Biology* **10**, 59-67 (2000).

198 Kirschner, M. & Mitchison, T. Beyond self-assembly: from microtubules to morphogenesis. *Cell* **45**, 329-342 (1986).
199 Heald, R. & Khodjakov, A. Thirty years of search and capture: The complex simplicity of mitotic spindle assembly. *J Cell Biol* **211**, 1103-1111 (2015).
200 Wollman, R. *et al.* Efficient chromosome capture requires a bias in the 'search-and-capture'process during mitotic-spindle assembly. *Current Biology* **15**, 828-832 (2005).
201 Clarke, P. R. & Zhang, C. Spatial and temporal coordination of mitosis by Ran GTPase. *Nature reviews Molecular cell biology* **9**, 464-477 (2008).
202 Tulu, U. S., Fagerstrom, C., Ferenz, N. P. & Wadsworth, P. Molecular requirements for kinetochore-associated microtubule formation in mammalian cells. *Current Biology* **16**, 536-541 (2006).
203 Maiato, H., Rieder, C. L. & Khodjakov, A. Kinetochore-driven formation of kinetochore fibers contributes to spindle assembly during animal mitosis. *J Cell Biol* **167**, 831-840 (2004).
204 Khodjakov, A., Copenagle, L., Gordon, M. B., Compton, D. A. & Kapoor, T. M. Minus-end capture of preformed kinetochore fibers contributes to spindle morphogenesis. *The Journal of cell biology* **160**, 671-683 (2003).
205 Tsai, C. Y. *et al.* Aurora-A phosphorylates Augmin complex component Hice1 protein at an N-terminal serine/threonine cluster to modulate its microtubule binding activity during spindle assembly. *Journal of Biological Chemistry* **286**, 30097-30106 (2011).
206 Johmura, Y. *et al.* Regulation of microtubule-based microtubule nucleation by mammalian polo-like kinase 1. *Proceedings of the National Academy of Sciences* **108**, 11446-11451 (2011).
207 Petry, S., Groen, A. C., Ishihara, K., Mitchison, T. J. & Vale, R. D. Branching microtubule nucleation in Xenopus egg extracts mediated by augmin and TPX2. *Cell* **152**, 768-777 (2013).
208 Kamasaki, T. *et al.* Augmin-dependent microtubule nucleation at microtubule walls in the spindle. *J Cell Biol* **202**, 25-33 (2013).
209 Lecland, N. & Lüders, J. The dynamics of microtubule minus ends in the human mitotic spindle. *Nature cell biology* **16**, 770-778 (2014).
210 Goshima, G., Mayer, M., Zhang, N., Stuurman, N. & Vale, R. D. Augmin: a protein complex required for centrosome-independent microtubule generation within the spindle. *The Journal of cell biology* **181**, 421-429 (2008).
211 Vasileva, V. *et al.* Molecular mechanisms facilitating the initial kinetochore encounter with spindle microtubules. *J Cell Biol*, jcb. 201608122 (2017).
212 Tanaka, T. U. Kinetochore–microtubule interactions: steps towards bi-orientation. *The EMBO journal* **29**, 4070-4082 (2010).
213 Grishchuk, E. L., Molodtsov, M. I., Ataullakhanov, F. I. & McIntosh, J. R. Force production by disassembling microtubules. *Nature* **438**, 384-388 (2005).
214 Joglekar, A. P., Bloom, K. S. & Salmon, E. Mechanisms of force generation by end-on kinetochore-microtubule attachments. *Current opinion in cell biology* **22**, 57-67 (2010).
215 Akiyoshi, B. *et al.* Tension directly stabilizes reconstituted kinetochore-microtubule attachments. *Nature* **468**, 576 (2010).

216 Hoyt, M. A., Totis, L. & Roberts, B. T. S. cerevisiae genes required for cell cycle arrest in response to loss of microtubule function. *Cell* **66**, 507-517 (1991).
217 Li, R. & Murray, A. W. Feedback control of mitosis in budding yeast. *Cell* **66**, 519-531 (1991).
218 Hardwick, K. G., Johnston, R. C., Smith, D. L. & Murray, A. W. MAD3 encodes a novel component of the spindle checkpoint which interacts with Bub3p, Cdc20p, and Mad2p. *The Journal of cell biology* **148**, 871-882 (2000).
219 Sudakin, V., Chan, G. K. & Yen, T. J. Checkpoint inhibition of the APC/C in HeLa cells is mediated by a complex of BUBR1, BUB3, CDC20, and MAD2. *The Journal of cell biology* **154**, 925-936 (2001).
220 Lara-Gonzalez, P., Westhorpe, F. G. & Taylor, S. S. The spindle assembly checkpoint. *Current biology* **22**, R966-R980 (2012).
221 London, N. & Biggins, S. Mad1 kinetochore recruitment by Mps1-mediated phosphorylation of Bub1 signals the spindle checkpoint. *Genes & development* **28**, 140-152 (2014).
222 Sharp-Baker, H. & Chen, R.-H. Spindle checkpoint protein Bub1 is required for kinetochore localization of Mad1, Mad2, Bub3, and CENP-E, independently of its kinase activity. *The Journal of cell biology* **153**, 1239-1250 (2001).
223 Howell, B. *et al.* Cytoplasmic dynein/dynactin drives kinetochore protein transport to the spindle poles and has a role in mitotic spindle checkpoint inactivation. *J Cell Biol* **155**, 1159-1172 (2001).
224 Kops, G. J. & Shah, J. V. Connecting up and clearing out: how kinetochore attachment silences the spindle assembly checkpoint. *Chromosoma* **121**, 509-525 (2012).
225 Hauf, S. *et al.* The small molecule Hesperadin reveals a role for Aurora B in correcting kinetochore–microtubule attachment and in maintaining the spindle assembly checkpoint. *J Cell Biol* **161**, 281-294 (2003).
226 Lampson, M. A., Renduchitala, K., Khodjakov, A. & Kapoor, T. M. Correcting improper chromosome–spindle attachments during cell division. *Nature cell biology* **6**, 232 (2004).
227 Lampson, M. A. & Cheeseman, I. M. Sensing centromere tension: Aurora B and the regulation of kinetochore function. *Trends in cell biology* **21**, 133-140 (2011).
228 Tanaka, T. U. *et al.* Evidence that the Ipl1-Sli15 (Aurora kinase-INCENP) complex promotes chromosome bi-orientation by altering kinetochore-spindle pole connections. *Cell* **108**, 317-329 (2002).
229 Manic, G., Corradi, F., Sistigu, A., Siteni, S. & Vitale, I. in *International review of cell and molecular biology* Vol. 328 105-161 (Elsevier, 2017).
230 Lerit, D. A., Smyth, J. T. & Rusan, N. M. Organelle asymmetry for proper fitness, function, and fate. *Chromosome Res* **21**, 271-286 (2013).
231 Tajbakhsh, S. & Gonzalez, C. Biased segregation of DNA and centrosomes—moving together or drifting apart? *Nature Reviews Molecular Cell Biology* **10**, 804 (2009).
232 Holt, C. E. & Bullock, S. L. Subcellular mRNA localization in animal cells and why it matters. *Science* **326**, 1212-1216 (2009).
233 Klar, A. J. Differentiated parental DNA strands confer developmental asymmetry on daughter cells in fission yeast. *Nature* **326**, 466 (1987).

234 Klar, A. The developmental fate of fission yeast cells is determined by the pattern of inheritance of parental and grandparental DNA strands. *The EMBO journal* **9**, 1407-1415 (1990).
235 Klar, A. J. Lessons learned from studies of fission yeast mating-type switching and silencing. *Annu. Rev. Genet.* **41**, 213-236 (2007).
236 Sinclair, D. A. & Guarente, L. Extrachromosomal rDNA circles—a cause of aging in yeast. *Cell* **91**, 1033-1042 (1997).
237 Armakolas, A. & Klar, A. J. Cell type regulates selective segregation of mouse chromosome 7 DNA strands in mitosis. *Science* **311**, 1146-1149 (2006).
238 Liu, P., Jenkins, N. A. & Copeland, N. G. Efficient Cre-loxP–induced mitotic recombination in mouse embryonic stem cells. *Nature genetics* **30**, 66 (2002).
239 Shinin, V., Gayraud-Morel, B., Gomès, D. & Tajbakhsh, S. Asymmetric division and cosegregation of template DNA strands in adult muscle satellite cells. *Nature cell biology* **8**, 677 (2006).
240 White, M. A., Eykelenboom, J. K., Lopez-Vernaza, M. A., Wilson, E. & Leach, D. R. Non-random segregation of sister chromosomes in Escherichia coli. *Nature* **455**, 1248 (2008).
241 Yadlapalli, S. & Yamashita, Y. M. Chromosome-specific nonrandom sister chromatid segregation during stem-cell division. *Nature* **498**, 251 (2013).
242 Tran, V., Lim, C., Xie, J. & Chen, X. Asymmetric division of Drosophila male germline stem cell shows asymmetric histone distribution. *Science* **338**, 679-682 (2012).
243 Xie, J. *et al.* Histone H3 threonine phosphorylation regulates asymmetric histone inheritance in the Drosophila male germline. *Cell* **163**, 920-933 (2015).
244 Li, P., Yang, X., Wasser, M., Cai, Y. & Chia, W. Inscuteable and Staufen Mediate Asymmetric Localization and Segregation of prosperoRNA during Drosophila Neuroblast Cell Divisions. *Cell* **90**, 437-447 (1997).
245 Melton, D. Translocation of a localized maternal mRNA to the vegetal pole of Xenopus oocytes. *Nature* **328**, 80 (1987).
246 Neuman-Silberberg, F. S. & Schüpbach, T. The Drosophila dorsoventral patterning gene gurken produces a dorsally localized RNA and encodes a TGFα-like protein. *Cell* **75**, 165-174 (1993).
247 McFaline-Figueroa, J. R. *et al.* Mitochondrial quality control during inheritance is associated with lifespan and mother–daughter age asymmetry in budding yeast. *Aging cell* **10**, 885-895 (2011).
248 Peraza-Reyes, L., Crider, D. G. & Pon, L. A. Mitochondrial manoeuvres: latest insights and hypotheses on mitochondrial partitioning during mitosis in Saccharomyces cerevisiae. *Bioessays* **32**, 1040-1049 (2010).
249 Katajisto, P. *et al.* Asymmetric apportioning of aged mitochondria between daughter cells is required for stemness. *Science* **348**, 340-343 (2015).
250 Du, Y., Ferro-Novick, S. & Novick, P. Dynamics and inheritance of the endoplasmic reticulum. *Journal of cell science* **117**, 2871-2878 (2004).
251 Lowe, M. & Barr, F. A. Inheritance and biogenesis of organelles in the secretory pathway. *Nature Reviews Molecular Cell Biology* **8**, 429-439 (2007).
252 Yamashita, Y. M., Mahowald, A. P., Perlin, J. R. & Fuller, M. T. Asymmetric inheritance of mother versus daughter centrosome in stem cell division. *Science* **315**, 518-521 (2007).

253 Januschke, J., Llamazares, S., Reina, J. & Gonzalez, C. Drosophila neuroblasts retain the daughter centrosome. *Nature communications* **2**, 243 (2011).
254 Conduit, P. T. & Raff, J. W. Cnn dynamics drive centrosome size asymmetry to ensure daughter centriole retention in Drosophila neuroblasts. *Current Biology* **20**, 2187-2192 (2010).
255 Salzmann, V. *et al.* Centrosome-dependent asymmetric inheritance of the midbody ring in Drosophila germline stem cell division. *Molecular biology of the cell* **25**, 267-275 (2014).
256 Wang, X. *et al.* Asymmetric centrosome inheritance maintains neural progenitors in the neocortex. *Nature* **461**, 947-955 (2009).
257 Izumi, H. & Kaneko, Y. Evidence of asymmetric cell division and centrosome inheritance in human neuroblastoma cells. *Proceedings of the National Academy of Sciences* **109**, 18048-18053 (2012).
258 Pereira, G., Tanaka, T., Nasmyth, K. & Schiebel, E. Modes of spindle pole body inheritance and segregation of the Bfa1p-Bub2p checkpoint protein complex. *EMBO J.* **20**, 6359-6370 (2001).
259 Anderson, C. T. & Stearns, T. Centriole age underlies asynchronous primary cilium growth in mammalian cells. *Current biology* **19**, 1498-1502 (2009).
260 Stewart, E. J., Madden, R., Paul, G. & Taddei, F. Aging and death in an organism that reproduces by morphologically symmetric division. *PLoS biology* **3**, e45 (2005).
261 Sinclair, D., Mills, K. & Guarente, L. Aging in Saccharomyces cerevisiae. *Annual Reviews in Microbiology* **52**, 533-560 (1998).
262 Shcheprova, Z., Baldi, S., Frei, S. B., Gonnet, G. & Barral, Y. A mechanism for asymmetric segregation of age during yeast budding. *Nature* **454**, 728-734, doi:10.1038/nature07212 (2008).
263 Lengefeld, J., Hotz, M., Rollins, M., Baetz, K. & Barral, Y. Budding yeast Wee1 distinguishes spindle pole bodies to guide their pattern of age-dependent segregation. *Nature cell biology* **19**, 941 (2017).
264 Davidow, L. S., Goetsch, L. & Byers, B. Preferential occurrence of nonsister spores in two-spored asci of Saccharomyces cerevisiae: evidence for regulation of spore-wall formation by the spindle pole body. *Genetics* **94**, 581-595 (1980).
265 Gordon, O. *et al.* Nud1p, the yeast homolog of Centriolin, regulates spindle pole body inheritance in meiosis. *The EMBO journal* **25**, 3856-3868 (2006).
266 Chant, J. & Pringle, J. R. Patterns of bud-site selection in the yeast Saccharomyces cerevisiae. *J Cell Biol* **129**, 751-765 (1995).
267 Pringle, J. *et al.* in *Cold Spring Harbor symposia on quantitative biology.* 729-744 (Cold Spring Harbor Laboratory Press).
268 Chant, J., Mischke, M., Mitchell, E., Herskowitz, I. & Pringle, J. R. Role of Bud3p in producing the axial budding pattern of yeast. *The Journal of cell biology* **129**, 767-778 (1995).
269 Halme, A., Michelitch, M., Mitchell, E. L. & Chant, J. Bud10p directs axial cell polarization in budding yeast and resembles a transmembrane receptor. *Current Biology* **6**, 570-579 (1996).

270 Roemer, T., Madden, K., Chang, J. & Snyder, M. Selection of axial growth sites in yeast requires Axl2p, a novel plasma membrane glycoprotein. *Genes & Development* **10**, 777-793 (1996).
271 Sanders, S. L. & Herskowitz, I. The BUD4 protein of yeast, required for axial budding, is localized to the mother/BUD neck in a cell cycle-dependent manner. *The Journal of Cell Biology* **134**, 413-427 (1996).
272 Lord, M., Yang, M. C., Mischke, M. & Chant, J. Cell cycle programs of gene expression control morphogenetic protein localization. *The Journal of cell biology* **151**, 1501-1512 (2000).
273 Lord, M. *et al.* Subcellular localization of Axl1, the cell type-specific regulator of polarity. *Current biology* **12**, 1347-1352 (2002).
274 Gao, X.-D. *et al.* Sequential and distinct roles of the cadherin domain-containing protein Axl2p in cell polarization in yeast cell cycle. *Molecular biology of the cell* **18**, 2542-2560 (2007).
275 Kang, P. J., Angerman, E., Jung, C.-H. & Park, H.-O. Bud4 mediates the cell-type-specific assembly of the axial landmark in budding yeast. *J Cell Sci* **125**, 3840-3849 (2012).
276 Kang, P. J., Sanson, A., Lee, B. & Park, H.-O. A GDP/GTP exchange factor involved in linking a spatial landmark to cell polarity. *Science* **292**, 1376-1378 (2001).
277 Marston, A. L., Chen, T., Yang, M. C., Belhumeur, P. & Chant, J. A localized GTPase exchange factor, Bud5, determines the orientation of division axes in yeast. *Current Biology* **11**, 803-807 (2001).
278 Park, H.-O., Sanson, A. & Herskowitz, I. Localization of Bud2p, a GTPase-activating protein necessary for programming cell polarity in yeast to the presumptive bud site. *Genes & development* **13**, 1912-1917 (1999).
279 Park, H.-O., Kang, P. J. & Rachfal, A. W. Localization of the Rsr1/Bud1 GTPase involved in selection of a proper growth site in yeast. *Journal of Biological Chemistry* **277**, 26721-26724 (2002).
280 Adams, A., Johnson, D. I., Longnecker, R. M., Sloat, B. F. & Pringle, J. R. CDC42 and CDC43, two additional genes involved in budding and the establishment of cell polarity in the yeast Saccharomyces cerevisiae. *The Journal of cell biology* **111**, 131-142 (1990).
281 Johnson, D. I. Cdc42: an essential Rho-type GTPase controlling eukaryotic cell polarity. *Microbiology and Molecular Biology Reviews* **63**, 54-105 (1999).
282 Longtine, M. S. & Bi, E. Regulation of septin organization and function in yeast. *Trends in cell biology* **13**, 403-409 (2003).
283 Liakopoulos, D., Kusch, J., Grava, S., Vogel, J. & Barral, Y. Asymmetric Loading of Kar9 onto Spindle Poles and Microtubules Ensures Proper Spindle Alignment. *Cell* (2003).
284 Yin, H., Pruyne, D., Huffaker, T. C. & Bretscher, A. Myosin V orientates the mitotic spindle in yeast. *Nature* **406**, 1013-1015, doi:10.1038/35023024 (2000).
285 Beach, D. L., Thibodeaux, J., Maddox, P., Yeh, E. & Bloom, K. The role of the proteins Kar9 and Myo2 in orienting the mitotic spindle of budding yeast. *Current Biology* **10**, 1497-1506 (2000).
286 Hwang, E., Kusch, J., Barral, Y. & Huffaker, T. C. Spindle orientation in Saccharomyces cerevisiae depends on the transport of microtubule ends along polarized actin cables. *The Journal of cell biology* **161**, 483-488 (2003).

287 Schwartz, K., Richards, K. & Botstein, D. BIM1 encodes a microtubule-binding protein in yeast. *Molecular biology of the cell* **8**, 2677-2691 (1997).
288 Lengefeld, J. *et al.* Spatial cues and not spindle pole maturation drive the asymmetry of astral microtubules between new and pre-existing spindle poles. *Molecular biology of the cell*, mbc. E16-10-0725 (2017).
289 Maekawa, H. & Schiebel, E. Cdk1-Clb4 controls the interaction of astral microtubule plus ends with subdomains of the daughter cell cortex. *Genes & development* **18**, 1709-1724 (2004).
290 Moore, J. K. & Miller, R. K. The Cyclin-dependent Kinase Cdc28p Regulates Multiple Aspects of Kar9p Function in Yeast. **18**, 1187-1202 (2007).
291 Hotz, M., Lengefeld, J. & Barral, Y. The MEN mediates the effects of the spindle assembly checkpoint on Kar9-dependent spindle pole body inheritance in budding yeast. *Cell Cycle* **11**, 3109-3116, doi:10.4161/cc.21504 (2012).
292 Kammerer, D., Stevermann, L. & Liakopoulos, D. Ubiquitylation regulates interactions of astral microtubules with the cleavage apparatus. *Current Biology* **20**, 1233-1243 (2010).
293 Leisner, C. *et al.* Regulation of mitotic spindle asymmetry by SUMO and the spindle-assembly checkpoint in yeast. *Current Biology* **18**, 1249-1255 (2008).
294 Meednu, N. *et al.* The spindle positioning protein Kar9p interacts with the sumoylation machinery in Saccharomyces cerevisiae. *Genetics* **180**, 2033-2055 (2008).
295 Hüls, D., Storchova, Z. & Niessing, D. Post-translational modifications regulate assembly of early spindle orientation complex in yeast. *Journal of Biological Chemistry* **287**, 16238-16245 (2012).
296 Hergovich, A. in *The Mitotic Exit Network* 265-277 (Springer, 2017).
297 Gruneberg, U., Campbell, K., Simpson, C., Grindlay, J. & Schiebel, E. Nud1p links astral microtubule organization and the control of exit from mitosis. *The EMBO Journal* **19**, 6475-6488 (2000).
298 Bardin, A. J., Visintin, R. & Amon, A. A mechanism for coupling exit from mitosis to partitioning of the nucleus. *Cell* **102**, 21-31 (2000).
299 Pereira, G., Höfken, T., Grindlay, J., Manson, C. & Schiebel, E. The Bub2p spindle checkpoint links nuclear migration with mitotic exit. *Molecular cell* **6**, 1-10 (2000).
300 Visintin, R. & Amon, A. Regulation of the mitotic exit protein kinases Cdc15 and Dbf2. *Molecular biology of the cell* **12**, 2961-2974 (2001).
301 Valerio-Santiago, M. & Monje-Casas, F. Tem1 localization to the spindle pole bodies is essential for mitotic exit and impairs spindle checkpoint function. *The Journal of Cell Biology* **192**, 599-614 (2011).
302 Longtine, M. S. *et al.* Septin-dependent assembly of a cell cycle-regulatory module in Saccharomyces cerevisiae. *Molecular and Cellular Biology* **20**, 4049-4061 (2000).
303 Barral, Y., Parra, M., Bidlingmaier, S. & Snyder, M. Nim1-related kinases coordinate cell cycle progression with the organization of the peripheral cytoskeleton in yeast. *Genes & development* **13**, 176-187 (1999).
304 Monje-Casas, F. & Amon, A. Cell polarity determinants establish asymmetry in MEN signaling. *Developmental cell* **16**, 132-145 (2009).

305 Caydasi, A. K. & Pereira, G. Spindle alignment regulates the dynamic association of checkpoint proteins with yeast spindle pole bodies. *Developmental cell* **16**, 146-156 (2009).
306 Bertazzi, D. T., Kurtulmus, B. & Pereira, G. The cortical protein Lte1 promotes mitotic exit by inhibiting the spindle position checkpoint kinase Kin4. *The Journal of cell biology* **193**, 1033-1048 (2011).
307 Scarfone, I. *et al.* Asymmetry of the budding yeast Tem1 GTPase at spindle poles is required for spindle positioning but not for mitotic exit. *PLoS genetics* **11**, e1004938 (2015).
308 Heil-Chapdelaine, R. A., Tran, N. K. & Cooper, J. A. Dynein-dependent Movements of the Mitotic Spindle inSaccharomyces cerevisiae Do Not Require Filamentous Actin. *Molecular biology of the cell* **11**, 863-872 (2000).
309 Vaughan, K. T., Tynan, S. H., Faulkner, N. E., Echeverri, C. J. & Vallee, R. B. Colocalization of cytoplasmic dynein with dynactin and CLIP-170 at microtubule distal ends. *Journal of cell science* **112**, 1437-1447 (1999).
310 Han, G. *et al.* The Aspergillus cytoplasmic dynein heavy chain and NUDF localize to microtubule ends and affect microtubule dynamics. *Current Biology* **11**, 719-724 (2001).
311 Ma, S. & Chisholm, R. L. Cytoplasmic dynein-associated structures move bidirectionally in vivo. *Journal of Cell Science* **115**, 1453-1460 (2002).
312 Lenz, J., Schuchardt, I., Straube, A. & Steinberg, G. A dynein loading zone for retrograde endosome motility at microtubule plus-ends. *The EMBO journal* **25**, 2275-2286 (2006).
313 Kobayashi, T. & Murayama, T. Cell cycle-dependent microtubule-based dynamic transport of cytoplasmic dynein in mammalian cells. *PLoS One* **4**, e7827 (2009).
314 Busson, S., Dujardin, D., Moreau, A., Dompierre, J. & De Mey, J. R. Dynein and dynactin are localized to astral microtubules and at cortical sites in mitotic epithelial cells. *Current biology* **8**, 541-544 (1998).
315 Gönczy, P., Pichler, S., Kirkham, M. & Hyman, A. A. Cytoplasmic dynein is required for distinct aspects of MTOC positioning, including centrosome separation, in the one cell stage Caenorhabditis elegans embryo. *The Journal of cell biology* **147**, 135-150 (1999).
316 Kotak, S. & Gönczy, P. Mechanisms of spindle positioning: cortical force generators in the limelight. *Current opinion in cell biology* **25**, 741-748 (2013).
317 Markus, S. M., Kalutkiewicz, K. A. & Lee, W.-L. Astral microtubule asymmetry provides directional cues for spindle positioning in budding yeast. *Experimental cell research* **318**, 1400-1406 (2012).
318 Lee, W.-L., Oberle, J. R. & Cooper, J. A. The role of the lissencephaly protein Pac1 during nuclear migration in budding yeast. *J Cell Biol* **160**, 355-364 (2003).
319 Li, J., Lee, W.-L. & Cooper, J. A. NudEL targets dynein to microtubule ends through LIS1. *Nature cell biology* **7**, 686-690 (2005).
320 Markus, S. M. *et al.* Quantitative analysis of Pac1/LIS1-mediated dynein targeting: Implications for regulation of dynein activity in budding yeast. *Cytoskeleton* **68**, 157-174 (2011).
321 Komarova, Y. *et al.* EB1 and EB3 control CLIP dissociation from the ends of growing microtubules. *Molecular biology of the cell* **16**, 5334-5345 (2005).

322 Watson, P. & Stephens, D. J. Microtubule plus-end loading of p150Glued is mediated by EB1 and CLIP-170 but is not required for intracellular membrane traffic in mammalian cells. *Journal of cell science* **119**, 2758-2767 (2006).
323 Caudron, F., Andrieux, A., Job, D. & Boscheron, C. A new role for kinesin-directed transport of Bik1p (CLIP-170) in Saccharomyces cerevisiae. *Journal of cell science* **121**, 1506-1513 (2008).
324 Markus, S. M. & Lee, W.-L. Regulated offloading of cytoplasmic dynein from microtubule plus ends to the cortex. *Developmental cell* **20**, 639-651 (2011).
325 Lee, W.-L., Kaiser, M. A. & Cooper, J. A. The offloading model for dynein function. *The Journal of cell biology* **168**, 201-207 (2005).
326 Yeh, E. *et al.* Dynamic positioning of mitotic spindles in yeast: role of microtubule motors and cortical determinants. *Molecular biology of the cell* **11**, 3949-3961 (2000).
327 Carminati, J. L. & Stearns, T. Microtubules orient the mitotic spindle in yeast through dynein-dependent interactions with the cell cortex. *The Journal of cell biology* **138**, 629-641 (1997).
328 Grava, S., Schaerer, F., Faty, M., Philippsen, P. & Barral, Y. Asymmetric recruitment of dynein to spindle poles and microtubules promotes proper spindle orientation in yeast. *Developmental cell* **10**, 425-439 (2006).
329 King, S. J. & Schroer, T. A. Dynactin increases the processivity of the cytoplasmic dynein motor. *Nature cell biology* **2**, 20-24 (2000).
330 Culver-Hanlon, T. L., Lex, S. A., Stephens, A. D., Quintyne, N. J. & King, S. J. A microtubule-binding domain in dynactin increases dynein processivity by skating along microtubules. *Nature cell biology* **8**, 264-271 (2006).
331 Kardon, J. R., Reck-Peterson, S. L. & Vale, R. D. Regulation of the processivity and intracellular localization of Saccharomyces cerevisiae dynein by dynactin. *Proceedings of the National Academy of Sciences* **106**, 5669-5674 (2009).
332 Moore, J. K., Li, J. & Cooper, J. A. Dynactin function in mitotic spindle positioning. *Traffic* **9**, 510-527 (2008).
333 Farkasovsky, M. & Küntzel, H. Cortical Num1p interacts with the dynein intermediate chain Pac11p and cytoplasmic microtubules in budding yeast. *The Journal of cell biology* **152**, 251-262 (2001).
334 Woodruff, J. B., Drubin, D. G. & Barnes, G. Dynein-driven mitotic spindle positioning restricted to anaphase by She1p inhibition of dynactin recruitment. *Mol. Biol. Cell* **20**, 3003-3011 (2009).
335 Markus, S. M., Kalutkiewicz, K. A. & Lee, W.-L. She1-mediated inhibition of dynein motility along astral microtubules promotes polarized spindle movements. *Current Biology* **22**, 2221-2230 (2012).
336 Knaus, M. *et al.* The Bud14p–Glc7p complex functions as a cortical regulator of dynein in budding yeast. *The EMBO journal* **24**, 3000-3011 (2005).
337 Markus, S. M., Punch, J. J. & Lee, W.-L. L. Motor- and tail-dependent targeting of dynein to microtubule plus ends and the cell cortex. *Curr. Biol.* **19**, 196-205 (2009).
338 Vogel, J. & Snyder, M. The carboxy terminus of Tub4p is required for gamma-tubulin function in budding yeast. *Journal of cell Science* (2000).

339 Bailly, E., Cabantous, S., Sondaz, D., Bernadac, A. & Simon, M.-N. N. Differential cellular localization among mitotic cyclins from Saccharomyces cerevisiae: a new role for the axial budding protein Bud3 in targeting Clb2 to the mother-bud neck. *J. Cell. Sci.* **116**, 4119-4130 (2003).
340 Cuschieri, L., Nguyen, T. & Vogel, J. Control at the cell center - The role of spindle poles in cytoskeletal organization and cell cycle regulation. *Cell Cycle* **6**, 2788-2794 (2007).
341 Oakley, B. R., Paolillo, V. & Zheng, Y. γ-Tubulin complexes in microtubule nucleation and beyond. *Molecular biology of the cell* **26**, 2957-2962 (2015).
342 Zimmerman, S. & Chang, F. Effects of γ-tubulin complex proteins on microtubule nucleation and catastrophe in fission yeast. *Molecular biology of the cell* **16**, 2719-2733 (2005).
343 Bouissou, A. *et al.* γ-Tubulin Ring Complexes and EB1 play antagonistic roles in microtubule dynamics and spindle positioning. *EMBO J.* **33**, 114-128 (2014).
344 Cuschieri, L., Miller, R. & Vogel, J. Gamma-tubulin is required for proper recruitment and assembly of Kar9-Bim1 complexes in budding yeast. *Mol. Biol. Cell* **17**, 4420-4434 (2006).
345 Paluh, J. L. *et al.* A mutation in γ-tubulin alters microtubule dynamics and organization and is synthetically lethal with the kinesin-like protein pkl1p. *Molecular biology of the cell* **11**, 1225-1239 (2000).
346 Li, S. *et al.* Cytoplasmic dynein's mitotic spindle pole localization requires a functional anaphase-promoting complex, γ-tubulin, and NUDF/LIS1 in Aspergillus nidulans. *Molecular biology of the cell* **16**, 3591-3605 (2005).
347 Rodriguez, A. S. *et al.* Protein complexes at the microtubule organizing center regulate bipolar spindle assembly. *Cell Cycle* **7**, 1246-1253 (2008).
348 Höög, G., Zarrizi, R., von Stedingk, K., Jonsson, K. & Maria, A.-K. Nuclear localization of γ-tubulin affects E2F transcriptional activity and S-phase progression. *FASEB J.* **25**, 3815-3827 (2011).
349 Ehlén, A. *et al.* Tumors with nonfunctional retinoblastoma protein are killed by reduced γ-tubulin levels. *J. Biol. Chem.* **287**, 17241-17247 (2012).
350 Eklund, G., Lang, S., Glindre, J., Ehlen, A. & Kristensson, M. The nuclear localization of γ-tubulin is regulated by SadB-mediated phosphorylation. **289**, 21360-21373 (2014).
351 Edgerton-Morgan, H. & Oakley, B. R. γ-Tubulin plays a key role in inactivating APC/CCdh1 at the G1–S boundary. *J Cell Biology* **198**, 785-791 (2012).
352 Nayak, T. *et al.* γ-Tubulin regulates the anaphase-promoting complex/cyclosome during interphase. *The Journal of cell biology* **190**, 317-330 (2010).
353 Alvarado-Kristensson, M., Rodríguez, M. J., Silió, V., Valpuesta, J. M. & Carrera, A. C. SADB phosphorylation of gamma-tubulin regulates centrosome duplication. *Nat. Cell Biol.* **11**, 1081-1092 (2009).
354 Sankaran, S., Crone, D. E., Palazzo, R. E. & Parvin, J. D. BRCA1 regulates γ-tubulin binding to centrosomes. *Cancer biology & therapy* **6**, 1853-1857 (2007).
355 Starita, L. M. *et al.* BRCA1-dependent ubiquitination of γ-tubulin regulates centrosome number. *Molecular and cellular biology* **24**, 8457-8466 (2004).
356 Sankaran, S., Starita, L. M., Groen, A. C., Ko, M. J. & Parvin, J. D. Centrosomal microtubule nucleation activity is inhibited by BRCA1-dependent ubiquitination. *Molecular and cellular biology* **25**, 8656-8668 (2005).

357 Choy, J. S. *et al.* Genome-wide haploinsufficiency screen reveals a novel role for γ-TuSC in spindle organization and genome stability. *Molecular biology of the cell* **24**, 2753-2763 (2013).
358 Colombié, N. *et al.* The Drosophila γ-tubulin small complex subunit Dgrip84 is required for structural and functional integrity of the spindle apparatus. *Molecular biology of the cell* **17**, 272-282 (2006).
359 Vardy, L. & Toda, T. The fission yeast γ-tubulin complex is required in G1 phase and is a component of the spindle assembly checkpoint. *The EMBO Journal* **19**, 6098-6111 (2000).
360 Hendrickson, T. W., Yao, J., Bhadury, S., Corbett, A. H. & Joshi, H. C. Conditional mutations in γ-tubulin reveal its involvement in chromosome segregation and cytokinesis. *Molecular Biology of the Cell* **12**, 2469-2481 (2001).
361 Prigozhina, N. L., Walker, R. A., Oakley, C. E. & Oakley, B. R. γ-Tubulin and the C-Terminal Motor Domain Kinesin-like Protein, KLPA, Function in the Establishment of Spindle Bipolarity inAspergillus nidulans. *Molecular biology of the cell* **12**, 3161-3174 (2001).
362 Prigozhina, N. L. *et al.* γ-Tubulin plays an essential role in the coordination of mitotic events. *Molecular biology of the cell* **15**, 1374-1386 (2004).
363 Müller, H., Fogeron, M.-L., Lehmann, V., Lehrach, H. & Lange, B. M. A centrosome-independent role for γ-TuRC proteins in the spindle assembly checkpoint. *Science* **314**, 654-657 (2006).
364 Mayer, C., Filopei, J., Batac, J., Alford, L. & Paluh, J. L. An extended anaphase signaling pathway for Mad2p includes microtubule organizing center proteins and multiple motor-dependent transitions. *Cell Cycle* **5**, 1456-1463 (2006).
365 Edgerton, H., Paolillo, V. & Oakley, B. R. Spatial regulation of the spindle assembly checkpoint and anaphase-promoting complex in Aspergillus nidulans. *Molecular microbiology* **95**, 442-457 (2015).
366 Shirayama, M., Zachariae, W., Ciosk, R. & Nasmyth, K. The Polo-like kinase Cdc5p and the WD-repeat protein Cdc20p/fizzy are regulators and substrates of the anaphase promoting complex in Saccharomyces cerevisiae. *The EMBO journal* **17**, 1336-1349 (1998).
367 Pereira, G. & Schiebel, E. Kin4 kinase delays mitotic exit in response to spindle alignment defects. *Molecular cell* **19**, 209-221 (2005).
368 Fraschini, R., D'Ambrosio, C., Venturetti, M., Lucchini, G. & Piatti, S. Disappearance of the budding yeast Bub2–Bfa1 complex from the mother-bound spindle pole contributes to mitotic exit. *The Journal of cell biology* **172**, 335-346 (2006).
369 Maekawa, H., Priest, C., Lechner, J., Pereira, G. & Schiebel, E. The yeast centrosome translates the positional information of the anaphase spindle into a cell cycle signal. *The Journal of Cell Biology* **179**, 423-436 (2007).
370 Zhang, S., Hemmerich, P. & Grosse, F. Centrosomal localization of DNA damage checkpoint proteins. *Journal of cellular biochemistry* **101**, 451-465 (2007).
371 Lesca, C. *et al.* DNA damage induce γ-tubulin–RAD51 nuclear complexes in mammalian cells. *Oncogene* **24**, 5165 (2005).
372 Hořejší, B. *et al.* Nuclear γ-tubulin associates with nucleoli and interacts with tumor suppressor protein C53. *Journal of cellular physiology* **227**, 367-382 (2012).

373 Hubert, T., Vandekerckhove, J. & Gettemans, J. Cdk1 and BRCA1 target γ-tubulin to microtubule domains. *Biochemical and biophysical research communications* **414**, 240-245 (2011).
374 Luca, F. C. *et al.* Saccharomyces cerevisiae Mob1p is required for cytokinesis and mitotic exit. *Molecular and Cellular Biology* **21**, 6972-6983 (2001).
375 Yoshida, S., Asakawa, K. & Toh-e, A. Mitotic exit network controls the localization of Cdc14 to the spindle pole body in Saccharomyces cerevisiae. *Current biology* **12**, 944-950 (2002).
376 Rock, J. M. & Amon, A. Cdc15 integrates Tem1 GTPase-mediated spatial signals with Polo kinase-mediated temporal cues to activate mitotic exit. *Genes & Development* **25**, 1943-1954 (2011).
377 Molk, J. N. *et al.* The differential roles of budding yeast Tem1p, Cdc15p, and Bub2p protein dynamics in mitotic exit. *Molecular biology of the cell* **15**, 1519-1532 (2004).
378 Mulvihill, D. P. & Hyams, J. S. Cytokinetic actomyosin ring formation and septation in fission yeast are dependent on the full recruitment of the polo-like kinase Plo1 to the spindle pole body and a functional spindle assembly checkpoint. *Journal of cell science* **115**, 3575-3586 (2002).
379 Tomlin, G. C., Morrell, J. L. & Gould, K. L. The spindle pole body protein Cdc11p links Sid4p to the fission yeast septation initiation network. *Molecular biology of the cell* **13**, 1203-1214 (2002).
380 Krapp, A., Schmidt, S., Cano, E. & Simanis, V. S. pombe cdc11p, together with sid4p, provides an anchor for septation initiation network proteins on the spindle pole body. *Current Biology* **11**, 1559-1568 (2001).
381 Binarová, P. *et al.* γ-Tubulin is essential for acentrosomal microtubule nucleation and coordination of late mitotic events in Arabidopsis. *The Plant Cell Online* **18**, 1199-1212 (2006).
382 Jensen, O. N. Modification-specific proteomics: characterization of post-translational modifications by mass spectrometry. *Current opinion in chemical biology* **8**, 33-41 (2004).
383 Khoury, G. A., Baliban, R. C. & Floudas, C. A. Proteome-wide post-translational modification statistics: frequency analysis and curation of the swiss-prot database. *Scientific reports* **1**, 90 (2011).
384 Stumpff, J., Kellogg, D. R., Krohne, K. A. & Su, T. T. Drosophila Wee1 interacts with members of the γTURC and is required for proper mitotic-spindle morphogenesis and positioning. *Current biology* **15**, 1525-1534 (2005).
385 Kim, H.-K. *et al.* De novo formation of basal bodies in Naegleria gruberi: regulation by phosphorylation. *The Journal of cell biology* **169**, 719-724 (2005).
386 Kukharskyy, V. *et al.* Complexes of γ-tubulin with nonreceptor protein tyrosine kinases Src and Fyn in differentiating P19 embryonal carcinoma cells. *Experimental cell research* **298**, 218-228 (2004).
387 Hegemann, B. *et al.* Systematic phosphorylation analysis of human mitotic protein complexes. *Sci. Signal.* **4**, rs12-rs12 (2011).
388 Kim, W. *et al.* Systematic and quantitative assessment of the ubiquitin-modified proteome. *Molecular cell* **44**, 325-340 (2011).

389 Tsai, C.-F. *et al.* Large-scale determination of absolute phosphorylation stoichiometries in human cells by motif-targeting quantitative proteomics. *Nature communications* **6**, 6622 (2015).
390 Sharma, K. *et al.* Ultradeep human phosphoproteome reveals a distinct regulatory nature of Tyr and Ser/Thr-based signaling. *Cell reports* **8**, 1583-1594 (2014).
391 Zhou, H. *et al.* Toward a comprehensive characterization of a human cancer cell phosphoproteome. *Journal of proteome research* **12**, 260-271 (2012).
392 Chi, Y. *et al.* Identification of CDK2 substrates in human cell lysates. *Genome biology* **9**, R149 (2008).
393 Mertins, P. *et al.* Integrated proteomic analysis of post-translational modifications by serial enrichment. *Nature methods* **10**, 634 (2013).
394 Povlsen, L. K. *et al.* Systems-wide analysis of ubiquitylation dynamics reveals a key role for PAF15 ubiquitylation in DNA-damage bypass. *Nature cell biology* **14**, 1089 (2012).
395 Wagner, S. A. *et al.* A proteome-wide, quantitative survey of in vivo ubiquitylation sites reveals widespread regulatory roles. *Molecular & Cellular Proteomics* **10**, M111. 013284 (2011).
396 Stuart, S. A. *et al.* A phosphoproteomic comparison of B-RAFV600E and MKK1/2 inhibitors in melanoma cells. *Molecular & Cellular Proteomics* **14**, 1599-1615 (2015).
397 Luerman, G. C. *et al.* Phosphoproteomic evaluation of pharmacological inhibition of leucine-rich repeat kinase 2 reveals significant off-target effects of LRRK-2-IN-1. *Journal of neurochemistry* **128**, 561-576 (2014).
398 Danielsen, J. M. *et al.* Mass spectrometric analysis of lysine ubiquitylation reveals promiscuity at site level. *Molecular & Cellular Proteomics* **10**, M110. 003590 (2011).
399 Huen, M. S., Sy, S. M. & Chen, J. BRCA1 and its toolbox for the maintenance of genome integrity. *Nature reviews Molecular cell biology* **11**, 138 (2010).
400 Lin, T.-c. C. *et al.* Phosphorylation of the yeast γ-tubulin Tub4 regulates microtubule function. *PLoS ONE* **6**, e19700 (2011).
401 Holt, L. J. *et al.* Global analysis of Cdk1 substrate phosphorylation sites provides insights into evolution. *Science* **325**, 1682-1686 (2009).
402 Ear, P. H. *et al.* Dissection of Cdk1-cyclin Complexes in vivo. *Proceedings of the National Academy of Sciences* (2013).
403 Karim, A. S., Curran, K. A. & Alper, H. S. Characterization of plasmid burden and copy number in Saccharomyces cerevisiae for optimization of metabolic engineering applications. *FEMS yeast research* **13**, 107-116 (2013).
404 Peng, Y. *et al.* Interaction of CK1δ with γTuSC ensures proper microtubule assembly and spindle positioning. *Mol. Biol. Cell* **26**, 2505-2518 (2015).
405 Cheong, J. K. & Virshup, D. M. Casein kinase 1: Complexity in the family. *The international journal of biochemistry & cell biology* **43**, 465-469 (2011).
406 Behrend, L. *et al.* Interaction of casein kinase 1 delta (CK1δ) with post-Golgi structures, microtubules and the spindle apparatus. *European journal of cell biology* **79**, 240-251 (2000).
407 Milne, D. M., Looby, P. & Meek, D. W. Catalytic activity of protein kinase CK1δ (casein kinase 1δ) is essential for its normal subcellular localization. *Experimental cell research* **263**, 43-54 (2001).

408 Andersen, J. S. *et al.* Proteomic characterization of the human centrosome by protein correlation profiling. *Nature* **426**, 570 (2003).
409 Greer, Y. E. & Rubin, J. S. Casein kinase 1 delta functions at the centrosome to mediate Wnt-3a–dependent neurite outgrowth. *The Journal of cell biology* **192**, 993-1004 (2011).
410 Huerta-Cepas, J., Serra, F. & Bork, P. ETE 3: reconstruction, analysis, and visualization of phylogenomic data. *Molecular biology and evolution* **33**, 1635-1638 (2016).
411 Winzeler, E. A. *et al.* Functional characterization of the S. cerevisiae genome by gene deletion and parallel analysis. *science* **285**, 901-906 (1999).
412 Huh, W.-K. *et al.* Global analysis of protein localization in budding yeast. *Nature* **425**, 686 (2003).
413 Shaner, N. C. *et al.* A bright monomeric green fluorescent protein derived from Branchiostoma lanceolatum. *Nature methods* **10**, 407 (2013).
414 Bitinaite, J. *et al.* USER™ friendly DNA engineering and cloning method by uracil excision. *Nucleic acids research* **35**, 1992-2002 (2007).
415 Gietz, R. D. & Schiestl, R. H. High-efficiency yeast transformation using the LiAc/SS carrier DNA/PEG method. *Nature protocols* **2**, 31 (2007).
416 Longtine, M. S. *et al.* Additional modules for versatile and economical PCR-based gene deletion and modification in Saccharomyces cerevisiae. *Yeast* **14**, 953-961 (1998).
417 Knop, M. *et al.* Epitope tagging of yeast genes using a PCR-based strategy: more tags and improved practical routines. *Yeast* **15**, 963-972 (1999).
418 Sherman, F. in *Methods in enzymology* Vol. 350 3-41 (Elsevier, 2002).
419 Rines, D. R., Thomann, D., Dorn, J. F., Goodwin, P. & Sorger, P. K. Live cell imaging of yeast. *Cold Spring Harbor Protocols* **2011**, pdb. top065482 (2011).
420 Huffaker, T. C., Thomas, J. H. & Botstein, D. Diverse effects of beta-tubulin mutations on microtubule formation and function. *The Journal of Cell Biology* **106**, 1997-2010 (1988).
421 Stearns, T. & Botstein, D. Unlinked noncomplementation: isolation of new conditional-lethal mutations in each of the tubulin genes of Saccharomyces cerevisiae. *Genetics* **119**, 249-260 (1988).
422 Gardner, R. G., Nelson, Z. W. & Gottschling, D. E. Degradation-mediated protein quality control in the nucleus. *Cell* **120**, 803-815 (2005).
423 Ratsima, H. *et al.* Independent modulation of the kinase and polo-box activities of Cdc5 protein unravels unique roles in the maintenance of genome stability. *Proceedings of the National Academy of Sciences* **108**, E914-E923 (2011).
424 Shulist, K. *et al.* Interrogation of γ-tubulin alleles using high-resolution fitness measurements reveals a distinct cytoplasmic function in spindle alignment. *Scientific reports* **7**, 11398 (2017).
425 Byers, B. & Goetsch, L. in *Cold Spring Harbor Symposia on Quantitative Biology.* 123-131 (Cold Spring Harbor Laboratory Press).
426 Byers, B. & Goetsch, L. Behavior of spindles and spindle plaques in the cell cycle and conjugation of Saccharomyces cerevisiae. *Journal of bacteriology* **124**, 511-523 (1975).
427 Harris, J., Shadrina, M., Oliver, C., Vogel, J. & Mittermaier, A. Concerted millisecond timescale dynamics in the intrinsically disordered carboxyl terminus of γ-tubulin induced by mutation of a conserved tyrosine residue. *Protein Science* **27**, 531-545 (2018).

428 Marschall, L. G., Jeng, R. L., Mulholland, J. & Stearns, T. Analysis of Tub4p, a yeast gamma-tubulin-like protein: implications for microtubule-organizing center function. *The Journal of cell biology* **134**, 443-454 (1996).
429 Toh, G.-L. & Lowndes, N. (Portland Press Limited, 2003).
430 Lowndes, N. F. & Murguia, J. R. Sensing and responding to DNA damage. *Current opinion in genetics & development* **10**, 17-25 (2000).
431 Knop, M. & Schiebel, E. Spc98p and Spc97p of the yeast γ-tubulin complex mediate binding to the spindle pole body via their interaction with Spc110p. *The EMBO Journal* **16**, 6985-6995 (1997).
432 Pereira, G., Knop, M. & Schiebel, E. Spc98p directs the yeast γ-tubulin complex into the nucleus and is subject to cell cycle-dependent phosphorylation on the nuclear side of the spindle pole body. *Molecular biology of the cell* **9**, 775-793 (1998).
433 Zhu, H. *et al.* Analysis of yeast protein kinases using protein chips. *Nature genetics* **26**, 283 (2000).
434 Jaspersen, S. L. *et al.* Cdc28/Cdk1 regulates spindle pole body duplication through phosphorylation of Spc42 and Mps1. *Developmental cell* **7**, 263-274 (2004).
435 Lacey, K. R., Jackson, P. K. & Stearns, T. Cyclin-dependent kinase control of centrosome duplication. *Proceedings of the National Academy of Sciences* **96**, 2817-2822 (1999).
436 Kovacs, L. A. S., Nelson, C. L. & Haase, S. B. Intrinsic and cyclin-dependent kinase-dependent control of spindle pole body duplication in budding yeast. *Molecular biology of the cell* **19**, 3243-3253 (2008).
437 Geiser, J. R., Sundberg, H. A., Chang, B. H., Muller, E. & Davis, T. N. The essential mitotic target of calmodulin is the 110-kilodalton component of the spindle pole body in Saccharomyces cerevisiae. *Molecular and Cellular Biology* **13**, 7913-7924 (1993).
438 Stirling, D. A., Welch, K. A. & Stark, M. Interaction with calmodulin is required for the function of Spc110p, an essential component of the yeast spindle pole body. *The EMBO Journal* **13**, 4329-4342 (1994).
439 Doxsey, S. J., Stein, P., Evans, L., Calarco, P. D. & Kirschner, M. Pericentrin, a highly conserved centrosome protein involved in microtubule organization. *Cell* **76**, 639-650 (1994).
440 Fry, A. M. *et al.* C-Nap1, a novel centrosomal coiled-coil protein and candidate substrate of the cell cycle–regulated protein kinase Nek2. *The Journal of cell biology* **141**, 1563-1574 (1998).
441 Lin, T.-c. *et al.* Cell-cycle dependent phosphorylation of yeast pericentrin regulates γ-TuSC-mediated microtubule nucleation. *Elife* **3** (2014).
442 Viswanath, S. *et al.* The molecular architecture of the yeast spindle pole body core determined by Bayesian integrative modeling. *Molecular biology of the cell* **28**, 3298-3314 (2017).
443 O'Toole, E. T. *et al.* Three-dimensional analysis and ultrastructural design of mitotic spindles from the cdc20 mutant of Saccharomyces cerevisiae. *Molecular biology of the cell* **8**, 1-11 (1997).
444 Winey, M. *et al.* Three-dimensional ultrastructural analysis of the Saccharomyces cerevisiae mitotic spindle. *The Journal of cell biology* **129**, 1601-1615 (1995).

445 Cohen, P. The regulation of protein function by multisite phosphorylation–a 25 year update. *Trends in biochemical sciences* **25**, 596-601 (2000).
446 Nash, P. *et al.* Multisite phosphorylation of a CDK inhibitor sets a threshold for the onset of DNA replication. *Nature* **414**, 514 (2001).
447 Deshaies, R. J. & Ferrell, J. E. Multisite phosphorylation and the countdown to S phase. *Cell* **107**, 819-822 (2001).
448 Holmberg, C. I., Tran, S. E., Eriksson, J. E. & Sistonen, L. Multisite phosphorylation provides sophisticated regulation of transcription factors. *Trends in biochemical sciences* **27**, 619-627 (2002).
449 Malleshaiah, M. K., Shahrezaei, V., Swain, P. S. & Michnick, S. W. The scaffold protein Ste5 directly controls a switch-like mating decision in yeast. *Nature* **465**, 101 (2010).
450 Lim, W., Mayer, B. & Pawson, T. *Cell signaling: principles and mechanisms*. (Taylor & Francis, 2014).
451 Ubersax, J. A. *et al.* Targets of the cyclin-dependent kinase Cdk1. *Nature* **425**, 859 (2003).
452 Moses, A. M., Hériché, J.-K. & Durbin, R. Clustering of phosphorylation site recognition motifs can be exploited to predict the targets of cyclin-dependent kinase. *Genome biology* **8**, R23 (2007).
453 Traven, A. & Heierhorst, J. SQ/TQ cluster domains: concentrated ATM/ATR kinase phosphorylation site regions in DNA-damage-response proteins. *Bioessays* **27**, 397-407 (2005).
454 Lee, S.-J., Schwartz, M. F., Duong, J. K. & Stern, D. F. Rad53 phosphorylation site clusters are important for Rad53 regulation and signaling. *Molecular and cellular biology* **23**, 6300-6314 (2003).
455 Lenz, P. & Swain, P. S. An entropic mechanism to generate highly cooperative and specific binding from protein phosphorylations. *Current biology* **16**, 2150-2155 (2006).
456 Oakley, C. E. & Oakley, B. R. Identification of γ-tubulin, a new member of the tubulin superfamily encoded by mipA gene of Aspergillus nidulans. *Nature* **338**, 662-664 (1989).
457 Oakley, B. R., Oakley, C. E., Yoon, Y. & Jung, M. K. γ-Tubulin is a component of the spindle pole body that is essential for microtubule function in Aspergillus nidulans. *Cell* **61**, 1289-1301 (1990).
458 Stearns, T., Evans, L. & Kirschner, M. γ-Tubulin is a highly conserved component of the centrosome. *Cell* **65**, 825-836 (1991).
459 Zheng, Y., Jung, M. K. & Oakley, B. R. γ-Tubulin is present in Drosophila melanogaster and Homo sapiens and is associated with the centrosome. *Cell* **65**, 817-823 (1991).
460 Horio, T. *et al.* The fission yeast gamma-tubulin is essential for mitosis and is localized at microtubule organizing centers. *Journal of Cell Science* **99**, 693-700 (1991).
461 Joshi, H. C., Palacios, M. J., McNamara, L. & Cleveland, D. W. γ-Tubulin is a centrosomal protein required for cell cycle-dependent microtubule nucleation. *Nature* **356**, 80-83 (1992).
462 Zheng, Y., Wong, M., Alberts, B. & Mitchison, T. Nucleation of microtubule assembly by a gamma-tubulin-containing ring complex. *Nature* **378**, 578-583 (1995).

463 Sobel, S. G. & Snyder, M. A highly divergent gamma-tubulin gene is essential for cell growth and proper microtubule organization in Saccharomyces cerevisiae. *The Journal of Cell Biology* **131**, 1775-1788 (1995).
464 Geissler, S. *et al.* The spindle pole body component Spc98p interacts with the gamma-tubulin-like Tub4p of Saccharomyces cerevisiae at the sites of microtubule attachment. *The EMBO journal* **15**, 3899 (1996).
465 Knop, M., Pereira, G., Geissler, S., Grein, K. & Schiebel, E. The spindle pole body component Spc97p interacts with the γ-tubulin of Saccharomyces cerevisiae and functions in microtubule organization and spindle pole body duplication. *The EMBO Journal* **16**, 1550-1564 (1997).
466 Jaspersen, S. L. & Winey, M. The budding yeast spindle pole body: structure, duplication, and function. *Annu. Rev. Cell Dev. Biol.* **20**, 1-28 (2004).
467 Knop, M. & Schiebel, E. Receptors determine the cellular localization of a γ-tubulin complex and thereby the site of microtubule formation. *The EMBO Journal* **17**, 3952-3967 (1998).
468 Bloom, J. & Cross, F. R. Multiple levels of cyclin specificity in cell-cycle control. *Nat. Rev. Mol. Cell Biol.* **8**, 149-160 (2007).
469 Hardwick, K. G. *et al.* Lesions in many different spindle components activate the spindle checkpoint in the budding yeast Saccharomyces cerevisiae. *Genetics* **152**, 509-518 (1999).
470 Braberg, H. *et al.* From structure to systems: high-resolution, quantitative genetic analysis of RNA polymerase II. *Cell* **154**, 775-788 (2013).
471 Baryshnikova, A. *et al.* Synthetic genetic array (SGA) analysis in Saccharomyces cerevisiae and Schizosaccharomyces pombe. *Methods in …* **470**, 145-179 (2010).
472 Tong, A. *et al.* Systematic genetic analysis with ordered arrays of yeast deletion mutants. *Science* **294**, 2364-2368 (2001).
473 Brachmann, C. B. *et al.* Designer deletion strains derived from Saccharomyces cerevisiae S288C: a useful set of strains and plasmids for PCR-mediated gene disruption and other applications. *YEAST-CHICHESTER-* **14**, 115-132 (1998).
474 Gietz, R. D. & Schiestl, R. H. High-efficiency yeast transformation using the LiAc/SS carrier DNA/PEG method. *Nat Protoc* **2**, 31-34, doi:10.1038/nprot.2007.13 (2007).
475 Markus, S. M., Omer, S., Baranowski, K. & Lee, W. L. Improved plasmids for fluorescent protein tagging of microtubules in Saccharomyces cerevisiae. *Traffic* **16**, 773-786 (2015).
476 Janke, C. *et al.* A versatile toolbox for PCR-based tagging of yeast genes: new fluorescent proteins, more markers and promoter substitution cassettes. *Yeast* **21**, 947-962 (2004).
477 Schindelin, J. *et al.* Fiji: an open-source platform for biological-image analysis. *Nature methods* **9**, 676-682 (2012).
478 Elena, S. & Lenski, R. Test of synergistic interactions among deleterious mutations in bacteria. *Nature* **390**, 395-398 (1997).
479 Phillips, P. C., Otto, S. P. & Whitlock, M. C. Beyond the average. 20-40 (2000).
480 Collins, S. R., Roguev, A. & Krogan, N. J. Chapter 1 1 Quantitative Genetic Interaction Mapping Using the E-MAP Approach. **470**, 205-231 (2010).
481 Baryshnikova, A. *et al.* Quantitative analysis of fitness and genetic interactions in yeast on a genome scale. *Nat. Methods* **7**, 1017-1024 (2010).

482 Turney, D., de los Santos, T. & Hollingsworth, N. M. Does chromosome size affect map distance and genetic interference in budding yeast? *Genetics* **168**, 2421-2424 (2004).
483 Kaback, D. B., Steensma, H. Y. & De Jonge, P. Enhanced meiotic recombination on the smallest chromosome of Saccharomyces cerevisiae. *Proceedings of the National Academy of Sciences* **86**, 3694-3698 (1989).
484 Zhu, Y. & Kuang, D. Construction of the physical map of yeast (Saccharomyces cerevisiae) chromosome V. *Cell Research* **2**, 25-34 (1992).
485 Schuyler, S. C., Liu, J. Y. & Pellman, D. The molecular function of Ase1p. *J Cell Biol* **160**, 517-528 (2003).
486 Zeng, X. *et al.* Slk19p is a centromere protein that functions to stabilize mitotic spindles. *The Journal of cell biology* **146**, 415-425 (1999).
487 D'Aquino, K. E. *et al.* The protein kinase Kin4 inhibits exit from mitosis in response to spindle position defects. *Molecular cell* **19**, 223-234 (2005).
488 Rauch, A., Nazarova, E. & Vogel, J. Analysis of microtubules in budding yeast. *Methods Cell Biol.* **97**, 277-306 (2010).
489 Kusch, J., Meyer, A., Snyder, M. P. & Barral, Y. Microtubule capture by the cleavage apparatus is required for proper spindle positioning in yeast. *Genes & Development* **16**, 1627-1639 (2002).
490 Palmer, R., Sullivan, D., Huffaker, T. & Koshland, D. Role of astral microtubules and actin in spindle orientation and migration in the budding yeast, Saccharomyces cerevisiae. *The Journal of cell biology* **119**, 583-593 (1992).
491 Segal, M. & Bloom, K. Control of spindle polarity and orientation in\textless i\textgreater Saccharomyces cerevisiae\textless/i\textgreater. *Trends in cell biology* (2001).
492 Theesfeld, C. L., Irazoqui, J. E., Bloom, K. & Lew, D. J. The role of actin in spindle orientation changes during the Saccharomyces cerevisiae cell cycle. *J Cell Biol* **146**, 1019-1032 (1999).
493 Gupta, M. L. *et al.* β-Tubulin C354 mutations that severely decrease microtubule dynamics do not prevent nuclear migration in yeast. *Molecular biology of the cell* **13**, 2919-2932 (2002).
494 Shaw, S. L., Yeh, E., Maddox, P., Salmon, E. D. & Bloom, K. Astral microtubule dynamics in yeast: a microtubule-based searching mechanism for spindle orientation and nuclear migration into the bud. *The Journal of cell biology* **139**, 985-994 (1997).
495 Addinall, S. G. *et al.* Quantitative fitness analysis shows that NMD proteins and many other protein complexes suppress or enhance distinct telomere cap defects. *PLoS Genet.* **7**, e1001362 (2011).
496 Thorsness, P. E. & Koshland, D. E. Inactivation of isocitrate dehydrogenase by phosphorylation is mediated by the negative charge of the phosphate. *Journal of Biological Chemistry* **262**, 10422-10425 (1987).
497 Weng, Q.-P. *et al.* Regulation of the p70 S6 kinase by phosphorylation in vivo analysis using site-specific anti-phosphopeptide antibodies. *Journal of Biological Chemistry* **273**, 16621-16629 (1998).
498 Hiscott, J. *et al.* Triggering the interferon response: the role of IRF-3 transcription factor. *Journal of interferon & cytokine research* **19**, 1-13 (1999).

499 Lin, R., Heylbroeck, C., Pitha, P. M. & Hiscott, J. Virus-dependent phosphorylation of the IRF-3 transcription factor regulates nuclear translocation, transactivation potential, and proteasome-mediated degradation. *Molecular and cellular biology* **18**, 2986-2996 (1998).
500 Brown, N. M. *et al.* Novel role of phosphorylation in Fe–S cluster stability revealed by phosphomimetic mutations at Ser-138 of iron regulatory protein 1. *Proceedings of the National Academy of Sciences* **95**, 15235-15240 (1998).
501 Krek, W., Marks, J., Schmitz, N., Nigg, E. A. & Simanis, V. Vertebrate p34cdc2 phosphorylation site mutants: effects upon cell cycle progression in the fission yeast Schizosaccharomyces pombe. *Journal of cell science* **102**, 43-53 (1992).
502 Mercurio, F. *et al.* IKK-1 and IKK-2: cytokine-activated IκB kinases essential for NF-κB activation. *Science* **278**, 860-866 (1997).
503 Gould, K. L. & Nurse, P. Tyrosine phosphorylation of the fission yeast cdc2+ protein kinase regulates entry into mitosis. *Nature* **342**, 39 (1989).
504 Gonzalez, G. A. & Montminy, M. R. Cyclic AMP stimulates somatostatin gene transcription by phosphorylation of CREB at serine 133. *Cell* **59**, 675-680 (1989).
505 García-Heredia, J. M. *et al.* Tyrosine phosphorylation turns alkaline transition into a biologically relevant process and makes human cytochrome c behave as an anti-apoptotic switch. *JBIC Journal of Biological Inorganic Chemistry* **16**, 1155-1168 (2011).
506 Dai, H. *et al.* Contribution of Bcl-2 phosphorylation to Bak binding and drug resistance. *Cancer research* **73**, 6998-7008 (2013).
507 Zheng, W. *et al.* Cellular stabilization of the melatonin rhythm enzyme induced by nonhydrolyzable phosphonate incorporation. *Nature Structural and Molecular Biology* **10**, 1054 (2003).
508 Littlepage, L. E. *et al.* Identification of phosphorylated residues that affect the activity of the mitotic kinase Aurora-A. *Proceedings of the National Academy of Sciences* **99**, 15440-15445 (2002).
509 Szczepanowska, J. *et al.* Effect of mutating the regulatory phosphoserine and conserved threonine on the activity of the expressed catalytic domain of Acanthamoeba myosin I heavy chain kinase. *Proceedings of the National Academy of Sciences* **95**, 4146-4151 (1998).
510 Michard, E., Dreyer, I., Lacombe, B., Sentenac, H. & Thibaud, J. B. Inward rectification of the AKT2 channel abolished by voltage-dependent phosphorylation. *The Plant Journal* **44**, 783-797 (2005).
511 Chen, Z. & Cole, P. A. Synthetic approaches to protein phosphorylation. *Current opinion in chemical biology* **28**, 115-122 (2015).
512 Robellet, X. *et al.* A high-sensitivity phospho-switch triggered by Cdk1 governs chromosome morphogenesis during cell division. *Genes & development* **29**, 426-439 (2015).
513 Park, H.-S. *et al.* Expanding the genetic code of Escherichia coli with phosphoserine. *Science* **333**, 1151-1154 (2011).
514 Chalker, J. M., Lercher, L., Rose, N. R., Schofield, C. J. & Davis, B. G. Conversion of Cysteine into Dehydroalanine Enables Access to Synthetic Histones Bearing Diverse Post-Translational Modifications. *Angewandte Chemie* **124**, 1871-1875 (2012).

515 Nakamura, Y., Gojobori, T. & Ikemura, T. Codon usage tabulated from international DNA sequence databases: status for the year 2000. *Nucleic acids research* **28**, 292-292 (2000).
516 Xie, J. & Schultz, P. G. An expanding genetic code. *Methods* **36**, 227-238 (2005).
517 Erlemann, S. *et al.* An extended γ-tubulin ring functions as a stable platform in microtubule nucleation. *J Cell Biol* **197**, 59-74 (2012).
518 Kõivomägi, M. *et al.* Dynamics of Cdk1 substrate specificity during the cell cycle. *Molecular cell* **42**, 610-623 (2011).
519 Pohl, T. J., Brewer, B. J. & Raghuraman, M. Functional centromeres determine the activation time of pericentric origins of DNA replication in Saccharomyces cerevisiae. *PLoS genetics* **8**, e1002677 (2012).
520 Wang, P. J. & Huffaker, T. C. Stu2p: A microtubule-binding protein that is an essential component of the yeast spindle pole body. *The Journal of cell biology* **139**, 1271-1280 (1997).
521 Winey, M. Genome stability: Keeping the centrosome cycle on track. *Current Biology* **6**, 962-964 (1996).
522 Albuquerque, C. P. *et al.* A multidimensional chromatography technology for in-depth phosphoproteome analysis. *Molecular & Cellular Proteomics* **7**, 1389-1396 (2008).
523 Jones, M. H. *et al.* Cell cycle phosphorylation of mitotic exit network (MEN) proteins. *Cell Cycle* **10**, 3435-3440 (2011).
524 Swaney, D. L. *et al.* Global analysis of phosphorylation and ubiquitylation cross-talk in protein degradation. *Nature methods* **10**, 676 (2013).
525 Chee, M. K. & Haase, S. B. B-cyclin/CDKs regulate mitotic spindle assembly by phosphorylating kinesins-5 in budding yeast. *PLoS genetics* **6**, e1000935 (2010).
526 Humphrey, L., Felzer-Kim, I. & Joglekar, A. P. Stu2 acts as a microtubule destabilizer in metaphase budding yeast spindles. *Molecular biology of the cell* **29**, 247-255 (2018).
527 Shapira, O. & Gheber, L. Motile properties of the bi-directional kinesin-5 Cin8 are affected by phosphorylation in its motor domain. *Scientific reports* **6**, 25597 (2016).
528 Goldstein, A. *et al.* Three Cdk1 sites in the kinesin-5 Cin8 catalytic domain coordinate motor localization and activity during anaphase. *Cellular and Molecular Life Sciences* **74**, 3395-3412 (2017).
529 Avunie-Masala, R. *et al.* Phospho-regulation of kinesin-5 during anaphase spindle elongation. *J Cell Sci* **124**, 873-878 (2011).
530 Castillo, A. R., Meehl, J. B., Morgan, G., Schutz-Geschwender, A. & Winey, M. The yeast protein kinase Mps1p is required for assembly of the integral spindle pole body component Spc42p. *The Journal of cell biology* **156**, 453-465 (2002).
531 Bailly, E., Cabantous, S., Sondaz, D., Bernadac, A. & Simon, M.-N. Differential cellular localization among mitotic cyclins from Saccharomyces cerevisiae: a new role for the axial budding protein Bud3 in targeting Clb2 to the mother-bud neck. *Journal of cell science* **116**, 4119-4130 (2003).
532 McMillan, J. N. *et al.* The morphogenesis checkpoint in Saccharomyces cerevisiae: cell cycle control of Swe1p degradation by Hsl1p and Hsl7p. *Molecular and cellular biology* **19**, 6929-6939 (1999).
533 Burton, J. L. & Solomon, M. J. Hsl1p, a Swe1p inhibitor, is degraded via the anaphase-promoting complex. *Molecular and cellular biology* **20**, 4614-4625 (2000).

534 Friedman, D. B. *et al.* Yeast Mps1p phosphorylates the spindle pole component Spc110p in the N-terminal domain. *Journal of Biological Chemistry* **276**, 17958-17967 (2001).
535 Holinger, E. P. *et al.* Budding yeast centrosome duplication requires stabilization of Spc29 via Mps1-mediated phosphorylation. *Journal of Biological Chemistry* **284**, 12949-12955 (2009).
536 Araki, Y. *et al.* N-terminal regions of Mps1 kinase determine functional bifurcation. *The Journal of cell biology* **189**, 41-56 (2010).
537 Schutz, A. R. & Winey, M. New alleles of the yeast MPS1 gene reveal multiple requirements in spindle pole body duplication. *Molecular biology of the cell* **9**, 759-774 (1998).
538 Shimogawa, M. M. *et al.* Mps1 phosphorylation of Dam1 couples kinetochores to microtubule plus ends at metaphase. *Current biology* **16**, 1489-1501 (2006).
539 Weiss, E. & Winey, M. The Saccharomyces cerevisiae spindle pole body duplication gene MPS1 is part of a mitotic checkpoint. *The Journal of cell biology* **132**, 111-123 (1996).
540 Hardwick, K. G., Weiss, E., Luca, F. C., Winey, M. & Murray, A. W. Activation of the budding yeast spindle assembly checkpoint without mitotic spindle disruption. *Science* **273**, 953-956 (1996).
541 Miller, M. E. & Cross, F. R. Distinct subcellular localization patterns contribute to functional specificity of the Cln2 and Cln3 cyclins of Saccharomyces cerevisiae. *Molecular and cellular biology* **20**, 542-555 (2000).
542 Edgington, N. P. & Futcher, B. Relationship between the function and the location of G1 cyclins in S. cerevisiae. *Journal of Cell Science* **114**, 4599-4611 (2001).
543 Miller, M. E. & Cross, F. R. Mechanisms controlling subcellular localization of the G1 cyclins Cln2p and Cln3p in budding yeast. *Molecular and cellular biology* **21**, 6292-6311 (2001).
544 Queralt, E. & Igual, J. C. Functional distinction between Cln1p and Cln2p cyclins in the control of the Saccharomyces cerevisiae mitotic cycle. *Genetics* **168**, 129-140 (2004).
545 Haase, S. B., Winey, M. & Reed, S. I. Multi-step control of spindle pole body duplication by cyclin-dependent kinase. *Nature cell biology* **3**, 38 (2001).
546 Hunter, T. & Plowman, G. D. The protein kinases of budding yeast: six score and more. *Trends in biochemical sciences* **22**, 18-22 (1997).
547 Shero, J. H. & Hieter, P. A suppressor of a centromere DNA mutation encodes a putative protein kinase (MCK1). *Genes & development* **5**, 549-560 (1991).
548 Neigeborn, L. & Mitchell, A. P. The yeast MCK1 gene encodes a protein kinase homolog that activates early meiotic gene expression. *Genes & development* **5**, 533-548 (1991).
549 Dou, Z. *et al.* Dynamic distribution of TTK in HeLa cells: insights from an ultrastructural study. *Cell research* **13**, 443 (2003).
550 Fisk, H. A., Mattison, C. P. & Winey, M. Human Mps1 protein kinase is required for centrosome duplication and normal mitotic progression. *Proceedings of the National Academy of Sciences* **100**, 14875-14880 (2003).
551 Howell, B. J. *et al.* Spindle checkpoint protein dynamics at kinetochores in living cells. *Current biology* **14**, 953-964 (2004).

552 Stucke, V. M., Silljé, H. H., Arnaud, L. & Nigg, E. A. Human Mps1 kinase is required for the spindle assembly checkpoint but not for centrosome duplication. *The EMBO journal* **21**, 1723-1732 (2002).
553 Xu, Q. *et al.* Regulation of kinetochore recruitment of two essential mitotic spindle checkpoint proteins by Mps1 phosphorylation. *Molecular biology of the cell* **20**, 10-20 (2009).
554 Liu, S.-T. *et al.* Human MPS1 kinase is required for mitotic arrest induced by the loss of CENP-E from kinetochores. *Molecular biology of the cell* **14**, 1638-1651 (2003).
555 Liu, X. & Winey, M. The MPS1 family of protein kinases. *Annual review of biochemistry* **81**, 561-585 (2012).
556 Lim, G. & Huh, W.-K. Rad52 phosphorylation by Ipl1 and Mps1 contributes to Mps1 kinetochore localization and spindle assembly checkpoint regulation. *Proceedings of the National Academy of Sciences* **114**, E9261-E9270 (2017).
557 Palframan, W. J., Meehl, J. B., Jaspersen, S. L., Winey, M. & Murray, A. W. Anaphase inactivation of the spindle checkpoint. *Science* **313**, 680-684 (2006).